PB91-136572

Projection of Response of Trees and Forests to Acidic Deposition and Associated Pollutants

NSI Technology Services Corp., Corvallis, OR

Prepared for:

Corvallis Environmental Research Lab., OR

Sep 90

U.S. Department of Commerce
National Technical Information Service
NTIS

TECHNICAL REPORT DATA
(Please read Instructions on the reverse before complett

1. REPORT NO.
EPA/600/3-90/096

2.

3.
PB91-136572

4. TITLE AND SUBTITLE
The Projection of Response of Trees and Forests to Acidic Deposition and Associated Pollutants

5. REPORT DATE
September 1990

6. PERFORMING ORGANIZATION CODE

7. AUTHOR(S)
A. R. Kiester,[2] E. D. Ford, [2]A. Avery, [3]C. Gay,[3] T. Droessler,[2]S. Bassow,[2]S. Cothern, &[2]K. Sorrenson

8. PERFORMING ORGANIZATION REPORT NO.

9. PERFORMING ORGANIZATION NAME AND ADDRESS
[1]USDA/FS;[2]U of WA; [3]NSI, ERL-Corvallis

10. PROGRAM ELEMENT NO.

11. CONTRACT/GRANT NO.

12. SPONSORING AGENCY NAME AND ADDRESS
US Environmental Protection Agency
Environmental Research Laboratory
200 SW 35th Street
Corvallis, OR 97333

13. TYPE OF REPORT AND PERIOD COVERED
Published Report

14. SPONSORING AGENCY CODE
EPA/600/2

15. SUPPLEMENTARY NOTES
1990. U.S. Environmental Protection Agency, Environmental Research Laboratory, Corvallis, OR.

16. ABSTRACT

In 1986 the National Acid Precipitation Assessment Program (NAPAP) established the Forest Response Program (FRP) to assess the effects of acidic deposition and associated pollutants on forests. Modeling studies were developed in parallel with both field studies on the pattern and trends of forest condition and physiological studies of seedlings, saplings, and branches of mature trees. The goals of the modeling effort were to simulate the dynamics of the processes by which acidic deposition and ozone affect tree physiological processes and therefore lead to changes in growth.

Results from models of the physiological function of leaves, branches, roots, xylem, and canopies are presented here. These models illustrate three aspects of the dynamics of these processes. First, growth and the effects of pollutants are stochastic processes; that is, they vary randomly over time. The models help to account for the large amount of variability seen in normal field conditions. Second, some physiological processes can compensate for the effects of acidic deposition or ozone. Third, pollutants may have more than one effect on tree growth, and these effects may be synergistic. The last two properties, compensation and synergy, can lead to nonlinearities in the response of trees, as occurs when compensation is overwhelmed.

The potential nonlinearities and the variabilities demonstrated by these models lead to the conclusions that 1) forest health effects may be developing that are not yet apparent, and 2) for regulation of acidic deposition and associated pollutants to have a detectable effect, regulatory changes will probably have to be of substantial magnitude.

17. KEY WORDS AND DOCUMENT ANALYSIS

a. DESCRIPTORS	b. IDENTIFIERS/OPEN ENDED TERMS	c. COSATI Field/Group

18. DISTRIBUTION STATEMENT
Release to Public

19. SECURITY CLASS *(This Report)*
Unclassified

20. SECURITY CLASS *(This page)*
Unclassified

21. NO. OF PAGES
219

22. PRICE

EPA Form 2220-1 (9-73)

INSTRUCTIONS

1. **REPORT NUMBER**
Insert the EPA report number as it appears on the cover of the publication.

2. **LEAVE BLANK**

3. **RECIPIENTS ACCESSION NUMBER**
Reserved for use by each report recipient.

4. **TITLE AND SUBTITLE**
Title should indicate clearly and briefly the subject coverage of the report, and be displayed prominently. Set subtitle, if used, in smaller type or otherwise subordinate it to main title. When a report is prepared in more than one volume, repeat the primary title, add volume number and include subtitle for the specific title.

5. **REPORT DATE**
Each report shall carry a date indicating at least month and year. Indicate the basis on which it was selected *(e.g., date of issue, date of approval, date of preparation, etc.)*.

6. **PERFORMING ORGANIZATION CODE**
Leave blank.

7. **AUTHOR(S)**
Give name(s) in conventional order *(John R. Doe, J. Robert Doe, etc.)*. List author's affiliation if it differs from the performing organization.

8. **PERFORMING ORGANIZATION REPORT NUMBER**
Insert if performing organization wishes to assign this number.

9. **PERFORMING ORGANIZATION NAME AND ADDRESS**
Give name, street, city, state, and ZIP code. List no more than two levels of an organizational hirearchy.

10. **PROGRAM ELEMENT NUMBER**
Use the program element number under which the report was prepared. Subordinate numbers may be included in parentheses.

11. **CONTRACT/GRANT NUMBER**
Insert contract or grant number under which report was prepared.

12. **SPONSORING AGENCY NAME AND ADDRESS**
Include ZIP code.

13. **TYPE OF REPORT AND PERIOD COVERED**
Indicate interim final, etc., and if applicable, dates covered.

14. **SPONSORING AGENCY CODE**
Leave blank.

15. **SUPPLEMENTARY NOTES**
Enter information not included elsewhere but useful, such as: Prepared in cooperation with, Translation of, Presented at conference of, To be published in, Supersedes, Supplements, etc.

16. **ABSTRACT**
Include a brief *(200 words or less)* factual summary of the most significant information contained in the report. If the report contains a significant bibliography or literature survey, mention it here.

17. **KEY WORDS AND DOCUMENT ANALYSIS**
(a) DESCRIPTORS - Select from the Thesaurus of Engineering and Scientific Terms the proper authorized terms that identify the major concept of the research and are sufficiently specific and precise to be used as index entries for cataloging.

(b) IDENTIFIERS AND OPEN-ENDED TERMS - Use identifiers for project names, code names, equipment designators, etc. Use open-ended terms written in descriptor form for those subjects for which no descriptor exists.

(c) COSATI FIELD GROUP - Field and group assignments are to be taken from the 1965 COSATI Subject Category List. Since the majority of documents are multidisciplinary in nature, the Primary Field/Group assignment(s) will be specific discipline, area of human endeavor, or type of physical object. The application(s) will be cross-referenced with secondary Field/Group assignments that will follow the primary posting(s).

18. **DISTRIBUTION STATEMENT**
Denote releasability to the public or limitation for reasons other than security for example "Release Unlimited." Cite any availability to the public, with address and price.

19. & 20. **SECURITY CLASSIFICATION**
DO NOT submit classified reports to the National Technical Information service.

21. **NUMBER OF PAGES**
Insert the total number of pages, including this one and unnumbered pages, but exclude distribution list, if any.

22. **PRICE**
Insert the price set by the National Technical Information Service or the Government Printing Office, if known.

ABSTRACT

In 1986, the National Acid Precipitation Assessment Program (NAPAP) established the Forest Response Program (FRP) to assess the effects of acidic deposition and associated pollutants on forests. Modeling studies were developed in parallel with both field studies on the pattern and trends of forest condition and physiological studies of seedlings, saplings, and branches of mature trees. The goals of the modeling effort were to simulate the dynamics of the processes by which acidic deposition and ozone affect tree physiological processes and therefore lead to changes in growth.

Results from models of the physiological function of leaves, branches, roots, xylem, and canopies are presented here. These models illustrate three aspects of the dynamics of these processes. First, growth and the effects of pollutants are stochastic processes; that, is they vary randomly over time. The models help to account for the large amount of variability seen in normal field conditions. Second, some physiological processes can compensate for the effects of acidic deposition or ozone. Third, pollutants may have more than one effect on tree growth, and these effects may be synergistic. The last two properties, compensation and synergy, can lead to nonlinearities in the response of trees, as occurs when compensation is overwhelmed.

The potential nonlinearities and the variabilities demonstrated by these models lead to the conclusions that 1) forest health effects may be developing that are not yet apparent, and 2) for regulation of acidic deposition and associated pollutants to have a detectable effect, regulatory changes will probably have to be of substantial magnitude.

PB91-136572

United States
Environmental Protection
Agency

Environmental Research
Laboratory
Corvallis, OR 97333

EPA/600/3-90/096
September 1990

Research and Development

The Projection of Response of Trees and Forests to Acidic Deposition and Associated Pollutants

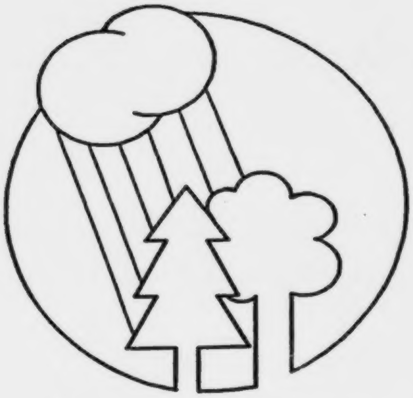

Forest Response Program

Major Program Output #5

United States
Environmental Protection
Agency

United States
Department of Agriculture
Forest Service

REPRODUCED BY
U.S. DEPARTMENT OF COMMERCE
NATIONAL TECHNICAL
INFORMATION SERVICE
SPRINGFIELD, VA 22161

EPA/600/3-90/096
September 1990

The Projection of Response of Trees and Forests to Acidic Deposition and Associated Pollutants

by

A. Ross Kiester,[1] E. David Ford,[2] Anne Avery,[2] Cheryl Gay,[3]
Terry Droessler,[3] Susan Bassow,[2] Steven Cothern,[2] and Kristin Sorrensen[2]

[1]USDA Forest Service
[2]Center for Quantitative Science
University of Washington
[3]NSI Technology Services Corp.

Project Officer

Roger Blair
US EPA Environmental Research Laboratory
Corvallis, OR 97333

The Forest Response Program is a cooperative program of the US Environmental Protection Agency and the USDA Forest Service with support from the National Council of the Paper Industry for Air and Stream Improvement, Inc.

Environmental Reseach Laboratory
US Environmental Protection Agency
200 SW 35th Street
Corvallis, OR 97333

TABLE OF CONTENTS

Abstract i

Preface viii

Acknowledgements ix

Abbreviations x

Executive Summary xi

1 INTRODUCTION

1.1 Forest Response Program Goals 1-1

1.1.1 The Three Policy Questions 1-1
1.1.2 Overall Strategy of the FRP 1-2
  1.1.2.1 Epidemiology/Field Ecology 1-2
  1.1.2.2 Physiology 1-3
  1.1.2.3 Modeling 1-4
1.1.3 Synthesis and the Projection of Response 1-4
1.1.4 The Uses of Models 1-5

1.2 Quality Assurance Program 1-6

1.3 Structure of the Document 1-7

2 DYNAMICS OF TREES AND STANDS

2.1 Stand Dynamics 2-1

2.2 Whole Tree Physiology 2-3

2.3 Sources of Variation in Response to Pollutants 2-3

2.3.1 Genetic Variation within Species 2-3
2.3.2 Variation within Forest Stands 2-4
2.3.3 Phenotypic Variation in Mature Trees Relative to Seedlings 2-4
2.3.4 Between Species: Red Spruce and Loblolly Pine 2-4

3 MECHANISMS OF ACTION OF ACIDIC DEPOSITION AND ASSOCIATED POLLUTANTS

3.1 Concepts of Pollutant Dose 3-1

3.1.1 Chronic Effects 3-1
3.1.2 Duration and Pattern of Dosage 3-1
3.1.3 Conditional Events 3-2

3.2 Specific Mechanisms 3-2
3.2.1 Tree Carbohydrate Balance 3-3
  3.2.1.1 Mechanisms 3-3
  3.2.1.2 Stochastic Processes 3-6
  3.2.1.3 Dosage Patterns 3-6

3.2.2 Winter Injury 3-7
  3.2.2.1 Mechanisms 3-7
  3.2.2.2 Stochastic Processes 3-7
  3.2.2.3 Dosage Patterns 3-7

3.2.3 Soil, Root, and Mycorrhizal Processes 3-8
  3.2.3.1 Mechanisms in the Acidification of Forest Soils 3-8
  3.2.3.2 Mechanisms of Tree Response to Changing Soil Conditions 3-11

3.2.4 Foliar Nutrient Balance 3-12
  3.2.4.1 Mechanisms 3-12
  3.2.4.2 Stochastic Processes 3-13
  3.2.4.3 Dosage Patterns 3-13

3.2.5 Water Relations 3-13
  3.2.5.1 Mechanisms 3-13
  3.2.5.2 Stochastic Processes 3-14

3.2.6 Population Processes 3-14
  3.2.6.1 Mechanisms 3-14
  3.2.6.2 Stochastic Processes 3-14

3.3 Mechanisms in Concert: The Whole Tree 3-14

4 MODELING APPROACH

4.1 The Basic Meta-Model 4-1

4.2 Mathematical and Computational Considerations 4-3

4.3 The Carbohydrate-based Approach 4-3

4.3.1 Carbon Allocation 4-3

4.3.2 The Model CARBON 4-5
4.3.3 Beyond CARBON 4-7

4.4 The Role of Morphology 4-9

5 MODEL: FOLIAR SENESCENCE

5.1 Workshop 5-1

5.2 Description 5-3

5.2.1 Foliar Life-Span (Mortality) 5-7
5.2.2 Photosynthetic Productivity 5-8
5.2.3 Ontogeny 5-8
5.2.4 Carbon 5-11
5.2.5 Nitrogen 5-13

5.3 Analysis 5-13

5.3.1 Ponderosa Pine 5-14
  5.3.1.1 Without Pollutant Stress 5-15
  5.3.1.2 Addition of Accelerated Senescence 5-17
5.3.2 Loblolly Pine 5-18
  5.3.2.1 Life-Span 5-19
  5.3.2.2 Multiplication Factor (Mult) 5-22
  5.3.2.3 Carboxylation Efficiency (k_c) 5-23
  5.3.2.4 Reduction Factor 5-24

5.4 Application 5-26

5.4.1 Loblolly Pine 5-27
  5.4.1.1 Ozone Concentration 5-27

5.4.2 Red Spruce 5-30

5.5 Conclusions and Critique 5-30

6 MODEL: BRANCH/FOLIAGE

6.1 Description 6-2

6.2 Analysis 6-9

6.2.1 General 6-9

6.2.2 Loblolly Pine 6-9
6.2.3 Red Spruce 6-15

6.3 Application 6-19

6.3.1 Loblolly Pine 6-19
    6.3.1.1 Photosynthetic Rate 6-19
    6.3.1.2 Foliage Longevity 6-19
    6.3.1.3 Respiration 6-21
    6.3.1.4 Photosynthetic Rate X Foliage Longevity 6-21

6.3.2 Red Spruce 6-22
    6.3.2.1 Dose 6-22

6.4 Conclusions and Critique 6-26

7 MODEL: SIMPLE WHOLE TREE

7.1 Description 7-3

7.1.1 Numerical Solution 7-8
7.1.2 Boundary Conditions 7-10
7.1.3 Parameterization 7-12
7.1.4 Cambial Hydraulic Conductivity -- Lc 7-13
7.1.5 Axial Hydraulic Conductivity -- Gamma 7-14
7.1.6 Run-Specific Input Requirements 7-14

7.2 Analysis 7-15

7.2.1 Effects of Varying Initial Conditions 7-16
7.2.2 Effects of Varying Boundary Conditions 7-16
7.2.3 Effects of Varying Physical Parameters 7-17
7.2.4 Model Performance 7-17
7.3 Application 7-24

7.4 Conclusions and Critique 7-26

8 MODEL: ROOTS/SOIL

8.1 An Analysis of Southern Soils with MAGIC 8-1

8.1.1 Root and Soil Processes Workshop 8-2
    8.1.1.1 Introduction 8-2
    8.1.1.2 Defining the Scope of the Problem 8-2

8.1.2 Modeling Background 8-7
8.1.3 Modeling Direction 8-8
8.1.4 Mechanisms of Nutrient Uptake 8-9

8.2 Description 8-11

8.2.1 Soil 8-11
8.2.2 Root Growth and Morphology 8-14
8.2.3 Nutrient Uptake Dynamics 8-15
8.2.3.1 Diffusion 8-15
8.2.3.2 Diffusion and Mass Flow 8-15

8.3 Analysis 8-18

8.3.1 Diffusion Case 8-18
8.3.1.1 Morphology 8-18
8.3.1.2 Nutrient Uptake Dynamics 8-18
8.3.2 Diffusion and Mass Flow Case 8-22
8.3.2.1 Morphology 8-22
8.3.2.2 Nutrient Uptake Dynamics 8-22

8.4 Application 8-22

8.4.1 Experimental Seedlings versus Mature Trees 8-22
8.4.2 Organic Soils versus Mineral Soils 8-26

8.5 Conclusions and Critique 8-26

9 MODEL: WHORL

9.1 Competition Models 9-1

9.1.1 Statement of the Problem 9-2

9.2 Description 9-5

9.2.1 Assumptions 9-6
9.2.2 Calculation 9-9
9.2.2.1 Initialization of Tree Crowns 9-9
9.2.2.2 Interception 9-10
9.2.2.3 Annual Growth 9-11

9.3 Analysis 9-11
9.3.1 Comparison to the APA Model 9-12
9.3.2 Variation Accounted for in Growth 9-14

9.3.3 Ten-year Simulation to Compare Shade-tolerant and Intolerant Canopies . 9-14

9.4 Application 9-17

9.5 Conclusions and Critique 9-17

10 SUMMARY AND CONCLUSIONS

10.1 Summary of the Feedback Structure of the Models 10-1

10.2 Summary of the Basic Assumptions of the Models 10-6

10.3 Summary of the Assumptions of Pollution Effects 10-7

10.4 Summary of the Sensitivity Studies 10-8

10.5 Conclusions from Modeling 10-10

10.6 Species Differences 10-12

10.7 Model Limitations and Uncertainties 10-12

10.8 Forests and Long Term Soil Effects 10-13

10.9 Detecting Pollution Effects: Critique 10-13

11 LITERATURE CITED

PREFACE

Research conducted by the Forest Response Program of the National Acid Precipitation Assessment Program and elsewhere has demonstrated a contradiction in the multitude of results. On one hand, field studies of forest condition in the United States have not revealed any statistically detectable, widespread chronic growth declines (although local declines have been documented). This lack of detectable effects is in large part due to the amount of natural variation in trees and stands. On the other hand, experimental studies on a variety of physiological processes of trees have demonstrated several potential mechanisms by which acidic deposition can affect tree and forest health.

The purpose of the present study was to develop a suite of models of components of tree physiological processes, including foliage senescence, branch growth, whole-tree carbohydrate translocation, soil-root function, and crown competition between individuals. Overall, the models help to interpret the significance of results of experimental work done on seedlings and branches in terms of potential effects on whole mature trees. They further develop our understanding of the mechanisms of cause and effect between acidic deposition and tree response.

The most striking result of the work is that dynamic behavior inherent in the model studies generate the same type of variability found in nature. This behavior results from the interactions of multiple mechanisms producing nonlinear responses. These nonlinear interactions arise from physiological and competitive compensation and synergy. Random variation (stochasticity) due to phenotypic plasticity and weather contributes even more to this variation. For example, the branching pattern of trees has an important random component, and this stochasticity itself is a compensating mechanism. This result sets limits on the detectability of a pollution response.

ACKNOWLEDGEMENTS

The authors wish to thank Lew Ladd, Peter Westerhagen, and Rupert Ford for help in the development and running of the models. We thank the National Center for Supercomputing Applications at the University of Illinois for supplying time on a CRAY X-MP. We thank Phil Dougherty, Robert Teskey, Lee Allen, David Vann, Andy Friedland, Carrie White, Eric Miller, Art Wiselogel, and Art Johnson for supplying crucially needed data and much useful discussion. Finally, we thank Jeff Sexton, Brenda Huntley, Lynn Arnaut, Jeff Brandt, Bryn Juntunen, and Greg Baumgardner for their help in the production of this document.

ABBREVIATIONS

APA	–	area potentially available
CSTR	–	continuously stirred tank reactor
EPA	–	Environmental Protection Agency
FRP	–	Forest Response Project
MPO	–	Major Program Output
NADP	–	National Atmospheric Deposition Program
NAPAP	–	National Acid Precipitation Assessment Program
OTC	–	open-top chambers
QA	–	Quality Assurance
QAPP	–	Quality Assurance Project Plan
USDA	–	United States Department of Agriculture
USFS	–	USDA Forest Service
SOS/T	–	State-of-Science/Technology
SWT	–	Simple Whole Tree

EXECUTIVE SUMMARY

The Forest Response Program (FRP) set out to answer three environmental policy questions:

1) Is there a significant problem of forest damage in North America that might be caused by acidic deposition, alone or in combination with other pollutants?

2) What is the causal relationship between air pollutants and forest damage?

3) On a stand or regional basis, what is the dynamic relationship between air pollutants and forest damage?

This report presents a suite of process-based models of tree physiology and growth to answer Question 3 and to integrate the results of research designed to answer Questions 1 and 2. Studies conducted on Question 1 to document the health of our forests found that, with the exception of damage in high montane red spruce forests in the northern Appalachians and to ponderosa pine in southern California, forest health is not showing widespread decline. On the other hand, research on Question 2 demonstrated several mechanisms by which acidic deposition and ozone can potentially damage trees and forests.

The models discussed in this report incorporate variability in environmental conditions and in tree processes. The models indicate that it is the natural variability found in trees and forests that probably explains the difference in results for Questions 1 and 2; ambient levels of pollution do result in tree damage, yet forests exposed to such levels of deposition seem to be healthy.

Five models were developed based on biological levels of organization. Each model can be studied and analyzed alone, or information from one model may be used as input to the next higher level of biological organization. The five models are:

- FOLIAR SENESCENCE
- BRANCH/FOLIAGE
- SIMPLE WHOLE TREE
- ROOTS/SOIL
- WHORL

The core of this report is the BRANCH/FOLIAGE Model, which has been applied to red spruce and loblolly pine.

Although the models are not yet complete, they raise a note of caution. Model results emphasize that forest processes are stochastic and there may be critical points where pollution overwhelms their compensatory abilities. As a result,

- forest health effects may be developing that are not yet apparent, and
- for regulations of acidic deposition and associated pollutants to have a detectable effect, regulatory changes will probably have to be of substantial magnitude.

SECTION 1. INTRODUCTION

The Forest Response Program (FRP) is a joint research program of the US Environmental Protection Agency (EPA), US Department of Agriculture Forest Service (USFS), and the National Council of the Paper Industry for Air and Stream Improvement, Inc., and it is a component of the National Acid Precipitation Assessment Program (NAPAP). The FRP's primary objective is to determine the nature and extent of the effects of acidic deposition and associated pollutants on trees and forests of the United States. This document, Major Program Output (MPO) #5 of the FRP, presents the projected effects of acidic deposition and associated pollutants on trees and forests.

1.1 FOREST RESPONSE PROGRAM GOALS

1.1.1 The Three Policy Questions

The objective of the FRP is to provide information that can be used to address three broad questions related to environmental policy (Schroeder and Kiester, 1989):

(1) Is there a significant problem of forest damage in North America that might be caused by acidic deposition, alone or in combination with other pollutants?

(2) What is the causal relationship between air pollutants and forest damage?

(3) On a stand or regional basis, what is the dynamic relationship between air pollutants and forest damage?

To address these issues, the FRP had to assess the present state of forest health, determine the causes of any changes in health, and, if air pollution is a contributor to changes, estimate the effects of various levels of pollution on forests. This information will be useful to EPA policy makers responsible for regulatory decisions and to those in the USFS involved in planning and forest management.

A primary observation in studies initiated under Policy Question 1 is that trees and forests possess a high degree of natural variation. To date, this variation has made it impossible to detect any widespread chronic effects of acidic deposition. Studies under Policy Question 2 have shown the existence of several mechanisms by which acidic deposition and ozone can affect trees and forests. The objective of this document is to reconcile these two results by calculating some aspects of long-term response to acidic deposition, thus addressing Policy Question 3.

Policy Question 3 has also been phrased as, "What is the dose-response relationship between acidic deposition, alone or in combination with other pollutants, and forest damage in North America?" The FRP has interpreted this in the context of forest biology to mean, "What are the dynamic relations between pollutants and tree and forest growth?" This interpretation emphasizes the dynamic nature of the relationship and it focuses on methods that allow the response of trees and forests to pollutants to be evaluated under alternative deposition scenarios.

1.1.2 Overall Strategy of the FRP

To cohesively integrate results from several fundamentally different kinds of research, the FRP adopted an approach based on the following biological levels of organization: seedling, branch, tree, stand, and region. There were two reasons for choosing this strategy. First, each level can be studied and analyzed in and of itself. Second, information at one level can be synthesized and used as input to another level. The levels and methods by which they are linked are shown in Figure 1-1.

One advantage of this modular approach is that it provides a framework that can accommodate results from both survey (epidemiology/field ecology) and experimental (physiology) types of research. Results from both types of research must be integrated to quantify and predict pollutant impacts on forest growth and to thus provide an answer to the third policy question. The biological levels are linked through statistical techniques and mathematical and computer simulation modeling.

1.1.2.1 Epidemiology/Field Ecology. Epidemiological and field ecological studies constituted the primary approach used to address Policy Question 1. This approach is characterized by broad surveys of forest health and a search for spatial or temporal patterns that may be related to environmental patterns such as air quality and atmospheric deposition. The inherent nature of forests is to change continuously over time. A decline of a tree species or forest is a negative trend, caused by the interaction of any number of abiotic and biotic factors, that is beyond the natural bounds of variability and normal changes.

Data from four principal sources have been analyzed to study trends and natural variability and to identify and estimate the extent and magnitude of any current forest decline. These sources are dendrochronological studies, USFS Forest Inventory and Analysis plots, fixed plot remeasurement studies, and spatial pattern or gradient studies. These studies are summarized in FRP MPO #1&2 and in a NAPAP document, State-of-Science/Technology Report (SOS/T) #16.

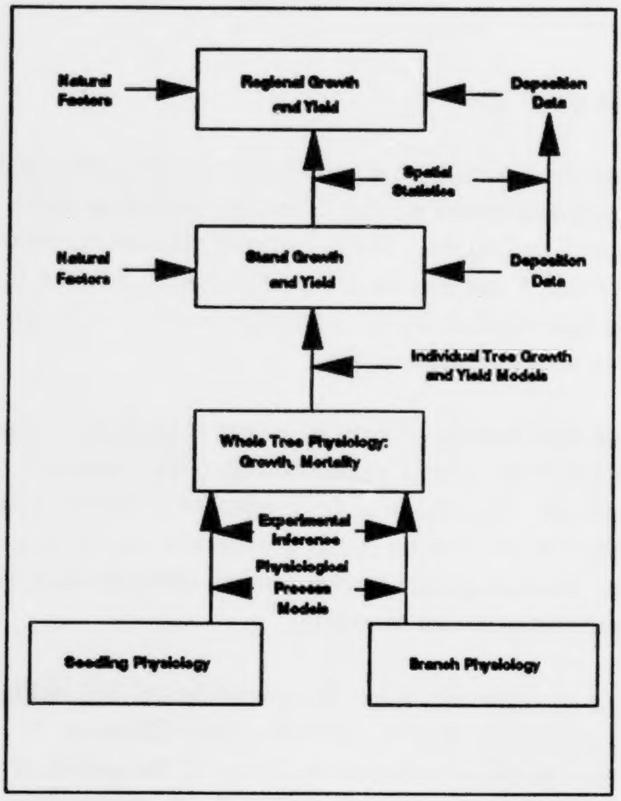
Natural Factors
Regional Growth and Yield
Deposition Data
Spatial Statistics
Natural Factors
Stand Growth and Yield
Deposition Data
Individual Tree Growth and Yield Models
Whole Tree Physiology: Growth, Mortality
Experimental Inference
Physiological Process Models
Seedling Physiology
Branch Physiology

Figure 1-1. Biological levels of organization.

1.1.2.2 Physiology. The physiological approach focuses on the effects of pollutants and other environmental stresses on the health of individual trees. Physiological studies are the main vehicle used to address Policy Question 2 on cause and effect. Studies include greenhouse, field, and controlled laboratory experiments with varying combinations of pollutants, as well as intensive field classification studies. Field studies also include cloud exclusion chamber experiments.

Examinations of the role of air pollutants in growth declines require that carefully designed experimental manipulations be performed. A substantial portion of FRP research examined the growth and physiological responses of tree seedlings to controlled exposures to air pollutants. Program scientists used growth chambers, continuously stirred tank reactors (CSTRs), open-top chambers (OTCs), and branch exposure chambers to conduct experiments. Treatments included ozone, gaseous sulfur and nitrogen compounds, and simulated acid rain and acid mist. Other environmental factors, such as drought stress, were sometimes included. Because these experiments were generally conducted over several years, two- to three-year exposure results are just becoming available.

Branch chamber exposure systems have been used to gain an understanding of how mature trees respond to pollutant exposure. Enclosure chambers can be used to exclude ambient air pollutants or to allow controlled doses of pollutants to be applied to intact branches with several age classes of needles. This approach enables the FRP scientists to study mature trees, and it is less expensive and technically simpler than working with whole trees.

MPO #3 summarizes the studies on seedlings, MPO #4 describes the physiological studies and combines these data with information from MPO #1&2 in an attempt to assess cause-effect relationships (also see NAPAP's SOS/T #18).

1.1.2.3 Modeling. Modeling has been performed by the Synthesis and Integration (S&I) Project, a unique component of the FRP. Because of its size, diversity, and decentralized nature, the FRP faced a special challenge to maintain a cohesive program. The modeling activities of the S&I Project helped in providing the overall technical focus of the FRP and in formulating answers to the policy questions that drive the program.

1.1.3 Synthesis and the Projection of Response

To predict tree and forest response to alternative pollutant scenarios, two tasks must be accomplished:

(1) The known experimental and field information must be synthesized; and

(2) models reflecting that synthesis must be created.

As Figure 1-1 illustrates, one of the ways that information was integrated in the FRP was through computer simulation models. These models may apply to a single level of organization or they may link two levels. For example, much of the experimental work in the program is conducted on seedlings. Therefore, the differences between seedling physiology and mature tree physiology must be understood. Models can help define and examine these differences. For the seedling/mature tree integration, physiological process models are used. Focusing on basic processes, rather than on responses in growth to exposure, allows some of the seedling results to be applied to mature trees.

Figure 1-1 also illustrates the parallel use of branch studies in developing an understanding of mature tree response. The results of branch studies contribute to process-level models and can help to improve the interpretation of seedling results.

At the stand level, integration can be achieved with models based on individual trees. Physiological process models that describe the mechanisms at work in individual trees are used to produce patterns of stand dynamics. This approach allows physiological mechanistic information to specify or describe the behavior of individual trees that are to be aggregated to produce the stand level of organization. Once the stand models are in place, spatial statistical techniques are used to suggest the appropriate regional aggregations. Unfortunately, model development has not yet reached this stage, although some progress has been made in the development of models of canopy competition.

A certain degree of uncertainty is involved when using a hierarchical or scaling-up approach. Seedlings are not equivalent to mature trees. Crucial differences exist that affect responses to air pollutants and other stresses. These differences include the ratio of photosynthetic to respiring tissue, canopy microclimate, leaf morphology, and water and nutrient regimes. Also, individual tree effects may be compensated or magnified at the stand level. The first step is to specify theories that describe and analyze these differences.

All the components of the modeling hierarchy have not been completed. However, syntheses and models for branches, whole trees, and to a very limited extent, stands, have been completed.

1.1.4 The Uses of Models

Several models, rather than a single monolithic model, are included in this report. By constructing an assemblage of models, the modeling effort can be more flexible, can produce early results, and can avoid over-reliance on any single model.

The models developed have at least two uses. First, they provide an understanding of how trees work and how pollutants might affect tree functioning. Second, they predict how trees and stands will respond in the future as the pollution environment changes. Because our overall understanding of tree and stand growth is limited, much of the report deals with the first use, building our understanding of cause and effect. Predictive use of the models is limited to general application. For example, the effects of frost damage on the growth of a single branch of red spruce are studied, but the models cannot be adapted to specific regions of the country or to specific stands in the field.

1.2 QUALITY ASSURANCE PROGRAM

Organizations that make environmentally related measurements (within or funded extramurally by the EPA) are required by EPA policy to participate in a formal, centrally managed and directed quality assurance (QA) program (Stanley and Verner, 1985). The goal of this QA program is to ensure that data used for policy formulation are technically sound and of known and documented quality. The EPA's QA policy applies to the FRP. The FRP QA program was developed and implemented using existing EPA guidance (e.g., EPA, 1976; 1979; 1982; 1983; 1986). The QA program focuses on quality assurance of the measurement process and is outlined in the QA Implementation Plan (EPA, 1987), which defines the QA policy in detail.

The goal of quality assurance of the measurement process is to carry out operations and procedures so that the data produced are of a specified quality within a stated level of uncertainty. In the FRP, data quality is specified quantitatively for each measurement variable in terms of precision and accuracy. These specifications were developed through a consensus of scientists and were expressed as data quality objectives. Precision was estimated by repeated measurements of the same materials using the same methods. Accuracy was estimated by the difference between a measured value and a primary standard, reference material, or equivalent method.

Four general activities were performed to assess data quality: planning, on-site auditing, comparability studies, and QA documentation. Further details can be found in MPOs #1 through #4 and in final QA reports being prepared.

QA planning required that funded projects prepare a QA project plan (QAPP). The QA staff reviewed each QAPP and made recommendations for improvement if necessary. Approval indicated that sufficient QA activities were planned for the project. QA project plans were developed for most FRP projects; the exceptions were those funded at the beginning of the FRP, before the QA program was fully implemented.

An annual, on-site system audit was required for each funded project. System audits involved a comprehensive review of the QA activities of the whole project as described in the QAPP. In addition, annual air monitor performance audits were implemented in projects that conducted controlled exposures that collected ambient air quality data. Air monitor audits focused specifically on calibration checks of project equipment in relation to audit equipment (the "standard").

The QA staff conducted 34, 48, 38, and 45 system audits for 1986, 1987, 1988, and 1989, respectively. Air monitors at 13, 21, and 23 sites were audited for the years 1987, 1988, and 1989, respectively. A report that highlights audit findings and recommended correction action was written for each audit. By policy, audit reports are confidential; they are distributed only to the project personnel and the QA staff. Most of the recommended corrective actions were technical and were worked out between the project personnel and the QA staff, later followed up by the QA staff. Occasionally, audit findings revealed management issues clearly outside of our charge; e.g., changes in project research direction or questions regarding cooperator interactions and funding. These issues were referred to the respective cooperative manager for resolution.

Comparability activities included promoting the use of similar measurement methods and equipment, and documenting differences among methods, laboratories, and field crews. For example, the QA project funded the development of four methods manuals (Baes et al., 1984; Evans and Dougherty, 1986; Robarge and Fernandez, 1987; Zedaker and Nicholas, 1988). These manuals contained recommended methods and were distributed for use in FRP-funded projects. Furthermore, the QA project funded 12 research initiatives on methods comparability, and managed four FRP-wide interlaboratory sample exchange programs. In 1988 there were 9, 31, and 24 FRP projects participating in the soil, water, and foliage sample exchanges, respectively. Finally, the QA staff helped coordinate and evaluate group training sessions for several field survey projects.

Documentation activities focused on promotion of thorough record-keeping within projects in order to document QA activities and allow assessment of data quality. Other activities included maintenance of QA project plans and audit reports, collection of project QA results, and formation of a database of project summaries and QC data.

QA activities in the FRP also provided information about the quality of data used to develop and calibrate the models discussed below. Within the modeling activities themselves an effort was made to apply QA principles to the process of coding the models into a computer language. A document entitled *C Programming Standards for the Forest Response Program* (Avery and Kiester, 1988) was developed for internal use. This document laid out the guidelines for coding that we felt were necessary to help ensure the production of quality code.

1.3 STRUCTURE OF THE DOCUMENT

This document has three main parts. First, Sections 2 through 4 provide the background for the specific models. Next, the models are described, analyzed, and applied in Sections 5 through 9. Finally, Section 10 presents the summary and conclusions based on these models.

This document is based on the work by the FRP and others on tree growth and the mechanisms of action of acidic deposition and associated pollutants (see Table 1-1). MPOs #1 through #4 summarize the remaining collective effort by FRP. NAPAP State-of-Science/Technology (SOS/T) Reports #16 and #18 provide further summaries and syntheses of almost all known results. MPO #4 and SOS/T #18 provide summaries and syntheses of work on the mechanisms of action of acidic deposition and associated pollutants. These documents provide the background necessary for much of the development of the models reported here. MPO #5 will also become a component of the NAPAP SOS/T Report #17, *Development and Use of Tree and Forest Response Models*.

background for the specific models. Next, the models are described, analyzed, and applied in Sections 5 through 9. Finally, Section 10 presents the summary and conclusions based on these models.

This document is based on the work by the FRP and others on tree growth and the mechanisms of action of acidic deposition and associated pollutants (see Table 1-1). MPOs #1 through #4 summarize the remaining collective effort by FRP. NAPAP State-of-Science/Technology (SOS/T) Reports #16 and #18 provide further summaries and syntheses of almost all known results. MPO #4 and SOS/T #18 provide summaries and syntheses of work on the mechanisms of action of acidic deposition and associated pollutants. These documents provide the background necessary for much of the development of the models reported here. MPO #5 will also become a component of the NAPAP SOS/T Report #17, *Development and Use of Tree and Forest Response Models*.

Table 1-1. Documents Associated with Major Program Output #5

DOCUMENT	TITLE	AUTHORS
Major Program Output #1&2	Extent and Magnitude of Recent Changes in Forest Condition and the Role of Air Pollution and Non-Air Pollution Factors	G.A. Reams, R. Vong, M. Böhm, K.G. Mattson, and L.Y. Arnaut
Major Program Output #3	Seedling Response to Sulfur, Nitrogen, and Associated Pollutants	C.E. Peterson, K.G. Mattson, and R.A. Mickler
Major Program Output #4	Response of Forest Trees to Sulfur, Nitrogen, and Associated Pollutants	K.G. Mattson, L.Y. Arnaut, G.A. Reams, S.P. Cline, C.E. Peterson, and R.J. Vong
NAPAP State of Science and Technology Report #16	Changes in Forest Health and Productivity in the United States and Canada	J. Barnard, A. Lucier, A. Johnson, R. Brooks, D. Karnosky, and P. Dunn
NAPAP State of Science and Technology Report #17	Development and Use of Tree and Forest Response Models	A.R. Kiester et al.

Table 1-1. **Documents Associated with Major Program Output #5**

DOCUMENT	TITLE	AUTHORS
Major Program Output #1&2	Extent and Magnitude of Recent Changes in Forest Condition and the Role of Air Pollution and Non-Air Pollution Factors	G.A. Reams, R. Vong, M. Böhm, K.G. Mattson, and L.Y. Arnaut
Major Program Output #3	Seedling Response to Sulfur, Nitrogen, and Associated Pollutants	C.E. Peterson, K.G. Mattson, and R.A. Mickler
Major Program Output #4	Response of Forest Trees to Sulfur, Nitrogen, and Associated Pollutants	K.G. Mattson, L.Y. Arnaut, G.A. Reams, S.P. Cline, C.E. Peterson, and R.J. Vong
NAPAP State of Science and Technology Report #16	Changes in Forest Health and Productivity in the United States and Canada	J. Barnard, A. Lucier, A. Johnson, R. Brooks, D. Karnosky, and P. Dunn
NAPAP State of Science and Technology Report #17	Development and Use of Tree and Forest Response Models	A.R. Kiester et al.

SECTION 2. DYNAMICS OF TREES AND STANDS

2.1 STAND DYNAMICS

The FRP considers stand-level dynamics to be the most useful aspect of trees for such an assessment. A stand of trees may be defined as a group of trees living in sufficient proximity to each other that the individual trees respond to similar environmental factors as well as to each other. Stands may be composed of a single species or of two or more species (mixed species), and they may contain individuals of nearly the same age (even-aged) or of different ages (uneven-aged). Trees that are not in stands are often called open-grown.

Stand dynamics are important in the assessment of pollutant effects for three primary reasons:

(1) Trees often live a long time, i.e., they are not just perennial species, they are long-lived, perennial species.

(2) Individual trees can be extremely interactive, i.e., neighboring trees influence each other and can often be competitive in such a way that a lack of vigor on the part of one tree may be advantageous to another.

(3) Trees are genetically variable and do not all respond in the same way.

In addition to these biological reasons, the stand is an important structural level from an economic viewpoint. At the stand level, predictions can be made on the amount of timber that a number of trees can produce; such a prediction cannot be made based on non-interacting individuals. Most forest economic theory deals with the interactive nature of trees in stands, as shown, for example, by Holley and Veal's (1977) analysis of the effects of fusiform rust at the stand level.

The stand has often been examined to assess the effects of deleterious environmental processes, such as the action of pathogens and insects. Some interactions cannot be assessed by examining individual trees only. Meineke (1917, 1928) observed that even if pathogens kill young trees in a stand, the effects on the total stand growth through time may be negligible, or even positive. Trees in stands compete with one another, and the death (or slower growth) of one tree may provide competitive advantages (e.g., more light or water) for others.

An assessment may also be done at a level other than stand level. For example, the population of individuals most sensitive to pollutants might be the target for assessments. In forestry, assessments might be performed based on the sensitivity of individual seedlings to the pollutant in question. This method is often recommended because it is easy and inexpensive, although it can give a misleading result due to the potential compensatory effects of competition within a stand.

Historically, the study of stand dynamics has been performed from two points of view: evolutionary ecology (Harper, 1977) and forestry (Assmann, 1970). From the evolutionary ecology point of view, reproduction is unquestionably of primary importance to organisms. Organisms that leave the greatest number of progeny are the most successful, assuming that these progeny are able to adapt to their environment. Much of evolutionary theory is devoted to understanding the dynamics of reproductive success. Growth is important only insofar as it influences reproduction. Many organisms do not reproduce until they have achieved a certain size, and reproductive output depends on size and, hence, growth. Trees are examples of both of these dependencies.

In general, foresters consider growth to be the most important variable in the study of stand dynamics. The growth rates and processes tell the forester when a given amount of wood will be available for harvest. Reproduction affects species composition and, thus, the growth of desired species in a stand. Success rates of seedlings can affect initial density and hence, growth rates. Ingrowth (the process by which new trees grow into a stand) can affect growth throughout the life of a stand.

From either point of view, reproduction is related to growth, and vice versa. The two points of view can be combined in an approach where growth is included by specifying the size of each individual tree. Thus, stand dynamics involve size, age, and time, and the processes of birth, death, and growth. The pattern of interdependencies of the various important processes can then be specified. It is these processes and their pattern of interdependencies that make up the dynamics of a stand. Any mechanism of pollution action that affects either the processes or their interdependencies affects stand dynamics and thus is important to consider in an assessment.

The synthesis of the two points of view can be illustrated through the use of a model designed to simulate the growth of physiologically and chronologically aged-structured populations. This model is based on the von Foerster partial differential equation as elaborated by Van Sickle (1977) and Oster (1977), and summarized in Metz and Diekmann (1986). The specific model for tree populations characterized by age, size, and time, was developed by Kiester (1988). The analyses involved with the model are not repeated here, but readers should note that the resulting equation of the dynamics of individuals characterized by size and age present an ideal case. More importantly, the model defines the real problem: the need for understanding the processes of birth, death and growth. In the past, forest models have often been statistical rather than process-based, but science has now developed to a point where process-based models are becoming the preferred method (Kiester, 1990).

2.2 WHOLE-TREE PHYSIOLOGY

If the distribution of physiologically structured populations defines the problem, then understanding whole-tree physiology is the first step in solving it. The processes by which a tree grows and interacts with the environment must be determined. Much of the discussion of Section 3 involves the integration of the various mechanisms controlling tree growth into a model of whole-tree function.

In summary, the stand may be the most relevant level of organization for the development of an assessment, but an understanding of whole-tree physiology is necessary to examine stand dynamics. No complete stand-level model based on whole-tree physiology currently exists. A series of models are available for different levels, ranging from parts of trees to stands that, when interpreted together, offer an assessment.

2.3 SOURCES OF VARIATION IN RESPONSE TO POLLUTANTS

A primary conclusion of MPO #4 is that variation occurs in the response of seedlings to experimental treatments and that similar variation is also observed in forest-based investigations. Four categories of variation are considered, as described in the following subsections.

2.3.1 Genetic Variation within Species

Results of experiments with loblolly pine seedlings have shown substantial genetic variation in response to ozone treatments (see MPO #3). Natural populations of ponderosa pine in southern California may have undergone change in response to ozone exposure (Henderson et al., 1989).

2.3.2 Variation within Forest Stands

Significant differences were found in mid-winter frost hardiness among individual red spruce trees on Whiteface Mountain, NY (see MPO #4). Observations have not determined if this is genetic variation or a product of stand structure and microclimate interactions. Variation among individual trees in physiological parameters such as time of growth initiation and starch concentration in the bark is known to occur (Kozlowski and Peterson, 1962; Kozlowski and Keller, 1966), and has been attributed to competition.

2.3.3 Phenotypic Variation in Mature Trees Relative to Seedlings

In addition to genetic variability, both within and between species, the conclusions of MPO #4 suggest that important sources of variability can occur that have not been investigated nor controlled during experimentation. These sources of variation may possibly include stage of phenological development, degree of stress from non-pollutant variables (water, temperature, light), and differences in rooting media. These sources of variation may provide an unspecified level of background variation that makes interpreting the results difficult. The question arises as to what levels of variation in growth naturally occur in trees and forests and whether this variation is greater or less than that occurring in experiment work. Some of the difficulties encountered in assessing tree-ring sequences (see MPO #1&2) suggest that, even in regions of established high pollutant loading, background variation in tree growth can be high relative to a pollution-induced signal.

Another source of variation is the true stochasticity (random variation) of the development process of trees. For example, patterns of branching appear to have important random components that provide flexibility in complex, dynamic environments and allow the actual branching pattern to vary with the environment.

2.3.4 Between Species: Red Spruce and Loblolly Pine

Two of the major species under investigation by the FRP, red spruce (*Picea rubens* Sargent) and loblolly pine (*Pinus taeda* L.), showed substantial differences in the type and magnitude of their responses to pollutant treatments (see Table 1 in Section 3.2.7). Generally, loblolly pine was sensitive to ozone as measured by effects on growth, photosynthesis, foliage health, and foliage longevity. Red spruce had no response to ozone other than in one long-term (two-year) experiment with saplings. In contrast, red spruce showed some negative responses to applied acid mist in growth and foliage condition, though not in photosynthetic rate. Loblolly pine exhibited no negative effects and actually demonstrated an increased growth in response to acid misting in some experiments. Red spruce showed increasing sensitivity to frost damage with decreasing pH in applied acid mist.

Red spruce and loblolly pine grow naturally in very different environments and have important differences in their biology and ecology (Walker, 1980; Barrett, 1980). Loblolly pine is a potentially fast-growing species that occurs in the southeastern United States. The period of shoot elongation is variable and can extend from early March through late August, depending on weather conditions. In wet seasons, up to five successive flushes of foliage-bearing shoots can occur, and the species is well known for its substantial response to the addition of nitrogen to the soil. Generally, foliage is held for two years only.

In contrast, red spruce on mountain tops in the eastern United States (the area of greatest concern) is a slow-growing tree with an annual period of shoot and foliage growth starting in June that lasts only four to five weeks. Red spruce typically holds foliage for longer than six years. Red spruce is often exposed to spring frost, mid-winter ice storms, and other freezing events that cause winter damage, and the species shows a morphological adaptation in the regeneration of foliage-bearing epicormic branchlets following such damage.

SECTION 3. MECHANISMS OF ACTION OF ACIDIC DEPOSITION AND ASSOCIATED POLLUTANTS

In this Section, the empirical background for the modeling effort is discussed. This background material is also summarized in MPO #4 and SOS/T #18. The concept of pollutant dose is addressed. Further discussion focuses on the specific physiological and ecological mechanisms of tree function that can be affected by acidic deposition and associated pollutants, followed by the patterns of whole-tree physiology. Thus, the specific functions and processes that occur in parts of trees are individually addressed and then combined to suggest how the tree as a whole will respond.

3.1 CONCEPTS OF POLLUTANT DOSE

3.1.1 Chronic Effects

In SOS/T #18, acute damage by pollutants is noted as the exception; the "far more common is the circumstance where the vegetation response to the cumulative dose of an air pollutant ... is sufficient to negatively impact growth, impact reproduction, alter nutrient cycling, alter metabolic processes or influence plant response to other stress factors." Chronic effects are the result of long-term or repeated exposure to low concentrations of a pollutant or pollutants. Generally, because exposure is prolonged, damage occurs in the context of exposure to multiple stress and multiple pollutants.

3.1.2 Duration and Pattern of Dosage

MPO #4 focuses on the conditions of pollutant application in physiological experiments. Exposure periods always have been shorter than might be expected under ambient conditions because experiments are of limited duration. On the other hand, dosage has frequently, but not invariably, been higher than might be expected under ambient conditions or even under alternative deposition scenarios of interest. In a review of ozone effects on woody plants, Reich (1987) concluded that while the effects of ozone on processes such as photosynthetic rate seem less for woody plants than for herbaceous annual plants, the duration of exposure over the life cycle of the plant can result in greater effects on growth. Ozone experiments produce less effect on slower growing species, and this difference may be involved in the apparent insensitivity of red spruce, a slower growing species, compared with loblolly pine. Only after a two-year experimental period did red spruce saplings show an effect of ozone treatment (Table

3-1 of Section 3.2.6). A primary conclusion of MPO #3 is that effects must be monitored at least one season after experimental ozone treatments have ended. In fact, because of the delayed response patterns and long life cycles of trees, exposure studies may need to be conducted over several years.

3.1.3 Conditional Events

Although experiments may demonstrate that damage due to a pollutant may occur under field conditions, actual damage in the environment may occur only with certain conditions not considered in the original experimentation. For example, substantial experimental evidence indicates that the application of acid mist at pH values across the range of ambient rainfall and cloud deposition results in a decreased rate of frost hardening (MPO #4). Furthermore, isolating mature tree foliage from the ambient cloud deposition on a mountain-top site and spraying the foliage with deionized water resulted in more frost-resistant foliage. However, the exact field conditions necessary to cause winter injury remain unclear. Johnson et al. (1986) have discussed the possible importance of particular combinations of warm periods during the winter, which result in some de-hardening, followed by a frost event. However, a recent synthesis of winter injury to red spruce suggests that red spruce may be vulnerable to mid-winter damage in the absence of a warm period (Adams and Eagar, 1989). Another conditional event is when high ozone levels and drought stress occur together, as can happen during the growing season of loblolly pine (Reich, 1987).

3.2 SPECIFIC MECHANISMS

In SOS/T #18 and MPO #4, six mechanisms are identified that should be addressed:

- carbohydrate balance,
- winter injury,
- soil processes,
- foliar nutrient balance,
- water relations, and
- population processes.

The carbohydrate balance of the tree is important because carbon-based compounds are the major structural elements of the tree. Ultimately, any theory of pollution influence must define its relation to the carbon economy through effects on photosynthetic rate, respiration, the shedding of plant parts, or changes in the carbon allocation patterns. Winter injury is considered because the effect of applied acid mist on frost hardiness is one of the clearest experimental results obtained with red spruce and because theories of damage have been developed. Similarly, a major conclusion of the FRP is that soil processes may be influenced at ambient acidities, and transplantation experiments of seedlings into soils of different origins show growth differences.

Application of acid mist causes a reduction in cuticle thickness, and differences in cuticle thickness are found along gradients of acidic deposition. This finding may be related to two possible mechanisms of influence: foliar nutrient balance and water relations. Changes in cuticle thickness may strongly influence these two processes, but both could change substantially with changes in carbohydrate balance and soil processes. Population processes are also a critical component. Generally, the individual tree, or part of it, has been the experimental unit, but estimating the effects on whole stands is an important objective.

3.2.1 Tree Carbohydrate Balance

3.2.1.1 Mechanisms. There are four primary ways in which pollutants can affect the carbon balance of trees:

- reduction in photosynthetic rate,
- increase in respiration rate,
- shedding of plant parts, particularly fine roots or foliage, or
- change in carbon allocation patterns.

Changes in photosynthetic rate, foliage longevity, and respiration rate are likely to interact as they affect growth. SOS/T #18 focuses on possible interactions in the relationships between sources and sinks of photosynthate. McLaughlin (1989) suggests that the capacity of foliage of some plants to respond to a decrease in the source-to-sink ratio by increasing net photosynthetic efficiency may be an important characteristic determining tree resilience to foliar damage, etc. A similar suggestion has been made by Mann et al. (1980). SOS/T #18 also refers to studies of white pine (*Pinus strobus* L.) that indicate increased dark respiration, decreased translocation, and reduced amounts and longevity of foliar biomass play a more significant role than suppression of photosynthetic rate in altering carbon in ozone-sensitive white pine trees.

The theory that growth is controlled by a balance between sources and sinks of photosynthate is an important one in the determination of pollutant effects. The basic theory (Figure 3-1) presents growth as a process involving photosynthesis at a source (foliage); translocation of photosynthate; and utilization of photosynthate in both respiration and production of cell material at a sink (a growing meristem). The whole process may be limited by rates of production, translocation, or utilization. Rates of translocation are driven by gradients in sucrose concentration and water potential (see Section 6), and the concentration gradients are in turn determined by rates of production, rates of utilization, and the distance between source (foliage) and sink (cambium). Two features can complicate this theory: the occurrence of storage and differential timing of periods of rapid photosynthesis and rapid growth. McLaughlin's suggestion above implies that if foliage amount is reduced, the total translocation flux can be maintained if the rate of photosynthesis per unit foliage increases, or possibly if previously stored starch becomes available for growth.

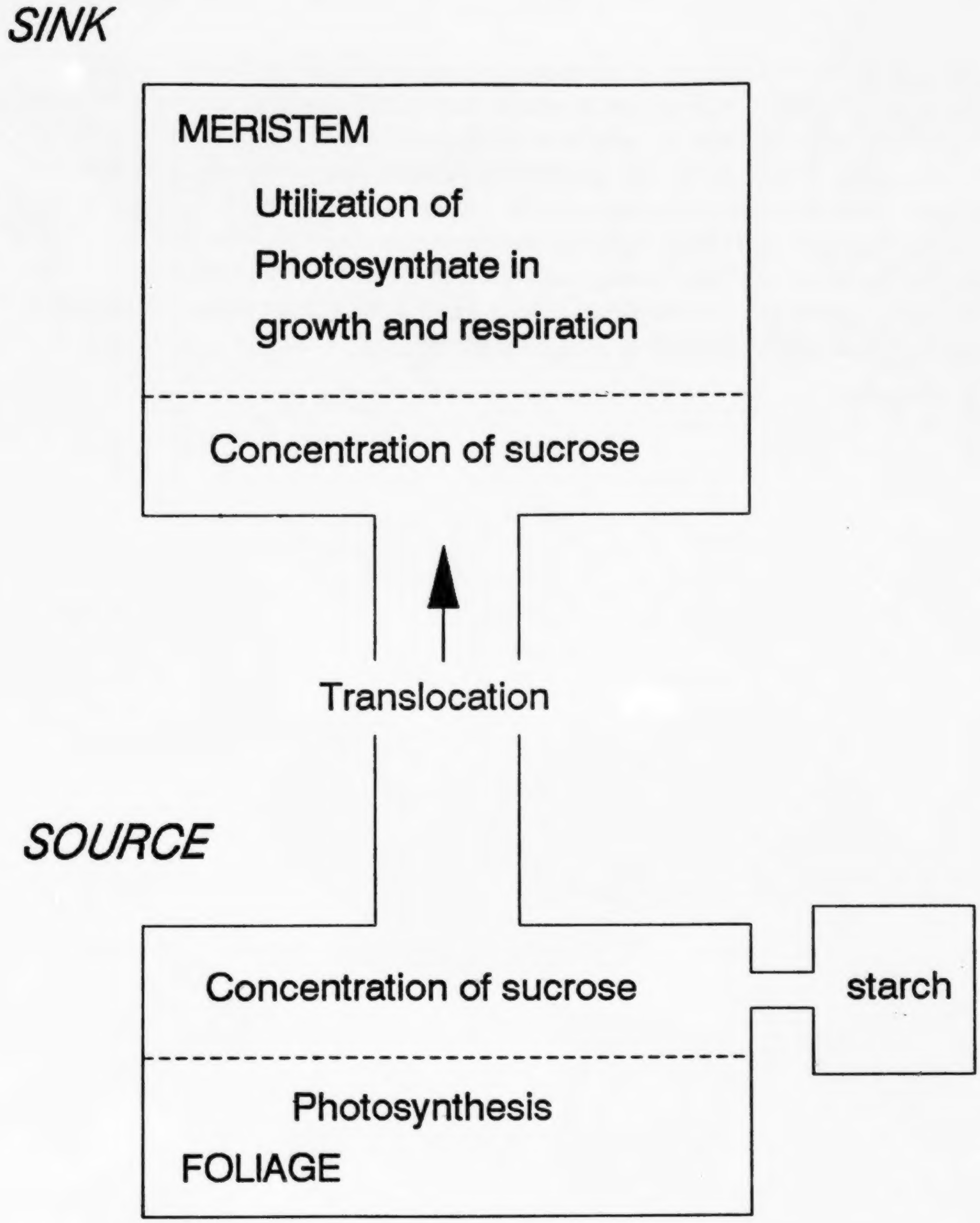
SINK
MERISTEM
Utilization of
Photosynthate in
growth and respiration
Concentration of sucrose
Translocation
SOURCE
Concentration of sucrose
starch
Photosynthesis
FOLIAGE

Figure 3-1. Representation of source-sink theory. The rate of supply of photosynthate from the source to the sink depends on concentration differences in sucrose that can be influenced by a number of factors, including photosynthetic rate.

Simulated acidic precipitation produced highly variable responses in growth of seedlings. In general, acidity did not appear to inhibit growth of most species, and in some cases it may have increased growth. At high acid concentrations (pH 3.0 or lower) foliar injury occurred in most species, and sulfate appeared to be more harmful than nitrate to red spruce seedlings.

Ozone may reduce seedling growth and photosynthesis in both seedlings and branches of mature trees. Results appeared to be species specific. Some genotypes of loblolly pine and ponderosa pine (*Pinus ponderosa* Laws) were especially sensitive and others, including western hemlock (*Tsuga heterophylla* (Raf) Sargent), other southern pine species, and several hardwood species may also be sensitive. The ozone levels required to produce reductions were typically higher than ambient concentrations.

MPO #3 and MPO #4 report that increasing acidity usually had no effect on photosynthetic rate or increased it only slightly, a result usually interpreted as a fertilization effect and thus dependent upon the experimental soil conditions. However, reductions in foliage mass occurred in response to pH below 3.0. Ozone was reported to have a substantial effect on photosynthetic rate of southern pines but little to no effect on red spruce. In seedling studies, considerable variation was observed both between species and between apparently identical experiments. Ozone almost invariably has been recorded as causing a decrease in foliage amount in conifers except for red spruce, which seems not to be affected. Increased respiration has been reported in response to both increased acidity and ozone, although generally fewer measurements have been made for respiration than for photosynthesis. One of the principal recorded effects of ozone on growth has been a reduction in root growth, although the same effect has not been observed consistently in red spruce. The red spruce seedlings, even in controlled studies, exhibited complex and varying responses to the environment; the response must be exhibited by at least 10% of the population to be detected.

SOS/T #18 concluded experimental evidence indicates that photosynthesis is inhibited at typical summer ozone levels measured over much of the eastern United States.

3.2.1.2 Stochastic Processes. There are three components to the stochastic element in a model for carbon dynamics. First, there is variation in the morphology and phenology of individual plant components. Second, substantial genetic variability occurs between individuals. Third, the weather provides a background of temporal variation in the growth process.

3.2.1.3 Dosage Patterns. There are marked contrasts between the apparent time scales of some mechanisms, such as photosynthetic rate and foliage mortality. These different time scales interact with the time scales of dosage patterns, making some aspects of the patterns more important than others. SOS/T #18 discusses also the possibility of physiological repair, particularly to ozone damage. If such repair can occur, then the effects of some patterns of dosage (such as short duration high levels of ozone) may be offset by physiological processes within the tree. Unfortunately, little is known about this possible repair process.

3.2.2 Winter Injury

3.2.2.1 Mechanisms. The FRP's investigation of frost hardening has focused on measuring the rate and degree to which autumn hardening of seedling material occurs under different levels of acidity. These experiments have consistently shown that the hardening process proceeds more slowly with greater acidity of applied mist. The seedling response was fairly linear as acidity increased, starting as high as pH 4.0.

Delay in hardening has also been reported following ozone exposure. Forest measurements have shown that foliage protected from ambient mist during summer growth and sprayed instead with deionized water had greater frost resistance the following winter. Tests on red spruce from several sources have shown that they did not achieve the same level of hardiness as balsam fir (*Abies balsamea* (L.) Mill.). Development of hardiness of current shoots lags behind that of older shoots.

Ideas on the details of the mechanisms by which acidic deposition and ozone increase the probability of winter injury are in flux (see MPO #4).

3.2.2.2 Stochastic Process. As a weather variable, frost is a stochastic process that needs to be defined in terms of temporal pattern of effect and mechanisms of damage.

3.2.2.3 Dosage Patterns. The manner in which dosage patterns might be extrapolated must be examined in more detail. First, winter injury may not be a mid-winter phenomenon, but rather it may be associated with early thawing followed by a return to cold conditions. This could occur in late winter and early spring when the de-hardening process is underway. In provenance (source) transfer experiments of other conifer species, the material sensitive to winter injury typically hardens more slowly in the autumn and to a lower mid-winter maximum and then dehardens to a potentially damaging level sooner in early spring. However, damage most frequently occurs in the spring as temperatures fluctuate during the warming process. Johnson et al. (1986) have reported that two major late-winter thaws in the past 30 years resulted in substantial needle browning in red spruce. Curry and Church (1952) have described the association between needle death and extended mid-winter thaws.

Extrapolation of results also suggests that winter injury is a frequently occurring phenomenon in red spruce. Evans (1986) described the morphology of injury as the consistent loss of all the needles of terminal shoot segments. However, Evans also showed that not all shoots died on a single tree. Thus, the ability for a tree to recover from winter injury is likely to be related to the amount of tissue lost as well as the effect of this loss on the carbon economy. The ability to recover might also depend on the morphological structure of branches and their capacity to allow re-growth. Frost-damaged branches of red spruce are known to exhibit a "witch's broom" proliferation of foliage-bearing shoots (epicormic shoots) from the main branch axis.

Thus, acidic deposition seems to increase the susceptibility of red spruce to winter damage, although it is not certain whether this is due to changes in frost tolerance, cuticular transpiration rates, or other process. Winter injury does not occur invariably each winter, and its potential effects will have to be examined as a stochastic process.

3.2.3 Soil, Root, and Mycorrhizal Processes

3.2.3.1 Mechanisms in the Acidification of Forest Soils. MPO #4 reports several observations that support the theory that changes in soil chemistry may occur due to acidic deposition. Trends similar to those that would be expected due to soil acidification have been observed along regional gradients of sulfate deposition and elevational gradients where deposition is believed to increase. Chemical changes in soil have been induced with artificial acidification, and mass balance analyses suggest that sulfate deposition will eventually lead to increased cation leaching.

MPO #4 reports that short-term responses of seedling root growth to simulated acid precipitation were highly variable, and no clear effects were evident. Direct effects of acidity on roots were not expected. However, indirect effects through changes in soil chemistry (sulfur and nitrogen fertilization, loss of cations, and mobilization of aluminum) were not discounted. Root growth in loblolly pine, quaking aspen (*Populus tremuloides* Michx.), Douglas-fir (*Pseudotsuga menziesii* (Mirb.) Franco), ponderosa pine, and lodgepole pine (*Pinus contorta* Douglas) seedlings was reduced by ozone exposure.

Binkley et al. (1987) reviewed the process of acidification of forest soils and simulated the possible effect of acidic precipitation. They described changes in the acidity of forest soils as a natural process and one that in plantations is closely related to the stages of the crop cycle.

Changes in acidity are mediated by processes that generate or consume hydrogen ions (H^+) and those that generate or consume organic acids stored in the soil. Binkley et al. (1987) state: "The total flux of H^+ in ecosystems is enormous, but fortunately only the net fluxes are important at the scale of ecosystem acidification (see Binkley and Richter, 1987)."

Important changes in acidity are caused by changes in the accumulation of organic matter as forests grow and subsequently decompose. Nutrients such as calcium and potassium ions (Ca^{2+} and K^+) retain their ionic character, and plants must have negative charges to balance these during uptake. These negative charges are provided through the formation of bicarbonate and organic acid anions. H^+ must be extruded from the roots in a quantity equivalent to the net accumulation. Through this process, growth results in acidification. Conversely, when biomass decomposes, the process is reversed. The net H^+ flux associated with nutrient uptake and storage in biomass is usually gauged as the total of the cations. However, some of the cations accumulated in living biomass may come from recycled detritus rather than from the exchange complex or other sources. Soil organic matter pools may also increase over time, and the net flux could be greater than the above-ground increment would indicate.

The net effect of H^+ in acidic deposition is often determined by the fate of the anion associated with the acidity. The process of reducing oxidized sulfur (S) and nitrogen (N) consumes acidity. Binkley et al. (1987) point out that southern forest soils are typically N deficient, and they assume in their simulations that S uptake is less likely to occur and, as far as acidification is concerned, is likely to be the major factor contributing to soil acidification. Other soils, particularly the upland organic soils of the spruce-fir zone, are not N limited and may even show substantial N leaching (Strader et al., 1989; Sasser and Binkley, 1989)

Binkley et al. (1987) suggest that some of the changes in soil condition in the South may be the result of continued change following reforestation, and that these changes may be influenced by natural processes. They were " ... confident that many forest soils are not in steady state with respect to long-term soil development or acidic deposition."

The process of soil acidification is complex because of the number of mechanisms involved, each of which may have a different importance in different environments. The soil system can be described in terms of a series of mechanisms that characteristically operate over different pH ranges. For example, the dissolution of calcium carbonate provides buffering capacity over the range pH 8.6 to 6.2, and the weathering of silicate provides buffering from pH 6.2 to 5.0. An important process in forest soils is the dissociation of the exchange complex from pH 5.2 to 4.0. Unlike the other buffering mechanisms, the anionic character of the exchange complex is associated with the soil material itself. Below pH 4.0, aluminum hydroxides begin to dissolve, releasing hydroxyl ions (OH^-) to buffer inputs of H^+. The inorganic component of most soils has large amounts of aluminum hydroxides. Thus, roots experience high aluminum concentration prior to damagingly low acidity.

Another important soil mechanism, particularly in relation to the effect of S inputs on the mineral component of soils, is the "salt effect". The addition of a salt can result in displacement of aluminum ions (Al^{3+}) from the exchange complex, which causes the dissociation of H^+ from aluminum. The ionic strength of precipitation in polluted regions is high and can lower the pH without changing the nature of the exchange complex. SOS/T #18 notes that as total ionic strength increases, concentration of trivalent cations (Al^{3+}) increases to the 3/2 power of bivalent ions (e.g., Ca^{2+} and Mg^{2+}) and to the third power of monovalent ions (H^+, K^+, Na^+). " ... Thus the introduction of mobile, mineral acid anions to an acid soil will cause an immediate increase in the concentration of Al in soil solution. Conversely, extremely acid soils will not produce solutions that are high in Al unless mineral acid anions are present in soil solution"(SOS/T #18).

SOS/T #18 suggests some evidence exists from the mass balance approach that natural cation leaching rates are substantially increased (two- to three-fold) by acidic deposition. SOS/T #18 focuses on long-term change with regard to changes in net cation budgets. "In most cases, some chance for change emerges over a period of decades if only exchangeable pools are considered, but little change is projected if total pools are considered .... Thus the actual rate of change is highly dependent upon unknown rates of mineral weathering and therefore remains very unclear." However, net cation change might vary substantially between soil horizons.

MPO #4 reports that along geographical gradients of increasing deposition, changes are observed in soil and forest floor chemistry; in particular, S increases. Along an Arkansas-Ohio gradient, a decrease in pH and an increase in exchangeable Al was found. The Ca:Al ratios along this gradient were similar to those associated with forest decline in Europe. In spruce-fir regions, elevational gradients of decreases in cations and increases in Al have been found. In addition to these correlative studies, changes in soil chemistry, particularly increases in Al concentrations, have been found in controlled lysimeter studies using simulated rainfall in the range of ambient acidities. These studies showed increases in Al concentrations after only six applications of acid and raised questions about the temporal pattern of exposure of roots to soil water containing different concentrations of Al. After reviewing FRP research and the ALBIOS project that examined Al and plant response in a number of catchments, MPO #4 authors concluded, "It is thus likely that Al toxicity due to acidic deposition is a stressor that contributes, along with other stressors, to some cases of tree dieback and forest decline." This was most likely the case for sensitive tree species (i.e., red spruce) in forests where

"... fine roots are concentrated in mineral soil horizons with less than 10% to 15% base saturation."

SOS/T #18 notes that typical S deposition values are in excess of tree S requirements, whereas N deposition is within the range of tree requirements (Cole and Rapp, 1981). The report states that, "Recently however, evidence has begun to surface to suggest that N deposition is excessive to certain forests in Europe and to high elevation forests of the eastern United States." Excessive N deposition could cause cation nutrient deficiencies or Al toxicity by acidifying soils and/or increasing mineral acid anion concentration in soil solution. In addition, recent studies of the effects of excessive ammonium (NH_4) deposition have shown that cation deficiencies and forest decline can be produced through above-ground processes.

3.2.3.2 Mechanisms of Tree Response to Changing Soil Conditions. SOS/T #18 reports that soil acidification is not usually the causal factor in hypotheses of red spruce decline, but Al^{3+} toxicity and/or Ca or magnesium (Mg) deficiency due to Al^{3+} inhibiting uptake are currently under serious consideration. The suggested effects of Al^{3+} are slowed growth of apical meristems, a possible increase in dark respiration, and altered translocation rates.

High Al:Ca ratios have been reported in soil solutions in the southern Appalachians. Experiments were conducted with red spruce seedlings in this same environment but with soils from Camels Hump, a region of observed decline, and with soils from forest sites at lower elevations in the same region. The seedlings grown in soil from Camels Hump had low growth rate and more Al^{3+} in their tissues than seedlings grown in other soils. Higher Al:Ca ratios in tree rings of red spruce have also been correlated with decreases in ring width.

MPO #4 reports the effects of acidity on root systems vary with species, although a substantial number of experiments have shown negative effects. One reason suggested for this variability is that the duration of the experiments is shorter than the time required for acidity to affect soil processes.

The results from soil chemistry models suggest further model development is required to incorporate the biological processes of root and soil systems. The stochastic nature of these processes, particularly in relation to dosage pattern, will be discussed after this development has taken place.

3.2.4 Foliar Nutrient Balance

3.2.4.1 Mechanisms. Leaf nutrient concentrations are normally affected by rainfall-induced leaching of nutrients from the leaf surface. Nutrient losses due to leaching usually occur in the following order: potassium, phosphorus, nitrogen, and calcium (K > P > N > Ca), and the rates often increase with foliage senescence, before abscission. MPO #4 and SOS/T #18 review the considerable evidence that acidic deposition enhances foliar leaching and increases nutrient concentrations in foliar throughfall. SOS/T #18 summarizes as follows: "Results of controlled exposure experiments with a variety of herbaceous, and broad-leaved and needle-leaved tree species, conducted by a variety of investigators with a variety of exposure conditions have consistently found a relationship of increased leaching of cation nutrients from foliage as the hydrogen ion concentration of the leaching solution increased..." Generally, cations are leached from exchangeable cation pools within the plant, which involves exchange reactions on the leaf surface. Cations may also move directly from the translocation stream within the leaf by diffusion and mass flow. The extent of the effects of leaching depends on the processes of nutrient recharge from elsewhere in the plant.

Normal leaching is considerable; throughfall typically accounts for 90% of the nutrient movement by leaching. Leaching losses are greatest for K, and lower for N and P. Except for K, litterfall exceeds leaching as a pathway of nutrient return to the soil (Switzer and Nelson, 1972). Leaching losses vary with different leaf types (Luxmoore et al., 1981; Waring and Schlesinger, 1985). New needles have the highest resistance to transport of internal foliar K, and old needles have the lowest resistance (Lovett et al., 1984).

The dynamics of nutrient flux in a canopy are considerable. For example, in canopy throughfall studies of lodgepole pine in southeastern Wyoming, most solute concentrations were found to be much higher in throughfall than in rainfall. Canopy evaporation accounts for a 27% increase of dissolved solids in throughfall, with other differences due to canopy leaching and washing of dry deposition. Throughfall is enriched most by K^+, Mg^{2+} and organic ions. Except for SO_4, wet deposition produces larger amounts of major elements than dry deposition. Canopy leaching is a major nutrient flux path, especially for K^+, Mg^{2+}, and SO_2 (Fahey et al., 1988). Changes in ion concentration gradients across canopy tissue surfaces appear to be important in regulating the flux rate of ions between canopy tissues and stem-flow throughfall (Olson et al., 1985).

SOS/T #18 describes the leaf cuticle as the first line of defense for a plant. Damage to the cuticle can lead to decreased water repellency and possibly to an increase in evaporation of water from the foliage. Resistance to nutrient flux decreases by as much as three times with increased pH and tissue age (Schafer, 1983). SOS/T #18 discusses the significance of this decrease with respect to the accelerated loss of Mg and possibly Ca. The hypothesis of Prinz (1987) states that ozone damages the cuticle, which allows acidic precipitation to more easily leach Mg, thus causing Mg deficiency. SOS/T #18 summarizes the current view: "As far as the foliar leaching portion of the hypothesis is concerned, the evidence would support the potential of acidic rain, fog, or cloud water to increase foliar leaching of magnesium, with or without the additional stress of ozone injury."

Tree stress would probably occur only when nutrient stress also exists. Soil conditions determine whether the amount of nutrients leached from the leaves can be compensated by increased absorption of nutrients through the roots. This situation makes evaluating the foliar leaching hypothesis difficult.

3.2.4.2 Stochastic Processes. Stochasticity in foliar leaching arises as a response to weather patterns, including rainfall and cloud immersion. Spatial variation in soil chemistry greatly influences the impact of leaching and may cause much of the variation in response.

3.2.4.3 Dosage Patterns. Weather features and occurrence patterns influence rain and cloud water chemistry, which determine the basic dose, or exposure, of a pollutant to the tree. Cuticular damage, which may be cumulative over time, can strongly affect the amount of dose received.

3.2.5 Water Relations

3.2.5.1 Mechanisms. Eamus et al. (1989) examined water relations of red spruce treated with acid mist and reported no effect on cuticular resistance or transpiration rates, but they did observe that treated trees exhibited symptoms of mild water stress. Interactions between experimental manipulations and other conditions can influence the water relations of trees and thus influence the experimental results. An example of this interaction has been observed in experiments on the effect of ozone on loblolly pine. Experimental work with seedlings clearly shows this species is sensitive to ozone. However, evidence suggests that under field conditions, mid-day reductions of photosynthesis occur in relation to both low internal water potentials in the plant and high vapor pressure deficit, and these reductions can occur for an extended period of time. Ozone concentrations are generally at their maximum during mid-day and late afternoon, and stomatal closure may minimize the ozone effect. A field experiment measuring photosynthetic rates in crowns of large trees is investigating the interaction by studying irrigated and non-irrigated treatments.

SOS/T #18 discusses other possible interactions between effects of pollutants and water relations. First, reduced carbohydrate production resulting in reduced root growth, as observed in experiments, may come to reduce water uptake capacity. Second, SOS/T #18 indicates that increased drought sensitivity of red spruce can be produced under greenhouse conditions with simulated acid rain at near-ambient conditions. This effects seems to be due to stimulated transpiration loss. In general, effects of acidic precipitation on cuticles may also have an effect on transpiration.

Water flow through soils appears to be a controlling factor of soil chemical processes. Within a given soil type, the balance between percolation and transpiration is controlled by root density and distribution in relation to the transpiration demand set by the foliage.

3.2.5.2 Stochastic Processes. The water status of trees is determined by weather and site conditions. Water status may influence the response of plants to pollutants and determine the nature of the dose received.

3.2.6 Population Processes

3.2.6.1 Mechanisms. Genetic variation in response to applied pollutants has been observed in all experiments in which effects have been observed, e.g., ozone sensitivity of loblolly pine, and frost resistance of red spruce. Thus, if pollutants are having an effect on growth of trees in stands, the responses will be variable. Some individuals will exert a competitive advantage. As cited in MPO #4, diversity decreases with proximity to point sources of pollution, which suggests that genetic variation may operate at the between-species level. For example, ponderosa pine populations of southern California differ in numbers and presence of ozone-resistant genotypes (Henderson et al., 1989).

3.2.6.2 Stochastic Processes. Genetic variation and competition are major variables in the growth of individual plants. Models must consider both when attempting to extrapolate from the effects of pollutants on individual trees to the effects on whole stands or populations.

3.3 MECHANISMS IN CONCERT: THE WHOLE TREE

SOS/T #18 states that plant growth may be thought of as "... a complex system of sources and sinks which has evolved under selective pressures for the efficient management of available resources. The relationship between leaf area and root area in a growing plant, for example, may be visualized as a dynamic balance between the allocation of carbon, water and mineral nutrients between growing roots and shoots. Exposure to atmospheric pollutants can disrupt that dynamic balance, resulting in alteration of growth, stress tolerance, or reproductive efficiency."

MPO #4 and SOS/T #18 suggest that multiple interactions of pollutant influence must be considered. The SOS/T #18 overview (Figure 3-2) focuses on the range of different influences that pollutants may have. MPO #4 presents an overview (Figure 3-3) of the interaction of plant parts in the growth process and discusses how these may be influenced.

These overviews are not contradictory, but the differences between them illustrate the task for modeling. The hypotheses must be translated into quantitative computer simulation programs. Information that is represented as a general influence or that can be satisfactorily depicted as such in diagrams must be made specific. Both figures show interactions between components of growth. In Figure 3-2, shifts in carbon allocations and the inhibition of fine root growth, as a result of changes in metal mobility, are linked to produce a weakened root system. In Figure 3-3, a comprehensive overview of the carbon economy is presented in terms of major components.

To properly extrapolate from experiments under controlled conditions, the effects of synergisms and compensating mechanisms must be estimated. Synergisms occur when the effect of acidic precipitation on two or more processes has a greater effect than can be estimated from studies of the individual processes themselves. Compensating processes may reduce an impact of damage estimated expected based on experiments on single processes. Theories must be developed that incorporate synergism and compensation into a more complete theory of pollution influence. Typically, synergism and compensation operate through more complex mechanisms than can be investigated through direct experimentation.

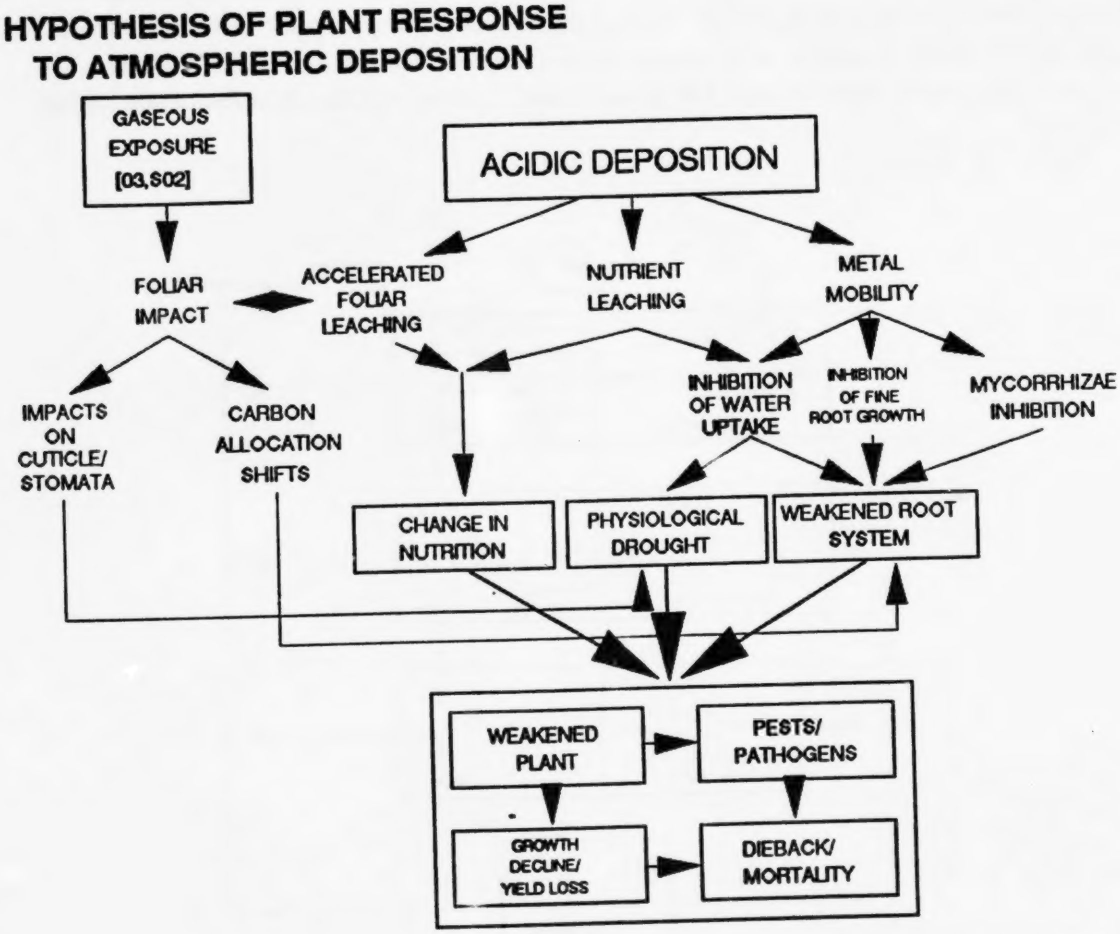
HYPOTHESIS OF PLANT RESPONSE TO ATMOSPHERIC DEPOSITION
GASEOUS EXPOSURE [03,S02]
ACIDIC DEPOSITION
FOLIAR IMPACT
ACCELERATED FOLIAR LEACHING
NUTRIENT LEACHING
METAL MOBILITY
IMPACTS ON CUTICLE/ STOMATA
CARBON ALLOCATION SHIFTS
INHIBITION OF WATER UPTAKE
INHIBITION OF FINE ROOT GROWTH
MYCORRHIZAE INHIBITION
CHANGE IN NUTRITION
PHYSIOLOGICAL DROUGHT
WEAKENED ROOT SYSTEM
WEAKENED PLANT
PESTS/ PATHOGENS
GROWTH DECLINE/ YIELD LOSS
DIEBACK/ MORTALITY

Figure 3-2. Potential interactions of component mechanisms in the effects of pollutants on tree and forest growth (from SOS/T #18).

A synergistic effect could occur through the effects of acid precipitation on soil and foliar processes. A small increase in foliar leaching and a small increase in soil leaching could, over time, have a marked effect upon growth. For example, Hari et al. (1987) proposed a complex sequence for the influence of acid precipitation on Finnish forests where an initial increase in nutrient mobilization in the soil is accompanied by a concomitant increase in tree growth. Under continued acid precipitation, however, nutrient leaching reduces nutrient levels in the whole ecosystem so that a rapid and dramatic decrease in growth occurs. Examining a theory of synergistic effects between root-soil and foliar response, will require a simulation of the rates at which foliage nutrient loss can be compensated for by increased nutrient uptake or mobilization within the tree.

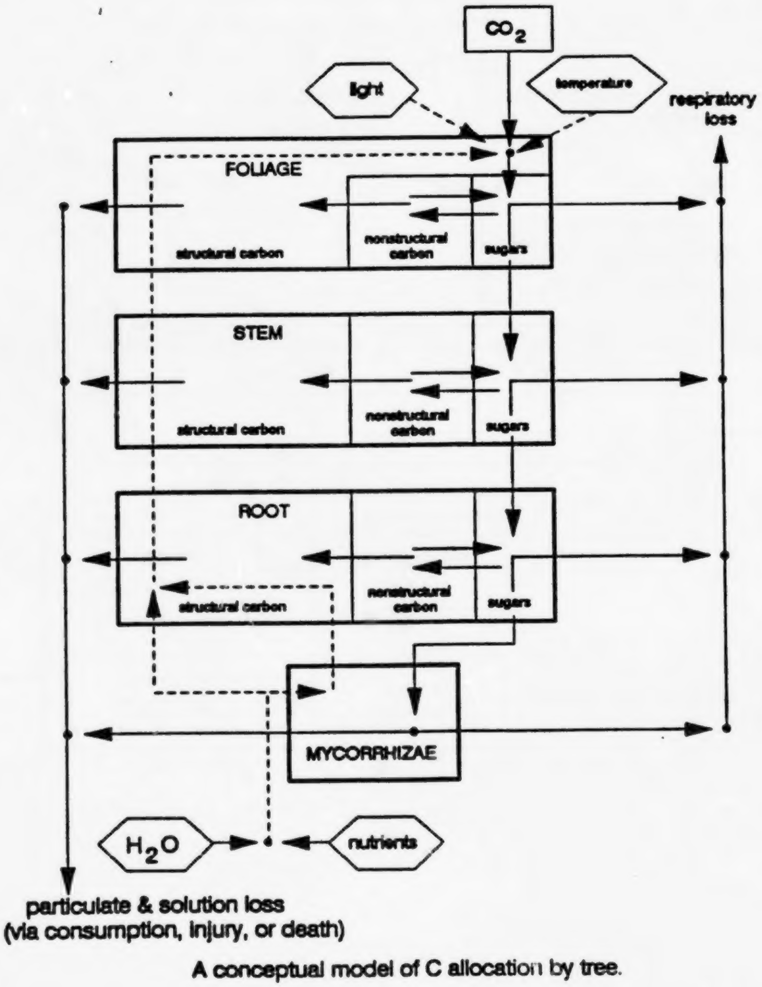
CO_2
light
temperature
respiratory loss
FOLIAGE
structural carbon
nonstructural carbon
sugars
STEM
structural carbon
nonstructural carbon
sugars
ROOT
structural carbon
nonstructural carbon
sugars
MYCORRHIZAE
H_2O
nutrients
particulate & solution loss
(via consumption, injury, or death)
A conceptual model of C allocation by tree.

Figure 3-3. Conceptual model of carbon gain, allocation, and loss and its influence on pathways of water and nutrient movement (from MPO #4).

A possible compensating mechanism in the response of forest stands to acidic precipitation may involve the interaction between the genetic variation in the response of individual trees and competition, which also results in differential growth rates. Theoretically, although acidic deposition might reduce the growth of some individuals within a stand, the overall effect would be a mitigation of the competition process. Thus, the reduction in growth for a whole stand might be less than that estimated only by experiments on the effects of acid precipitation on individual trees. An assessment would require the simulation of the spatial and temporal characteristics of growth rates between trees as affected by competition and genetically determined sensitivity to acidic precipitation (Webb and Burkhart, 1988).

Table 3-1. Comparison of the Effects of Experimental Application of Acid Mist and Ozone Treatments to Red Spruce and Loblolly pine (from findings presented in MPO #4)

EXPERIMENTAL TREATMENT	RED SPRUCE	LOBLOLLY PINE
Acidity on roots	1 negative effect 3 no effect	no effects
Tolerance to Al concentrations in rooting solution	root and shoot growth reduced at 200 to 800 μmole/L	tolerant to 3000 μmole/L
Acidity on mycorrhizal root tips	no effects	not applicable
Acidity on photosynthesis	no negative effects	no negative effects
Acidity on foliar condition	sensitive at pH < 2.5	insensitive, but treatment levels > 3.0
Acidity on height growth	no effects	some positive effects
Acidity on frost hardiness	3 negative effect	not applicable

Table 3-1. (continued)

EXPERIMENTAL TREATMENT	RED SPRUCE	LOBLOLLY PINE
Ozone on photosynthesis	declining trend in seedling experiments but not statistically significant. negative effect in 2-year sampling experiments.	all studies report negative effects
Ozone on foliage mass	3 no effect	all 8 studies report negative effects
Ozone on foliage condition	1 of 2 studies negative effect	all 4 experiments negative effect
Ozone on height growth	insensitive	7 of 8 studies report reduced growth
Ozone on root growth	3 no response	4 reduced root amount
Ozone on mycorrhizae	not applicable	1 reduced

SECTION 4. MODELING APPROACH

The information reviewed in the two previous sections leads to the basic structure of the models, the questions that need to be asked of those models, and, in some cases, the data necessary to calibrate the models. The models must contend with uncertainty and lack of knowledge both of normal tree and stand function and of the effects of pollutants on those functions.

The modeling performed by the FRP is uncertain in terms of the details of proposed mechanisms and the functional forms or parametric values used to model them. These uncertainties reflect our current state of knowledge about the general mechanisms of tree physiology and growth. As realized by the FRP, any investigation of the effects of pollutants must also consider alternative hypothesized mechanisms.

4.1 THE BASIC META-MODEL

Models have been constructed that simulate the effect of damage on tree processes, as measured and investigated within the FRP. The particular task of the modeling effort has been the following:

- Describe the functional interaction between the components of tree growth and so capture the potential for either synergism or compensation between a damaging process and the natural processes of forest growth, and
- Incorporate the uncertainties of variable tree growth rate and pollution dose as stochastic components.

In the study of acid precipitation effects, no consistently accepted theory exists that can be expressed in a single, unified model. This is true partially because individual species, as well as the forests in which they grow, are very different biologically and ecologically. This is particularly true for the two principal species studied by the FRP -- loblolly pine and red spruce.

With this in mind, the objective has been to construct a number of simulators to examine the different, and possibly mutually exclusive, theories of tree growth or response. For example, the simulator of foliage and branch growth of red spruce (Section 6) describes the species' characteristic process of regrowth after damage as a morphological and physiological process. This enables the interactions between incidence of damage (both frequency and intensity) and ability to recover (in terms of photosynthetic rate, foliage amount and number of potential growing points) to be examined under the assumptions of the model.

The areas that the FRP has focused on in modeling physiological processes are shown in Figure 4-1. With the exception of direct attempts to model the relationship between nutrient levels and photosynthetic rates (Section 5) and to simulate nutrient dynamics and root growth in structured soils (Section 8), the modelers have concentrated on processes and their influence on carbon gain and loss. This focus is a reflection of the current knowledge of tree physiology and the interactions between nutrient gain and its effect on growth. It also reflects a decision to model the connection between different components of growth explicitly in terms of morphology and transport. For each aspect of tree and forest growth studied, a first attempt was made to develop a general structure for the temporal and spatial interactions of physiological processes. Due to a combination of choice, which was guided by emphasis in the FRP, and the complexity of the problem being studied, the progress made has been greater in some areas than in others.

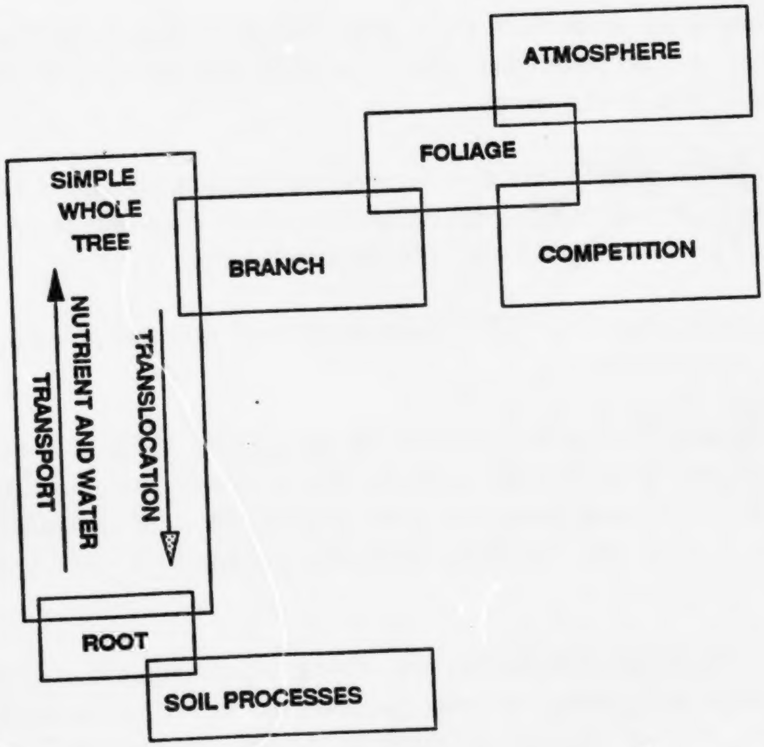

Figure 4-1. Schematic representation of the simulators constructed for modeling the effects of pollutants on tree and forest growth.

The most important requirement is that the model structure be functionally correct in the description of mechanisms of response, especially for mature trees and forests. This is the most scientifically demanding aspect of the modeling task. Theories on the effects of pollution and on the processes that control the growth of large trees are constantly evolving. This dynamic nature of the information has important implications for the way that we develop and use our models.

Models must be constructed to assess the relative importance of different mechanisms, separately and in combinations, and perhaps with different emphasis on various regions and conditions of pollutant load. Models are simply quantitative representations of theory, and, in different geographical regions, theories that emphasize different aspects of pollution influence are being developed. No single global model will be adequate or appropriate for the purposes of the FRP; thus, the construction and use of different models, not just one model with different parameters, is necessary.

4.2 MATHEMATICAL AND COMPUTATIONAL CONSIDERATIONS

All models produced are computer simulations. Much attention has been given to the modularity and readability of the code. Simulators have been constructed that can be used to examine the principal questions being asked in pollution research (Figure 4-1), but the simulators must be used in an interrogative way that is relative to a particular set of questions. The attempt to represent growth as a stochastic process has placed considerable demands on computational resources.

4.3 THE CARBOHYDRATE-BASED APPROACH

4.3.1 Carbon Allocation

That pollutants may influence the relative distribution of photosynthate between plant parts was an important initial hypothesis. In a comprehensive experiment with red spruce seedlings grown in different soils and exposed to a range of acid misting and ozone exposures, Taylor et al. (1986) demonstrated that although photosynthetic rate per unit foliage was not significantly different between treatments, the growth proportions of the seedlings produced were significantly different; i.e., changes in allocation occurred. Changes in allocation could have commercial and functional importance: a reduced relative bole weight would have economic significance, and reduced foliage or root weight could lead to an imbalance in the growth process.

Thornley (1972) was the first to express plant growth explicitly as a dynamic process of interacting parts. His two-compartment differential equation model comprised of root and shoot growth simulated allocation as a process that changes in response to environmental variation. The model was based on the proposition that a functional balance is maintained between roots and shoot. A certain amount of root is required to absorb the necessary N from the soil for both root and shoot growth; similarly, a certain amount of foliage is required to produce sufficient photosynthate for the plant's growth (both root and shoot). The assimilated C and N are assumed to be transported between plant parts along concentration gradients. Growth in either the root or shoot requires concomitant growth in the other. Therefore, the model simulates a balance achieved between root and shoot growth in a changing environment.

This "carbon-partitioning" model, which has been developed and refined (Mäkelä and Sievänen, 1987), was initially developed for cultured plants of genetically indeterminate growth, plants in which limitations to growth were likely to be determined by N availability and photosynthate produced. Unfortunately, this approach to modeling the balance between total uptake of C and N and subsequent distribution to different plant parts cannot be applied to trees in a straightforward manner. Trees exhibit distinct temporal differences in the growth of different meristems, particularly roots and foliage. Furthermore, a major part of their growth is in wood production, and tree growth continues for years rather than days, although models of the type described by Thornley (1972) are most effective in representing growth over the time span of days.

McMurtrie and Wolf (1983) developed a structurally more complex model for trees that incorporated foliage, wood, and fine roots and described the relationships between these components in terms of the production, utilization, and allocation of carbohydrates. Their objective was to predict tree growth over a plantation cycle. The model is formulated as a set of simple differential equations. Production of photosynthates is determined by the amount of light interception, and light interception is determined by the amount of foliage present. All material, including wood, is considered to continually use photosynthate for respiration. Unlike Thornley (1972), McMurtrie and Wolf (1983) used constant partitioning coefficients of photosynthate; they did not simulate a functional balance between root and foliage as a dynamic interaction as no direct experimental work is available to support such an assumption for mature tree growth. Litterfall, branch loss, root death, and turnover were also incorporated.

By varying the partitioning coefficients in McMurtrie and Wolf's model, different patterns of growth, including the accumulation of woody tissue, were predicted. The model, based on carbon dynamics, predicts forest death to occur when the demand for carbohydrate for respiration exceeds photosynthate produced. The lifespan of the forest depends on the allocation coefficients used, in particular, the allocation to woody material; as allocation to woody material is increased, mortality is hastened by increased respiration losses. A critical feature of the McMurtrie and Wolf (1983) model is that, from canopy closure onwards, foliage and fine root growth are assumed to balance losses of foliage and fine root due to litterfall, consumption, and turnover.

4.3.2 The Model CARBON

For the purposes of the FRP, there is an advantage in developing a model that will predict the growth of an entire stand, as McMurtrie and Wolf's (1983) model does. However, the McMurtrie and Wolf model lacks the ability to make independent manipulations of the principle features of growth that might be influenced by pollution, such as, foliage age and differential rates of foliage mortality, and changes in photosynthetic rate. The model CARBON retained the ability to make predictions over the time scale of a stand rotation, but if incorporated three different features (Figure 4-2) (Ford and Bassow, 1988; Bassow, Ford and Kiester, 1990):

- foliage was structured according to age classes, each of which had a photosynthetic rate and mortality;
- a functional link was simulated between root and foliage amounts so that changes in one could induce changes in the other according to various required rules; and
- a technique was used establishing the priorities of carbon distribution in the allocation procedure.

In Figure 4-2, the sequence in priority order is specified as respiration, foliage, fine root amount, and wood production. However, in simulation, this sequence could be changed.

In the model CARBON, photosynthate is totaled from a series of foliage age classes and is allocated according to the following priority system:

- Respiration, which is calculated according to the size of each tree component, foliage, fine root and branch, bole, and thick root. Each component has its own specific respiration rate.
- The new foliage cohort. The size of this is determined by a series of possible controlling factors. It cannot exceed the previous year's increment by more than a certain amount, which simulates the limit of branch-supporting capacity. The total foliage amount must not exceed a pre-set maximum amount.

- Fine root amount, set to be a specified fraction of the total foliage amount.
- The remaining photosynthate, deemed to increment wood weight.
- Reproduction and production of secondary compounds are not included.

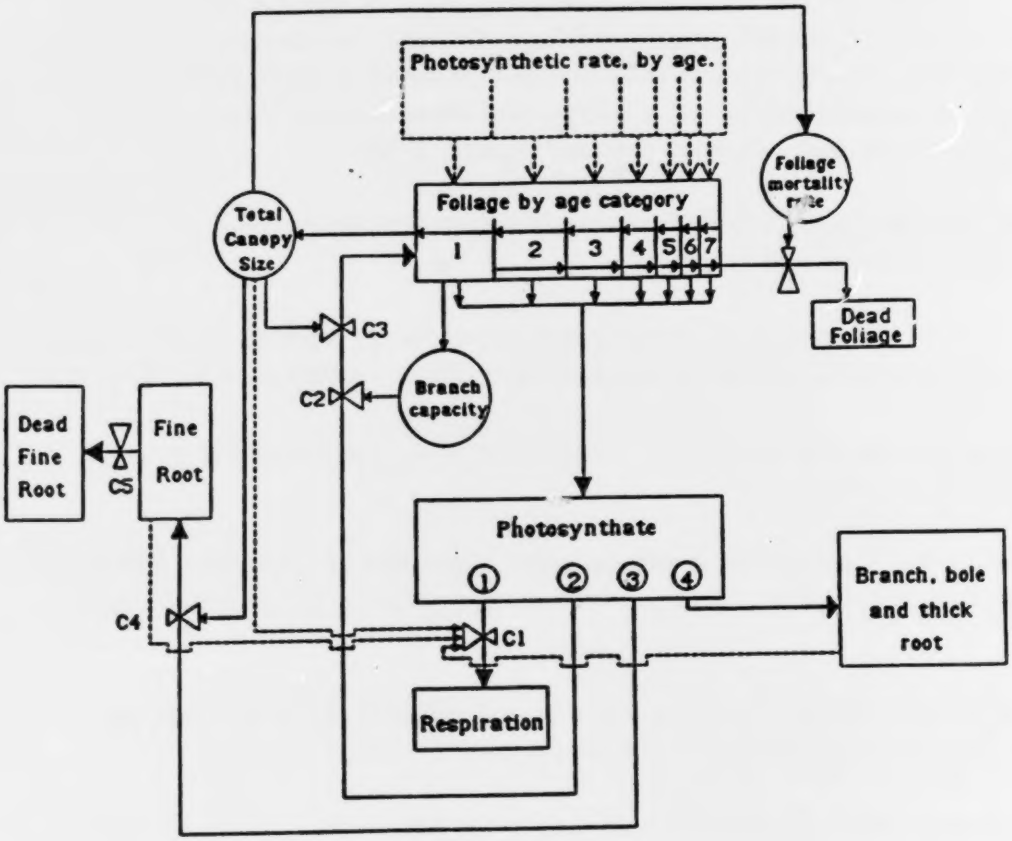
Photosynthetic rate, by age.
Foliage mortality rate
Total Canopy Size
Foliage by age category
1
2
3
4
5
6
7
Dead Foliage
C3
Branch capacity
C2
Dead Fine Root
C5
Fine Root
Photosynthate
①
②
③
④
Branch, bole and thick root
C4
C1
Respiration

Figure 4-2. A schematic representation of the model CARBON. Solid lines represent the flow of carbon, dotted lines represent the effect of various conditions on that flow.

4.3.3 Beyond CARBON

Although CARBON is able to simulate pollutant effects such as the reduction of a photosynthetic rate of particular foliage categories, the predictions made were determined by two important features of the model (Ford and Bassow, 1988). These features were weaknesses of most previous carbon-based tree growth models (Bassow et al., 1990). CARBON requires that (1) a limit be set to the maximum amount of foliage that can develop, and (2) respiration be the first process satisfied in the allocation priority. Ford and Bassow (1988) found that when pollutant effects operated to reduce the rate of foliage increment, the wood increment rate was reduced and the life of the forest was prolonged. Thus, the point when respiration became the major consumer of the photosynthate produced was postponed. Although the value of parameters could be changed and even made dynamic with respect to the growth process, it was necessary to establish a limit to foliage amount and to prioritize the respiration demand for photosynthate use to obtain similar results between CARBON and the previous carbon-based tree growth models.

Developments have also been made in the general class of physiologically based whole-stand models of forest growth. Mäkelä (1986) incorporated the pipe model theory of Shinozaki et al. (1964a,b) in a model to describe carbon balance. She interpreted the pipe model theory as a constant ratio between the cross-sectional sapwood area of the stem and the total foliage above that point. She used the same principle of functional balance between fine root amount and foliage as modeled by Thornley (1972); the pipe model theory was used to determine the annual carbon allocation for stem growth of trees and stands in the forest. For instance, high rates of photosynthesis and nutrient uptake, if combined with low sapwood respiration rates and a low rate of conversion from sapwood to heartwood, imply a relatively high growth rate. Interestingly, in this context the pipe model theory predicts that as the average pipe length increases (i.e., as the tree grows taller) the relative growth rate declines. Thus, a maximum tree height is approached.

However, as a theory on which to base at least part of the allocation process, the pipe model theory has some major drawbacks. The apparent linear relationship between sapwood area and leaf area has been questioned. Dean and Long (1986) found that the ratio between the sapwood cross-sectional area and the total leaf area above that point varied within the crowns of sapling and mature lodgepole pine; the regression lines for saplings and mature trees had very different slopes. Also, sapwood area tapered from breast height to the base of the live crown. They concluded that the relationship between the sapwood area and leaf area could best be explained by a nonlinear regression. Whitehead et al. (1984) suggested that there is a linear relationship between foliage area and the product of sapwood area and wood permeability. An alternative hypothesis to the pipe model theory states that the width of recent growth rings is a function of the carbohydrate produced by the canopy rather than a response to its demand for water.

A direct simulation of the factors controlling foliage amount as part of the growth process is required. In particular, such factors are necessary to simulate the effects of fertilization or pollutants on forests, which increase or decrease foliage amount in the canopy.

The following conclusions are drawn from experience with this class of whole-stand, physiologically-based growth models. The conclusions relate to their potential use in predicting the effects of pollution on tree growth.

- A description of the allocation process that simulates the relationships between plant parts as they are influenced by the environment and the requirements of structural balance, particularly in relation to the amount of wood relative to other plant parts, is required. Cannell (1985) showed that the partitioning ratios among plant parts change with fluctuations of internal and external conditions throughout the life of a plant.

- Factors that control the production and mortality of foliage need to be expressed directly; they should not be addressed as balancing features that artificially constrain canopy development to approach a maximum value. The carbon-based models tend to predict that mortality is the result of excess respiration over photosynthesis, yet this prediction is most frequently made on the basis of respiration per unit weight. Estimates of plant surface area are required.

- Tree mortality occurs for individuals and not whole stands. Tree mortality due to competition occurs naturally throughout a major proportion of the life of most forest stands and is related to the dynamics of foliage increment and loss. Processes other than carbohydrate deficit may initiate mortality.

- Carbon gain, a continual and obvious physiological activity of trees, is a factor that any model of forest growth must try to explain. However, the processes of photosynthesis and respiration, although being the focus of the previously described models, may not actually control the growth process. Nutrition and stand water relations can change as stand growth and development occur, and both may be important factors affected by pollutants.

4.4 THE ROLE OF MORPHOLOGY

Models are structured to describe the connections between plant parts in terms of their morphology, to permit some aspects of the damage and recovery experienced by trees in relation to pollutants to be directly simulated, and to permit two important theories of the control of plant growth to be tested. These two theories are the following:
(1) morphogenetic constraints on patterns of carbon allocation in plants exist (Watson and Casper, 1984); and (2) photosynthesis is dependent on growth rate and vice versa (Gifford and Evans, 1981).

Watson and Casper (1984) examined three questions about the process of photosynthesis:

- To what extent do morphological subunits (i.e., branches) produce the photosynthate needed for their own growth and maintenance?
- To what degree is photosynthate moved freely among organs within a branch?
- To what extent is photosynthate moved among branches?

Watson and Casper reviewed evidence about the modular structure of plants, particularly in relation to physiological function, and they developed the concept of the integrated physiological unit. Shortly after formation as a unit of branch or stem, the integrated physiological unit functions autonomously. Supporting evidence for this concept comes from the modular structure of many plants, the changing patterns of translocation due to age and life stage, and particularly the role of the arrangement of leaves on the stem (phyllotaxy) in determining the patterns of assimilate (photosynthate) movement.

A model structure based on branch units provides a more realistic simulation of the synthesis and utilization of photosynthate. It permits consideration of the importance of storage and transport and enables an accounting of cambial surface area on different branch segments; thus, it permits a more accurate calculation of respiration. However, along with a more detailed consideration of the spatial aspects of synthesis, transport, storage, and utilization, it would be necessary to consider the timing of these events and probably to refine the time increment of models from a yearly to a seasonal level. Modeling at the seasonal level would allow the incorporation of differences between species that may be crucial to understanding the variability in their response to pollutants (e.g., foliage structure).

Reynolds et al. (1980) described the development of a carbon budget model for loblolly pine in which assimilate was distributed among synthesis, storage, and new growth. Three sub-models were considered at different vertical levels in the canopy. The use of a storage sub-compartment is important in simulating loblolly pine growth because shoot growth occurs in a number of flushes during the year, and this number varies with height in the canopy. The model did not explicitly simulate growth in relation to the geometric structure of branch and foliage, but estimates of the rate at which carbon moves from foliage and arrives at assimilating tissues were made on the basis of carbon balance estimates and a review of translocation data for the species.

Watson and Casper (1984) also questioned whether allocation should continue to be considered primarily in terms of carbon: " ... The preponderant use of dry weight as a measure of allocation reflects an underlying assumption that assimilate is the critical currency limiting plant growth. Its adequacy as currency has been questioned recently ... and there is a growing sense that its death knell has been sounded." Perhaps nutrient limitations on photosynthesis should also be considered an important factor limiting plant growth. Seemann et al. (1987) found that a linear relationship exists between CO_2-saturated photosynthetic rates and leaf N content, and that lower N availability reduces the ability of plants to acclimate from shade to sun. Field (1983) has suggested that the C production in an entire canopy is maximized when leaf N is distributed in concert with maximum light intensities received by the leaves.

Finally, the role of morphology and phenology in the construction of models must be emphasized. Morphology provides constraints on the modeling process; the shape of the tree must be predicted as well as the mass. Although this constraint may seem an added burden for the modeler, it provides a very different way of assessing the effectiveness of a model. The strategy of mixing morphology and physiology into the unified study of "functional morphology" has accounted for many recent successes in animal physiology and should be equally successful in tree physiology.

SECTION 5. MODEL: FOLIAR SENESCENCE

Research indicates that major impacts of atmospheric pollution center on alteration of mortality patterns, photosynthetic productivity and nutrient relations. For this reason, these three activities and the interactions between them form the framework of the foliar processes model.

Foliar states change dynamically as a function of both season and maturity. This model was developed to describe changing foliar function associated with these two influencing factors. One of the most consistently observed responses to pollution exposure is accelerated senescence. Using the model, the impact of changes in senescence timing is explored, while other parameters driven by seasonality remain constant.

The issue of senescence resulting from altered carbon allocation to the needle cohort is addressed in the BRANCH/FOLIAGE model, which focuses on a higher level of biological organization than the FOLIAR SENESCENCE model.

5.1 WORKSHOP

A workshop was held in the fall of 1988 to discuss the development of a foliar process model designed to explore the physiological processes affected by acid deposition and ozone (O_3). A conceptual model was presented in the context of the overall FRP modeling plan. The purpose of the workshop was to solicit comments and recommendations from the participants, regarding the specifics of the physiological processes involved and potential data sources. Major concern focused on the complexity of the problem and the limited time remaining in the program. The discussions emphasized issue prioritization and simplification to facilitate future research efforts. The approach was dictated by policy needs of the program and the time available.

The group recommended the use of an empirical photosynthesis model based on physiological facts. The general empirical photosynthesis model provides a particular advantage since measurements have been made for various pollutants, allowing a direct application of the experimental data to the photosynthesis model. However, proper parameterization would be impossible, even though the enzymatic biochemical models have the strongest basis. The panel agreed that the best strategy was to combine photosynthesis and respiration into net photosynthesis rather than to differentiate between respiration and production. A link between nutrient dynamics and ontogeny would then be developed.

The phenomenon of nutrient dynamics is the most complex of the foliar modeling effort and is poorly understood. However, the foliar model must simulate nutrient concentration to fully examine acidic deposition effects. Of the primary mineral elements (Ca, K, Mg, and N), N was chosen as the preferred single nutrient on which to focus. Data on N and Mg concentration were available for some species, and some of the nutrient work had been conducted along with photosynthesis measurements. The driver of the initial nutrient supply was assumed at the outset.

Leaching processes are not amenable to mechanistic modeling, since the mechanisms that cause ions to enter foliage tissue or come out of foliage into surface wetness are not well understood. In addition, the affected pools cannot be measured. Instead, a typical flux was established and modified by ozone concentration or acid concentration. The studies are necessarily highly empirical to account for this influx and efflux of ions from the foliage.

The branch model provides the foundation from which the foliage model operates, providing the connection between foliage classes. The interaction between the foliage and branch models focuses on net carbohydrate production and needle longevity, with movement of carbohydrate between branch and foliage. The branch model provides information on the sinks that limit carbohydrate resources for the needles.

The processes of photosynthesis and influx/efflux of foliar nutrients occur in the foliage. Yet, factors limiting these processes involve components beyond the foliage mass itself, extending to branch wood bole and even roots. Nutrient dynamics begins with soil uptake via the roots, followed by allocation/reallocation. Ozone affects carbohydrate reserves and the movement and allocation of C between organs of the whole plant. The consequences of continual pollutant impact on the photosynthetic apparatus and carbohydrate production are of particular concern.

The panel remained divided on (1) the question of how to allocate C between foliage and branch, and (2) information requirements for the simulation of C allocation and transport. The information required for simulation of allocation includes distance, concentrations, internal sink/source relationships, as well as a differentiation between response of individual tissues.

To address these issues, model development would involve parallel in-depth efforts on branch and foliage components, with some work on whole-tree transport and C allocation processes. Results from the branch and foliage effort should be useful to the FRP and for the Integrated Assessment. Whereas time and information constraints would not allow completion of the whole-tree simulation effort, information from the whole-tree inquiry will be used to aid in interpretation of branch model results and to provide needed groundwork for evolving programs beyond the FRP.

5.2 DESCRIPTION

As indicated by the workshop, a simulator of foliar processes would be expected to address the dynamics of (1) tissue ontogeny, i.e., the pattern of its growth, maturation and senescence; (2) carbohydrates; and (3) nutrients. Equally important are the interactions between these three primary functions, as illustrated in Figure 5-1.

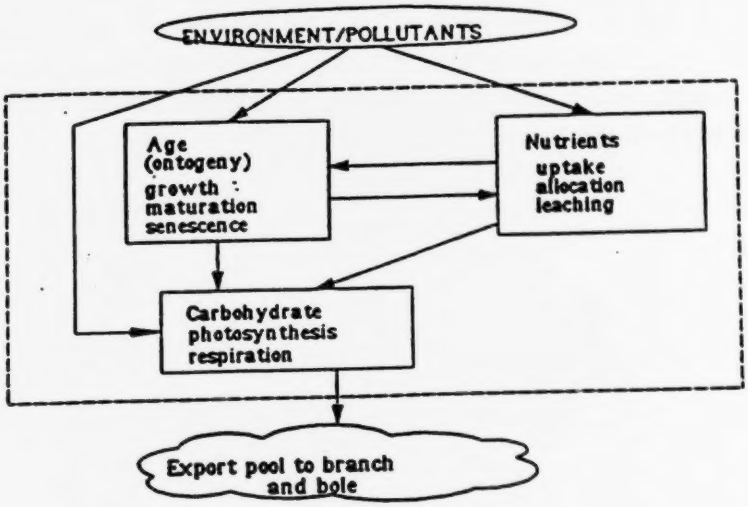
ENVIRONMENT/POLLUTANTS
Age
(ontogeny)
growth
maturation
senescence
Nutrients
uptake
allocation
leaching
Carbohydrate
photosynthesis
respiration
Export pool to branch and bole

Figure 5-1. Diagram of a simplified model of foliar processes, including the points of interaction between environment/pollution and the internal physiological processes associated with maturation, and nutrient and carbon dynamics.

The purpose of this model is to explore changing foliar function due to environmental conditions, including the presence or absence of pollutants. This focus makes it desirable to specify particular environmental conditions. Weather conditions are simulated, although the model can easily accommodate a weather data file.

The model simulates normally occurring activities of the needles on a conifer branch segment, with a branch segment defined as that portion of the branch elongating during a single growth flush. The simulator addresses processes occurring within any single cohort of needles (Figure 5-2). The following is an overview of the approach used in model development.

To address mechanisms that drive changes in nutrient status, ontogenic state, and net carbon productivity, increased resolution is required for the processes and interrelationships illustrated in Figure 5-1. In model development, the coupling of processes (structure of arrows) was emphasized, rather than the detailed simulation of the individual processes (boxes). The boxes are biologically meaningful aggregations of processes that are amenable to further expansion as process models at increasingly higher levels of detail. The pollutants of interest include ozone and acidic deposition. Pollution responses are represented simply. Characteristics of acidic deposition exposure include amount, pH, and N concentration. Simulated responses to acid deposition include (1) increase in cuticle weathering (resulting in increased wettability); (2) the establishment of concentration gradients between apoplast and cuticle surface; and (3) a reduction in frost hardening rates.

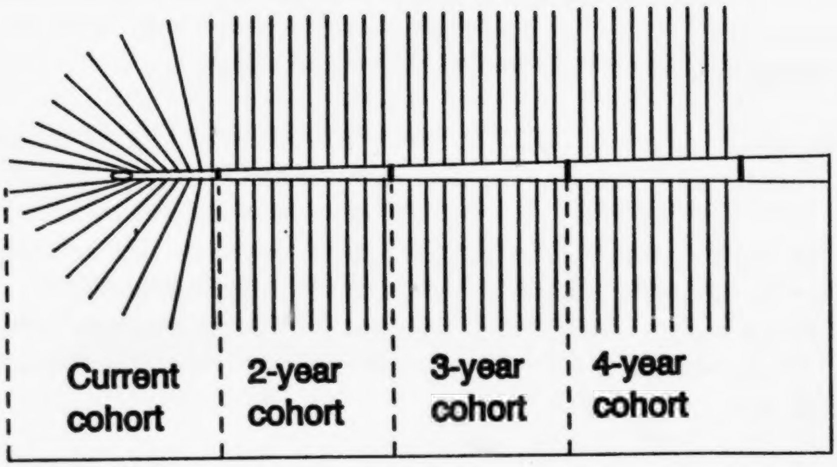
Current cohort
2-year cohort
3-year cohort
4-year cohort
Temporal needle age

Figure 5-2. Schematic of a branchlet with four flushes of needles. The foliar model simulates behaviors occurring on a single flush of needles of the branchlet, from the beginning of needle expansion until all needle tissue has senesced.

Ozone exposure is represented by average ambient concentration over the daylight hours of each day. The treatment of ozone effects is confined to chronic rather than acute exposures and includes simulated cumulative and transitory effects. The cumulative effect is a reduction in the potential life-span of exposed needle tissue; each episode of ozone exposure reduces the tissue life-span from that expected at the onset of exposure. The immediate effects, which apply only during the day of exposure, consist of a transient reduction in the potential net photosynthesis for that day.

Assumptions concerning the foliage environment include (1) a non-limiting water supply, and (2) a location on an open-grown tree with negligible self-shading. The tree is assumed to function as a dominant/codominant tree, as opposed to a suppressed or declining tree.

Because of the highly dynamic nature of foliage, a daily time step for the simulation of foliar processes is used to optimize the balance between computation efficiency and representation, although the model includes sufficient physiological detail to support diurnal simulation. The model will be exercised at hourly resolution to facilitate comparisons with the daily "average" predicted values.

The hypothesis of general pollutant effect used in the foliar processes model is that pollutant effects act in concert with other environmental factors to modify the normal rates of changes in foliar state. Deposition of the mineral elements affects foliar activities by altering the normal fluxes in foliar mineral nutrients. The resultant change in nutrient content can either enhance or reduce photosynthetic productivity. Additionally, ozone can transiently impair processes involved in photosynthetic productivity. Ozone also has the chronic effect of general structural degradation, appearing as premature senescence.

The foliage is physically separated from other elements of its environment by boundaries between needle and branch wood, and between needle and atmosphere. Elements external to the system include moisture, temperature, sunlight, and chemical components in the atmosphere and precipitation. External elements providing input to and accepting output from the system include branch-wood and bole input (nutrient supply from the roots, through the xylem stream in the bole), as well as export of carbohydrate and nutrients to the branch-wood, bole, and the rest of the tree.

Input information to the system includes environmental descriptors characterizing weather and pollutant exposure. Supply of nutrients from the roots through the bole is currently simulated with simple functions, but it can also be input from a linked system of simulators. Branch autonomy is not a required assumption. Specification of carbohydrate input can either be zero (autonomous) or non-zero (non-autonomous).

Output from the system is of two types: material and information. Material flowing from the needles is net carbohydrate available for branch- and bole-wood growth and respiration. Information generated within the model and passed to other elements of a whole-tree modeling system include descriptors of foliar state, such as fresh and dry weight.

Thermal time (degree-days) is used as a general indicator of physiological activity and is calculated as the difference between the daily average temperature and a defined temperature minimum (here assumed to be 0° C). All computations based on "time" in the model refer to thermal time, or degree-days. The effects of soil temperature on physiological activity (and the delaying effects of snowpack on needle growth) have not been included.

The simulator is deterministic in nature, with a single random element introduced through the weather simulation algorithm.

5.2.1 Foliar Life-Span (Mortality)

The impact of leaf aging depends on the environment. The observed decline in photosynthetic capacity with leaf age often reflects nutrient reallocation to more productive positions in the canopy (Chabot and Hicks, 1982).

Branch extension is resource limited and is thus influenced by the growing conditions of the tree and the demands placed on the resources (Cochrane and Ford, 1978). Branch production can provide an early checkpoint for physiological changes that may eventually affect the whole tree. Alteration of needle longevity influences branch production, the spatial distribution of foliage, and relative photosynthate allocation to branch and stem wood (Sheppard and Ford, 1987).

Age-related declines in photosynthetic capacity reduce C yield from a leaf. In both evergreen and deciduous species, a rapid increase to a maximum photosynthetic rate typically occurs, followed by a gradual decline until senescence and death. In some evergreen conifers, maximum photosynthetic rates decrease at a rate of approximately 30% to 50% per year in a roughly exponential fashion (Chabot and Hicks, 1982).

Changes in the specific foliar area (i.e., weight/area) can be complex. Immediately after formation, the foliage may gain in weight and subsequently, with increasing shade, may lose weight (Ford, 1982a). Foliage plays a role in the storage of material for new shoot and foliar growth (Gordon and Larson, 1968), but the flexibility of this system and the factors that control the balance between the use of currently produced and stored photosynthate are only partially understood (Little, 1970).

5.2.2 Photosynthetic Productivity

Net carbohydrate available for non-foliar parts of the plant is the amount produced through photosynthesis minus that expended by the foliage through respiration. The net productivity of the tree also depends on the carbohydrate expenditure associated with needle formation and maintenance (Sheppard and Ford, 1987). The leaf must remain productive long enough to return the carbohydrates used during formation.

The amount of carbohydrate produced by foliage is directly related to the photosynthetic capacity, the amount of productive foliage, and the rate at which carbohydrate is actually being produced (often less than the potential rate). In addition, nutrient status of the foliage is instrumental in determining productivity (Birk and Matson, 1986). To this end, foliar nutrient concentrations fluctuate in association with leaf maturity, season, and physiological stress (Maksymowich, 1973; Yang et al., 1983). Acidic deposition may also play a role in changing foliar nutrient content (van Praag and Weissen, 1986).

Foliar nutrient status plays a tremendous regulatory role in determining synthetic capacity of the foliage, and it therefore must be addressed in the model. Both the inherent internal cycles of nutrient movement and the effects of external influences on nutrients must be addressed.

5.2.3 Ontogeny

One effect of atmospheric pollution is a reduction in foliar life-span (McLaughlin, 1985; Miller et al., 1982). The productivity of a healthy leaf halfway through its expected life span is much greater than the productivity of a damaged leaf of the same chronological age that is ready to drop. Descriptions of foliar age, therefore, must include physiological age and cannot be based solely on the amount of time elapsed since formation.

The ontogeny component of the foliar model determines physiological status of the foliage cohort with respect to tissue maturity (Figure 5-3). This component plays a central role because of the governing influence of tissue maturity on function. Included foliar state descriptors include the following: frost hardiness, cuticle integrity, area live and area senesced, and maturity range of all live needle tissue. Ontogenic state changes as a function of weather and previous ontogenic state, with the rate of change constrained by characteristic patterns of species behavior.

Growth, maturation, and senescence are determined by an extension of the growth curve concept. Potential needle expansion assumes a generally sigmoid pattern, represented by the Gompertz equation (Gompertz, 1825). This simulated potential expansion reflects the cell wall loosening pattern occurring during the expansion period, during which the cell walls follow a pattern of increasing then decreasing plasticity. A fixed time frame is assumed during which elongation will be allowed to occur. Under optimal expansion conditions, needle expansion follows the pattern described by the sigmoid function. If during the expansion period a condition occurs that restricts the expansion of the needles, growth rate also is reduced. The occurrence of a growth restriction at any time in the expansion period will thus prevent the needles from attaining their potential maximum size. The needle cohort cannot accelerate growth rates to compensate for transient growth restrictions.

Life expectancy of tissues on a given foliage cohort varies, with particular tissues more ephemeral than others. The range in longevity has been attributed to the proximity to meristematic tissues. Tissue closer to meristematic tissue has a longer life span than tissue farther away (Thomas and Stoddart, 1980; Ticha, 1981).

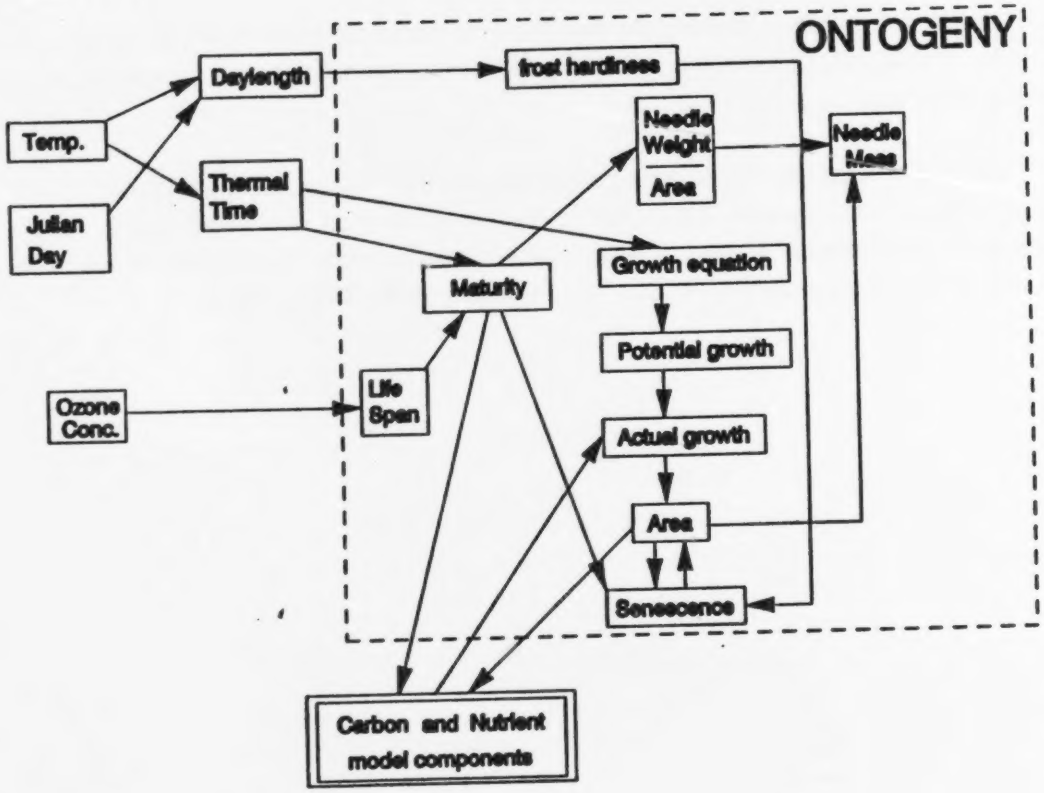
ONTOGENY
Daylength
Temp.
Julian Day
Thermal Time
frost hardiness
Needle Weight
Area
Needle Mass
Growth equation
Maturity
Potential growth
Ozone Conc.
Life Span
Actual growth
Area
Senescence
Carbon and Nutrient model components

Figure 5-3. Interrelationships within the ontogeny component of the foliar model.

The first-emerging needle tissue is assumed in the model to be the most ephemeral, and tissue expanding last is the most durable. Upon emergence, the first-emerging needle tissue is assigned an expected life span, *s*, in degree-days. The value of *s* is characteristic of the species, and is an input parameter. The life span of the most durable tissue is a multiple of *s*, and tissue emerging between the first and last has a life expectancy linearly related to its time of emergence.

Tissue age is predicted as a normalized value, and it is the ratio of elapsed thermal time since the beginning of needle expansion (degree-days) to expected life span (degree-days). "Age" represents the change in tissue vigor and the accumulation of errors in the synthetic mechanisms, which occur over time. Accumulated stress progressively decreases the value of the life span.

Leaf mass/unit area is determined as a function of age, and it changes dynamically over time. Foliar leaf weight is calculated by multiplying the live needle by the mass/unit area associated with a particular tissue age. Leaf area is considered to be live, or functional area, only. Abscission of senescent tissue is assumed to occur immediately on death.

Frost hardiness (used in the red spruce simulation) is determined using a method derived by Cannell et al. (1985), based on day-length and temperature.

5.2.4 Carbon

The interrelationships associated with the C portion of the foliar model are illustrated in Figure 5-4. Landsberg's (1986) empirically derived photosynthesis equations are employed to compute potential net photosynthetic productivity as a function of vapor pressure, temperature, photon flux density, and stomatal conductance. Leaf temperature is assumed equal to ambient air temperature (Waring and Franklin, 1979). Photosynthetic productivity is reduced from the predicted potential by the presence of ozone or by a reduction in leaf N.

Because energy and gas exchange by conifer needles appears insensitive to wind speed beyond a rather low threshold (e.g., 5 cm/s) (Running et al., 1987), wind speed is not included as an influential factor in the photosynthesis calculations. Quantum efficiency in this model is unchanged by tissue frost hardiness, although Öquist and Strand (1986) found a 10% decrease in the mean photosynthetic quantum efficiency of hardened primary needles of Scots pine seedlings when compared with the efficiency of non-hardened needles.

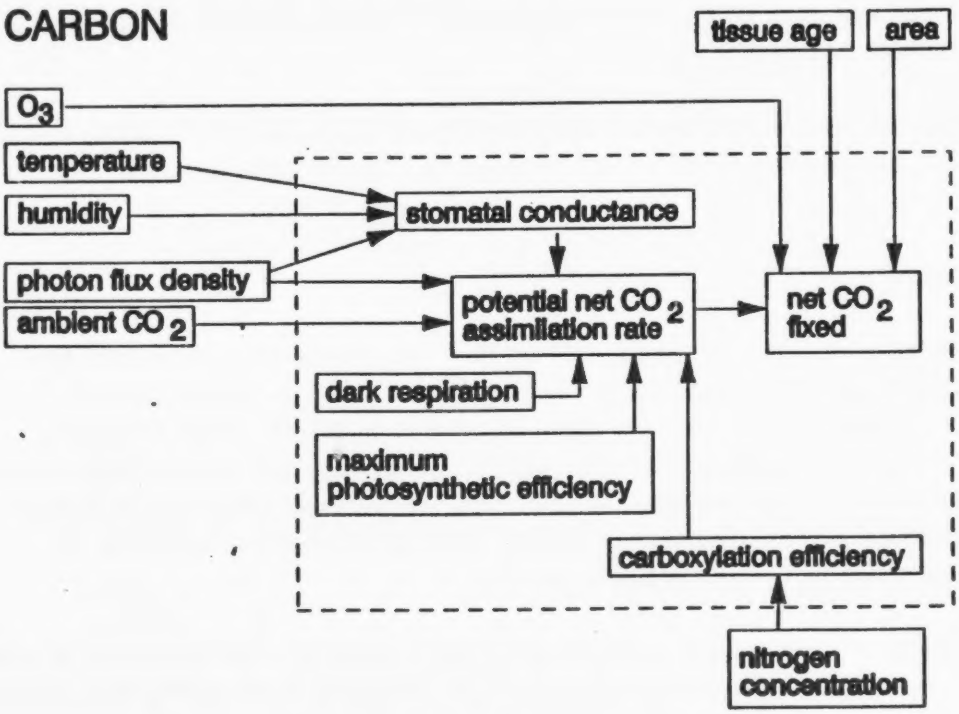
CARBON
tissue age
area
O3
temperature
humidity
stomatal conductance
photon flux density
ambient CO2
potential net CO2 assimilation rate
net CO2 fixed
dark respiration
maximum photosynthetic efficiency
carboxylation efficiency
nitrogen concentration

Figure 5-4. Interrelationships within the carbon component of the foliar model.

5.2.5 Nitrogen

Figure 5-5 illustrates internal relationships of the nutrient components of the foliar model. Changing internal leaf N sinusoidal oscillation represents seasonal fluxes in N supply per unit dry mass of needles through the xylem stream to the leaves, and it is computed as a function of Julian day and normalized tissue age. The minimum N concentration required to support structure and the maximum N concentration are input parameters. The oscillation in N concentration is damped as a linear function of tissue age to represent the decreasing N sink strength of the tissue as it ages. Nitrogen susceptible to leaching is considered to be present in the apoplast solution and is calculated as the amount exceeding the minimum required for the maintenance of dry weight.

Total needle N reaches maximum soon after emergence, dropping to the minimum value required for structure at death, and it oscillates seasonally between these limits with a yearly period. The oscillation has been calibrated to concur with regression equations by Landsberg et al. (1984). The damping effect of advanced age represents age-related export of labile, or non-structural, N.

Cuticle wettability increases with duration and severity of exposure, and the effect of acidic deposition on cuticle function is simulated as a weathering phenomenon. With increased exposure, the cuticle becomes more wettable, increasing retention of moisture during a precipitation event. The enhanced wettability increases cuticular exposure to acid precipitation induced leaching because of the increase in wetted leaf area. Acidic deposition "exposure" on a leaf is thus modeled as a function of leaf area, precipitation amount (Eddleman, 1988), wettability, and chemical composition of the precipitation liquid.

5.3 ANALYSIS

The analysis of model behavior is presented in two parts using simulations calibrated for two species. First, the ponderosa pine version of the model is used to illustrate general model behaviors and activities. Second, the loblolly pine version of the model is employed for a sensitivity analysis, illustrating the sensitivity of response to changing values of particular calibration parameters.

5.3.1 Ponderosa Pine

The yearly cycle of day-length and temperature (or degree-day accumulation) for the ponderosa pine simulation runs is representative of a flat (non-mountainous) site located at 45° North latitude. Daily degree-day accumulation throughout the year ranges from a high of 10 (mid-summer) to a low of 0 degree-days (mid-winter) per day.

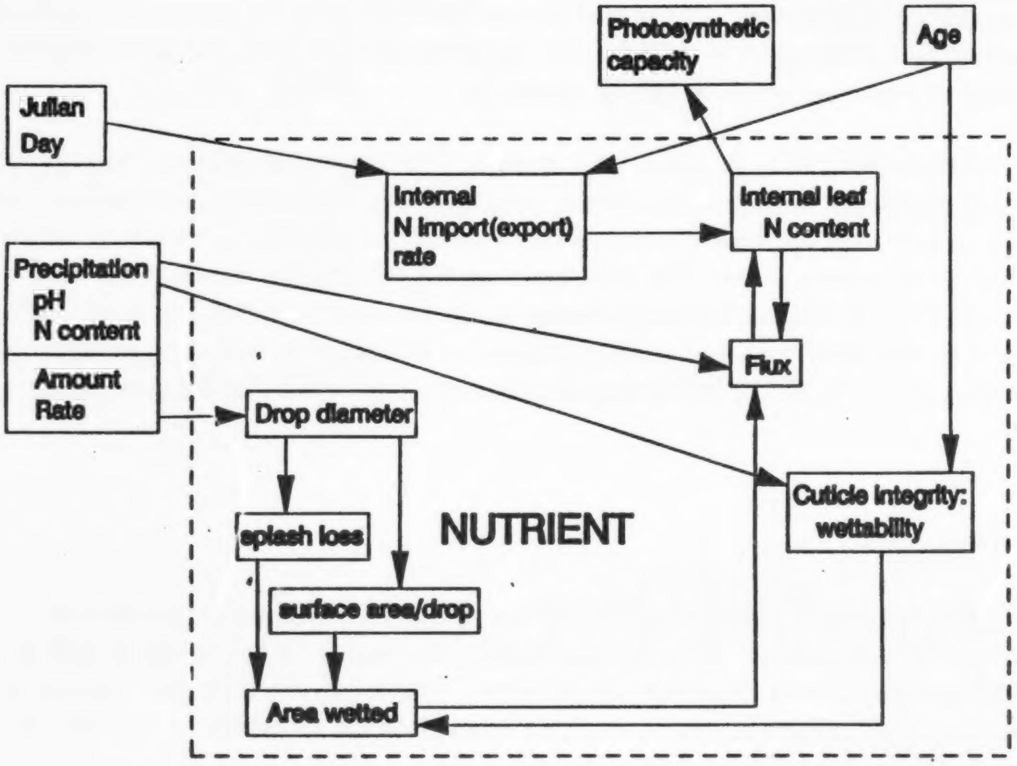
Photosynthetic capacity
Age
Julian Day
Internal N import(export) rate
Internal leaf N content
Precipitation pH N content
Amount Rate
Flux
Drop diameter
Cuticle integrity: wettability
splash loss
NUTRIENT
surface area/drop
Area wetted

Figure 5-5. Interrelationships within the nutrient (nitrogen) component of the foliar model.

5.3.1.1 Without Pollutant Stress. Figure 5-6 shows model output from a model run in which needle growth was simulated without the addition of environmental stress. Figure 5-6a reflects changing needle area over time. Tissue expansion begins at thermal time 0 and continues for 600 degree-days, at which time the maximum surface area of 0.25 m^2 is reached. Senescence of the most ephemeral (first expanded) needle tissue begins at 1000 degree-days.

Simulated senescence is a function of thermal time and represents the loss of functional needle area. Senescence rates, therefore, accelerate during the warm periods of the year, when degree-day accumulation is high, and slow during the cold winter months, as illustrated by the irregular decline in live leaf area.

Photosynthetic productivity of the cohort is a function of the amount of live area and its maturity (Figure 5-6b). Productivity peaks at the time of the completion of expansion and then declines. This pattern of productivity is initially governed by the aging of the tissue, and later by the combination of decreased leaf area and maturation of the remaining needle area.

The changing kill temperature (T_k) associated with frost hardening (Figure 5-6c) is governed by the changing daylength (a consistent pattern through the year) and by minimum air temperatures (T_{min}), which are more capricious. Throughout the life span of this needle cohort, the occurrence of frost was introduced as a random element, overlaid on the consistent pattern of changing day-lengths. The yearly trends in the rise and fall of frost hardiness (killing temperature) remain consistent, whereas the daily changes in hardiness vary from year to year.

Needle dry mass (Figure 5-6d) initially follows a pattern similar to area expansion, but it diverges as the tissue ages due to an increase in relative dry weight with maturity.

Total tissue N content (Figure 5-6e) generally follows the trends observed in area and dry weight changes, while N concentration, shown as a fraction of dry weight, shows the pattern of a damped sinusoidal oscillation (Figure 5-6f) introduced by the oscillating seasonal supply to the needles, with the damping effect driven by maturation.

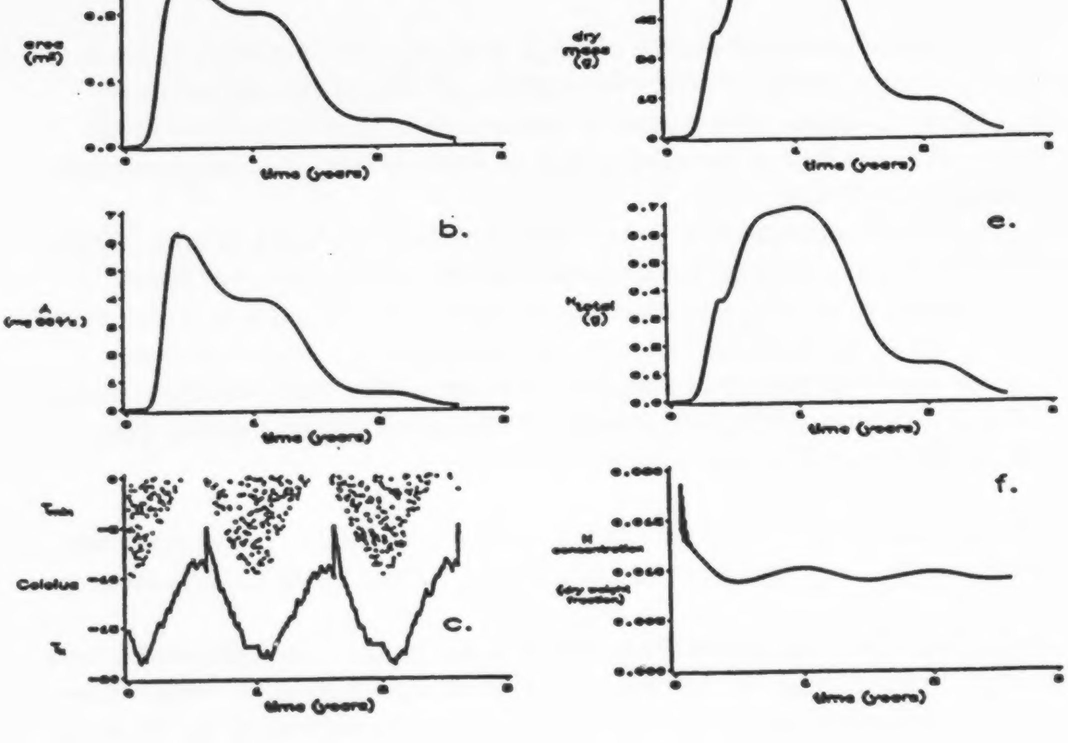

Figure 5-6. Simulated change throughout the needle cohort life span (years) with respect to: a) surface area, m_2 of live needle tissue; b) photosynthetic potential, mg CO_2 fixed/s; c) semi-random frost occurrences (T_{min}, ° C) and resulting changes in frost hardiness, indicated as killing temperature (T_k, ° C); d) dry mass (g) of live needle tissue; e) total N, (g); and f) total N, represented as a fraction of dry weight of the living needle tissue.

5.3.1.2 Addition of Accelerated Senescence. The chronic effects of ozone exposure are simulated by a cumulative reduction in life span for every day of exposure. Figure 5-7 shows the impact of daily reductions in life span of 0%, 0.25%, 0.5% and 1% per day, plotted over thermal time. These life span reduction values produce simulated senescence patterns that correspond with field observations of early needle senescence on ponderosa pine growing in the southern Sierra Nevada (Miller et al., 1982). The precise ozone exposure history of these particular trees is unavailable, so the relationship between particular ambient ozone concentrations and resultant percentage reductions is unclear.

Senescence rates increase as a result of an acceleration of maturation of all needle tissue in the cohort. The tissue does not simply die sooner. Photosynthetic capacity is tied to tissue maturity and, since the stressed needles age faster, their net productivity declines earlier than that of unstressed needles. Cumulative photosynthetic productivity (Figure 5-8) is therefore reduced significantly. This photosynthetic reduction is due to the increased senescence rate alone, without inclusion of the immediate pollution-induced effects transiently reducing net photosynthesis.

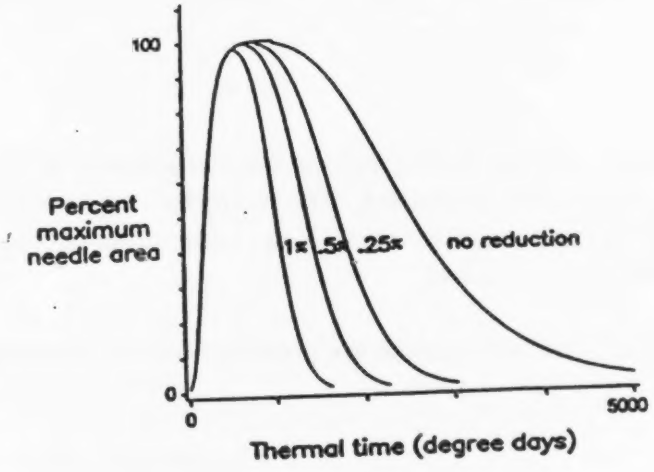

Figure 5-7. Expansion and senescence of one needle cohort, with life-span reduced by 0%, 0.25%, 0.5%, and 1% per day.

5.3.1.2 Addition of Accelerated Senescence. The chronic effects of ozone exposure are simulated by a cumulative reduction in life span for every day of exposure. Figure 5-7 shows the impact of daily reductions in life span of 0%, 0.25%, 0.5% and 1% per day, plotted over thermal time. These life span reduction values produce simulated senescence patterns that correspond with field observations of early needle senescence on ponderosa pine growing in the southern Sierra Nevada (Miller et al., 1982). The precise ozone exposure history of these particular trees is unavailable, so the relationship between particular ambient ozone concentrations and resultant percentage reductions is unclear.

Senescence rates increase as a result of an acceleration of maturation of all needle tissue in the cohort. The tissue does not simply die sooner. Photosynthetic capacity is tied to tissue maturity and, since the stressed needles age faster, their net productivity declines earlier than that of unstressed needles. Cumulative photosynthetic productivity (Figure 5-8) is therefore reduced significantly. This photosynthetic reduction is due to the increased senescence rate alone, without inclusion of the immediate pollution-induced effects transiently reducing net photosynthesis.

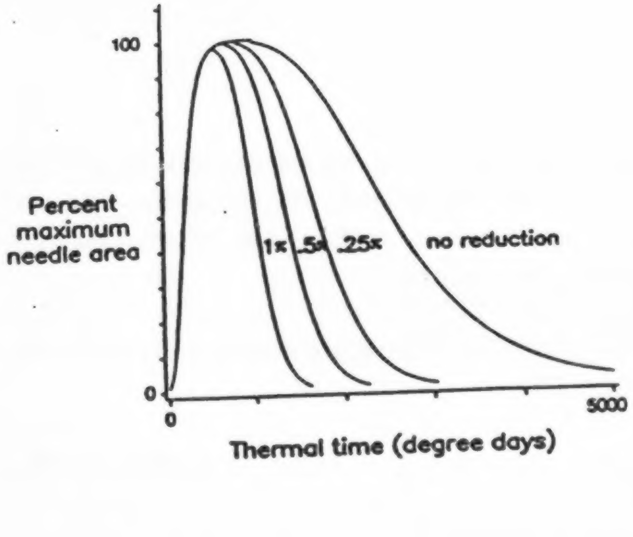

Figure 5-7. Expansion and senescence of one needle cohort, with life-span reduced by 0%, 0.25%, 0.5%, and 1% per day.

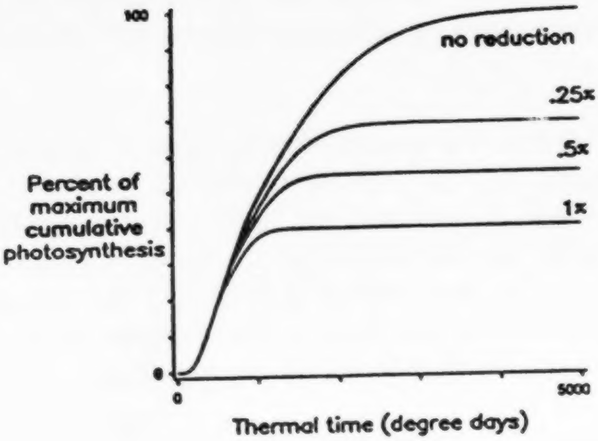

Figure 5-8. Percent of expected cumulative photosynthesis, associated with life span reductions in Figure 5-7.

5.3.2 Loblolly Pine

Sensitivity analysis provides insight into the internal characteristics of the simulation system as it has been constructed. The sensitivity of the system to changes in parameter values was tested (sensitivity analysis), and information concerning the error structure of the simulator was obtained.

The results of the sensitivity analysis are presented for the following growth constants:

1) life span	5500 degree-days
2) multiplication factor (mult)	1.7
3) carboxylation efficiency (k_c)	0.03 μmol/m/s/μbar

and the pollution-effect factor:

4) reduction factor - 0.01

Default values of the parameters tested are indicated beside the parameter name. Loblolly pine produces multiple flushes of foliage within a single year. Calibration parameters have been chosen to reflect behavior of a cohort appearing in the first flush.

5.3.2.1 Life Span. The life span value in the loblolly pine version of the foliar model has been defined as 5500 degree-days. This is the amount of thermal time expected to elapse between the beginning of tissue expansion and the appearance of the first senescence (typically seen as the browning of needle tips). The life span value was varied from 2000 to 6000 degree-days by increments of 1000 degree-days.

The attainment of the maximum foliar area of 0.25 m^2 is unaffected (Figures 5-9 and 5-10) as long as life span values remain greater than the time marking the end of the expansion period. The life span value of 2000 degree-days is short enough to allow senescence to begin before the attainment of the maximum foliar area. The amount of growth occurring is unaffected, but the amount of live tissue area is reduced due to senescence. Not only is the time of complete senescence of the foliar cohort delayed with extended life span, but the slope of the decline in leaf area changes.

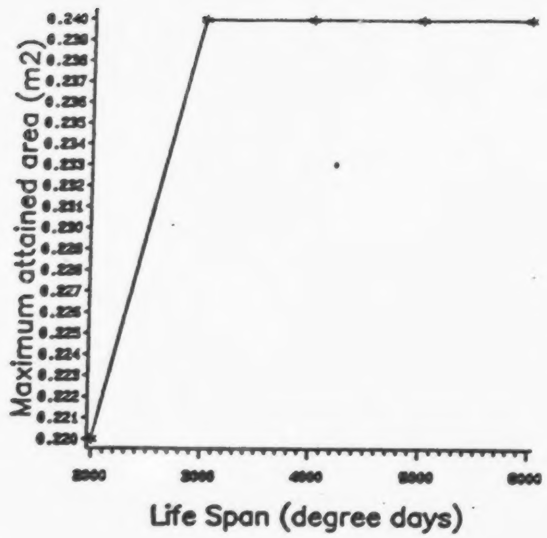

Figure 5-9. Maximum attained foliage area associated with life span values ranging from 2000 to 6000 degree-days.

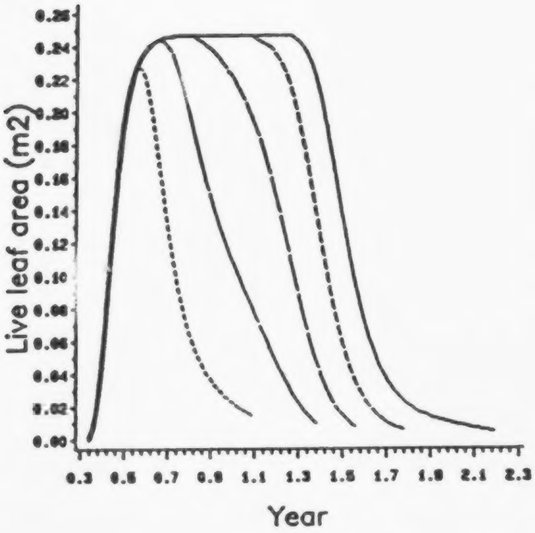

Figure 5-10. Live foliage area over time (years), with life-span values of 2000, 3000, 4000, 5000 and 6000 degree-days (reading from left to right).

In loblolly pine, dry mass per unit area (tissue density) follows a symmetric parabolic pattern, increasing steadily in the early stages of leaf life, then decreasing again with the onset of senescence: a general scheme of construction prior to the period of maximum tissue productivity, followed by rigorous disassembly before tissue death. Because of the symmetric rise and fall in tissue density over age, the curves of mass over time match the live leaf area plots. This result contrasts with the behavior of ponderosa pine, for which tissue density increases steadily with advancing maturity without the decline associated with structural disassembly. More biomass remains in the senescent ponderosa pine needles, so that plots of dry mass in ponderosa pine are offset to the right from the corresponding live area curves.

Cumulative net photosynthesis (Figure 5-11) increases with life span in a nearly linear manner. With increasing life span, cumulative photosynthesis drops increasingly below a linear reduction. The proportion of older, or less productive, tissue increases with an increase in life span.

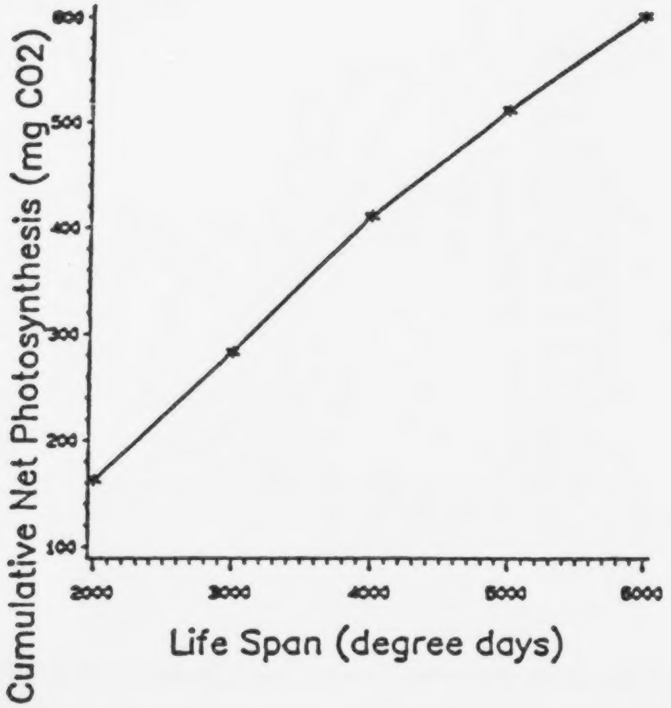

Figure 5-11. Cumulative net photosynthesis associated with life span values ranging from 2000 to 6000 degree-days.

5.3.2.2 Multiplication Factor (Mult). The value of mult describes the life span relationship of the most durable tissue to that of the most ephemeral. Loblolly pine has a defined mult value of 1.7, ponderosa pine a value of 5.0. Figure 5-12 illustrates the effects of mult values ranging from 1 to 5 on live foliage leaf area. Extension of the life of the cohort beyond two years makes the seasonal effects on leaf area more visible. Senescence is driven by the accumulation of thermal time (degree-days), accelerating in the summer months and slowing in the winter. The seasonal change in thermal time accumulation is responsible for the oscillation of the lines on the right-hand side of the leaf area curves. A mult value of 1 means that the life spans of the most durable and most ephemeral tissues are the same. Therefore, mult = 1 indicates that the right half of the live leaf area curve is similar to the left, yet inverted. Increasing mult values decrease the slope of the senescence curve. Increased mult values cause the tissues to age more slowly and increase the duration of the productive period of older tissues.

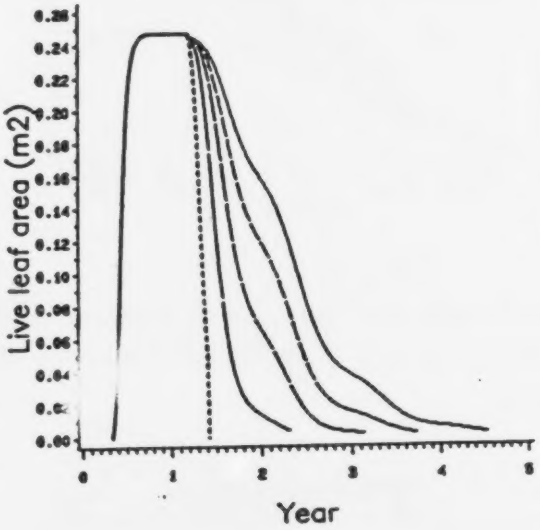

Figure 5-12. Live foliage area over time for mult values 1, 2, 3, 4 and 5 (reading from left to right).

5.3.2.3 Carboxylation Efficiency (k_c). Carboxylation efficiency, k_c, establishes the level of productivity of the foliage present. Cumulative photosynthesis increases linearly with increased k_c. There is no effect from k_c on maximum area, on senescence patterns, or on dry matter accumulation. Expected effects of changes in k_c arise through altered C allocation patterns, which are determined at a level of biological organization beyond the level of individual needle groups and are simulated in the branch/foliage model.

5.3.2.4 Reduction Factor. Unpublished data illustrating the effects of ozone exposure on foliar life span in loblolly pine seedlings are illustrated in Figures 5-13 and 5-14 (Duke Forest Project: Allen et al., personal communication).

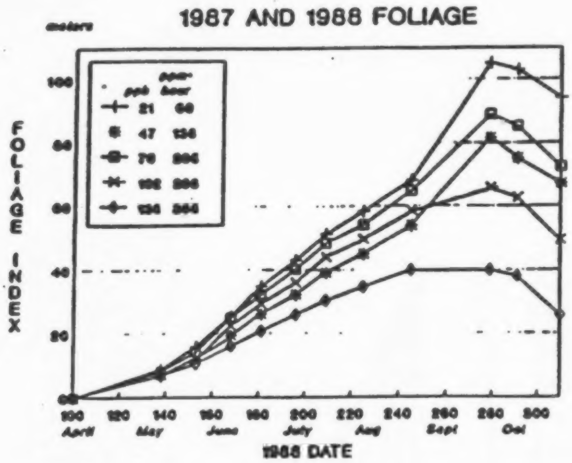

Figure 5-13. Changing total foliage index over time, in seedlings exposed to ozone concentrations ranging from 60 to 396 ppb (data from Allen et al., personal communication).

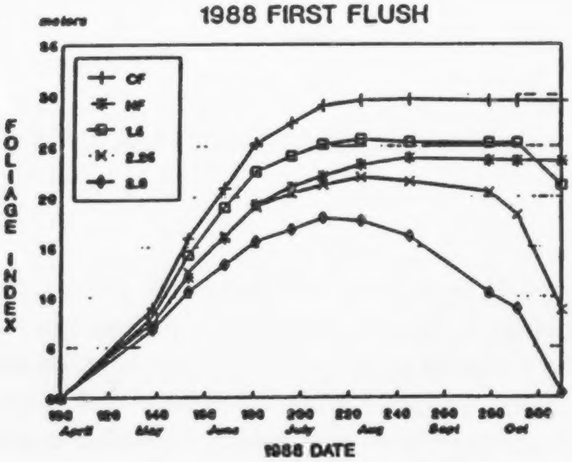

Figure 5-14. Changing foliage index in a single flush over time, in seedlings exposed to ozone concentrations ranging from 60 to 396 ppb (unpublished data from Allen et al.).

Figure 5-13 shows the impacts of exposure on all foliage produced over 1987 and 1988, and Figure 5-14 shows greater detail in the first flush to appear in 1988. These observations have been used as a general guideline to indicate the magnitude of the senescence response.

The daily fractional reduction of life-span due to the presence of ozone is computed using the following exponential saturation function:

$$\textit{fraction-loss} = 0.01\ (1.0 - e^{\mathrm{reduction\_factor[ozone]}})$$

The exponent of the equation, reduction_factor, ranges from -0.015 to -0.005. The default value in the loblolly pine simulation is -0.01. As the values of the reduction_factor become more negative, they increase the severity of the effect of increasing ozone concentrations. The effects of changing the reduction_factor value are tested with daily ozone concentrations of 100 ppb. With the most negative reduction_factor of -0.015, and a simulated ozone exposure of 100 ppb, senescence begins while the foliage is still expanding (Figure 5-15).

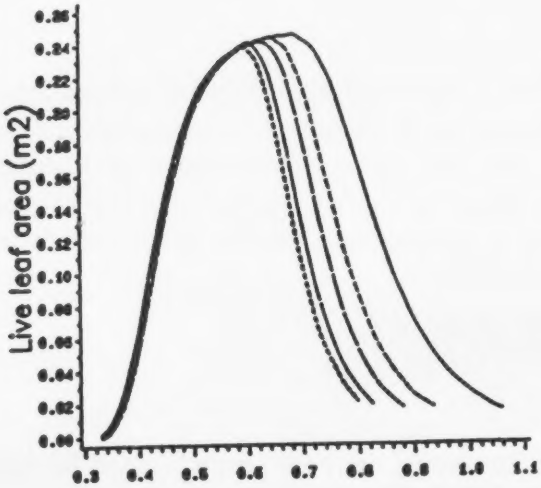

Figure 5-15. Live foliage area over time, with reduction_factor values of -0.015, -0.0125, -0.01, -0.00725, and -0.005 (reading from left to right).

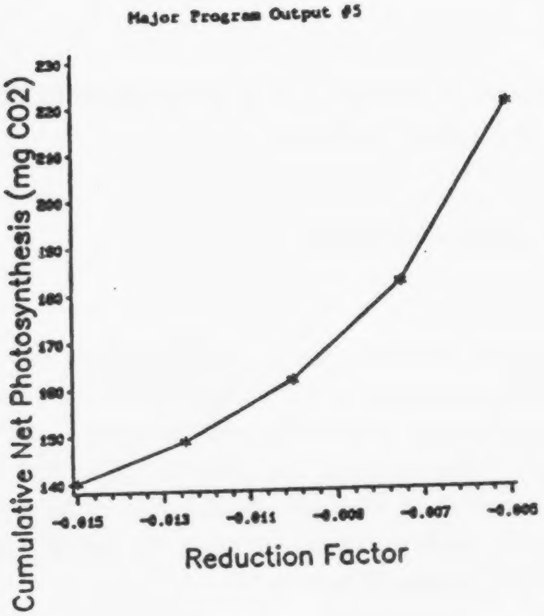

Figure 5-16. Cumulative net photosynthesis over time, as affected by reduction_factor values ranging from -0.015 to -0.005.

Cumulative net photosynthesis (Figure 5-16) declines exponentially with more negative values. The influence of the reduction_factor on live leaf area is shown in Figure 5-15. The effect of increasingly negative values of the reduction_factor is the same as the effect of increasing the ozone concentrations. Adjustment of the value of the reduction_factor is thus a calibration method for the sensitivity of the species to ozone damage.

5.4 APPLICATION

As indicated above, the model has been parameterized for ponderosa and loblolly pine, and, to a limited extent, for red spruce. Some parameters have been adapted from other species when not available for the species of concern. Calibration of the model for the various species entails specification of the following:

(1) cumulative thermal time (degree-days) at which expansion begins and ends,

(2) expected maximum needle surface area after expansion,

(3) expected life span of the most ephemeral needle tissue,

(4) value of the multiplication factor (mult) defining the difference in life span between most durable and most ephemeral needle tissues:

$$life\_span_{durable} = mult \times life\_span_{ephemeral}$$

5) maximum carboxylation efficiency of the needle tissue (k_c),

6) the relationship between tissue maturity and its dry weight per unit area,

7) the maximum and minimum N concentrations (fraction dry weight) of the needles, and

8 value of the reduction_factor indicating the effect of ozone exposure on life span reduction.

5.4.1 Loblolly Pine

The site description used in the loblolly pine simulations corresponds to the Savannah River Plant, in the upper coastal plain of South Carolina (Birk and Matson, 1986).

Total dry mass of the needle tissue is computed based on age and area. The change in specific dry mass (g/m^2) is approximated with a simple parabola, using data from Johnson (1984) and Allen et al. (personal communication). Dry mass ranges from a minimum of 190 g/m^2 on emergence (age 0) to a maximum of 300 g/m^2 at normalized age 0.5, dropping again to the minimum at senescence (age 1).

5.4.1.1 Ozone concentration. Sasek and Richardson (1989) reported that chronic exposure of loblolly pine to low levels of ozone resulted in cumulative, exposure-dependent damage and photosynthetic inhibition. They also pointed out that different aged needle flushes may vary as much as 80% in exposure response because of differences in cumulative ozone doses.

In the foliar model this cumulative damage is simulated by a cumulative reduction of the expected life span. For each day on which the foliage is exposed to ozone, the current life span is reduced by a fraction, depending on ozone concentration. The reduction in life span ranges from 0% (at 0 ppb ozone) to an upper limit of 1% per day. The influence of ozone concentration is tested by fixing ozone concentration at constant values (0 to 350 ppb) for every day of the cohort life. The dynamics of seasonal ozone fluctuations are not included.

In the loblolly version of the model, maximum foliar area (Figure 5-17) is affected at levels above 100 ppb, since these higher levels result in the onset of senescence before the end of the expansion period. Slopes of the senescence curves (Figure 5-18) become more acute with increased ozone levels, as older tissues mature at progressively higher rates. The differences in impact between lower ozone concentrations are greater than those at higher concentrations. Cumulative net photosynthesis (Figure 5-19) decreases rapidly with increasing ozone concentrations, due to the fact that an acceleration of senescence results in more rapid declines in photosynthetic capacity.

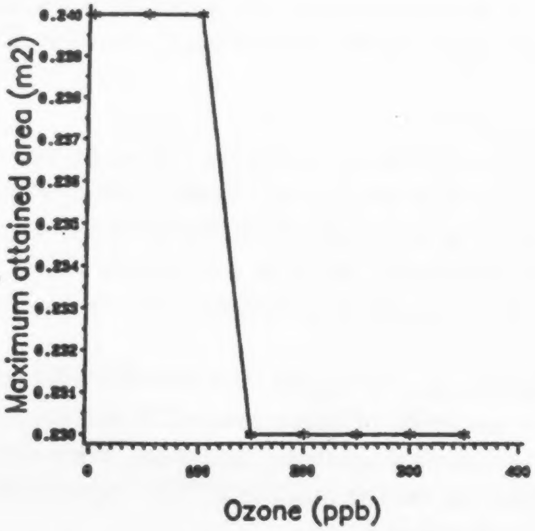

Figure 5-17. Maximum attained foliage area over simulated ozone concentrations ranging from 0 to 200 ppb.

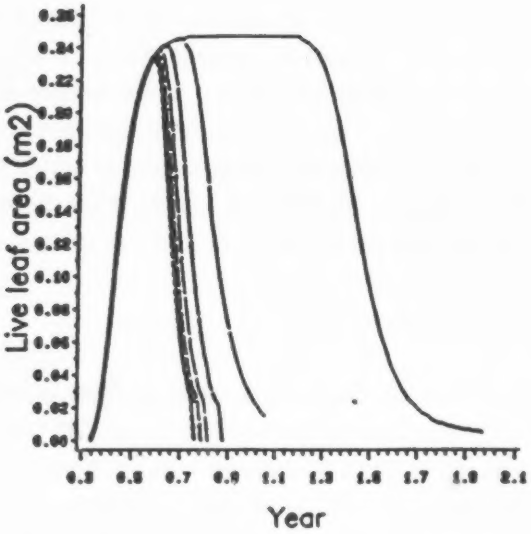

Figure 5-18. Live foliage area over time, with simulated ozone concentrations ranging from 0 to 200 ppb.

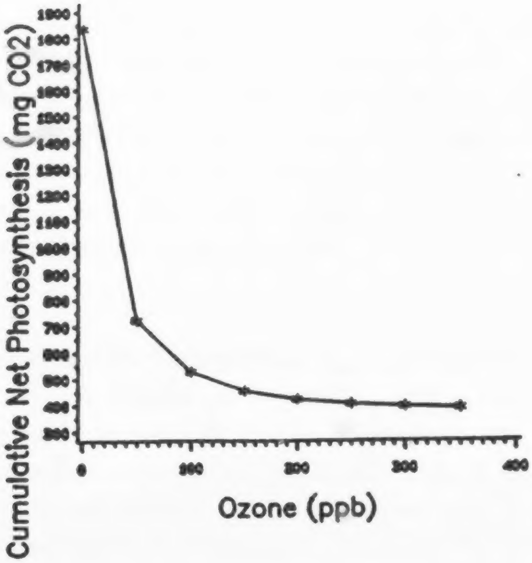

Figure 5-19. Cumulative net photosynthesis over time, with simulated ozone concentrations ranging from 0 to 200 ppb.

5.4.2 Red Spruce

The main difference between the red spruce model and those for the other two species is the importance of the frost-hardening computations. Performance of the red spruce version can be evaluated by sensitivity analysis of the effects of increased life span and decreased carboxylation efficiency. The autumn frost hardening calculations are from Cannell et al. (1985). Assuming that the temperature at which frost kill occurs, T_k, is initially declared to be -5° on August 15, the value of T_k is increased or decreased each day as a linear function of the difference between T_k and the minimum air temperature:

$$\Delta T_k = A + B\,(T_{min} - T_k)$$

Rapid hardening in response to short day lengths or frost is included by decreasing the value of A, once a critical short day length, or frost, is received. If the day's minimum temperature is lower than the killing temperature T_k, the shoots will be killed. Spring de-hardening is computed in an analogous manner to the calculation of hardening. Results of the frost hardening calculations are shown in the ponderosa pine section, above.

5.5 CONCLUSIONS AND CRITIQUE

Observed pollution responses in field and controlled-exposure studies are often unclear or inconsistent. Ozone responses tend to be more evident than responses to the influence of acidic deposition, since the magnitude of the experimental ozone responses is great enough to differentiate it from variation inherent in normal systems. Responses to ozone exposure include reductions in photosynthesis rates (Tjoelker et al., 1989; McLaughlin et al., 1982); altered dark respiration rates; and altered C translocation patterns in exposed foliage (Adams et al., 1988). Observations that invariably appear include early foliar senescence (Guderian, 1985) and reduced foliar biomass (Adams et al., 1988).

Sasek and Richardson (1989) have characterized the effects of chronic doses of ozone on photosynthesis in loblolly pine. Their results suggest changes in light-harvesting and biochemical efficiencies, as well as changes in the activity of rubisco and in the regeneration rate of RuBP. Chlorophyll and carotenoid conditions per unit leaf area were also reduced at high ozone treatments in older flushes. Stomatal control did not seem to be affected in loblolly pine. These types of responses are not unique to ozone exposure but are also associated with the natural process of senescence.

The foliar model was developed to provide a systematic way of simulating the seasonal and age-related changes in foliar condition. Through understanding the expected transients, the unexpected nature of these changes of pollutant exposure behaviors can be more readily assessed.

The primary hypothesis tested in the foliar model is that an increase in the rate of maturation is responsible for the majority of the observed pollution responses. If this is so, simulation of increased rates of maturation and senescence, coupled with the associated reductions in synthetic capacity, should mirror the foliar responses to pollutant exposure.

In the process of maturation, cells continually repair and re-synthesize functional elements. As the cells proceed through the senescence process, re-synthesis slows, and the component compounds are instead exported to more vigorous tissues. Disassembly of the chloroplast structures is reflected in a decline in net photosynthesis.

Accelerated senescence patterns have been simulated to correspond with observed mortality rates arising from ozone exposure. The resulting associated reductions in photosynthesis are significant. Further exploration of the parallels between ozone-induced senescence and senescence occurring in the absence of the pollution stresses is necessary.

Regarding the responses to acidic deposition, substances are known to leach into and out of the leaves, at rates for various compounds that are related to the composition and timing of deposited moisture. Information is insufficient concerning the source of the lost (or destination of the gained) materials, the mechanisms and time required for recharge of sources, and the impact of depletion (or enhancement) of these sources on the functions of coupled processes. In addition, more information is necessary about the relationship between leachates and the physiological mechanisms to which they are linked to predict response mechanisms and resultant effects.

SECTION 6. MODEL: BRANCH/FOLIAGE

The rationale for making a model of branch and foliage growth was described in Section 4. Branch structure defines the natural connections between foliage of different age categories. A cost function for foliage production and maintenance is defined by calculating the amount of wood required to produce the branches. Watson and Casper (1984) have described morphogenetic constraints on patterns of C allocation. These can be investigated with a branch model, and possible differences between species can be explored. Perhaps most importantly, branch production by trees is known to be a stochastic process (Cochrane and Ford, 1978) and one that should be directly analyzed (Waller and Steingraeber, 1985). This stochasticity may influence foliage production.

The objective of BRANCH/FOLIAGE was to relate foliage growth, photosynthetic performance, and foliage mortality to wood production. This was achieved in three stages:

Stage I.	A simulator for branch growth and foliage development was constructed that generated branching patterns typical of those found in pine. The growth of new foliage was made from photosynthate produced by the branch, but the amount of foliage growth was limited by the competing requirement of photosynthate to produce the supporting wood for the branch. This was calculated according to mechanical principals specified by McMahon and Kronauer (1976). Photosynthetic production in this simulator was calculated as net production, g material/g/time.
Stage II.	The photosynthesis routine described in Section 5 was incorporated so that photosynthetic production in the branch simulator was calculated as carbon dioxide uptake, mm $CO_2/m^2/h$. This provided the ability to examine one aspect of how environmental change may influence growth. It also required that respiration of branch and foliage be calculated, which appears as a second cost function in the development and growth of the branch.
Stage III.	Simulators were constructed for the particular morphological and phenological patterns of loblolly pine and red spruce. Morphological rules were specified as probabilities based on field measurements, thus introducing a stochastic element into the growth process. For each species a unique feature was required in the

design of a species-specific simulator. For loblolly pine, which can produce multiple shoot flushes in a year, the phenology had to be adapted. Red spruce produces epicormic shoots that develop in response to the loss of the normal main branch that can occur in a severe frost. Epicormic branches arise along the main branch axis at the site of normal branch whorls. However, their growth is delayed until the normal branches at that point are at least 5 years old; thus, substantial damage is required for epicormic branches to grow vigorously. The origin of epicormic shoots is most likely dormant buds (Stone and Stone, 1943; Stone, 1953). A simulator was constructed that mimicked frost damage and recovery.

6.1 DESCRIPTION

A full description of the simulator constructed at Stage I is given in Ford and Ford (in press), with only a mechanistic summary presented here. Branch growth and the export of photosynthate to mainstems are the result of interactions between five processes (Figure 6-1):

1) morphological development,

2) foliage growth,

3) production of net photosynthate,

4) the active period of growth for different meristems; i.e., phenology, and

5) branch wood thickening.

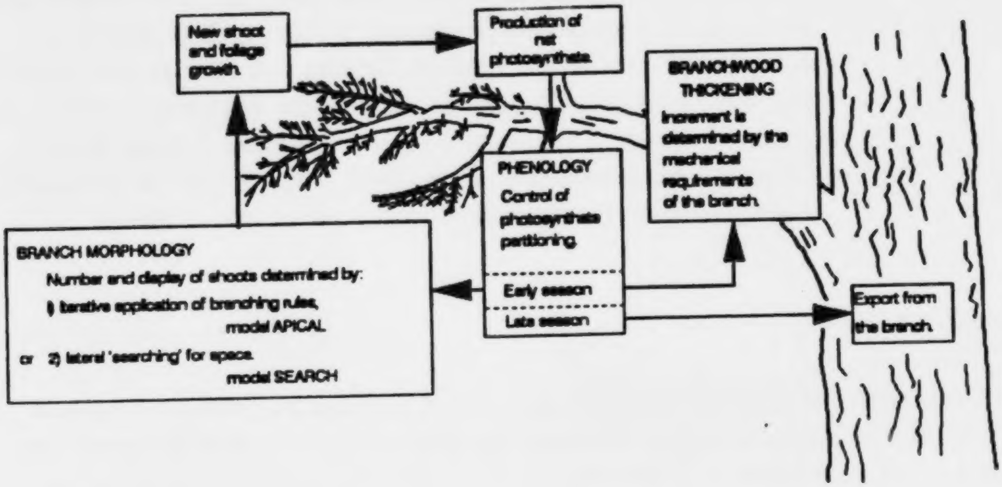
New shoot and foliage growth.
Production of net photosynthate.
BRANCHWOOD THICKENING
Increment is determined by the mechanical requirements of the branch.
PHENOLOGY
Control of photosynthate partitioning.
Early season
Late season
BRANCH MORPHOLOGY
Number and display of shoots determined by:
i) iterative application of branching rules, model APICAL
or 2) lateral 'searching' for space. model SEARCH
Export from the branch.

Figure 6-1. Diagrammatic representation of the sequence of processes in branch growth.

The active period of annual growth is considered to be in two phases. The first phase occurs in spring and early summer when all of the photosynthate produced goes to shoot extension, its associated foliage production, and branch thickening. Branch thickening is calculated as the requirement to maintain the branch in a specified curvilinear posture in the vertical plane (McMahon and Kronauer, 1976). The number of new shoots on the branch, or branchlets, and their angles relative to each other and to their parent branchlet are species-specific and defined by sets of rules in Stage III. In the second phase of growth, when shoot elongation, foliage increment, and branchwood thickening are complete, the photosynthate produced is considered to be exported to the mainstem of the tree. Photosynthate produced at any position on the branch is assumed available for growth, either for thickening or extension and foliage development, at any other position on the branch. A more detailed alternative to this assumption – where the movement of photosynthate within a branch itself may be determined by the balance between sink strength, source activity, and translocation distance – is considered in Section 6.

At Stage II the carbon economy of the branch was modeled in terms of net photosynthesis and respiration. Details of the photosynthesis equation used are given in the previous section. Respiration was calculated in two parts; growth respiration, G_R, and maintenance respiration, M_R after Hunt and Loomis (1979), who argued that respiration should be linked to growth rather than photosynthesis.

$$R = G_R\,(dW/dt) + M_R W$$

Hunt and Loomis (1979) included estimates for G_R and M_R, and subsequently we explore a range of values. Note that there is no temperature dependence for G. The values for G are argued on the basis of interconversions, so they should be applied to both the synthesis of sucrose in the foliage and its subsequent conversion to cell materials in the cambium or the shoot. A similar approach was advanced by Barnes and Hole (1978). Our model does not incorporate the interconversions between soluble and storage carbohydrate, so the more sophisticated approach for calculating respiration advanced by Penning de Vries et al. (1979) is not justified. They showed through experimentation that respiration increased with the reserve carbohydrate content and that growth respiration exponentially decreased in the dark.

Values for respiration were taken from a study of loblolly pine by Kinerson (1975), who published values for both actively growing and dormant stems. Because the dormant value was insensitive to temperature changes compared with the active condition, it was used as the maintenance respiration rate for the branch surface area.

- For foliage we assume that M_R is defined by the dark respiration term, *Rd*, and set to 0.2 mm $CO_2/m^2/s$.

- For branchwood we calculate a surface area at the start of the year and then use an estimate of respiration as measured for bark during the dormant period, but at summer ambient temperature levels, as our estimate of M_R, M_resp_rate = 102 mg $CO_2/m^2/h$, [function maint_resp] (see Kinerson, 1975, Figure 6-4).

- We make a combined estimate of G_R for branchwood and foliage using the variable, G_resp_rate, which we initially set to 0.3 [function growth_resp].

- The export-to-stem material was also subject to both G_R and M_R. M_R will vary according to the surface area of the trunk and roots, and because this depends on the size of the tree, these respiration values can only be calculated if we make a whole tree rather than an individual branch estimate of production. Generally, simulated loblolly pine branches were found to grow for between 5 and 6 years, typical for the stand from which we have obtained the data for the model.

Assuming that the production from successive simulated years represents contributions from branches 1, 2, ... , 6 and that there are four branches per whorl, then production by the whole crown of the tree can be estimated. Kinerson (1975) published regression equations for the mass of roots and the surface area of trunk boles as a function of diameter at breast height (dbh). Branch measurements were made on trees approximately 20 years old, with a dbh of 20 cm. This figure was used to estimate tree mass components.

At this point, estimates of annual respiration for the bole and roots can then be subtracted, assuming that the size of the tree remained constant at 20 cm dbh. M_R is calculated for the trunk using M_resp_rate = 102 mg $CO_2/m^2/h$ and a trunk surface area of 2791 cm^2, and for root respiration using rootm_resp_rate = 0.01 g/g/day (after Hunt and Loomis, 1979) and the root mass of 31781 g. The remainder of the export to trunk is then subject to growth respiration at the rate of G_resp_rate. The final total is an estimate of the biomass increment of the tree external to the foliage and branchwood increment.

Calculations for maintenance respiration were applied at each iteration of the model calculation. Growth respiration was calculated as a proportional deduction from potential growth.

For red spruce, the same procedure was used to calculate the respiration of branches, but not for stems and roots. Our interest and the data (where possible) concern old mature trees, usually older than 120 years. Biomass estimates are not available for these trees. Also, as discussed below, the simulated red spruce branches live for much more variable periods of time than those of loblolly pine, and a mean tree size could not be computed.

At Stage III, field data were used to calculate probability rules for the generation of numbers of new branchlets produced by each growing point, along with their relative lengths, after methods described by Cochrane and Ford (1978). Within the model, the APICAL version for morphological rules was used as described in Ford and Ford (in press). Absolute lengths achieved by the growing branchlets are determined by the photosynthate produced by the whole branch and the numbers of shoots among which the photosynthate must be distributed, the branch thickening, and respiration required. Rules for the production of branchlet numbers and the relative lengths vary by order of branchlet and by the length of the parent shoot segment from which the branchlet is being produced. Estimates of foliage longevity were also obtained by field observations, although subsequent data from pollution exposure experiments were used.

For red spruce a 20-day period of shoot extension was used, which is typical for this species when growing in the mountainous environments where decline has been observed (Vann, personal communication). The extension period of loblolly pine is much more variable and typically extends up to 90 days covering two flushes, or even longer when more flushes are produced. The standard used was two consecutive flushes, 60 and 30 days long, respectively, with a total growing period of 225 days. Over the total extension period of 90 days, shoot extension proceeds at varying rates, typically showing a small resting time between the major extension periods. Accordingly, it was appropriate to investigate the possibility that a proportion of the photosynthate produced during this extended period of time might be exported to the trunk, and simulations of this export were made.

A major addition to the model was required to simulate the production and growth of epicormic branchlets by red spruce. The production of epicormic branchlets is a typical response of pine to injury; e.g., spruce budworm defoliation stimulates their production by balsam fir (Batzer, 1973), they are produced by white fir in response to pruning (Cosens, 1952) and by Douglas-fir in response to needle blight infection (Lanner and Bryan, 1981). The precise position at which epicormic branchlets are produced varies according to the species. In montane Douglas-fir, extensive epicormic branching along the main stem of the tree has been observed, with substantial variation between individuals (Bryan and Lanner, 1981).

Observations were made of the incidence and development of epicormic branchlets, relative to the normal branching pattern, of red spruce on Whiteface Mountain, NY. These observations compared undamaged branches with cases where there was apparent damage and regrowth. In the undamaged situation, branching pattern followed that of a typical spruce type (Figure 6-2) except that order-2 branchlets tended to continue to grow for only five or six years (although foliage retention was typically between 6 and 12 years). This results in a considerable mass of foliage supported on branchlets that subtend no actively growing apices. At whorl positions 5 or 6 years back from the order-1 apex, one, two or occasionally three epicormic buds appeared on the upper surface of the order-1 branch immediately next to the point of connection of the two order-2 branches. On undamaged trees these epicormic branchlets tended to produce substantial (>1.0 cm) extension increments, only after the neighboring order-2 branchlets that were normally produced ceased to have active shoot extension.

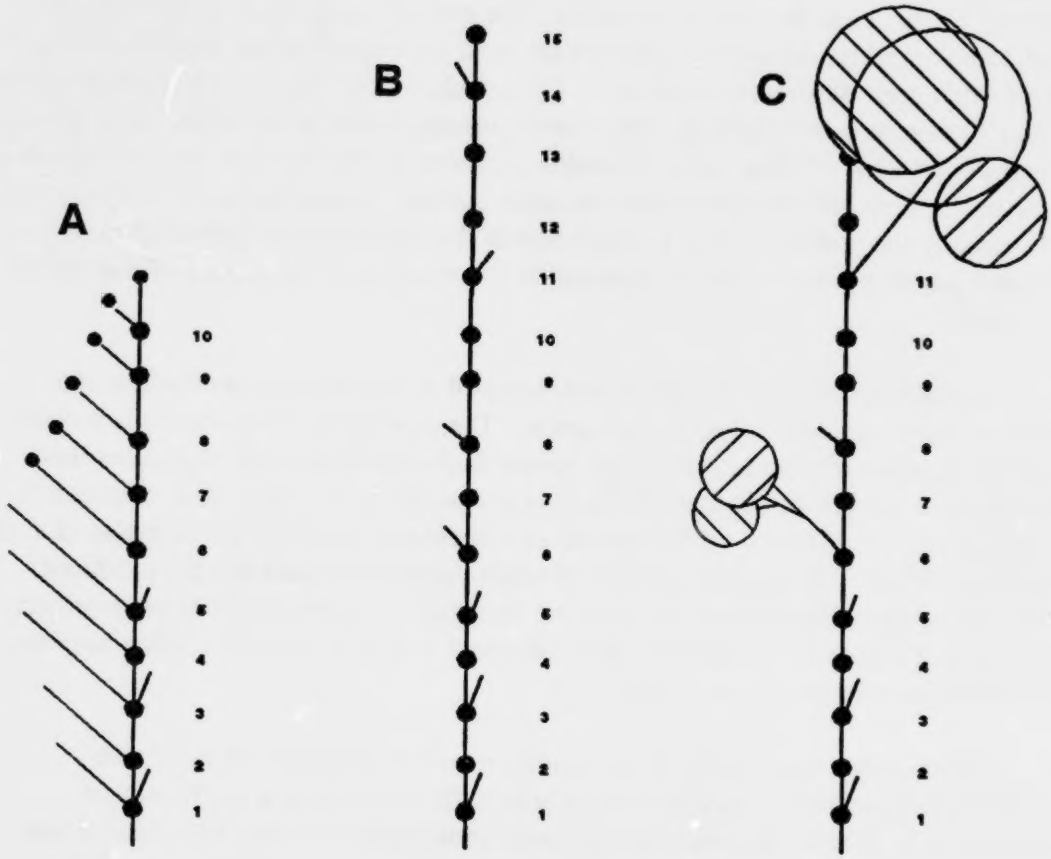

Figure 6-2. Diagram of the origin of epicormic branchlets along the main axis of red spruce branches and the generation of "foliage islands" as a branch grows. Diagram A represents the branch after 10 years of growth; order-2 branchlets formed between years 6 and 10 still have active apical buds, and epicormics only grow at the base of older branchlets. Diagram B shows a sequence of epicormic branch origins (original branches not shown). Diagram C represents epicormic branch growth and shows how successive generations of new epicormic branches are produced and how "islands" of foliage develop.

On damaged trees it was apparent that epicormic branchlets were produced, or tended to survive, when normal order-2 branchlets did not. On branches that had clearly been damaged, the branchlets of order-2 having origins as epicormics were distinctive in that they were above the plane of the order-1 branch axis. This is very different from normal order-2 branching which remains in the plane of the main axis or droops gracefully below it. Also, epicormic branches generally had a more acute angle relative to the main order-1 axis. Besides these distinctive traits, sucessive generations of epicormic branches were observed growing in a "stacked" fashion. It is this phenomenon that leads to typical clumps, or islands of foliage, situated above the original order-1 main branch axis and frequently quite close to it in the horizontal plane (Figure 6-2). At most, there were four generations of stacked epicormic branchlets observed and, assuming that a growing axis must be six years old before it produces epicormics, a minimum estimated age for such a foliage clump is 24 years. Once epicormics start growing as normal branches; i.e., with a dominanant leading bud, they generate buds and have the same relative lengths of shoot by orders of branching as are found on normal undamaged branches.

Two features were introduced to the branch model to simulate this process of epicormic growth and development. First, as a feature of the "normal" branching rules developed for red spruce, a probability function was developed for the initiation and growth of epicormic branchlets based on the collected field data. This produced zero, one, or two epicormics on the main branch axis at junction positions between order-2 branchlets and the main stem -- once the order-2 branchlet had lost its terminal bud either due to the normal rules of suppression found in red spruce branchlets or, as will be discussed later, due to frost damage. Epicormic branchlets grew according to weighting functions in the same way that "normally" produced branchlets grow, producing small annual extensions.

The second feature introduced into the branch model are periods of major damage simulated by the loss of the leader of the main branch; that is, the order-1 bud dies, and an apical control is then established for each epicormic. At this point the parent has living foliage that continues to exist until its normal mortality point, but no new shoots are produced on the parent branching system. A proportion of the photosynthate produced by the order-2 branchlets at the junction of the parent shoot where an epicormic has established control is allocated to the growth of that epicormic. This proportion was determined by calibrating the model production of epicormic shoot lengths against field data. The remainder of the photosynthate from the old parent branchlet foliage is allocated to cambial growth and respiration of the wood of the parent branch. The weight supported by the parent branch is greatly reduced, and, according to calculations using the McMahon and Kronauer (1976) equations no wood increment would be required. However, small rings do continue to form on such branch sections, and an arbitrary increment of 0.1 mm is added.

Each of the epicormics proceed to grow as if they were parent branches and produce both "normal" and epicormic branchlets. At the next major frost, they lose their own terminal apex, and control is transferred to any epicormics they may have. Currently, this procedure is implemented in a synchronous way, with epicormics across the whole branch transferring control to the new generation at the same time. Therefore, the repeat of a major frosting at less than a five-year interval will cause branch death because no new epicormics will have been formed to take control. Photosynthate produced by all the epicormics is summed, the photosynthate required for parent branch thickening, growth, and maintenance respiration is subtracted, and the remainder of the photosynthate is considered to be export to trunk.

The model distinguishes between two types of frost damage: removal of high-order branchlets (see photographs in Evans, 1986) and the removal of order-1 apices. These are treated as endemic damage at a low annual frequency and major damage that occurs at a lower frequency, respectively.

6.2 ANALYSIS

6.2.1 General

Extensive simulations were made with the models developed at Stage 1, with the results reported in Ford et al. (in press). The principal findings are that morphology influences tree response; morphological variation is a source of variation that defines one aspect of the stochastic process.

The model simulates branch growth as a balance between positive and negative feedbacks. In the early years of branch growth, foliage development is rapid and more photosynthate is available to produce foliage than in later years. As the branch elongates and foliage develops further from the tree, more branchwood is required to support the growing foliage. The photosynthate exported from the branch to the trunk increases as foliage increases, but then decreases as the demand for supporting branchwood increases.

Simulations show how the set point between the two feedback systems can be specified by phenology and morphology. For the export of photosynthate, an optimum period for branchlet growth can be defined when there is a balance between the amount of photosynthate invested in foliage production and the return of photosynthate obtained from the foliage to the trunk.

Branchlet production was simulated as nonstationary over the branch lifetime. Two morphological systems for this were examined: APICAL, which specifies branchlet proliferation according to length and order of parent branchlets and which was adapted for both the loblolly pine and red spruce models; and SEARCH, which simulates inhibition of branchlet production according to local crowding and competition for light. The SEARCH algorithm also includes interaction with branchlet phenology, which has a substantial effect on the timing and amount of photosynthate exported to the trunk.

Analyses of Stage II and Stage III of the model were jointly and independently conducted for the two species simulated.

6.2.2 Loblolly Pine

The parameters used in the model are listed in Table 6-1. The photosynthesis data, obtained from P. Dougherty and R. Teskey, University of Georgia, were provided as typical values of A_{max} for mature foliage obtained on an FRP project. The data were translated into a value for k_c, the limiting parameter of the quadratic equation used to simulate photosynthetic rate. Estimates of respiration rate were calculated as previously described.

Table 6-1. Loblolly Pine Branch Model Input Data

Photosynthesis Constants:		*McMahon and Kronauer Constants:*	
Mass of needles(g/cm):	0.700000	alpha:	1.500000
Init photo rate- sun:	0.000	beta:	1.500000
Init photo rate (g/g/da):	0.000	kd:	0.001500
Photosynthetic decay:	0.000977	kh:	0.001500
Foliage mortality start:	2	Branchwood density (g/cm^3):	0.45
Foliage mortality end:	2	Young's modulus (Pa):	20,000,000
		Diameter at tip (cm):	0.20
Morphology Constants:		*Phenology Constants:*	
Angle to trunk (rad):	0.00		
Whorl branch angle (rad):	1.00	Start day of growing season:	50
Epicormic angle (rad):	0.50		
Weighting of order-2 :	0.70	Days in growing season:	225.0
Weighting of order-3 :	0.40		
Weighting of order-4 :	0.40	Number of flushes:	2

An annual weather pattern from Dougherty and Teskey was used to calculate hourly photosynthesis. This photosynthesis was summed over five-day periods to calculate branchlet extension, foliage growth, branch wood production, and respiration by branch materials.

The most startling result was that, without adjusting the parameters, the model produced branches that survived for 5, 6, or 7 years (Figure 6-3), which is the typical age of branches in the forest. During this time, the branches produced 10 or 12 shoot extension increments. The spatial pattern of branching was very similar to that of measured branches (Figure 6-4).

As previously described, the production of new branchlets from a parent branchlet is determined by the length and order of the parent and is subject to a probability distribution based on field data. Branchlet production is reflected not only in the spatial variation in the pattern of growth but in other outputs, including the estimated total export to trunk. After 72 runs, using a different random number seed for each run, there was a five-fold difference in export to trunk (Figure 6-5).

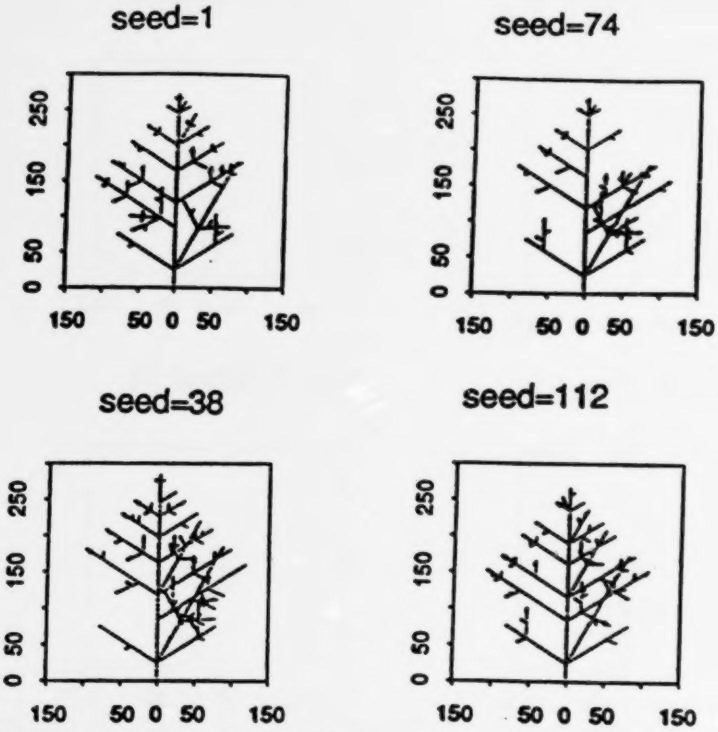

Figure 6-3. Four simulated loblolly pine branches showing differences in morphology that result in differences in growth and export to the stem. Solid lines support foliage.

Kinerson (1975) estimated the net primary production of a 13-yr-old stand of loblolly pine, with mean dbh of 16.75 cm, to be 1463 g C/m^2/yr. The plot had a stand density 1445 trees per hectare, equivalent to almost 7 trees per square meter. On the basis of this calculation, the net production per tree was 10241 g C. This value is slightly greater than the minumum estimated from the simulation runs (Figure 6-5) in which the model was parameterized on the basis of 20-cm dbh trees.

The 72 simulations (Figure 6-5) were divided according to branch survival (5, 6, or 7 years); the maximum, mean, and minimum foliage amount held at each age was examined (Figure 6-6). The difference in the pattern of mean foliage amount between branches that lived five and six years was small relative to the differences of foliage amount held by branches in the sixth or seventh years. As the branches age they are unable to support as much foliage. These differences are almost certainly related to the early production of lateral branches; the lateral branches produced in the first whorls require less support material and a smaller surface area than those produced in later whorls.

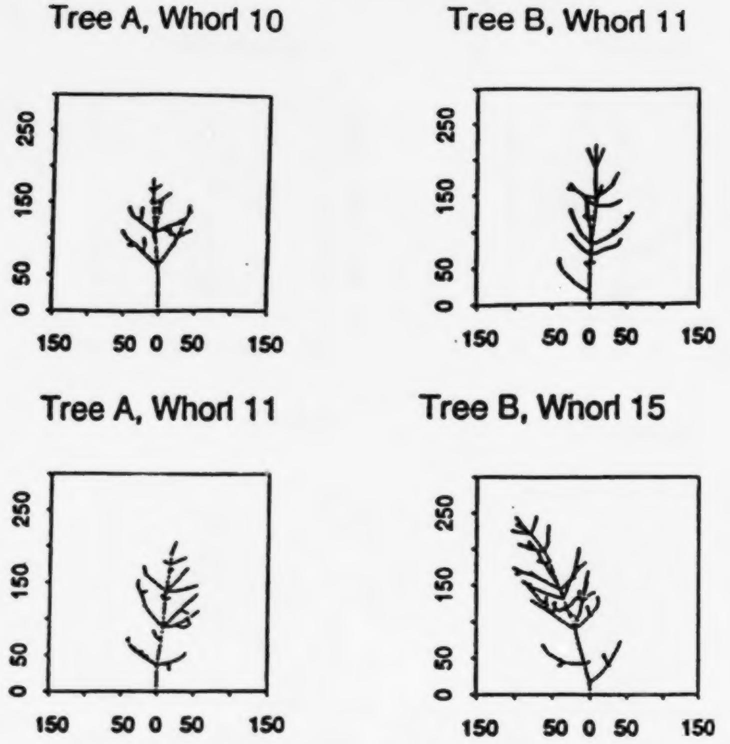
Tree A, Whorl 10
Tree B, Whorl 11
Tree A, Whorl 11
Tree B, Whorl 15
0
50
150
250
150
50
0
50
150

Figure 6-4. Actual branch dimensions from loblolly pine branches taken from two whorls on two trees.

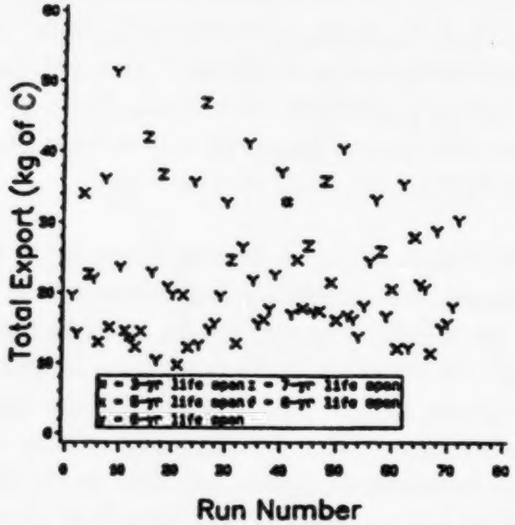

Figure 6-5. Total export to the trunk by run number for seventy-two random seeds that produced branch life spans of three, five, six, seven, and eight years.

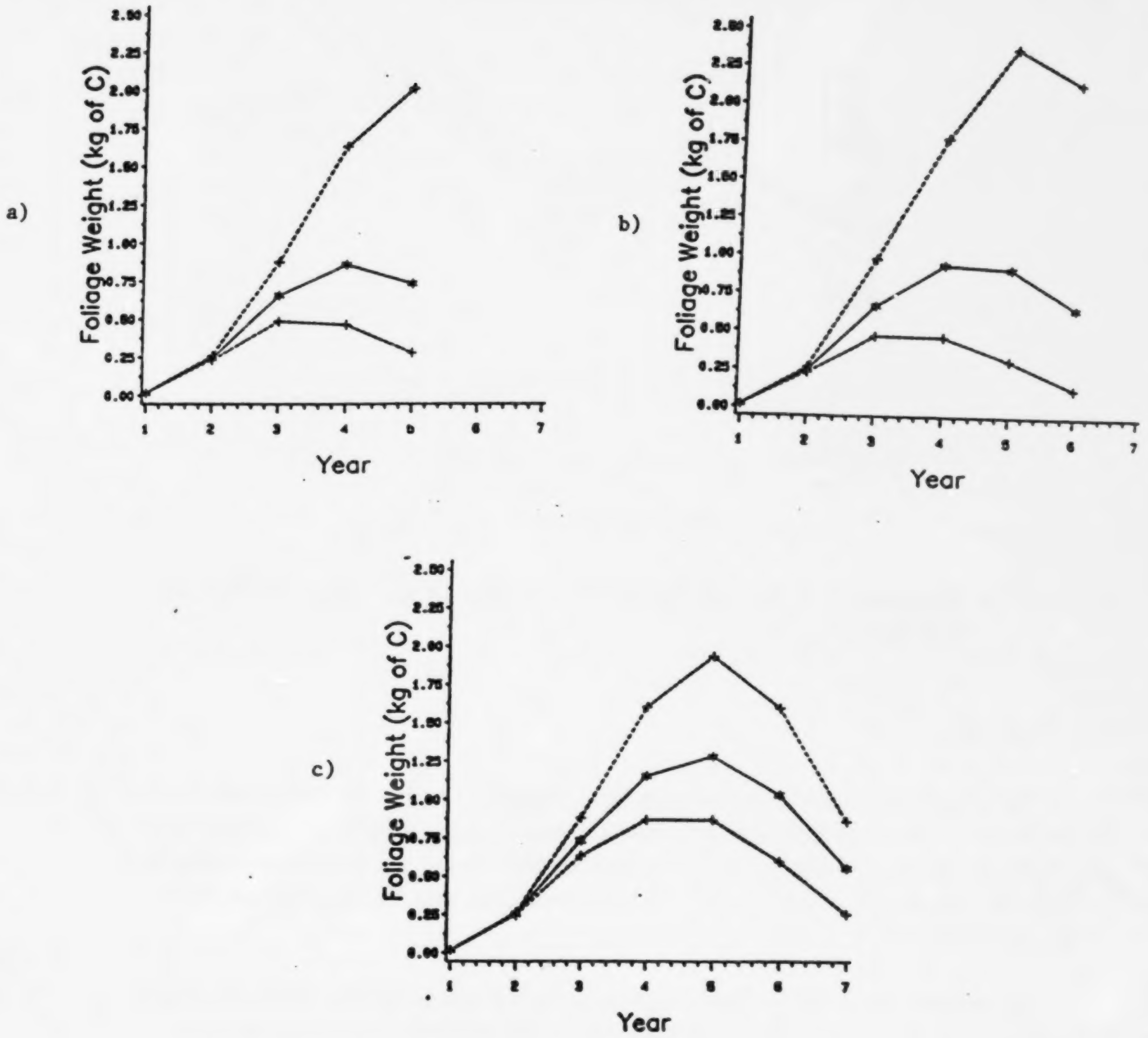

Figure 6-6. Average, minimum foliage weight for (a) 20 random number seeds that produced 5-year-old branches; (b) 42 random number seeds that produced six-year-old branches; and (c) eight random number seeds that produced seven-year-old branches.

The most important parameter that had no direct measured value was the porportion of photosynthate that was designated as export to trunk during the 90-day period of shoot extension, percent export. Simulations varying this parameter over the range 0.25 to 0.4 (Figure 6-7) for the same initial random number seed showed a nonlinear response in export to trunk over the range 0.25 to 0.35.

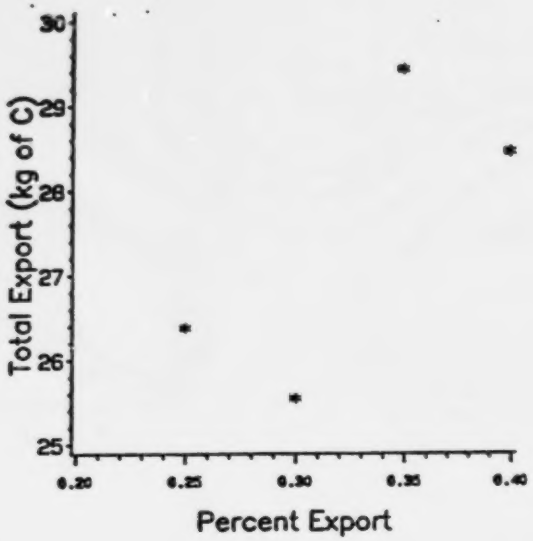

Figure 6-7. Total export to the trunk for selected percent export rates following the first flush.

6.2.3 Red Spruce

The phototsynthesis values used are from Taylor et al. (1986). These values are for seedlings; no data are available for mature canopy foliage. Baseline input data for the model are given in Table 6-2. All branches on the mature red spruce trees observed on Whiteface Mountain had produced epicormic branches, and the original "normal" foliage had been lost.

The model was tested by observing tree growth patterns with no major or minor frost damage (Figure 6-8). Undamaged branches typically lived 27 years, grew to a length of 3.75 m, and produced epicormic branches that grew up to 0.8 m. This result should not be considered as any type of baseline because damage and regrowth are integral parts of the biology and ecology of trees.

Table 6-2. Input Parameters for the Red Spruce Simulation Model

Photosynthesis Constants:		*McMahon and Kronauer Constants:*	
Mass of needles (g/cm):	0.160000		
Kcmax:	0.035	alpha:	1.500000
Dark resp (mm/m^2/s):	0.2	beta:	1.500000
Maint resp (mg/m^2/h):	51.0	kd:	0.001500
Growth resp (g/g):	0.40	kh:	0.001500
Photosynthetic decay:	0.000317		
Foliage mortality start:	6	Branchwood density (g/cm^3):	0.45
Foliage mortality end:	12	Young's modulus (Pa):	40,000,000
Probability of tip damage:	0.05	Diamter at tip (cm):	0.20
Pct sup foliage exported:	0.75		

Morphology Constants:		*Phenology Constants:*	
Angle to trunk (rad):	0.00		
Whorl branch angle (rad):	1.00	Start day of growing season:	165
Epicormic angle (rad):	0.50	Days in growing season:	125
Weighting of order-2:	0.70		
Weighting of order-3:	0.70		
Weighting of order-4:	0.70		
Weighting of order-5:	0.70		
Weighting of order ≥6:	0.70		
Whorl size:	4		

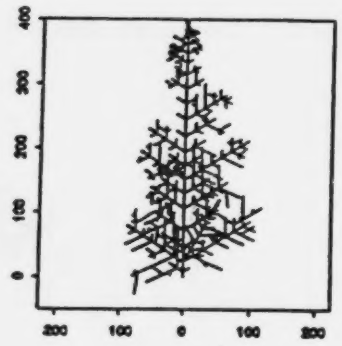

Figure 6-8. Growth pattern with no major or minor frost damage.

Two types of frost damage are considered: a regular removal of tips with a set probability of 0.05, 0.10, or 0.15, and a major frost damage simulation that transfers apical control to epicormic branches. The transfer of apical control to epicormic branches introduces a major source of variation into the pattern of growth. The small difference in probabilities of epicormic production determine survival. This is illustrated by the application of a regular 12-year major frost damage interval applied to simulations with four different random number seeds (Figures 6-9, 6-10, and 6-11).

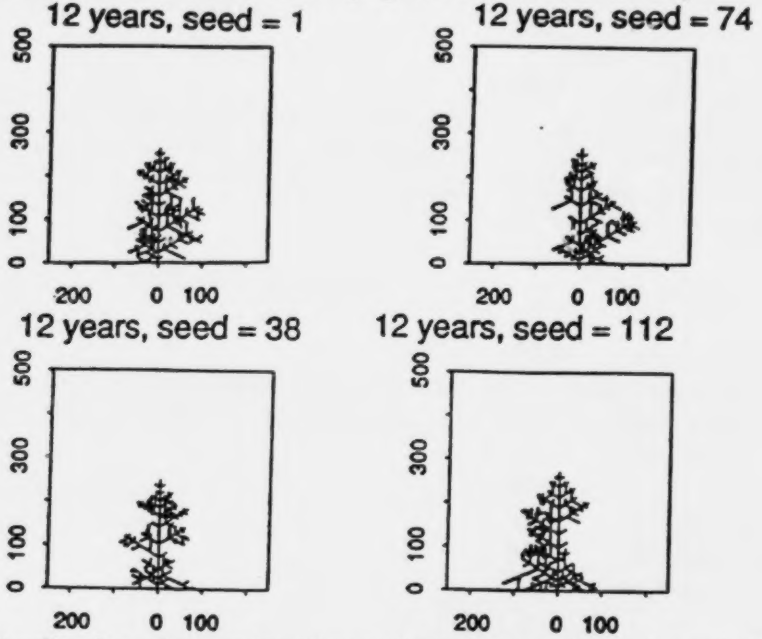

Figure 6-9. Application of a regular 12-year frost damage interval applied to simulations with four different random number seeds.

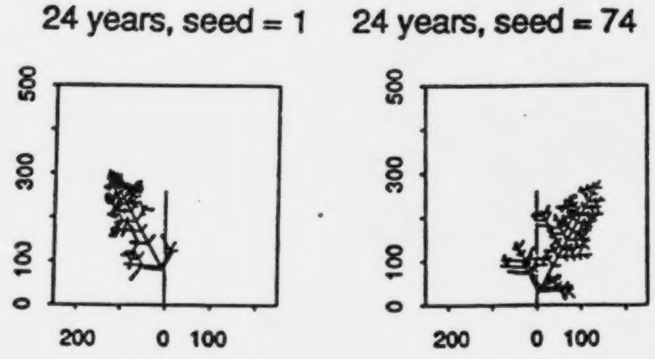

Figure 6-10. Two branches from Figure 6-9, here at year 24, survived a major frost of year 12 through the growth of epicormic branches.

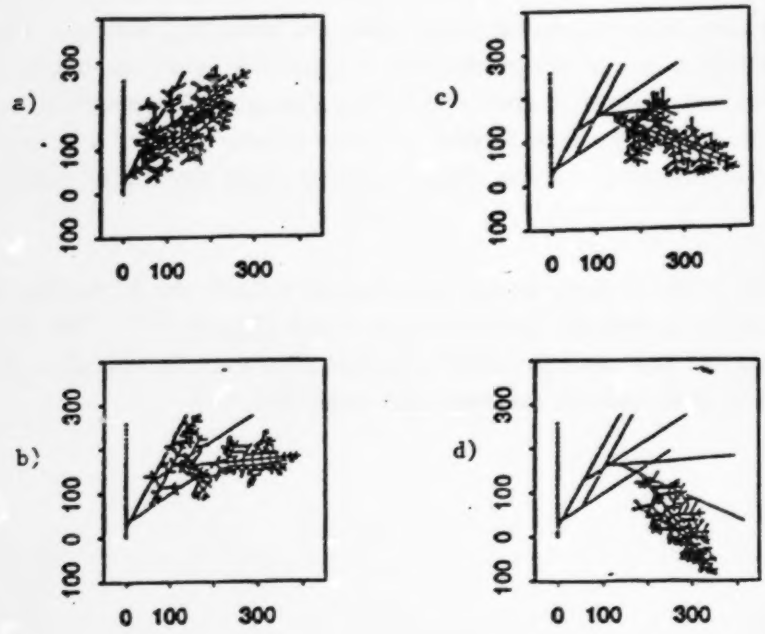

Figure 6-11. Simulation of red spruce branch growth, for random seed number 74, showing its structure prior to major frosting in the winter following years (a) 36, (b) 48, (c) 60, and (d) 72, after which it died.

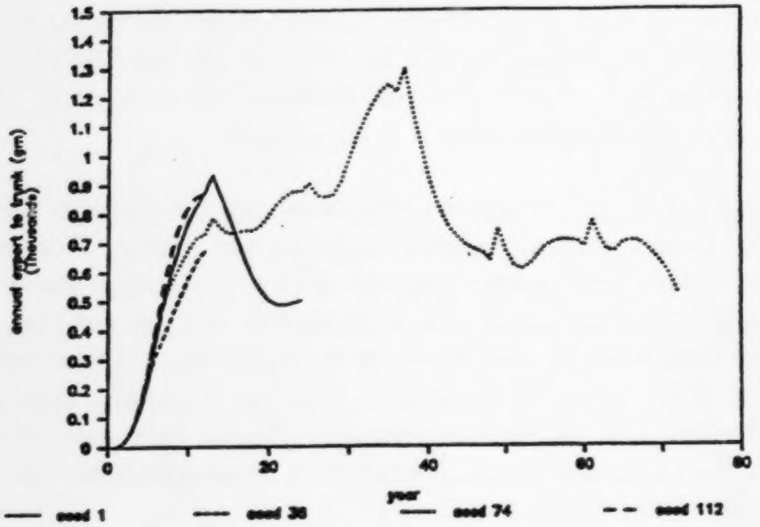

Figure 6-12. Carbohydrate export to trunk for the lifetimes of branches shown in Figures 6-8 through 6-10. Major variations in seed 74 output netted differences in the numbers of active epicormics.

With all other parameters in the model equal, the four simulations produce branches of very similar total length, but rather different branching patterns. Part of this variation in morphology is due to the production of epicormic branches that, in the simulation, are permitted to flourish after major frost damage. Consequently, only two branches survived the first major frost at year 12. One branch survived a second major frost at year 24 and continued to survive regular 12-year major frosts until it died after year 72.

The export to trunk for these simulated branches reflects the fluctuating pattern of foliage amount during a branch's lifetime and at death (Figure 6-12). The branch that survived for 72 years had just one epicormic branchlet after year 12, two after year 24, two after year 36, one after year 48, and two after year 60.

6.3 APPLICATION

6.3.1 Loblolly Pine

6.3.1.1 Photosynthetic rate. Experimental results have clearly shown the effect of ozone on the photosynthetic rate of loblolly pine. The photosynthetic rate, K_c, was varied over a range of 0.01 to 0.05; 0.03 is the calculated value from measured data on forest canopy foliage. The highest photosynthetic rate resulted in greater early foliage amount and quicker branch death (Figure 6-13). Export to trunk during the life span of the branch varied very little in simulations with K_c values of 0.04 and 0.03 (Figure 6-14). However, for values below 0.03, there was a linear decline in export to trunk. The occurrence of such optima is discussed in Ford et al. (in press).

6.3.1.2 Foliage Longevity. Foliage mortality is strongly influenced by ozone level. Kress et al. (personal communication) measured mortality over a range of doses. At 47 ppb, an intermediate to low ozone dosage, only half of an annual foliage cohort survived to the end of its initial season, compared with no survival for 102 ppb and close to 80% for 21 ppb. The condition of 47 ppb was simulated in 24 runs with different random number seeds (Figure 6-15). In the 24 simulations, there was a markedly bimodal response between the four- and five-year-old branches. The minimum value of total C export per tree over the life span of a branch was 4.0 kg, whereas branches with standard foiliage longevity export around 10.0 kg of C.

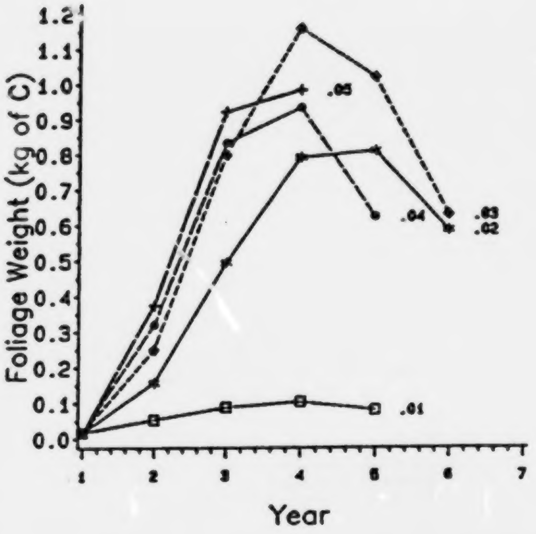

Figure 6-13. Foliage weight for selected carboxylation rates.

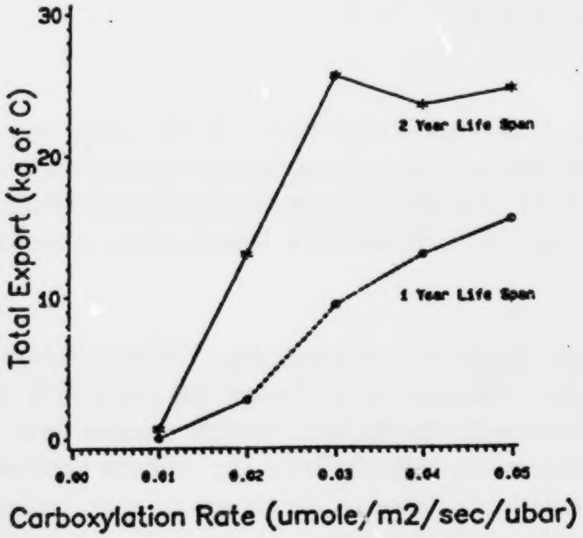

Figure 6-14. Total export of carbon to the trunk for selected carboxylation rate and foliage life spans.

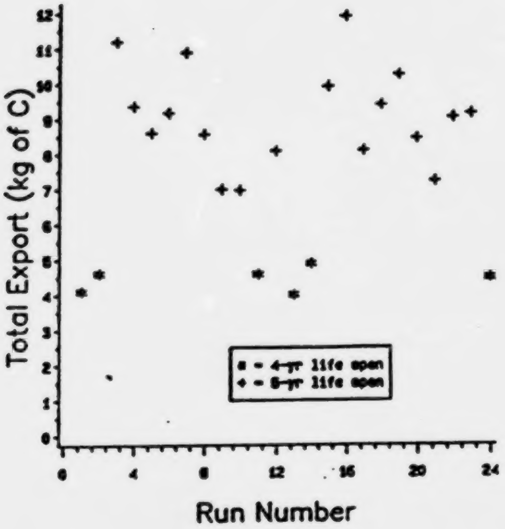

Figure 6-15. Total export to the trunk for foliage mortality set to one year for 24 random number seeds.

6.3.1.3 Respiration. Branchwood respiration rate was varied over the range of 85 to 120 mg CO_2/m^2hr, which produced an apparently nonlinear response over the higher part of the range (Figure 6-16). The approximate 20% increase in respiration rate from the estimated value of 102 mg CO_2/m^2hr caused a 14% decrease in the amount of C exported to the trunk.

6.3.1.4 Photosynthetic Rate x Foliage Longevity. The simulation that varied K_c over a range from 0.01 to 0.05 was repeated for foliage that had a 50% survival rate at the end of its first year (Figure 6-16) for the same random number seed. Export to trunk at a K_c of 0.03 was reduced by 38%, similar to the estimate obtained by comparing minimum values for 24 simulations. However, the reductions were considerably greater as values of K_c decreased below 0.03; reductions were less if K_c was increased. Thus, at $K_c = 0.02$, export to trunk for the greater rate of foliage death was 23% of that at the normal rate (Figure 6-14).

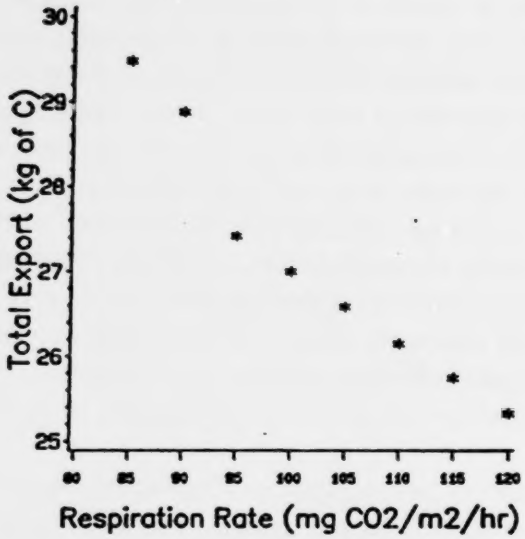

Figure 6-16. Total export to the trunk for selected maintenance respiration rates.

6.3.2 Red Spruce

6.3.2.1 Dose. As described in Section 3, frost damage is a conditional dose. Dose has not yet been precisely quantified, which is not surprising considering that conditional doses require an experimental analysis to be performed before they can be specified. A recent review of work sponsored by the FRP on air pollution and winter injury of red spruce concluded:

> Experiments in controlled conditions and in the field indicate that both ozone and acidic cloudwater can increase the probability of winter injury in red spruce by tissue freezing and possibly desiccation. Natural mechanisms to account for the increased winter injury observed in high elevation forests cannot be excluded, but, on the basis of the observations summarized here, the hypothesis that air pollution

predisposes red spruce growing at high elevations to winter injury is tenable (Adams and Eagar, 1989).

Two levels of damage have been mentioned: a regular endemic pattern and severe injury. DeHayes et al. (1989) reported annual surveys of visible injury in April 1986, 1987, 1988. They recorded an average foliar injury ranging from 8.6 to 12.2% that occurred on 34% to 46% of the trees. In contrast, Johnson et. al. (1986) have discussed the more rapid period of decline of montane red spruce in New England and New York over the last two decades. They have drawn attention to an apparent region-wide synchronization of reported winter damage with return times on the order of 5 to 10 years, although with closer time intervals in some cases. From tree ring and climate analysis, they suggested that the combination of warm late summer and cold early winter temperatures adversely affected the trees, presumably through frost damage. Johnson et. al. also noted theories of summer drought influence on the condition of the trees. In a summary of red spruce winter injury research, Adams and Eagar (1989) stated that " ... Current-year needles of red spruce reach midwinter hardiness levels that are barely sufficient to survive temperatures commonly encountered in midwinter; any natural or anthropogenic disturbance that could decrease midwinter cold tolerance of red spruce by just a few degrees (3 to 5 °C) would be likely to place the species in jeopardy."

Clearly, acidic precipitation causes red spruce foliage to be more susceptible to frost damage. However, there is no obvious and agreed mechanism by which the conditional effect would operate. Accordingly, the FRP has examined the joint effects of a regular loss of individual shoots of 5%, 10%, and 15% per year, and a severe damage with a return frequency of 8, 12, and 16 years. There are three stochastic processes in operation:

- new branchlets are generated at different positions on the branch;
- the effects of a frost event are randomly distributed across the branchlets; and,
- the survival of epicormic shoots is related to the first process and the interaction of the shoots with the environment.

We have simulated conditions in which both the annual percent damage and the repeat interval for major frost damage have been varied (Table 6-3).

The simulations show the sensitivity of branch growth to the frequency of major frost damage and the variability in the growth process. The low frequency of major damage (i.e., 16-year return cycle and 5% and 10% annual removal) seems to permit the branch to live longer than is likely. It may be that the cost function for the branches that develop "islands" of foliage is not adequately specified. To evaluate the similarity of simulations, the covariance of export to trunk with longevity must be examined.

Table 6-3. Simulation of Different Major Frost Return Cycles in Combination with an Annual Frost Damage Level of 5%

Major frost cycle (yr)	Simulation data			Branch survival (yrs)	Return to trunk per branch life	Annual return to trunk
8	seed	#year	export	Mean 8	Mean 1740	Mean 217
	1	8	1715			
	38	8	1883			
	74	8	1978			
	112	8	2124	4th and 5th	4th and 5th	4th and 5th
	149	8	2042			
	186	8	889	8	1883	235.4
	223	8	1883	8	1883	235.4
	260	8	1403			
10	seed	#year	export	Mean 16.25	Mean 10889	Mean 670.1
	1	10	3053			
	38	10	3204			
	74	10	3283			
	112	10	3720	4th and 5th	4th and 5th	4th and 5th
	149	10	3456			
	186	10	1661	10	3204	320.4
	223	60	66493	10	3283	328.3
	260	10	2242			
12	seed	#year	export	Mean 43.0	Mean 11399	Mean 265.1
	1	24	12570			
	38	12	4001			
	74	72	52871			
	112	12	5451	4th and 5th	4th and 5th	4th and 5th
	149	12	4931			
	186	100	253627	12	5451	454.25

Table 6-3. (continued)

Major frost cycle (yr)	Simulation data			Branch survival (yrs)	Return to trunk per branch life	Annual return to trunk
	223	100	78084	24	12570	523.75
	260	12	3153			
14	seed	#year	export	Mean 53.25	Mean 41186	Mean 773.4
	1	14	5971			
	38	14	5896			
	74	42	26027			
	112	56	17532	4th and 5th	4th and 5th	4th and 5th
	149	14	6247			
	186	86	74775	42	26027	619.7
	223	100	161682	56	17532	313.1
	260	100	31359			
16	seed	#year	export	Mean 79.0	Mean 97382	Mean 1232.7
	1	100	113110			
	38	16	6895			
	74	100	50222			
	112	100	109088	4th and 5th	4th and 5th	4th and 5th
	149	16	7334			
	186	100	208382	100	75569	755.7
	223	100	208459	100	109088	1090.9
	260	100	75569			
18	seed	#year	export	Mean 76.0	Mean 141144	Mean 1857.2
	1	100	143083			
	38	18	7565			
	74	100	270000			
	112	100	121864	4th and 5th	4th and 5th	4th and 5th
	149	18	7796			
	186	100	249097	100	121864	1218.6
	223	100	315509	100	143083	1430.8
	260	72	14240			

6.4 CONCLUSIONS AND CRITIQUE

Loblolly pine and red spruce, the species of principal interest in the FRP, show marked differences in their biology and in their sensitivity to pollutants. Loblolly pine is a rapidly growing species of potentially high productivity. The output provided by the model suggests that mature loblolly pine would be sensitive to small reductions in photosynthetic rate and foliage longevity. These two reported effects could act synergistically to decrease growth. The simulation of the combined effect of early foliage loss and decreased photosynthetic rate suggests for the amount of foliage loss tested (i.e., 50% loss at the end of the first year of growth) that no photosynthetic rate in the measured range is likely to provide compensation. Further analysis is required to examine the effects of smaller amounts of foliage loss, for which data are recently available (L. Allen, personal communication), and to examine the variability in the interaction between the two processes. The stochastic nature of branch growth is complex. There are large differences between branches of different ages, yet substantial variation exists between branches of the same age. Thus, to determine the various effects that pollution may have on trees, a substantial amount of simulation is required.

The production of epicormics following foliage damage is a very important compensating mechanism for red spruce. In a simulation of recurring major damage every 16 years, branches were still growing at 100 years, the maximum number of runs permitted by the model. This may be in excess of the natural duration of branch growth, although red spruce trees live for about 350 years. For an annual frost damage cycle of eight years, branches would rarely survive beyond the first frost. The sensitive range seems to be between 8 and 16 years, the two extremes, but it needs to be more precisely defined.

The two models, although designed for two very different species, strongly suggest that natural variation in patterns of development are likely to have a major effect on our ability to detect the effects of pollution on tree growth. For both models, the values of simulated outputs do not have frequency distributions that are easy to classify. The discontinuities implicit in an annual occurrence of death either when growth rates are high (loblolly pine), or through major frost damage (red spruce), produce discontinuities in the output variables.

A strength of the models is their multiple outputs; they predict morphology, longevity, and productivity. Of course, these are not orthogonal outputs, but they do offer some potential for developing a system of inference. We envisage that an attempt could be made to do that through simulation. The requirements for computation would be substantial but not prohibitive. We discuss the general problem of inference for complex models of this type in the Conclusions.

The models can be questioned on biological grounds. For example, an important untested assumption is that photosynthate created on any branchlet is equally available for use throughout the whole branch. There are conditions under which this assumption may break down and have an important effect on the functioning of the branch model can be examined by using the translocation model described in the next section. However, the assumption requires experimental analysis of the fundamental aspects of tree physiology. This is true for most of the assumptions made by the FRP. Another example is the interaction between growth physiology and frost damage. Research has clearly demonstrated that acid mist increases susceptibility to frost, but the question of how and under what conditions is not presently specified in sufficient detail to make refinements or to propose a detailed use of the model.

SECTION 7. MODEL: SIMPLE WHOLE TREE

The basic model of plant growth described by Thornley (1972) links root and shoot growth with the dynamics of their respective uptakes of nutrients and C. While this model may be logically correct for plants in general, implementing the model for trees is difficult. Because trees are large, transport between components must be explicitly represented. Also, trees have endogenous growth rhythms that are treated under phenology in the branch models, as well as source-sink dynamics that change over time. Source-sink dynamics are important considerations in the response of trees to pollutants.

Source-sink dynamics are important when considering branch growth. The branch models assume that all photosynthate produced within a branch is available for growth or respiration by any other part of the branch. Conversely, field studies of pollution influence on mature tree foliage consider the branch as a sampling unit. The growth of the branch is assumed to be independent of other parts of the tree; the branch exports photosynthate but does not import it. This is also the assumption of branch autonomy theory and the branch models. Modelers and experimenters have jointly established two very different assumptions: 1) during the first year of growth, photosynthate is freely mobile within a branch, and 2) after the first year of growth, photosynthate is unidirectional between the branch and the tree. In addition to these general assumptions, investigations have reported that ozone (MPO #4) and sulfur dioxide (Lorenc-Plucinska, 1984; 1986) have specific effects on translocation.

Three components of the Simple Whole Tree (SWT) model have been developed: TRANS, HYDRA, and an integration of TRANS into SWT. The translocation model (TRANS) describes the movement of water, mineral salts, and organic substances from one part of the plant to another when source and sink strengths are varied. HYDRA is a model for water movement in the plant. Although is is essential to a complete description of the dynamics of plant growth, it is not discussed here because it is not essential to our present interpretations of source-sink dynamics. The third component is a model for variation in sink strength, which is critical to the complete understanding of source-sink dynamics. This model integrates TRANS into the SWT model but has no independent name. The integration is described in the Section 7.4.

Translocation research, specifically the translocation of carbohydrates, dates back well into the 19th century. Sieve tubes and solution flow were identified by Hartig in 1837 (Parthasarathy, 1975). The most important concept in modeling translocation is the specific mass transfer (SMT) rate (Canny, 1973), with the product of concentration and speed of translocation measured in $g/hr/cm^2$. Concentration is in units of g/cm^3 and speed is in units of cm/hr. Mass transfer has units of g/hr and is the product of SMT and the cross-sectional area of the sieve tube.

Bassow (1989) reviewed mechanisms and models of translocation. Münch pressure-driven flow has gained the widest acceptance (Figure 7-1). However, the mechanism inducing translocation is still greatly debated. Although Münch pressure-driven flow is emerging as the favored mechanism, Fensom (1981) recently identified several problems. If a higher concentration of sucrose exists in cell A, the source region, than in cell B, the sink region, the osmotic pressure will be greater in A than in B. Water flows into cell A due to the higher osmotic pressure, and the resulting hydrostatic pressure drives solution into cell B. Water fluxes out of the sink by reverse osmosis.

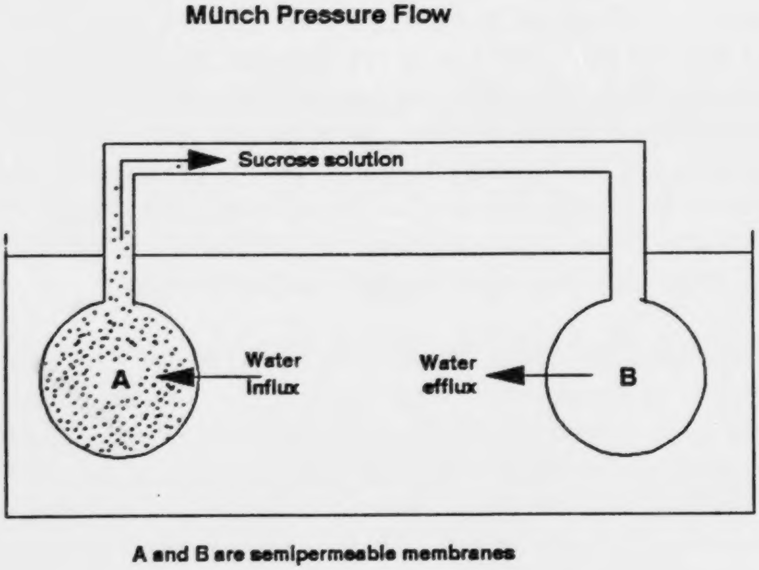

Figure 7-1. Diagram illustrating how Münch pressure-driven flow would explain flow of solution.

Until equilibrium is reached, a net flow of solution exists along the concentration gradient. This pressure-driven flow can be to maintained by a high concentration of sucrose at the source region, by phloem loading, and to maintain a lower concentration of sucrose at the sink region, by phloem unloading. In conifers, the application of Münch pressure-flow theory is debated because microscopic investigation of the sieve pores frequently shows plugs of material that could act as a barrier to the postulated fluid flow.

7.1 DESCRIPTION

Figure 7-2 illustrates the sieve tube and the variables incorporated in our model (based on Tyree et al., 1974, and Smith et al., 1980). The variables are:

$C(x,t)$	concentration of sucrose as a function of distance down the sieve tube, x, and time, t
$\bar{V}$	partial molar volume of sucrose
$P(x,t)$	hydrostatic or turgor pressure gradient as a function of time
L_p	peripheral membrane hydraulic conductivity
r	radius of the sieve tube
ψ_0	external water potential of the xylem
R	universal gas constant
T	absolute temperature.

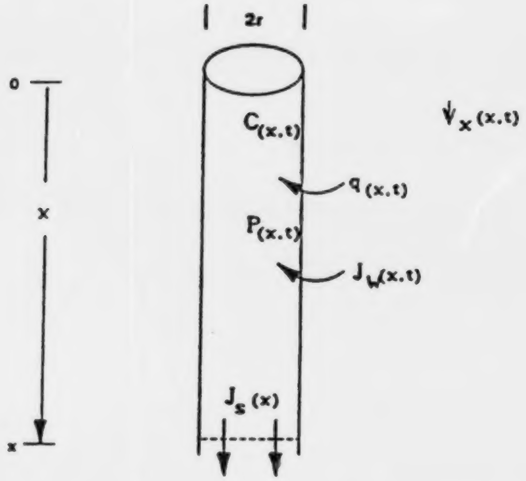

Figure 7-2. Diagram of Sieve Tube Model, based on Tyree et al. (1974) and Smith et al. (1980).

The equation for the conservation of water volume can be written as an expression of the time rate of change of the water volume in a control volume of the sieve tube of length Δx, as follows:

$$(\partial/\partial t)\,[1-VC(x,t)]\,A\Delta x = J_s(x_1)\,[1-VC(x_1)]A + 2\pi r\Delta x J_w(x) - J_s(x_2)[1-VC(x_2)]A \tag{1}$$

with the passive water influx defined as:

$$J_w(x) = L_p[\psi_0(x) - P(x) + C(x)RT] \tag{2}$$

and the velocity or volume flux at x:

$$J_s(x) = -\gamma(\partial P/\partial x)(x) \tag{3}$$

When the expressions for the passive water influx and the volume flux are substituted, all terms are divided by a factor of $A^*\Delta x$, and the value of $\Delta x \rightarrow 0$, the conservation of water equation can be rewritten as:

$$\begin{aligned}(\partial/\partial t)[1-VC(x,t)] + (\partial/\partial x)[-\gamma(\partial P/\partial x)(1-VC(x,t))] \\ = (2L_p/r)[\psi_0(x,t)-P(x,t)+C(x,t)RT]\end{aligned} \tag{4}$$

The conservation of sucrose can be expressed as a time rate of change of the sucrose moles in a control volume of the sieve tube of length, Δx:

$$(\partial C/\partial t)(x,t)A\Delta x = q(x)\Delta x + AJ_s(x_1)C(x_1)-AJ_s(x_2)C(x_2) + (\delta/\Delta x)[C(x_1)-C(x_2)] \tag{5}$$

Upon substitution for the volume flux, J_s, division by $A^*\Delta x$, and allowing $\Delta x \rightarrow 0$, the previous equation can be rewritten as:

$$\partial C/\partial t(x,t) + \partial/\partial x[-\gamma(\partial P/\partial x)C(x,t) + \delta(\partial C/\partial x)] = q(x)/A \tag{6}$$

where δ is the diffusion coefficient, and $q(x)$ is the loading and unloading function.

These two conservation equations can be solved to describe the variability of sieve tube flow with time. In particular, given the environmental conditions, initial conditions for the concentration of sucrose along the length of the sieve tube, and the boundary conditions of the pressure, one can calculate the evolution of sucrose concentration gradient and the pressure gradient that the concentrations induce. The environmental conditions include the water potential regime of the xylem, the loading and unloading rates of the sucrose, as well as the species-specific biological parameters. The equations are nonlinear partial differential equations that necessitate a numerical solution.

Our requirement was to develop a time-dependent, non-steady-state model (TRANS) of translocation of sucrose within the phloem, which was considered as an annulus rather than a single sieve tube.

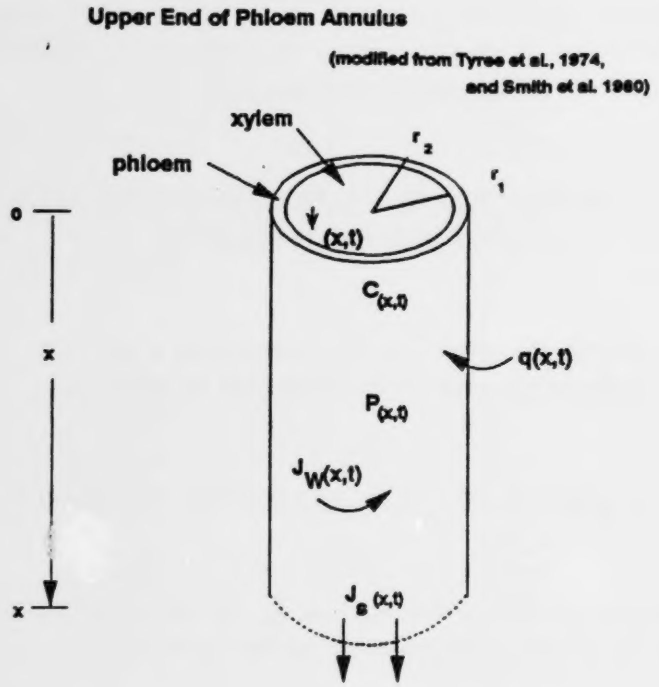
Upper End of Phloem Annulus
(modified from Tyree et al., 1974, and Smith et al. 1980)
xylem
phloem
r_2
r_1
0
x
x
$\psi_{(x,t)}$
$C_{(x,t)}$
q(x,t)
$P_{(x,t)}$
$J_W(x,t)$
$J_s(x,t)$

Figure 7-3. Diagram of variables to be included in TRANS.

Figure 7-3 incorporates the variables and parameters for TRANS. All parameters as indicated are functions of x and t, distance and time:

ψ_x = xylem water potential (bars)

q = sucrose loading and unloading rate (mol/min/cm^2 of peripheral membrane)

J_w = passive water flux (cm^3/min/cm^2 of peripheral membrane)

C = sucrose concentration in the phloem (mol/cm^3)

P = hydrostatic or turgor pressure in the phloem (bars)

J_s = average fluid velocity (cm/min or ml/min/cm^2 of phloem cross-sectional area)

The passive water influx and efflux can be expressed as:

$$J_w[x] = L_c\{\psi_x[x]-P[x]+C[x]RT\} \tag{7}$$

where:

$J_w[x]$ = water flow across the cambium in position element x (water that flows from the xylem to the phloem, or from the phloem to the xylem, depending on the sign of the flow)

$L_c[x]$ = hydraulic conductivity of the cambium in element x

$\psi[x]$ = water potential in the xylem in element x

$P[x]$ = hydrostatic or turgor pressure in element x

$C[x]$ = sucrose concentration in element x

R = universal gas law constant, 83.141 cm^3 bar/mol K

T = absolute temperature (K)

The average fluid velocity, or flux rate, is expressed as:

$$J_s[x] = -\gamma[\partial P/\partial x][x] \tag{8}$$

Where, in this case, γ = hydraulic conductivity of the annulus.

The equations for conservation of water and sucrose from Smith et al. (1980) can be reworked with: 1) annulus geometry replacing the tubular geometry; and 2) flow of sucrose and water allowed across both ends. Equations (4) and (6) from above then become:

$$(\partial/\partial t)[1-VC(x,t)] =$$

$$[2\pi r_1 L_c/A][\psi_0(x,t)-P(x,t) + C(x,t)RT] + (\partial/\partial x)[\gamma(\partial P/\partial x)(1-VC(x,t))] \tag{9}$$

Equations 9 and 10 assume that the vertical diffusion rate is negligible compared with the bulk flow as driven by Münch Pressure flow.

A linear combination of the above two equations is taken to obtain one equation with no time derivatives. This is a second-order differential equation in P:

$$O = Vq(x)/A + 2\pi r_1 L_c/A[\psi_x(x)-P(x) + C(x)RT] + (\partial/\partial x)[\gamma(\partial P(x)/\partial x)] \tag{11}$$

This equation can be rewritten as:

$$(\partial^2 P(x))/\partial x^2 + (-2\pi r_1 L_c/A\gamma)P(x) = -Vq(x)/A\gamma - 2\pi r_1 L_c/A\gamma[\psi_x(x)+C(x)RT] \tag{12}$$

$$\text{or:} \quad (\partial^2 P(x))/\partial x^2 + \alpha P(x) = f(x) \tag{13}$$

Where:

$$\alpha = (-2\pi r_1 L_c)/A\gamma$$

$$f(x) = (-Vq(x))/A\gamma[-2\pi r_1 L_c/A\gamma][\psi_x(x)+C(x)RT]$$

The other main equation is:

$$(\partial C(x))/\partial t = q(x)/A + \gamma[\partial^2 P(x)/\partial x^2]C(x) + \gamma[(\partial P(x))/\partial x][(\partial C(x))/\partial x] \tag{14}$$

Equations 13 and 14 are the major equations of the simulation.

7.1.1 Numerical Solution

Equation (13) is used to solve for the pressure gradient, given the initial concentration gradient. The concentration gradient can then be updated using Equation (14) for the time rate of change of the sucrose concentration. These two steps iterate forward through time.

Equation (13) can be approximated as follows:

$$(\partial^2 P(x))/\partial x^2 = 1/\Delta x^2\{P_{(i-1)}-2P_i+P_{(i+1)}\} \qquad (15)$$

so:

$$1/\Delta x^2\{P_{(i-1)}-2P_i + P_{(i+1)}\} + \alpha P_i = f_i \qquad (16)$$

or:

$$\alpha P_{(i-1)} + \beta P_i + \alpha P_{(i+1)} = f_i \qquad (17)$$

where: $\alpha = 1/\Delta x^2$

and $\beta = \alpha - 2/\Delta x^2$

or: $[-2\pi r_1 L_c/A\gamma] - 2/\Delta x_2$

The initial pressure at the top of the annulus is assumed to be: P(0,0) = P_a, and the initial pressure at the bottom of the annulus is assumed to be: P(0,N+1) = P_b.

For n vertical segments in the annulus, there are n unknown values for the pressure, and n equations to solve, given an initial estimate for the boundary conditions for the pressure, P(0,0) and P(0,N+1). The system of equations is uniquely solvable by simple matrix multiplication: $\underline{A}\ \underline{x} = \underline{b}$, in which we want to solve for the x vector of pressures, given the entries of the $\underline{A}$ matrix and the right-hand side, or the $\underline{b}$ vector.

$$\begin{array}{cccccccc}
\beta & \alpha & 0 & 0 & 0 & \ldots & P_1 & f_1-\alpha P_a \\
\alpha & \beta & \alpha & 0 & 0 & \ldots & P_2 & f_2 \\
0 & \alpha & \beta & \alpha & 0 & \ldots & P_3 & f_3 \\
0 & 0 & \alpha & \beta & \alpha & \ldots & P_4 & f_4 \\
0 & 0 & 0 & \alpha & \beta & \ldots & \ldots & \ldots \\
. & . & . & . & . & \ldots & P^n & f_n-\alpha P_b
\end{array} \qquad (18)$$

This was encoded in the computer language C using the function *sparse*() described by Press et al. (1988). The function *sparse*() was selected over the function *tridiag*() because of the numerical derivative approximation used.

The following equation was used to determine the time rate of change of the sucrose at each position along the annulus.

$$(\partial C(x))/\partial t = q(x)/A + \gamma[\partial^2 P(x)]/\partial x^2)C(x) + \gamma[\partial P(x)/\partial x][\partial C(x)/\partial x] \tag{19}$$

The average rate of change of concentration at any time can be approximated by:

$$(\partial C/\partial t)_i = \gamma C_i[(1/\Delta x^2)(P_{(i-1)}-2P_i+P_{(i+1)})] + [\gamma(1/(4\Delta x^2))[(C_{(i+1)}-C_{(i-1)})(P_{(i+1)}-P_{(i-1)})]+q_1 \tag{20}$$

Notice that the subscripts refer to the distance step, x, all within a single time step, t. A Runge-Kutta scheme was used to obtain the average time derivative of several estimates: one at time $t = t_1$, two different estimates at $t = t_i + 1/2\Delta t$, and one estimate at $t = t_1 + \Delta t$. This average derivative is used to step the concentration gradient forward in time:

$$(C_i)^* = C_i + (\partial C/\partial t)_i{}^*\Delta t \tag{21}$$

Where C_i^* is the new concentration and $(\partial C/\partial t)_i$ is an average rate of change of sucrose concentration over the time interval.

The concentration of sucrose at each point is updated in time, which includes the effects of sugar loading and unloading at that position, during that time step, and the effects of flow induced by the pressure gradient.

7.1.2 Boundary Conditions

Smith et al. (1980) assumed no flow across the ends of the sieve tube they modeled (i.e., the flux equaled zero), which simplified their calculations.

Here, TRANS represents a portion of the tree trunk or branch axis that is connected at the ends to the rest of the trunk or branch. The assumption of zero flux is inappropriate. In the FRP applications, the boundaries are usually not true "ends", but rather they are arbitrary boundaries imposed to study the behavior of the flow within the segment. Consequently, a new scheme was adopted.

The physiological process of translocation is very slow, at most on the order of 100 cm/hr, and generally very smoothly changing, particularly along the trunk of the tree. Consequently, the estimate used to update the values of the boundary pressure for the following time step was the model-predicted value of the pressure from the previous time step. That is, the calculations for what is happening within the domain of interest are used to update the boundary conditions for the next time step.

Thus:

$$P(t+1,0) = P(t,1) \tag{22}$$

$$P(t+1,N+1) = P(t,N) \tag{23}$$

The model predicts P(t,1) and P(t,N), as it solves for the pressure for segments 1 through N, inclusively. The boundary conditions for the next time step were set according to the model prediction in the last time step.

Assumptions must also be made for the boundary condition values at $x = 0$, and $x = N+1$, as the estimate in Equation (20) above uses values of the pressure and concentration at position (i - 1) and (i + 1). Smith et al. (1980) assumed no flow across the endpoints, which implied that:

$$\partial P/\partial x(0,t) = \partial P/\partial x(L,t) = 0 \tag{24}$$

and $$\partial C/\partial x(0,t) = \partial C/x(L,t) = 0 \tag{25}$$

These two equations imply that:

$$\partial C/\partial t(0,t) = q(0,t)/A \tag{26}$$

and $$\partial C/\partial t(L,t) = q(L,t)/A \tag{27}$$

Smith et al. (1980) assumed that if there is no flux across the endpoints, the partial time derivative will also be zero, except for any effect of loading or unloading directly at the boundary. Here we assume that due to the slow, smooth nature of translocation:

$$\partial P/\partial x(t+1,0) = \partial P/\partial x(t,1) \tag{28}$$

and $$\partial C/\partial x(t+1,0) = \partial C/\partial x(t,1) \tag{29}$$

And at the other end of the annulus:

$$\partial P/\partial x(t+1,N) = \partial P/\partial x(t,N-1) \tag{30}$$

and $$\partial C/\partial x(t+1,N) = \partial C/\partial x(t,N-1) \tag{31}$$

This would imply that:

$$\partial C/\partial t(t+1,0) = \partial C/\partial t(t,1) \tag{32}$$

and $$\partial C/\partial t(t+1,N) = \partial C/\partial t(t,N-1) \tag{33}$$

Thus, the boundary conditions of the sucrose partial rate of change will be updated by the estimate of the model prediction of the sucrose partial rate of change, within the domain and closest to the boundaries (i.e., one distance step in from each end). A test of these boundary conditions is given in the results of the simulations.

7.1.3 Parameterization

Smith et al. (1980) observed model output concentrations of sucrose along their path in a sieve tube of length 0.6 m, ranging from approximately 0.0004 to 0.0002 mol/cm^3, from the top of the sieve tube to the bottom. Tyree et al. (1974) observed similar concentration gradients: 0.0005 and 0.001 mol/cm^3 at the top of their 0.3-m and 25-m sieve tubes, respectively, to 0.0 mol/cm^3 at the bottom. These estimates were used as the approximate range for the initial concentration gradients for TRANS.

If initial estimates are too high, pressures are induced that are considerably greater than those observed. On the other hand, if the initial concentrations are set too low, the phloem develops a negative pressure. Tyree et al. (1974) considered this situation as representing plasmolysis and indicative of the phloem ceasing to translocate. Tyree et al. also suggest that for translocation to occur over a very long distance, as induced by Münch pressure-driven flow, the concentrations must be kept high. This was observed with TRANS. For the short-distance simulations, the initial concentrations were set at values ranging from 0.0003 to 0.00024 mol/cm^3. When this estimate of the gradient was used for very long distance simulations, plasmolysis occurred or negative pressures were observed. If the initial concentrations were set at higher levels, then positive pressures were observed. The initial estimates of the pressure boundary conditions were 2.8 and 2.7 bars, which usually gave a damped evolution of the boundary condition.

7.1.4 Cambial Hydraulic Conductivity -- Lc

TRANS is a model of whole phloem flow patterns, in contrast to the single sieve tube flow of the Smith et al. (1980) models. The estimates of peripheral hydraulic conductivity (L_p) must be converted into the hydraulic conductivity of the cambium (L_c). L_c assumes that water flows across the whole cambial tissue rather than preferentially along rays that connect the xylem and the phloem. Smith et al. (1980) used the estimate for $L_p = 2.5 \times 10^{-7}$ cm/bar/sec which can be converted into 1.5×10^{-5} cm/bar/min. Tyree et al. (1974) used a range of 2 to 5×10^{-7} cm/bar/sec, which can be converted to 1.2 to 3.0×10^{-5} cm/bar/min.

To convert an estimate of L_p into an estimate of L_c, the ratio of the volume to the surface area exposed (or normal) to the hydraulic flow is used. This means of converting the parameter value is more accurate than a simple scaling up in size. The ratio for conversion is:

$$L_p{*}(A_s/V_s) = L_c{*}(A_p/V_p) \tag{34}$$

Where:

A_s = surface area of one sieve tube

V_s = volume of one sieve tube

A_p = inner surface area of phloem annulus

V_p = volume of phloem

L_p = peripheral membrane hydraulic conductivity of one sieve tube

L_c = cambial hydraulic conductivity of phloem annulus

Thus:

$$Lc = (V_p/A_p) * L_p * (A_s/V_s) \tag{35}$$

For a single sieve tube of radius, r, and height, h:

$$\text{Volume} = \pi r^2 h$$

$$\text{Surface area} = 2\pi rh$$

For an annulus:

$$\text{Volume} = (r_2^2 - r_1^2)\pi h$$

and the surface normal to the flow from the xylem to the phloem is:

$$\text{Surface area} = 2\pi r_1 h$$

So, for the sieve tube geometry, the surface area to volume ratio is $2/r$. For the annulus, the surface area to volume ratio is $2r_i/(r_2^2 - r_1^2)$.

Assuming a radius of the sieve tube of 6×10^{-4} cm (Smith et al., 1980), an inner radius of 5.0 cm and an outer radius of 5.002 cm for the annulus, and a peripheral membrane hydraulic conductivity for a single sieve tube of 2.0×10^{-5} cm/bar/min (Tyree et al., 1974; Smith et al., 1980), then the cambial hydraulic conductivity, L_c, can be calculated by:

$$L_c = 2/r^* L_p^* (r_2^2 - r_1^2)/2r1 = 1.3336 \times 10^{-4} \text{ cm/bar/min} \qquad (36)$$

This value for cambial hydraulic conductivity is used in the simulations.

7.1.5 Axial Hydraulic Conductivity -- Gamma

Gamma (γ), or the hydraulic conductivity along the main axis of flow, is converted in a fashion similar to L_c. Tyree et al. (1974) calculated the hydraulic conductivity of the sieve tube, L (their notation), by applying Poiseuille's law of flow to the sieve plates and the sieve lumen separately. The resultant estimate of $\gamma = 15$ cm^2/min/bar is used for the hydraulic conductivity of the phloem annulus. The implications of higher and lower estimates of this hydraulic conductivity were explored by simulation.

7.1.6 Run-Specific Input Requirements

A water potential gradient, $\psi(x,t)$, and loading and unloading rates of sucrose, q(x,t), must be specified at each time step through the model run. The loading points may represent junctions where branches connect to the bole or where foliage is connected to the branch, depending upon the spatial orientation of the simulation. The unloading of sucrose for growth and respiration will ultimately be modeled as a Michaelis-Menten process. However, in the following simulations, all sinks or utilization components will be proportional to the concentration of sucrose at that point, and the potential sink strength will be represented as a proportionality constant, k_u, or the proportion of sucrose utilized to the total sucrose available at that time at that position. This approximates a high potential sink strength as defined by Ho (1988). Actual observed sink strength may be less than the potential sink strength if the translocation is insufficient to supply the sink.

The unloading rates have two distinct categories. The first is concentration-dependent unloading at a very low rate (a low k_u) along the entire length of the transport. Biologically, this represents respiration and growth of wood along the translocation path. The second is unloading at a high rate at an active terminal flush of roots or shoots. In this case, the concentration-dependent unloading is a relatively high proportion of the sucrose concentration at that position at that time (a high k_u).

7.2 ANALYSIS

Instabilities can arise in the model and are identified by a sudden change in the spatial pattern of concentration. These mathematical artifacts of the method of solution should not be given biological explanations. The instabilities arise if the distance step (in cm) is too small, or if the distance step is smaller than the time step (in min). Additionally, instabilities arise when the loading rates are an order of magnitude too great. The Courant condition for stability, as presented in Press et al. (1988), takes the form:

$$1 \geq (.\upsilon.\Delta t)/\Delta x \tag{37}$$

Zimmermann (1971) suggested that average fluid velocities for coniferous tree species is between 18 to 20 cm/hr. For white fir (*Abies concolor*), Crafts and Crisp (1971) suggested that assimilate translocation velocity is between 5 to 6 cm/hr. Also, Peel (1975) suggested reasonable translocation velocities in trees to be between 10 to 100 cm/hr. With the units converted to centimeters and minutes, the Courant condition is generally satisfied for the range of translocation speeds estimated for coniferous trees, with a distance step size of 2 cm and a time step size of 2 min.

7.2.1 Effects of Varying Initial Conditions

If the initial sucrose concentrations are too low, the simulation yields negative pressure. Tyree et al. (1974) described this as plasmolysis, or negative pressures in the phloem. They suggested that for long distance flow to occur in the sieve tubes, there must to be a sufficient concentration of sucrose in the sieve tubes. This corresponds with the results TRANS produces; if the initial sucrose concentrations are too low, the pressures in the phloem are negative. As the concentration rises through time with the loading rate, the pressures eventually become positive. This startup requirement to eliminate the negative pressure values can be avoided by selecting appropriately scaled initial values of the concentration gradient.

If the concentration gradient is initially set too high, the pressures appear to become infinite. Thus, the exact setting of the initial concentrations is not crucial, because the system tends to evolve and smooth or change the concentration values. However, the approximate range of initial concentrations is important to quantify, so that the simulation does not take several hours to balance the computation to some more realistic estimate that has positive pressure values.

7.2.2 Effects of Varying Boundary Conditions

As discussed above, the following boundary conditions were assumed:

$$P(t+1,N+1) = P(t,N) \text{ and } P(t+1,0) = P(t,1),$$

These boundary condition assumptions yield results in which the edge of the domain is closely related to the patterns just interior from the boundary. This is exactly as the boundaries should be, in contrast to simulations in which the boundary pressures are set at a given value, constant in time, and the time derivative of the concentration at the boundaries is set at zero. The latter represents a fixed flux rate across the boundaries through time. In those cases, the simulation results appear to change within the domain due to the loading and unloading regime, but the boundaries remained fixed. Thus, a significant difference developed between the boundaries and the points just interior from the boundaries.

This is quite unrealistic. The ad hoc method of updating the boundary conditions by utilizing information from within the domain of the model seems to yield far more appropriate and interpretable results.

7.2.3 Effects of Varying Physical Parameters

Several physical parameters must be specified for the model, e.g., parameters for vertical and lateral hydraulic conductivities, radius and thickness of the annulus, proportion of annulus cross-sectional area that are sieve tube lumens, and temperature. Some of these parameters are likely to be species specific. Others parameters, such as the temperature and radius, should be specified for a given simulation run.

Several simulations were run to explore the effects of the conductivities, L_c and gamma. The simulations with low conductivities demonstrated a slower accumulation of sucrose at the points of loading. The ridges surrounding the loading points slowly rise. This fills the regions between the ridges more slowly. Parameters such as the vertical and lateral hydraulic conductivities are seldom empirically measured, yet they are important for modeling translocation.

On the basis of the exploratory runs, the following physical parameter estimates were used:

$L_c = 1.3336 \times 10^{-4}$ cm/bar/min

$\gamma = 15$ cm^2/min/bar

$r_2 = 5.002$ cm

$r_1 = 5.0$ cm

The proportion of annulus cross-sectional area that are sieve tube lumens = 1.0, and temperature = 297 K.

7.2.4 Model Performance

The model was used to investigate three hypotheses of interest to the theory of carbon dynamics in trees: 1) branches can be thought of as autonomous, as exporting but not importing carbon; 2) total tree size or height may limit translocation; and 3) increasing water potential gradients may limit translocation in tall trees. Details are only presented for the simulation of branch autonomy.

Simulations were made of both short and long branches. The short branch is simulated as an annulus that is 40 cm in length, i.e., 20 distance steps of 2 cm. Foliage is considered to be along the entire length so that the loading rate is constant along the length as 6.0×10^{-7} mol/cm/min. There is a concentration-dependent unloading factor along the entire length; k_u being 1.0×10^{-4} cm^3/min/cm. The long branch was simulated as an annulus 100 cm in length, or 50 distance steps. The foliage is only located along the apical 40 cm, with the same photosynthetic rates as for the shorter branch. Thus, net photosynthesis is the same for the long branch and the short branch. Again, a constant unloading rate exists along the entire length as cambial growth and respiration; hence, the longer branch has a greater net sink than the shorter branch because the branchwood's length must be supported.

Specific mass transfer for a short branch reached equilibrium in less than 20 simulated minutes. The longer branch approaches a steady state more slowly and specific mass transfer rates are lower at the end of the annulus than for the short branch (Figures 7-4 through 7-7).

The effect of apical shoot growth was simulated for both branch lengths. Sink strength is equivalent to the removal of sucrose at a rate that achieves 1 cm of shoot extension per day.

Although a transient time of adjustment exists, after the first 60 to 80 min a steady state is approached. The flux of sucrose is reversed by the addition of a substantial sink and flows toward the newly growing shoot both at the branch mid-point and trunk connection point. However, this is not so for the long branch.

The specific mass transfer rate at the midpoint and at the branch trunk junction end of the annulus are still positive, indicating that the branch is continuing to export photosynthate to the trunk.

A series of additional simulations were made to examine the effects of different conditions between the trunk and branch on the process of translocation and growth in the branch itself. A theory of branch development (Figure 7-8) can be specified in relation to its relative "productivity" or export of material to the trunk, or "utilization" import from trunk to branch. This trajectory may be modified by pollutant influence, as discussed below.

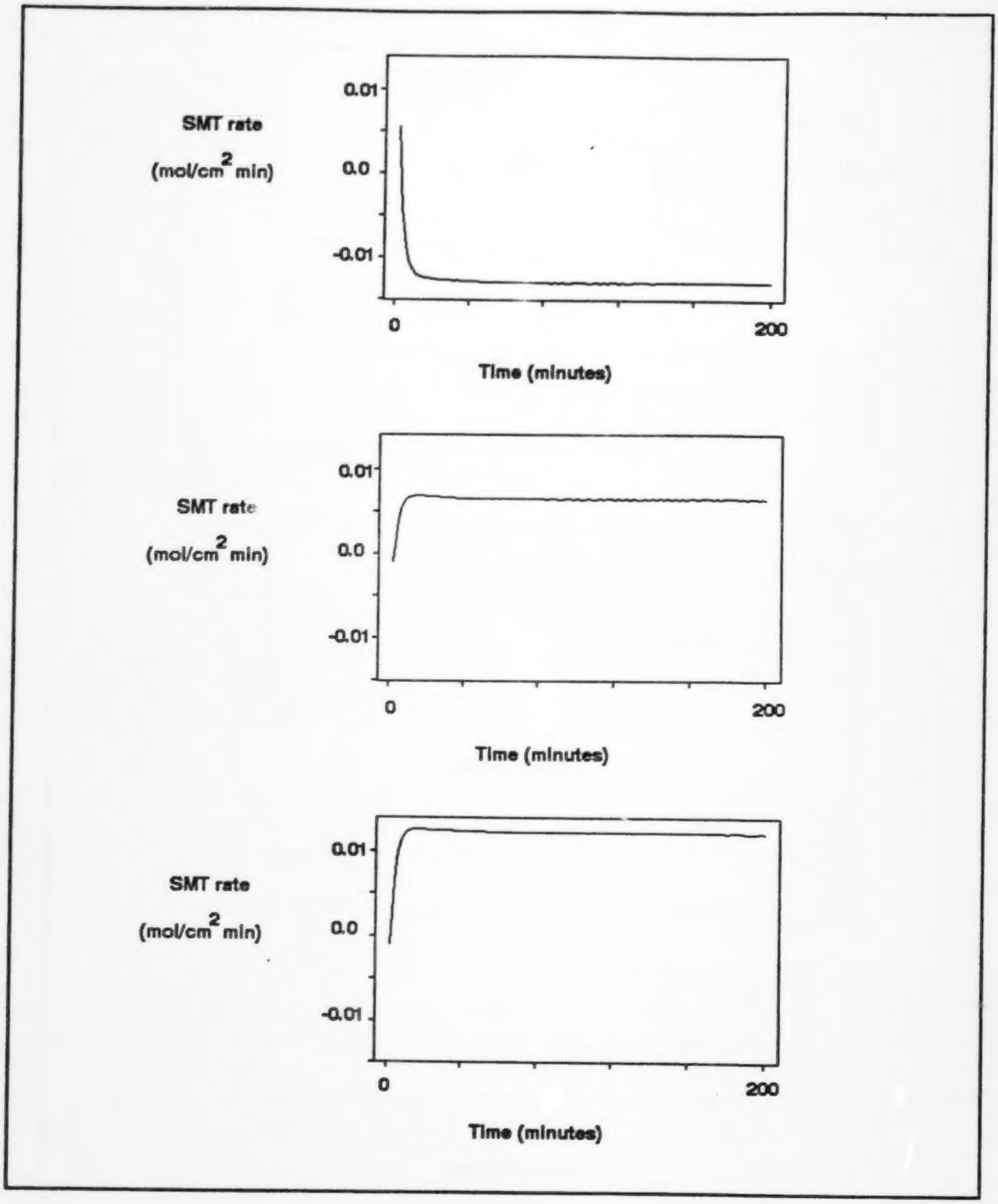

Figure 7-4. Specific mass transfer rates for a short branch at three positions along the phloem annulus: a) apical end, position 1, b) 30 cm from the apical end, position 15, and c) branch-trunk junction or end of the annulus, position 20.

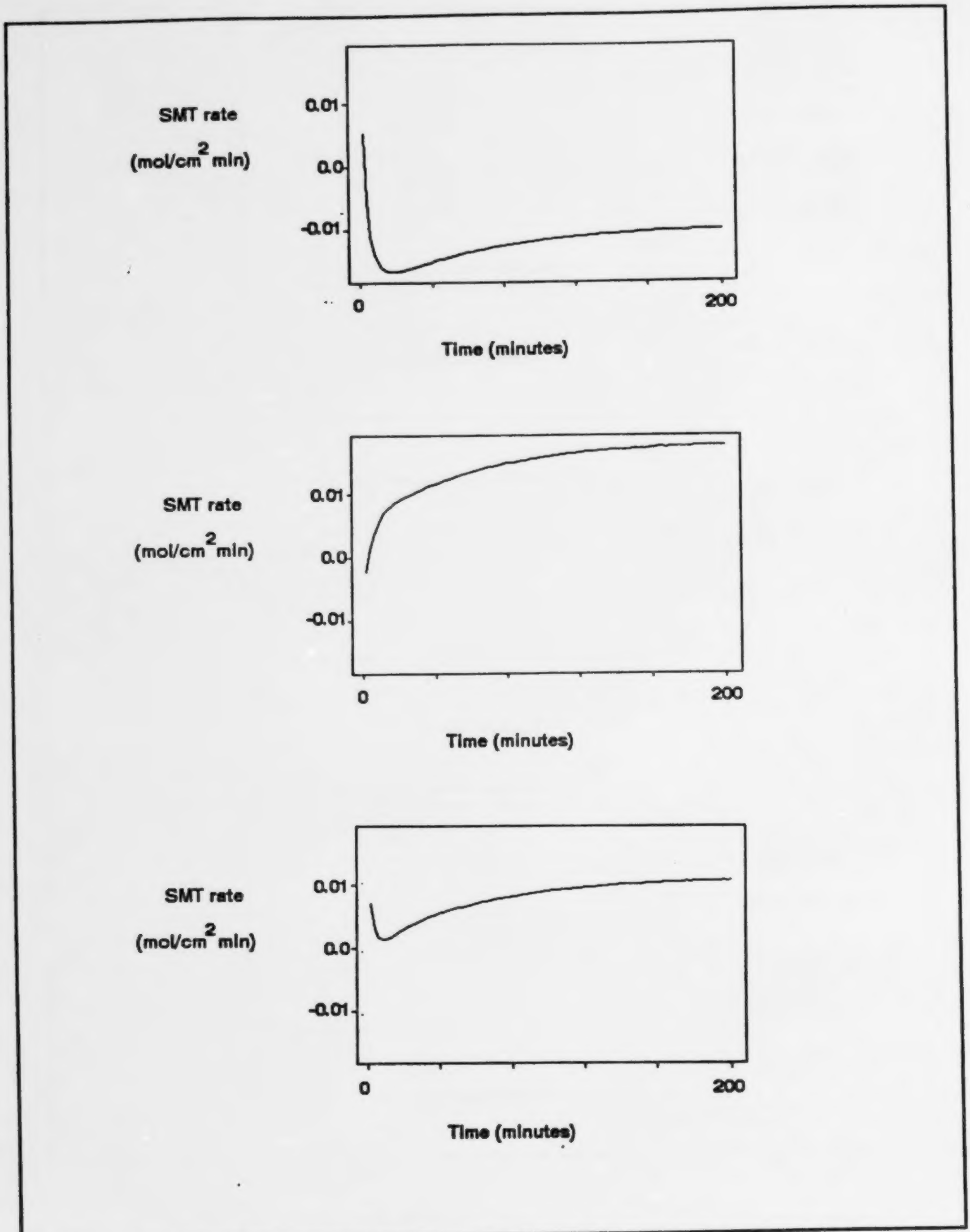

Figure 7-5. Specific mass transfer rate at three positions along the phloem annulus: a) the apical end, position 1, b) 50 cm from the apical end, position 25, and c) the branch-trunk junction, or end of annulus, position 50.

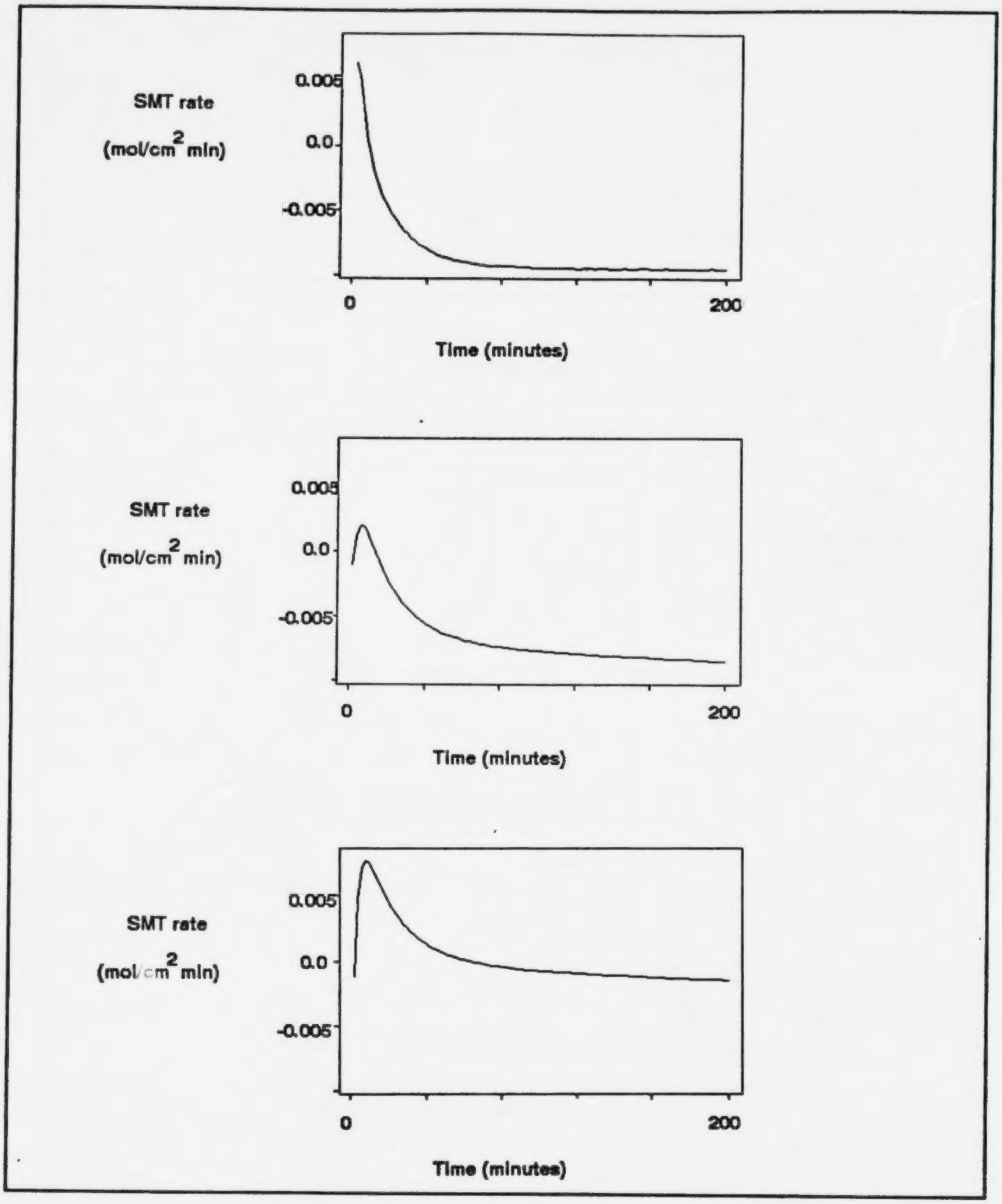

Figure 7-6. Specific mass transfer rates at three positions along a short branch with an active shoot flush: a) the apical end, position 1, b) 30 cm from apical end, position 15, and c) the branch-trunk junction, end of annulus, position 20.

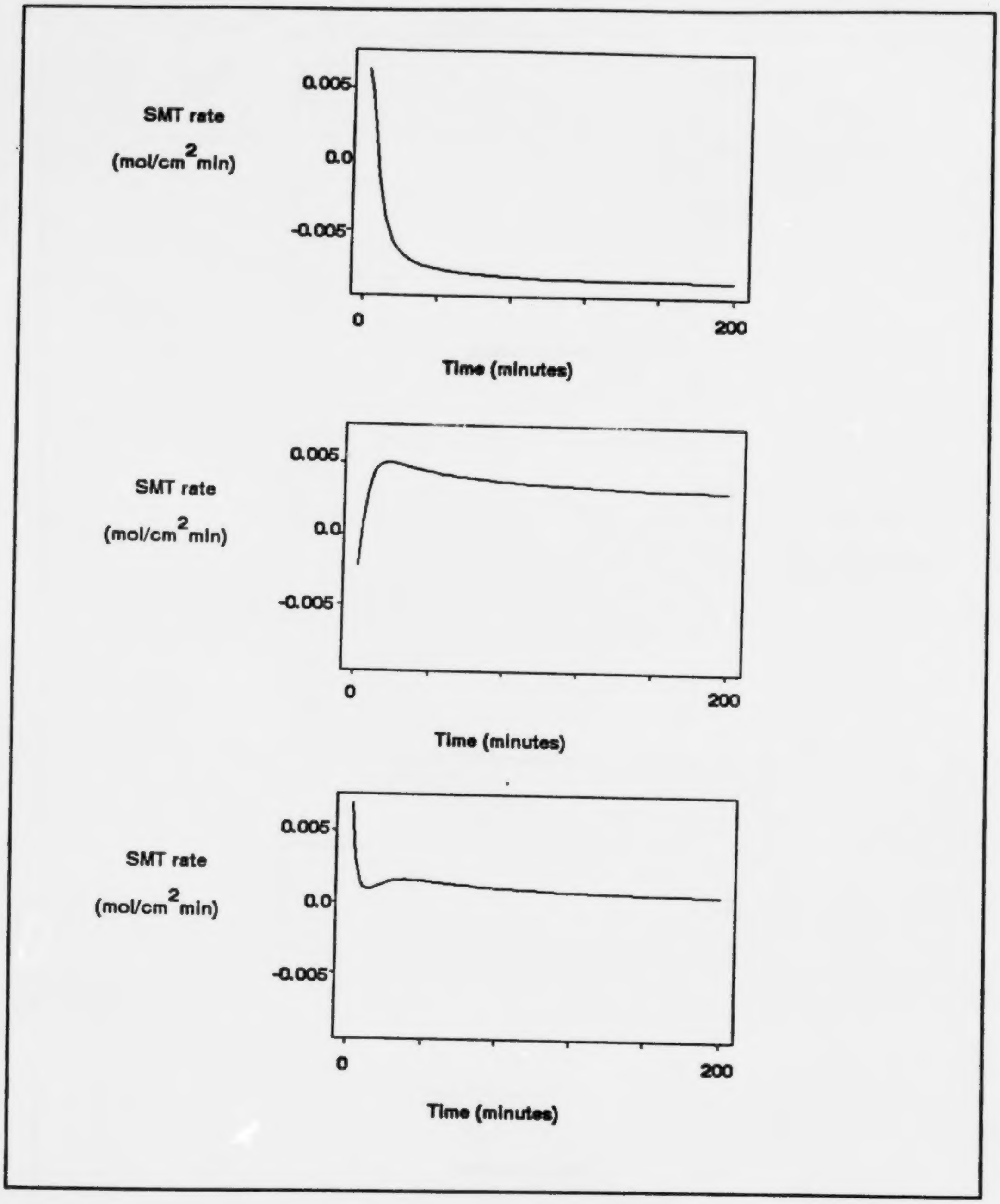

Figure 7-7. Specific mass transfer rates at three positions along the phloem annulus with shoot flush on a long branch: a) apical end, position 1, b) 50 cm from apical end, position 25, and c) branch-trunk junction, end of annulus, position 50.

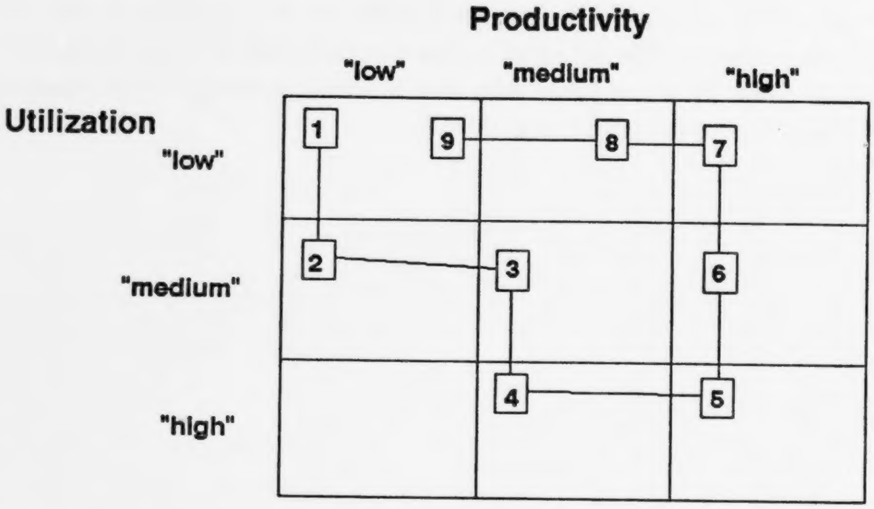

Figure 7-8. A sample trajectory of a branch as it grows throughout its life on a grid of relative production rates and relative utilization rates.

Simulations of translocation along complete trunks of trees show, as expected, that in taller trees translocation restricts the flux of sucrose. However, this process needs to be defined precisely in terms of time constants for specific temporal patterns of photosynthate production along trunks of specified structure.

In addition, the translocation of material along trunks substantially changes the vertical profile of water potentials. Simulations were limited by computational facilities; the effects of low water potentials on translocation within tall trees can be more thoroughly investigated with the use of a supercomputer. These preliminary simulations comparing translocation within a short tree under different water potential regimes illustrate that translocation is reduced with even slight reductions in the water status of the tree. If very low water potentials were reached within the top of a tall tree, this limitation could be even more significant. Understanding the interactions of the water-transport time dynamics and potentials within the xylem, as well as the time dynamics of the carbohydrate production, loading, and unloading within the phloem, will contribute to the modeling process.

7.3 APPLICATION

A simple, rather severe condition of pollutant action was simulated--a halving in the photosynthetic rate. This simulation is illustrated in the two branch types shown above, a short and a long branch. The effect of reduced photosynthetic rate during the time of shoot extension (Case 3) is compared with that of shoot extension alone (Case 2) and no shoot extension (Case 1) (Figures 7-9 and 7-10).

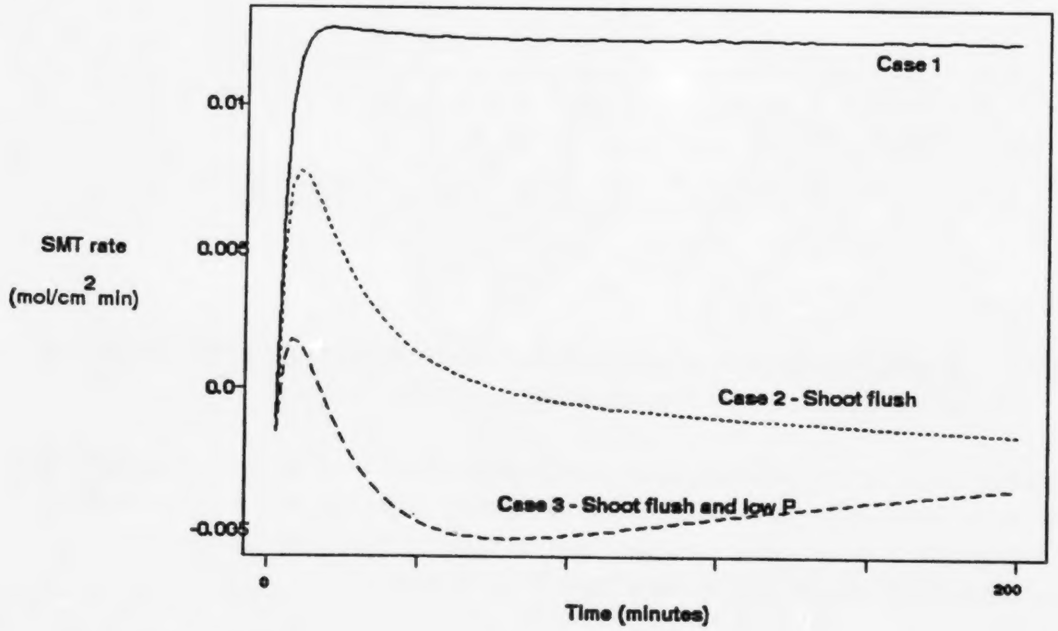

Figure 7-9. The specific mass transfer rates of the short branch for the three cases at the branch-trunk junction end of the branch, position 20.

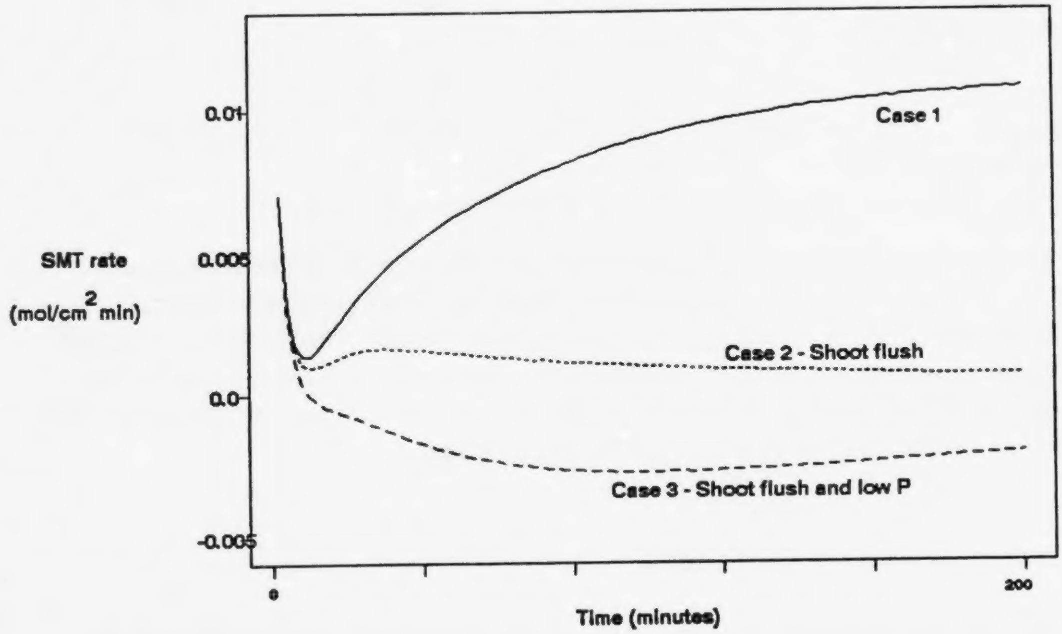

Figure 7-10. The specific mass transfer rate of the long branch for the three cases at the branch-trunk junction end of the branch, position 50.

The following table summarizes the specific mass transfer rates at the branch-trunk junction end of the branch after the 200 minutes of simulation:

Table 7-1. Specific Mass Transfer Rates at the End of the Branch After 200 Minutes, for the Long and the Short Branch

	Case 1 Base Case	Case 2 Shoot Flush	Case 3 Shoot Flush and Low P
SMT Rate of Short Branch ($g/hr/cm^2$ phloem)	2.5159	-0.3071	-0.6941
SMT Rate of Long Branch ($g/hr/cm^2$ phloem)	2.2044	0.1195	-0.4308

The simulated decrease in photosynthetic rate increases the effective sink size of the branch. The short branch is a net sink during shoot growth, and so a reduced photosynthetic rate simply increases the apparent sink strength. On the other hand, the long branch remains a net source of photosynthate, continuing to export to the trunk during the shoot flush period. Reducing the photosynthetic rate completely reverses this and changes the long branch to a net sink for photosynthate.

7.4 CONCLUSIONS AND CRITIQUE

The general conclusion from this study is that if pollution operates through the photosynthetic process, either in the reduction of photosynthetic rate or foliage amount, the translocation process may modify the observed effect on tree growth.

Direct application of this model to give precise figures to the general result requires the following:

1) Questions must be asked about specific branch and tree structures. It must be possible to define the length of pathways of interest, the variation in range of photosynthesis to be considered, and possible variations in foliage density per length of shoot. These conditions can be defined, at least in part, through the results in MPO #4 and the branching models.

2) The model must be implemented on a supercomputer. This is not a large task. Other models have transferred easily.

3) A model for transpiration and water movement along trunks and branches that was written in concert with this model (Haskins, in preparation) and that uses a very similar mathematical and computational procedure should be incorporated. Because it does not directly analyze pollution effects, this working model is not presented in this document.

4) TRANS is the central part of SWT. However, a principal requirement of SWT is a calculation of a *Potential Sink Strength* (Ho, 1988) for growing meristems. This acts as an attractor for sucrose, and sets up the gradient that is used in TRANS as the basis for translocation. Expanding cells create an expanding volume with a low concentration of sucrose into which sucrose is drawn through the translocation process (i.e., the sink becomes extended).

The observations have led to new directions in the modeling effort. At present, the model is developing along the following lines:

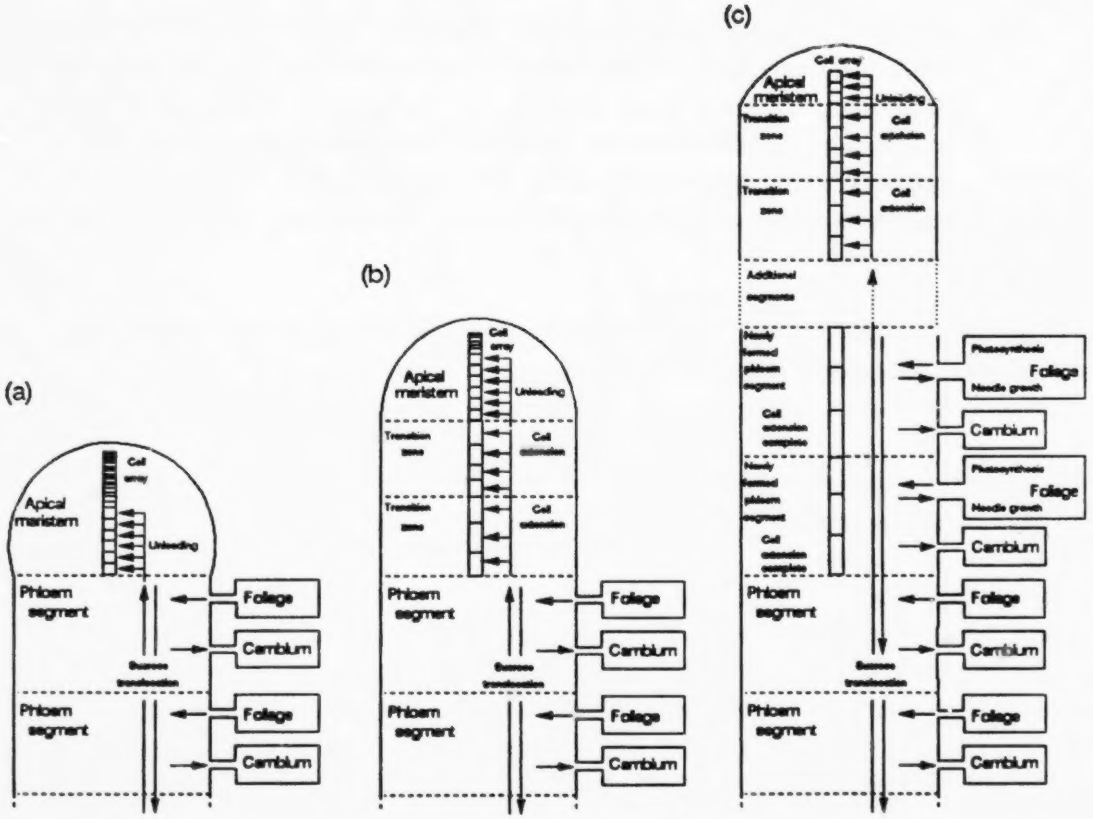
(a)
Apical meristem
Cell array
Unloading
Phloem segment
Sucrose translocation
Phloem segment
Foliage
Cambium
Foliage
Cambium
(b)
Apical meristem
Cell array
Unloading
Transition zone
Cell extension
Transition zone
Cell extension
Phloem segment
Sucrose translocation
Phloem segment
Foliage
Cambium
Foliage
Cambium
(c)
Cell array
Apical meristem
Unloading
Transition zone
Cell expansion
Transition zone
Cell extension
Additional segments
Newly formed phloem segment
Cell extension complete
Newly formed phloem segment
Cell extension complete
Phloem segment
Sucrose translocation
Phloem segment
Photosynthesis
Foliage
Needle growth
Cambium
Photosynthesis
Foliage
Needle growth
Cambium
Foliage
Cambium
Foliage
Cambium

Figure 7-11. Three stages in the growth of a shoot apex: a) phloem segments have both loading and unloading components and are an integral part of the TRANS model; b) the apical meristem produces transition zone segments depending upon the rate of supply of sucrose, determined by simulated enzymatic rates; and c) transition zones undergo longitudinal expansion and form new phloem segments that become part of TRANS.

At the start of the growing season, the meristem tissue of the bud is assumed to contain a number of small dimensioned cells typically found in apical meristems. These are organized in a linear distance from the connection of the bud to its supporting stem section (Figure 7-11). In the simulation, these cells are represented as an array of single cells, 15 x 15 x 15 microns with 1 micron thick cell walls. Each is a mean cell found in the cross-sectional area of the simulated apex. Sucrose is unloaded into this meristem from the terminal section of the phloem, and, depending upon the time interval and availability of sucrose, cells in the array commence a combined elongation and increase in area. At this stage, individual cells reach their full cross-sectional area, 30 x 30 microns with cell walls of 2 microns, but their elongation is arbitrarily restricted to 100 microns, one tenth of their full potential length of 1000 microns. This restriction ensures that the available sucrose is utilized by a number of cells within the meristem.

The total length of the elongated cells within the meristem is permitted to increase until the total extended length is 1 cm, equivalent to 10 fully extended cells. The cells in this extension then create a transitional zone (Figure 7-11b) which has its own phloem and forms the penultimate section of the phloem. Elongation of these cells continues until either they have reached their maximum permitted length of 1000 microns or they have passed through five transitional zones. Sucrose is unloaded into the cells in the transitional zones by the same processes as in other zones. However, a flux of water, in addition to sucrose, is simulated that is equivalent to the volume of new cell tissue created. The growth of cells in the meristem continues to take place as described above.

At each iteration of the simulation, after the new elongation growth has been calculated for each cell, a reallocation is made between the cells in the array and the 1-cm sections of phloem (Figure 7-11c). At this point, cells may pass from a transitional zone to a new shoot zone on which foliage development commences. All growth is calculated using the Michaelis-Menton coefficients described for cellulose formation, assuming the same rate for respiration as described above.

SECTION 8. MODEL: ROOTS/SOIL

ROOT/SOIL originated in the studies of Binkley et al. (1987, 1989) and in a workshop held by the FRP on the influence of acidic deposition on root and soil processes.

8.1 AN ANALYSIS OF SOUTHERN SOILS WITH MAGIC

Binkley et al. (1987, 1989) conducted an important modeling exercise with the Model for the Acidification of Groundwater in Catchments (MAGIC) (Cosby et al., 1985) on the potential effects of acidic precipitation on soils. This was discussed earlier along with FRP work on the effects that acidic precipitation may have on soil chemistry and, subsequently, on root function and tree growth. Binkley et al. (1987, 1989) concluded that:

> The models currently available do not simulate changes in forest productivity as a result of changing (soil) nutrient availability, and they do not include changes in the acid strength of the exchange complex.

These computer simulations examined the potential effects of sulfate adsorption patterns on acidification. Nitrogen is assumed to be taken up by the trees and does not contribute to the acidification process. However, recent work suggests that for upland forest soils, all available N may not be taken up (Strader et al., 1989); consequently, it may be a component of the acidification process. By amount, N is the most important soil nutrient; determining its dynamics of deposition, circulation within the ecosystem, and loss is critical for understanding acidification.

In their simulations, soil is represented as a monolith. This presents possible problems as discussed by Binkley et al. (1987, 1989). When the monolith was increased in depth, the apparent resistance to acidification was increased. This does not consider soil mixing processes in the soil, or the lack thereof. Also, Binkley et al. stated that:

> When sulfate adsorption capacity was increased from the values typical of the upper rooting zone (2 $\mathrm{mmol_c/kg}$) to a level more typical of lower soil horizons (8 $\mathrm{mmol_c/kg}$) acidification effects were delayed by about 20 years.

Measurements in a loblolly pine plantation that were taken between 5 and 25 years since the plantation was started showed the greatest acidity change in the surface horizons. Forest soils are highly horizontally stratified. The surface horizons contain the greatest concentrations of roots and biological activity (Ford and Deans, 1977; Grier et al., 1980).

The model used by Binkley et al. (1987, 1989) in their simulations is a lumped parameter equilibrium model of intermediate complexity based on processes involving a few major soil properties (Cosby et al., 1985). The model was designed to "include terms to describe the important phenomena controlling a system's chemical response to acidic deposition, yet be restricted in complexity so that they can be implemented on diverse systems with a minimum of prior data." The authors included soil cation exchange reactions, soil and aqueous phase Al reactions, gaseous and aqueous phase CO_2 reactions, and formulation of electroneutrality. Spatial heterogeneity was not incorporated in the model. Because of Binkley et al.'s (1987, 1989) results, particularly their field observations of surface horizons showing change to forest and acidification processes, further model developments should de-aggregate the model to account for spatial heterogeneity. The fundamental requirement is to study the differential occupancy of the vertical horizons by root systems and the transport between horizons that result from both physically and biologically induced processes. For example, if acidification occurs in the surface horizons, can root systems easily adapt by exploiting lower horizons more effectively? In this modeling approach, procedures have been developed that simulate differential root growth in soil horizons as a function of the conditions within each horizon and the transport of water between horizons.

8.1.1 Root and Soil Processes Workshop

The FRP sponsored a workshop held in New Orleans in March, 1989. Scientists working in the field were asked to specify the minimum properties of a simulator of the interaction of roots and soil. The following is a summary of the workshop report.

8.1.1.1 Introduction. The purpose of the workshop was to develop the approach that should be taken to model the effects of acidic deposition on forest soils and the subsequent effect on tree and stand growth. Soil systems are complex, and a relatively small amount of research has been conducted on root growth and function compared with above-ground plant parts. Nevertheless, acidic deposition may influence tree and forest growth through the soil-root system. Given our current understanding and our objective of simulating the possible influence of acidic deposition on tree growth, how best can the soil-root system be simulated and how can models be used effectively?

8.1.1.2 Defining the Scope of the Problem. Studies indicate that acidic deposition influences soil processes, which in turn affect the growth of roots and trees. Models to effectively simulate the effect of acidic deposition on soil processes have only recently been developed. A variety of interactions between acidic deposition, the soil, and the root system exist that must be defined and prioritized. This may be the most logical starting point to model below-ground processes affecting tree growth.

The group discussed the following types of effects from acidic deposition relative to below-ground processes:

- soil-mediated,
- direct effects on roots,
- above-ground mediated, and
- root-mediated changes (inputs to above-ground).

The direct effects on roots were not considered because atmospheric inputs to roots are considered soil-mediated even if they are only transported through the soil. Because above-ground mediated effects were not part of this workshop, subsequent discussions focus on soil-mediated changes and inputs from roots to the above-ground parts.

Root and soil processes were defined by the following categories:

(1) soil morphology,

(2) soil factors that affect root growth,

  a) factors that may be affected by acidic deposition

  b) factors not affected by acidic deposition

(3) root factors that affect soils,

(4) requirements of roots (through soil only), and

(5) outputs of roots to above-ground parts of tree.

The following discussion focuses on characteristics of the below-ground ecosystem that should be considered in the development of a soil and root modeling system.

Soil Morphology

Soil horizons should be included in a simulation model. Definitions are available according to soil taxonomy. The top horizon, if present, would be an organic layer, followed by a variable number of mineral horizons. If a soil consists of the minimum two layers, one organic layer and one mineral, the relative importance of the mineral versus the organic layers must be considered. Site-specific definitions can be obtained by choosing a set of major soil types at specific sites. The horizons can be defined one of two ways: by statistical methods (a representative look at what the soil is at present) or by a first principles view (which considers the origin of the soil). The time scales for horizon type and depth can likely be constant (e.g., for daily or weekly root growth), whereas time scales of other soil properties may vary depending on root growth in the model.

Recommendations for defining the soil morphology of a system in a soil and root model are as follows:

- Use standard soil taxonomy and available soil descriptions (e.g., DDRP) to define soil horizons.
- Choose a set of specific sites of major soil types to gather information.
- Use the statistical approach for initial conditions (that includes unknown anthropogenic inputs already part of soil), i.e, "initializer."
- Use first principles approach later in the process along with consideration of soil properties; i.e., "continuing dynamics."
- List horizon type (one of four types) and depth and most other physical properties as constants; other soil properties can be lumped by factors such as temporal variability, sensitivity to acidic deposition, information available relevant to acidic deposition, etc.

Soil Properties

The soil properties are factors that affect (or correlate with) root growth and they can be subdivided into physical, chemical, and biological properties. The ways these properties affect root growth can be separated into several categories: through water and nutrient uptake (U), respiration/growth (G), export, and death. The properties also vary in their susceptibility to change that is caused by acidic deposition; 1=not affected; 2=not likely affected; 3=possibly affected; 4=affected). The following list includes some physical, chemical, and biological properties of importance, defines the properties involved in uptake (U) and growth (G) of the root, and rates the effect, if any, of acidic deposition on each.

Physical

- Bulk Density (G) (2)
- Soil water potential - direction of movement (U,G) (1)
- Soil water content - % water-filled/air-filled pores (U,G) (1)
- Porosity - pore size distribution in cm^3/cm^3 (U,G) (1)
- Mechanical resistance - penetometer reading (G) (1)

Chemical

- Buffering powers - cation exchange capacity (4)
- Initial soil solution concentration - with increased S, H^+, and N:Mg, Ca, P, and K decrease and Al increases (4)
- Diffusion coefficients - by element (1)
- Mass flow (1)
- Oxygen availability - vapor pressure (2)
- Carbon content (3)

Biological

- Herbivory - Collembola, nematodes, fungi (3)
- Symbionts - Mycorrhizae (3)
- Competitors - Decomposers (3)

In formulating the list of soil properties, several points of discussion were made. Although root growth occurs quantitatively, qualitative changes take place. The fine roots uptake water and nutrients. If growth is concentrated in fine roots, it is considered quantitative. If growth undergoes a transition to thick roots and storage/maintenance roots, it is considered qualitative. How and when does root growth transition occur? When does uptake occur? In a grid cell framework, which provides a three-dimensional grid for the root (which maintains a constant thickness) to grow, the focus is on fine root uptake and growth (i.e., incremental quantitative growth).

Of the chemicals affecting root growth, H^+, N, and S enter the soils by acidic deposition. The increase of these chemicals in the ecosystem decreases the P, K, Ca, and Mg in the system, and increases the Al. The problem in modeling these increases and decreases in the chemical concentrations in the ecosystem is that the changes in the chemical contributions can be positive or negative, depending on other variables within the ecosystem.

Mycorrhizae in forest ecosystems require nutrients from the trees. Under different circumstances, they have positive or negative influences. For example, without acidic deposition, they can increase uptake by augmenting the surface area uptake in the roots, thus increasing storage potential and potential transport to above-ground portions of the tree. Mycorrhizae may also protect against infection by other disease agents. If root growth is at a minimum, mycorrhizae may deplete carbohydrate reserves. Under acidic deposition (i.e., N inputs), increased root growth may succeed mycorrhizal growth and result in decreased mycorrhyzae density. The fine root qualitative growth includes two cell populations: root and mycorrhizae.

Root Factors that Affect Soil/Nutrient Cycling

Four root factors were determined to affect the soil: mycorrhizae, exudates (organic acids), turnover (death) of fine roots, and effects on soil morphology. Also discussed were the above-ground factors affecting soil, including foliar leaching (throughfall) and litterfall/decomposition.

Root Requirement from the Rest of the Tree

Roots are constantly interacting with the rest of the tree, namely the trunk, branches, and foliage. The exchange of necessary elements and compounds between the above-ground and below-ground tree components is highly dependent on the rate of nutrient uptake and photosynthesis. For example, the rate of root growth increases with increasing levels of photosynthesis; during photosynthesis the nutrient requirements of the roots, i.e., carbohydrates, ions, and inorganic acids, are met.

Root Export to the Rest of the Tree

Roots export water, N (in the form of nitrate or ammonium), and essential elements, such as Ca, Mg, and Al. The following points were made during the discussions of root requirements and root export:

How can nitrate and ammonium from natural versus acidic deposition be differentiated in the model? The division should be possible using National Atmospheric Deposition Program (NADP) data in the model. Another problem in the model concerns the reaction of carbohydrates as they move down a tree, because carbohydrates react differently in the presence of nitrate versus ammonium.

As pH is lowered in the system, decomposition and mineralization rates slow down. Therefore, decomposition and mineralization rates must be assumed from the literature for different pH levels in the model.

The leakage rate was questioned for carbohydrate transport through the roots. The high estimate for fixed C leakage was stated to be 30%. Due to the association of mycorrhizae and fungi to the leakage, leakage was ignored in the model; replacing leakage with a constant was not acceptable.

8.1.2 Modeling Background

In addition to the workshop, models available in the literature were examined. Models of root growth and mineral nutrient responses are not as developed as are those modeling above-ground processes. The mechanisms of nutrient uptake include the morphological characteristics of root systems; how morphological characteristics change temporally during the course of root development are not well understood. However, understanding these mechanisms is crucial for any calculation of nutrient uptake per unit volume of soil.

Some existing models can simulate branching patterns. A model developed by Lungley (1973) is based on a numerical developmental approach. It differs from its predecessors by taking a disaggregate approach to the root system that focuses on detail at the individual root level rather than modeling system length as a function of biomass. The model was also one of the first to consider root branching as a function of lateral root order. It also emphasizes that elongation rates and inter-branch distances vary between root members of any one order and with respect to time for any one member under uniform conditions. Elongation and inter-branch distances are also strongly influenced by environmental factors, such as temperature, nutrient supply, and soil properties.

Three-dimensional models of growth are even fewer in number. Due to the opacity of the root environment, the task of observing the morphology of a root system while maintaining its spatial integrity is difficult. Henderson et al. (1983) formulated a model in which root growth is considered inherently regular, but the heterogeneous environment produce a final patterns of growth that appear irregular. Based on the detailed spatial measurement of seven excavated root systems, they hypothesized that bends, which are caused by fluctuations and obstructions in the soil environment, and forks, caused by damage to a growing root, are properties of the site and soil type. Conversely, lateral branching is determined by internal mechanisms. They developed an empirical model for the spatial distribution of structural roots at a fixed time, without attempting to describe their development. The rules of the model were evaluated in order to determine which, if any, were unnecessary to produce realistic structural representations. It was observed that the most critical factors influencing realistic simulations were the variances of the fitted distributions describing the morphological events (bends, forks, etc.).

Work on roots has tended to be independent of work on shoot growth except for simple allometric relationships or approaches using root:shoot ratios (Reynolds and Thornley, 1982; Johnson and Thornley, 1987; Mäkelä and Sievänen, 1987). A departure from these approaches has recently appeared in models that attempt to link shoot and root growth (Porter, Klepper and Belford, 1986). However, no models account for localized effects of nutrients (Drew and Saker, 1978) or for soil structure (Russell, 1977), although a start is being made on the description of these effects (see Fitter, 1985; Fitter, 1987).

8.1.3 Modeling Direction

A simulation to predict the change in soil processes must include the processes directly related to biological function, including N and Al dynamics, and soils must be treated as stratified. Attempts should be made to examine physical, chemical, and biological transport processes. The objective of this work has been to construct such a simulator.

8.1.4 Mechanisms of Nutrient Uptake

The rate of nutrient uptake must ultimately be a function of their concentration at the root surface; however, experiments have shown that uptake becomes limiting at concentrations that are usually below that of the ions in the bulk soil solution (Robinson and Rorison, 1983). In most instances the rate of uptake is governed not by the ability of the ions to move across the plasmalemmata of the roots but rather by the rate of ion movement through the soil either in the solution flow generated by transpiration or by nutrient diffusion through the soil water. The same effect can be achieved by root growth into unexploited regions of the soil (Nye and Tinker, 1977). The simulation of nutrient uptake by a plant can be represented by nutrient and root movement through the soil (Baldwin et al., 1973; Baldwin and Nye, 1974; Robinson and Rorison, 1983). The aim of this work is to simulate these two processes and their interaction.

Under these assumptions, Baldwin et al. (1973) formulated an approximate steady-state nutrient transport model. The model, later used by Robinson and Rorison (1983), consists of the following equations (symbols are defined in Table 8-1.):

For transport by solute diffusion only:

$$C_1 = C_{1a} - [I/4\pi Db]\ [1 + (\ln(\pi a^2 L_v))/1 - \pi a^2 L_v] \tag{1}$$

For transport by diffusion with mass flow of solution:

$$C_1 = I/2\pi av + [(C_{1a} - (I/2\pi av))/1 - (av/2Db)]\ [(\pi a^2 L_v)^{av/2Db} - \pi a^2 L_v/1 - \pi a^2 L_v] \tag{2}$$

Table 8-1. List of Symbols for Steady-State Nutrient Transport Model (after Robinson & Rorison, 1983)

Symbol	Definition	Units
C_l	Solute concentration in bulk soil solution	mol/cm^3
C_L	Solute concentration at root surface	mol/cm^3
D	Solute diffusion coefficient in soil	cm^2/s^1
I	Solute inflow rate per unit root length	mol/cm/s
I_{max}	Maximum potential inflow	mol/cm/s
b	Solute buffer power in soil, dMv/dCl	—
L_v	Root length per unit soil volume	cm/cm^3
a	Root radius	cm
v	Water flux	cm^3/cm^3/s

These equations are true if the nutrient depletion zones that extend throughout the volume of soil are occupied by roots; uptake rate is then proportional to L_v. This situation is unlikely for individual roots if they penetrate previously unexploited soil. In such cases, uptake is proportional to the rate of outward spread of the edge of the depletion zone around the root, $2(DT)^{1/2}$ (Baldwin and Nye, 1974).

The differences between root uptake by diffusion only and root uptake via diffusion and mass flow are the subject of the initial explorations with ROOT/SOIL. These differences also characterize the distinction between seedlings grown in experimental conditions (which use uptake by diffusion) and larger trees grown in the field (which use uptake by both diffusion and mass flow). In addition, the organic soils characteristic of red spruce tend to provide nutrients more by diffusion, whereas the mineral soils characteristic of loblolly pine provide nutrients by both diffusion and mass flow. The model can aid in the interpretation of experimental seedling studies and provide insight into the varying effects that soil acidification may have on the soils of red spruce and loblolly pine. In the simulations presented below, the diffusion case is similar to red spruce, and the diffusion plus mass flow is similar to loblolly pine.

8.2 DESCRIPTION

8.2.1 Soil

An integral part of nutrient uptake in soils by roots is moisture uptake. To simulate moisture uptake, knowledge or assumptions about movement in the soil matrix are required. The model can characterize the physical and chemical attributes of the soil matrix. This has involved identification and inclusion of essential physical and chemical soil characteristics.

The environmental spatial matrix (ESM) and the cubic grid components (CGC) from which the ESM is constructed provide a natural means of following the progress of individual roots as they grow through the soil and remove nutrients from the matrix.

The basic form of the physical description of the soil for the grid was suggested at the Forest Response Program Soil-Root workshop in New Orleans. The soil consists of four basic horizons:

- The O layer (organic material)
- The M1 layer (the first mineral horizon; at or near the surface)
- The M2 layer (the second mineral horizon, characterized by the presence of one or more of the following: silicate clay, iron, aluminum, or humus)
- The M3 layer (the third mineral horizon, characterized by carbonates and/or soluble salts, and exhibiting cementation and either temporary or permanent saturation)

The workshop participants determined the minimum complement of physical parameters required to specify chemical and biological processes in soils to be the following:

- bulk density
- soil water potential: direction of water movement
- porosity: pore size distribution
- soil water content: % water-filled/air-filled pores, and
- soil strength.

Bulk Density and *Particle Density* are determined by the primary constituents of the horizon. The bulk density array and the vertical coordinate of the current root tip are passed to the function establish_density. This function calculates a "weighted" density based on the root tip's relative position within the horizon, the average bulk density of the horizon, and the depth of the horizon.

For example, consider a root tip that has grown 5 cm downward in the matrix (relative to a surface position of 0 cm). The O horizon has been defined as being 7 cm in depth, with an average bulk density of 0.7 g/cm^3. The bulk density of the soil at the point of interest is determined as follows:

0.7/7 = 0.1; (the bulk density increment/layer)

ceiling(7/2) = 4; (the relative position within the horizon at which the average density occurs)

5-4 = 1; (the number (positive or negative) of layers to either side of the midpoint layer)

0.7 + 0.1(1) = 0.8 g/cm^3

Soil Water Potential (ψ) is characterized in the manner described by deWit and van Keulen (1972). Based on bulk density, porosity, and the pore space distribution (described below), each layer in the matrix is initialized to a calculated volumetric soil water content. Differences in the soil water content between layers define the potential between layers; hydraulic conductivity and diffusivity of the soil control the volume of water that is exchanged between layers. Net flow between horizons will depend on the potentials of each horizon based on the moisture characteristic (or release) curve of the involved horizons.

Porosity of a given layer in the matrix is estimated using the standard formula:

pore space percentage = 100 - (bulk density/particle density)(100)

This formula provides an estimate of the total pore volume based on the estimated bulk density at the specified depth within the horizon of interest and the average particle density for that horizon (based on its primary constituents).

Thomasson (1978) defined the structure of soil as "the assemblage of aggregates (peds) and voids (pore space) including voids between and within aggregates."

Thomasson uses the term "storage space" to indicate the sum of the terms. Using his work, a description of soil structure is provided by two categories of pore size:

a) Air capacity (C_a) percent of bulk soil volume; pores greater than about 60μm in diameter determine the volume of air equilibrated for saturation to 0.05 bar suction.

b) Available water (A_v) percent of bulk soil volume; pores between 60 and 0.2μm in diameter determine the volume of water held between 0.05 and 15 bar suction.

Pritchett and Fisher (1987) use the terms "noncapillary pores" and "capillary pores" to characterize (a) and (b), respectively.

The two terms summarize important aspects of soil structure. Air capacity reflects the ability of the soil to accept and transmit excess rainfall and to allow exchange of air between atmosphere and rhizosphere; it primarily represents the volume of coarse pores and fissures between peds in structured soils and particles in coarse-textured soils. Available water is the reserve that supports plant growth during periods when potential transpiration exceeds rainfall. It consists mainly of pore space within peds, but it excludes the finest pores that retain water at suctions greater than 15 bar. These fine pores can occupy 30% of the soil volume in clay soils, and as little as 5% in sands.

Two simplifications are combined to provide a reasonable approximation of changes in pore space distribution as a function of depth. The first is based on the empirical findings by many investigators that pore space, particularly those occupied by large pores, is reduced as the bulk density of the soil increases. When this theory is combined with the method used to characterize the bulk density of the grid, an attempt can be made to determine the percentage of noncapillary versus capillary pore space occupying the total pore space at a certain level. This relationship is expressed as:

$$\text{noncapillary space fraction} = e^{-(\text{bulk density estimate} * \text{scaling constant})}$$

Soil Water Content. Once the capillary space fraction has been determined, the initial water content is considered equivalent to that term (i.e., this is the amount of water in retention storage). Water in detention storage will depend on the permeability of the horizons; that is, the water may move laterally to stream channels, or downward to satisfy capillary moisture deficits.

Soil strength, or mechanical impedance, is primarily a function of bulk density and water content. As water content increases, soil strength decreases; however, related air availability also decreases. Decreased soil strength may increase percent root penetrative ability, but reduced air availability may decrease it. As bulk density increases, penetrative ability decreases.

Currently, it is assumed that the anaerobic contributions to bulk density do not amplify the detrimental effects of soil strength on growth; impedance is considered to be a scaling decrement to growth based on bulk density.

8.2.2 Root Growth and Morphology

The model simulates the growth and morphological change of an individual root and the root system according to four categories of morphological change identified by Henderson et al. (1983a); that is, at a given node[1], one of four things may occur:

(1) The root may continue growing in the same vertical and horizontal direction that it did in the previous increment, with

    (a) a lateral initiated at that point, or
    (b) no lateral initiated at that point.

(2) The root might bend, changing its horizontal and/or vertical directional vectors of growth, with

    (a) a lateral initiated at the point of bending, or
    (b) no lateral initiated at the point of bending.

(3) The root might fork into two roots of "equal" dominance, which would continue growing with their own new branching angles and azimuths.

(4) The root might end in a proliferation of small terminal roots proliferating at random away from the terminus.

The data used to estimate the probabilities of these events is from Henderson et al. (1983a).

---

[1] A node has two contemporaneous definitions: (1) a physical node, corresponding to the end of a root, and (2) a temporal node, corresponding to a simulation decision point reached after some specified amount of growth.

For purposes of initial simplicity, it is assumed that there is no lag between the initiation of a lateral and its growth (i.e., it will grow at the same rate as other segments in the time step immediately following its "emergence").

An illustration of how the system is used is graphically presented in Figure 8-1. Figure 8-1 is for a single order 0 root with higher order roots branching from it. Each "dot" represents a temporal/physical node in the growth process, and is labeled for identification. Each "branch" is labeled by the order of branching to which it belongs. Certain nodes are also labeled depending on whether or not bending and/or lateral initiation occurred at that point. The arrows in the lower portion of the figure between node identifiers represent pointers between the nodes; the node nearest the head of a particular arrow is said to be "pointed to" by the node at the distal end of the same arrow. Thus, information that is classified by branching order may also be retrieved in a linear fashion according to the particular root to which it belongs.

8.2.3 Nutrient Uptake Dynamics

8.2.3.1 Diffusion. The equations for diffusion are the compartmentalized flows implied by Equation 1.

8.2.3.2 Diffusion and Mass Flow. The relationship for water movement within a soil column (deWit and van Keulen, 1972) is:

$$\mathrm{Flow}_N = \mathrm{Da}_N * (\mathrm{WC}_{N-1} - \mathrm{WC}_N)/\mathrm{TCOM} + \mathrm{Ka}_N \qquad (3)$$

where Da_N is the average diffusivity between compartments N-1 and N, expressed in cm^2/day; Ka_N is the average conductivity between compartments N-1 and N, expressed in cm/day; WC is the water content of the compartment according to the index, expressed in $\mathrm{cm}^3/\mathrm{cm}^3$; and TCOM is the constant thickness of compartments in the matrix, expressed in cm.

This equation assumes that a volume of soil has been divided into a series of adjacent compartmentalized columns, each having a number of compartments equal to the number of layers in the matrix. Basically, the analysis is a compartmentalization of Equation 2. There is no horizontal movement, a common feature in unsaturated soils in the field (Marshall and Holmes, 1988). Thus, the bulk movement in the matrix can be considered to be the collective sum of movement in each of the columns. The net flow into a given compartment in a given column is the difference of flow into the compartment and flow out of the compartment:

$$\text{NetFlow}_N = \text{Flow}_N - \text{Flow}_{N+1} \tag{4}$$

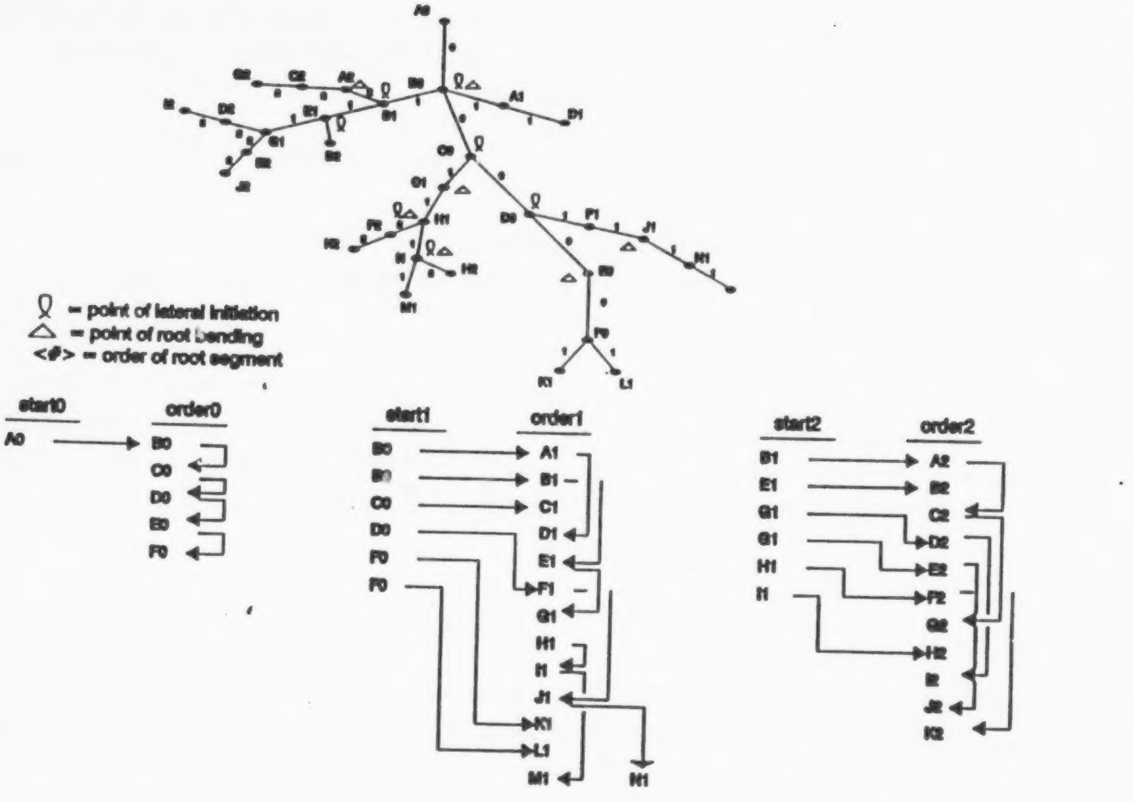
= point of lateral initiation
= point of root bending
<#> = order of root segment
start0
order0
A0
B0
C0
D0
E0
F0
start1
order1
A1
B1
C1
D1
E1
F1
G1
H1
I1
J1
K1
L1
M1
N1
start2
order2
A2
B2
C2
D2
E2
F2
G2
H2
I2
J2
K2

Figure 8-1. Example of root structure representation.

The average diffusivity and average conductivity are calculated using the "wet-weighted" average of the water contents between adjacent layers and are expressed as follows:

$$Da_N = (WF * D_{N-1} + D_N)/(WF + 1), \text{ where } WF = WC_{N-1}/WC_N \quad (5)$$

$$Ka_N = (WF * K_{N-1} + K_N)/(WF + 1), \text{ where } WF = WC_{N-1}/WC_N \quad (6)$$

The diffusivity and conductivity curves are incorporated into the model as tabulated functions; work is currently in progress to estimate these curves based on the pore size distribution data for a given soil. The net flow equation using these values will approximate water movement in the matrix, except at the point where two horizons interface, in which case the flow is calculated as:

$$Flow_N = Ca_N * (P_{N-1} - P_N + TCOM)/TCOM \quad (7)$$

where the potentials (P), at each time-step and for each compartment, are calculated from the water contents with the suction curves of the appropriate soil in each compartment.

The nutrient transport by mass flow equation has limited applicability because it assumes a constant water flux. However, for a highly mobile ion, such as nitrate, which is carried primarily by convection, the flux density of the solute can be approximated by:

$$q_s = q_w C \quad (8)$$

The variable q_s is the solute flux density, q_w is the water flux density, and C is the quantity of the solute in unit volume of solution. If it is assumed, as it has been thus far in the development of the model, that resources within a unit volume of soil are readily available to a given root in that volume of soil, then the removal of nutrient by a given root length will be:

$$N_r = I \, L_v \quad (9)$$

The nutrient removed will be approximated by the solute inflow rate in cm^2/time multiplied by the root length in the volume of soil (in cm/cm^3).

The amount of water removed by transpiration as a function of time is considered to be constant as a function of time and root surface area; it is approximately 2 cm of water per day per cm of root length.

This method of calculating the net mass flow between compartments has an inherent problem. The net flow must be calculated over a sufficiently brief time interval to avoid unstable oscillation about the true functional form. In fact, this time interval has been benchmarked to be on the order of seconds, as opposed to the original simulation time step of one day. This yields untenable run-time durations, an event which prompted the implementation of another algorithm to avoid redundant computation.

A data structure was constructed to maintain a history of those columns in the matrix that had been penetrated by roots. Once this occurs, the column must be monitored at each time step to calculate water and nutrient movement within it. However, if a column has not been penetrated, under the assumptions of the model, it will have the same water and nutrient content as any other unoccupied column in the matrix; therefore, a single movement calculation will suffice for all of these columns. As the matrix fills with roots, the calculation time for the entire matrix will approach the complete enumeration calculation method, but for a sparsely occupied matrix, the computational time savings will be extensive.

8.3 ANALYSIS

8.3.1 Diffusion Case

8.3.1.1 Morphology. Simulations have been made for root growth spreading from a point in a 25cm x 25cm x 25cm block of soil. Figure 8-2 shows the pattern of root morphology after 23 days. The root system is similar to observed systems, although precise assessment techniques, which are not readily available, have not been applied.

8.3.1.2 Nutrient Uptake Dynamics. Estimations of nitrate removal at sequential depths in the soil show quite a disjointed pattern as the root system penetrates to different regions. Figure 8-3 shows nitrate uptake as a diffusion process only; the model was very sensitive to the rate of emergence of lateral roots. Root tips were considered to cease growing if their nutrient uptake fell below a threshold value. A low value of new root tip emergence reduced the exploitation of new soil areas and, therefore, the uptake of nitrogen.

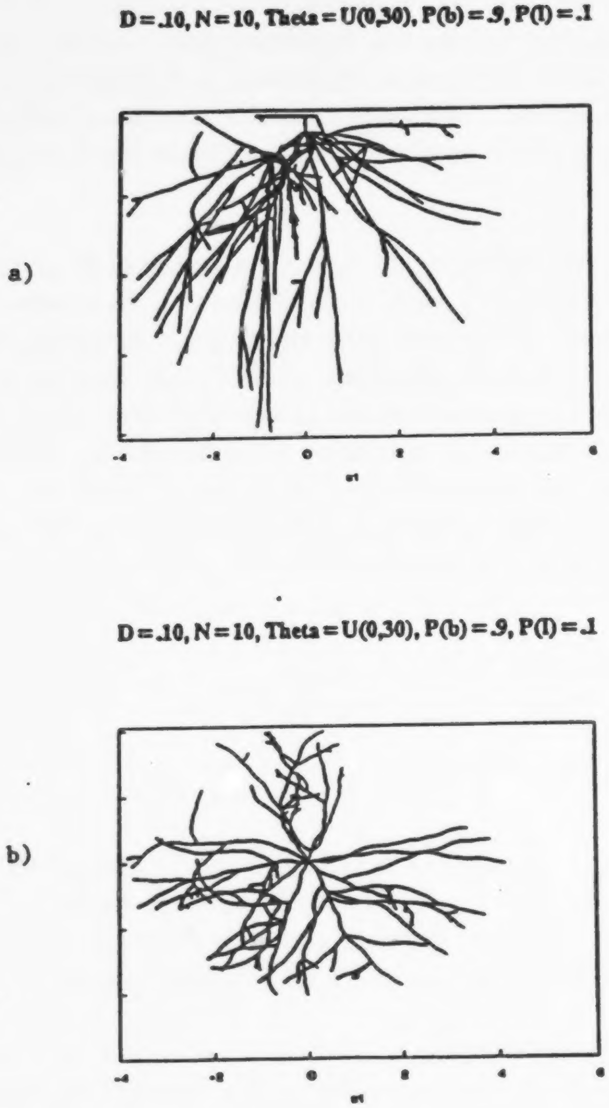

Figure 8-2. Simulated root system after 23 days with nutrient uptake only by diffusion; a) lateral view and b) projection from above.

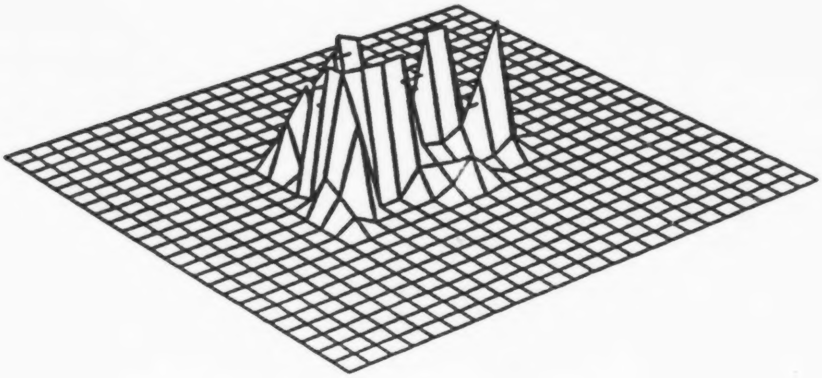

NO$_3$ Uptake Map at 0-1 cm Depth
Diffusion Only

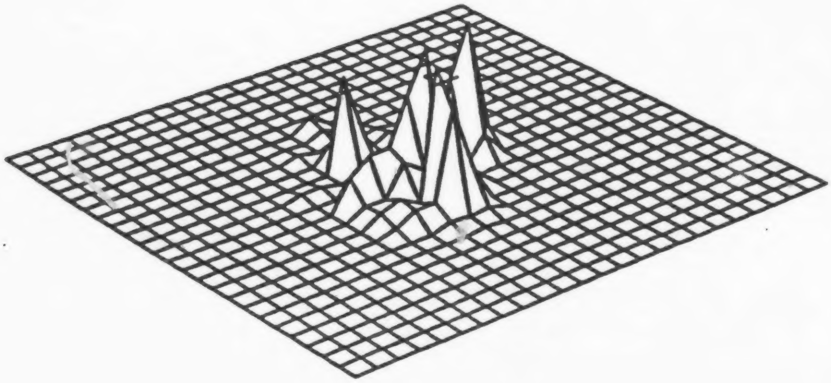

NO$_3$ Uptake Map at 2-3 cm Depth
Diffusion Only

Figure 8-3. Nitrate uptake by diffusion only at various soil depths after 33 days.

NO$_3$ Uptake Map at 3-4 cm Depth
Diffusion Only

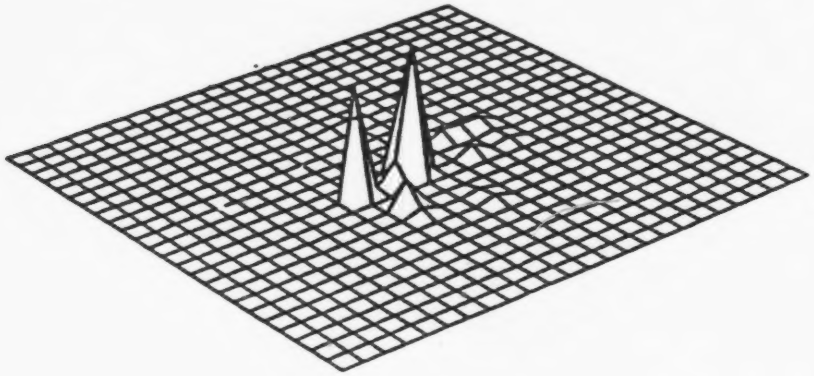

NO$_3$ Uptake Map at 5-6 cm Depth
Diffusion Only

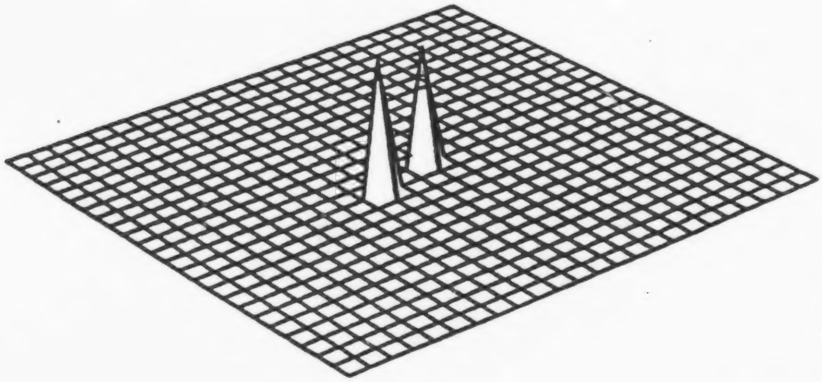

Figure 8-3. (continued) Nitrate uptake by diffusion only at various soil depths after 33 days.

8.3.2 Diffusion and Mass Flow Case

Nutrient removal by diffusion can be markedly contrasted with removal by both mass flow and diffusion. Growth in a southern forest soil that had been classified in four soil horizons (Buol, Hole, and McCracken, 1973) was simulated. A standard rate of water uptake per unit length of root and a uniform root growth rate over the period was specified.

Characteristics of a Southern Forest Soil

Horizon	Depth, cm	Mean Bulk Density	Particle density
O	1	1.43	2.65
A	9	1.43	2.65
B	10	1.51	2.65
C	15	1.29	2.60

8.3.2.1 Morphology. A root growth pattern in which diffusion and mass flow processes occurred for 23 days (Figure 8-4) shows the development of a similar pattern to that obtained with diffusion alone. However, the patterns diverge considerably with more time (more than 40 days).

8.3.2.2 Nutrient Uptake Dynamics. After 35 days, the influence of the incorporation of mass flow into the nutrient uptake equation can be seen (Figure 8-5). There is a less disjointed pattern of uptake, and roots remain in a more central location rather than showing the lateral "exploration" under the diffusion only case.

8.4 APPLICATION

8.4.1 Experimental Seedlings versus Mature Trees

Although the results presented above are only indicative of the differences between diffusion and diffusion with mass flow, they do provide a cautionary note for the interpretation of seedling studies' relevance to mature trees.

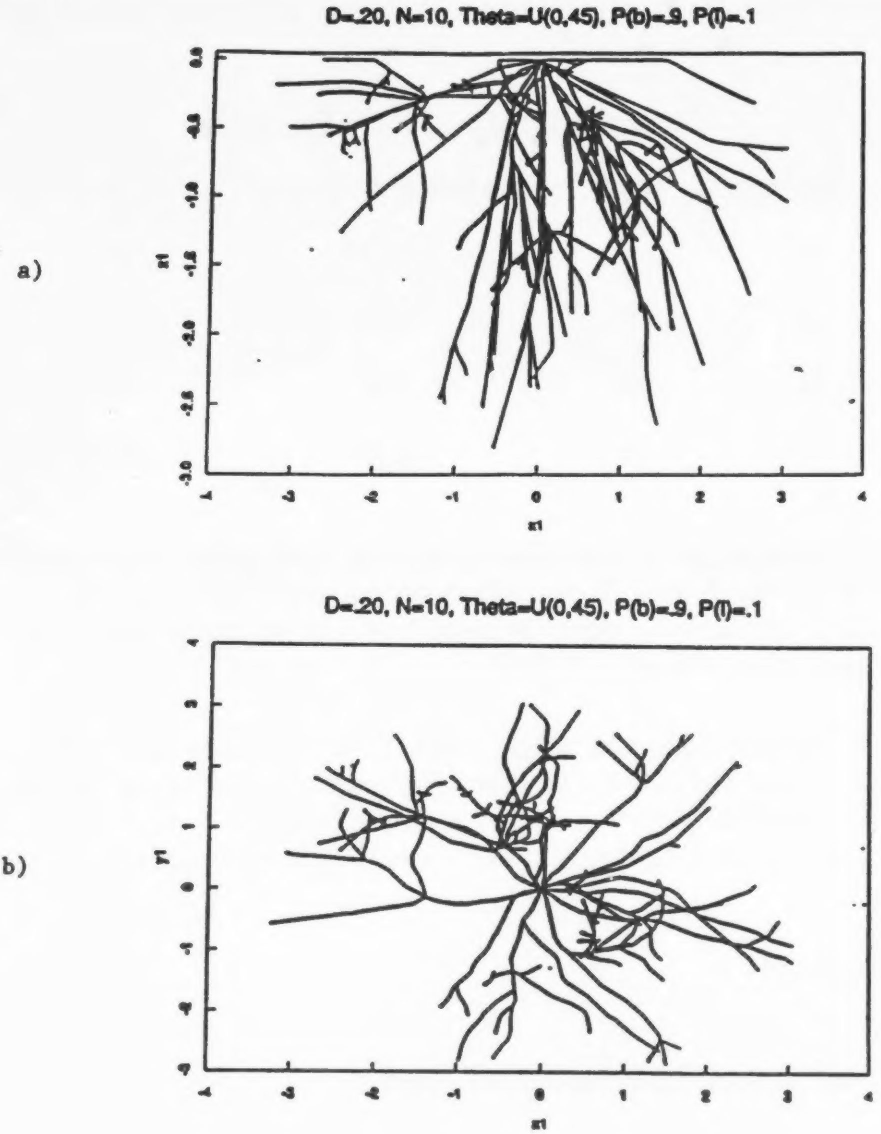

Figure 8-4. Simulated root system after 23 days with nutrient uptake by diffusion and mass flow; a) lateral view and b) projection from above.

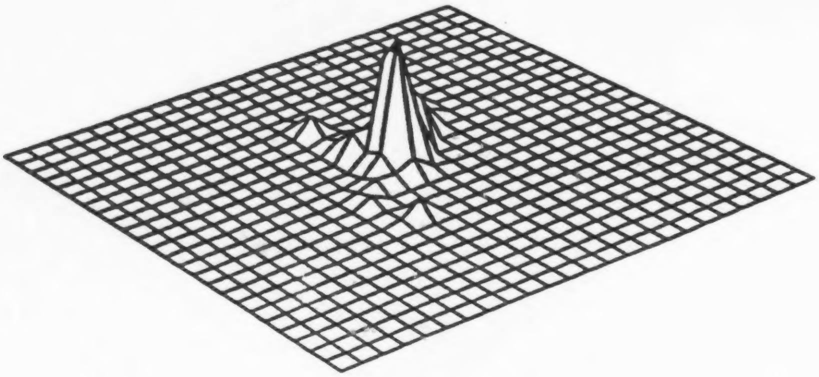

NO$_3$ Uptake Map at 0-1 cm Depth
Diffusion and Mass Flow

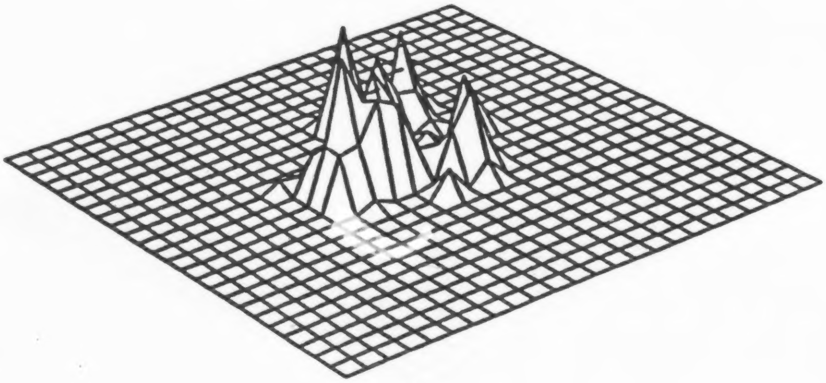

NO$_3$ Uptake Map at 2-3 cm Depth
Diffusion and Mass Flow

Figure 8-5. Nitrate uptake by diffusion and mass flow at various soil depths after 33 days.

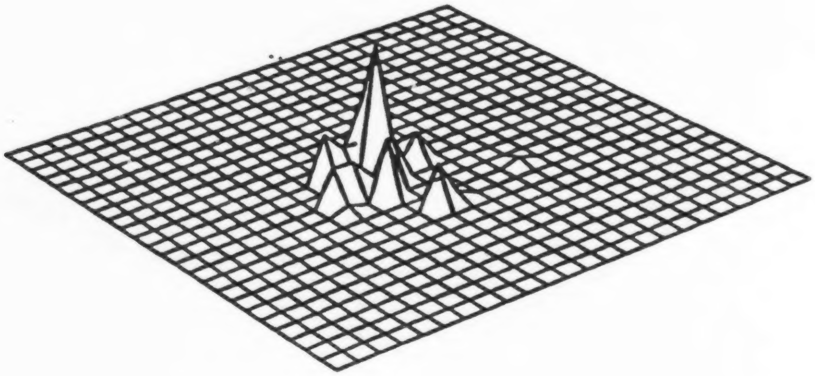

NO_3 Uptake Map at 4-5 cm Depth
Diffusion and Mass Flow

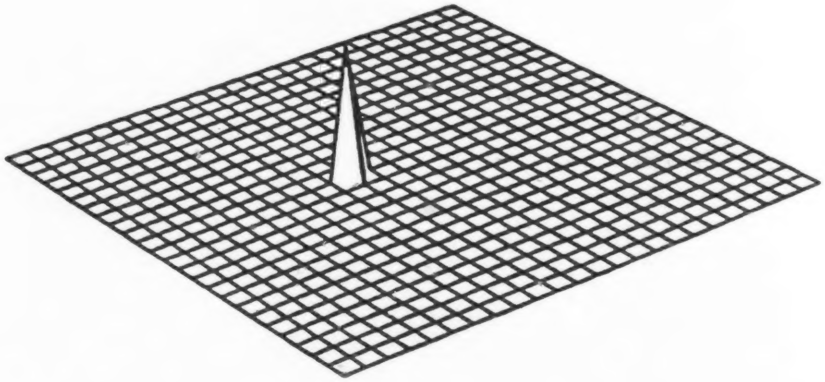

NO_3 Removal Map at 6-7 cm Depth
Diffusion and Mass Flow

Figure 8-5. (continued) Nitrate uptake by diffusion and mass flow at various soil depths after 33 days.

8.4.2 Organic Soils versus Mineral Soils

The results indicate that there may be important differences between uptake patterns shown by red spruce and loblolly pine. This implies that specific modeling efforts for each species will have to be undertaken.

8.5 CONCLUSIONS AND CRITIQUE

These models are still being evaluated. The water movement segment of the model is semi-continuous, the time step used for water potential calibration must be considerably smaller to avoid oscillations to the point of instability. This seems to be an inherent problem in many differential equation-based models and is currently being considered for revision in favor of an algorithm more computationally efficient. In addition, the model requires a substantial amount of run time; for example, even on a Cray X/MP supercomputer; a 35-day simulation took about six hours.

Additional aspects of soil chemistry must be added to the model in order to study the effects of acidic deposition on the root/soil system. Soil water movement is crucial to any consideration of acidification and this is currently the stumbling block to obtaining a usable simulator. The patterns of root growth are not deterministic. Any simulation that was attempted used the same approach as that adopted in the branch models, which was to examine the effects of variability. This would require an assessment of how many runs one needs before approaching a convergence.

SECTION 9. MODEL: WHORL

The precise spatial location of trees affects the rate at which changes in growth and distribution occur. Competition between trees is comprised of two interacting processes occurring over three-dimensional space: 1) resource distribution and acquisition, and 2) growth and resource allocation.

To describe the interaction between these processes, models must define the structural and physiological properties of plants in relation to the environmental factors for which they compete. The models must describe the competition process with respect to different species, changes over time, and different spatial or environmental conditions.

9.1 COMPETITION MODELS

Competition is important in any discussion of the growth rate of forests. Consider x_i individuals in a forest of area A and each with a relative growth rate r_i (mass/mass/time). Then the total growth of the forest, G, for a given period of time is

$$G = (1/A)\ \Sigma^{N}_{i=1} x_i r_i$$

Extensive field studies have shown that the values of relative growth rate (r_i) for individuals are not independent. Spatial correlation can occur in r_i values if competition exists between plants. Pollution can also have an effect on r_i. Experimental studies have identified genetic variability in sensitivity to ozone (MPO #4). The observations of field investigations suggest that natural selection for less ozone-sensitive species may have already occurred (Henderson et al., 1989). During a growth period, some individuals may be more sensitive to ozone than other individuals. The degree to which natural selection can affect forest growth rates needs to be addressed.

Competition and pollution effects can operate as canopy processes, and their effects on *G* (total forest growth) may not be independent. Sorrensen (1989) has constructed a simulator of competition as a canopy process. The simulator can represent pollutant effects as foliage retention and function, and by the relationship between the amount of photosynthate produced by a tree and the tree growth rate.

Past competition models focused on the outcome of competition rather than on the processes involved in competition. Competition determines individual plant size and distribution with the system (Harper, 1967), it and can result in the spatial uniformity of large plants (Ford, 1975) and survivors (Kenkle, 1988). Modeling attempts to reproduce these observed patterns, which can be accomplished using general hypotheses about competition for space (e.g., Bella, 1971; Gates et al., 1979; Ford and Diggle, 1981; Nance et al., 1988; Bonan, 1988). However, the interaction between resource acquisition and growth/allocation is not addressed in these hypotheses. Therefore, the question posed in these models is whether competition is one-sided (i.e., only larger neighbors influence the competitive outcome of smaller subjects), symmetric or asymmetric (i.e., linear or nonlinear interaction), or a first- or second-order interaction (i.e., nearest neighbor or distant neighbors determine competitive outcome).

Harper (1968) noted that plants can respond to competition by changing their form -- a "plastic" response. Plasticity is an inherited characteristic (Khan et al., 1976a; 1976b). In trees, plasticity has been observed in the physiological characteristics of upper versus lower canopy foliage (Leverenz and Jarvis, 1980), stem height-diameter allometry (Cannell et al., 1984), and shoot extension (Franco, 1986). These observations suggest an ability to respond as proposed in the modular theory of growth (Franco, 1986), which describes plants as having components that respond differentially to environmental stimuli such as resources or contact with another component. According to this theory, a plant does not compete with its neighbors; rather, components of a plant compete with and respond to components of its neighbors or of itself. This theory requires the consideration of multi-dimensional interactions of neighboring plants, a consideration emphasized by the mathematically rigorous definitions included in the overlapping disk model of Gates et al. (1979). Multi-dimensional interactions imply that the effect of one neighbor on a subject may depend on other neighbors of either or both trees. The exact pattern of plant space overlap, or the determination of precisely which components of the subject and neighbors interact, is needed to predict the outcome under plastic growth. This specification is required to predict the potential effects of pollution relative to the competition process.

9.1.1 Statement of the Problem

The basis for the above discussion of features that must be included in a mathematical model of competition is the conceptual model of competition. The conceptual model presents competition as a process in which resource acquisition and growth/allocation are linked over time (Figure 9-1). The structure of a tree determines its acquisition of resources within the community. The allocation of those resources determines the new structure of the plant and its capacity for future resource allocation.

Linking these two processes is particularly important when competition spans several phases of community or stand development, when the primary insufficient resource is assumed to be light, and when trees are the population that is modeled.

These factors are important because crown plasticity implies that the growth process dynamically affects the resource acquisition process. Growth with plasticity is not simply described by height or stem diameter increment. Furthermore, models based on competition for space that describe plant space and growth without considering plasticity, ignore the second link between resource acquisition and growth and allocation. They repeat the first link over time:

resource acquisition = fn(height, neighbors) ———> height growth,
resource acquisition = fn(height, neighbors) ———> height growth.

Incorporation of plasticity dramatically influences the model form.

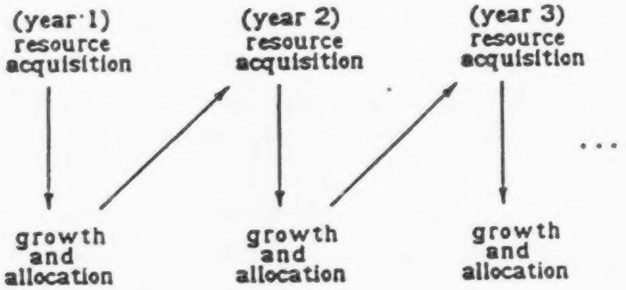

Figure 9-1. Competition represented as a two-part process. The structure of a tree determines its acquisition of resources within the community. The allocation of those resources then determines the new structure of the plant and its capacity for future resource acquisition.

Because competition mechanisms cannot be assumed to stay constant over time, they must be studied under different conditions that influence any interactions of spatial pattern and growth phase effects, such as those suggested by Cochrane and Ford (1978) and Kenkel (1988).

The model WHORL represents both of the component processes of competition represented in Figure 9-1. The model provides sufficient detail to link these processes together over time. Plasticity and multi-dimensional interaction are incorporated. This requires some degree of biological specificity (e.g., for a particular species or time phase), but it results in an increased ability to describe different spatial patterns and growth phases.

Competition indices usually characterize the above-ground space that a tree occupies in one of three forms: the two-dimensional form, the area potentially available (APA) form, and the three-dimensional form.

The most common form is two dimensional; a projection of the calculated space occupied by a plant onto the x,y plane (Bella, 1971; Ek and Monserud, 1974; Gates et al., 1979; Bonan, 1988). Overlapping disk models comprise the largest group of this form. Each tree is assigned a disk-shaped zone representing its assumed crown projection; the disk radius is typically proportional to height or stem diameter. Neighbors are defined as two trees having overlapping disks, with the overlapped portion divided according to their relative sizes. The usable zone of a tree is determined by removing or "downweighting" the disk area occupied by neighbors. The usable zone, or a comparison of it to the tree's original area (e.g., a ratio), becomes the competition index. Mitchell (1975) makes a similar comparison by applying the ratio of the foliage volume available to the foliage volume of an open-grown tree. The volume available is calculated by assuming that crown length is altered symmetrically by neighbor interaction. Because of this assumption, the ratio of two cone surfaces equals the ratio of the two disk projections; the latter ratio forms the competition index. Thus, although the estimation of foliage volume is an important conceptual difference between these models, the actual comparison of available to potential volume is quite similar.

The second model form, area potentially available or APA (Moore et al., 1973; Nance et al., 1988), recognizes that the space an individual tree occupies can extend beyond its crown radius. Non-overlapping polygons are constructed around each tree by drawing perpendicular tessellations between the subject and each of its near neighbors. A tree uses the area within its polygon. The tessellation is generally located between the subject and its neighbor according to their relative sizes, allowing more space for the larger tree (Moore et al., 1973). The location may also be constrained in proportion to the expected crown radius of an open-grown tree (Nance et al., 1988). A crown radius constraint ensures that available space is not extremely angular, and it also allows for the possibility that some of the resource space may go unallocated to an individual. Without a constraint, all space is allocated.

The third model form considers the three-dimensional plant structure (Ford and Diggle, 1981; Hatch et al., 1975). The size of a plant is assumed to decrease according to the degree to which the "cones of influence" of larger plants overtop it. The angle of the cones of influence can be a function of sun angle (Hatch et al., 1975), species, or time and stage of competition (Ford and Diggle, 1981). The three-dimensional models recognize the three-dimensional nature of crown competition, but they assume uniform crown geometry with only size varying. In addition, they address only one-sided interaction.

9.2 DESCRIPTION

Crowns are usually asymmetric and differ in structure with size. This assumption clearly departs from the assumptions required of two-dimensional models (e.g., Gates et al., 1979; Ford and Diggle, 1981). Furthermore, the exact position of trees, relative to clumps of trees or more open areas, affects the shape of the crown. These consequences of crown plasticity govern the model form. A model must describe the multiple interactions of trees in three dimensions. Incorporating these ideas over time results in a tree-growth algorithm such that crown components first grow in response to the detailed pattern of resource acquisition and then create the new pattern for the following year.

WHORL represents a tree as a series of whorls stacked along a center axis (Figure 9-2). Interaction between trees is primarily described by the interaction between whorls that overlap either horizontally or vertically. This interaction consists of a reduction in foliage density and radiation flux in the area of the overlap. The interaction between overlapping foliage from different trees is considered in successive cubes down through a vertical column and radiation intercepted in that cube is apportioned to the parent tree of that foliage. Foliage density and available radiation determine the interception or resource uptake at each point in the tree. Growth of each tree is related to the total radiation intercepted and new growth produces a new structure for the next competition cycle. Foliage receiving radiation below a fixed level is assumed to die.

This pattern determines growth, which can occur independently among whorls and among sectors of a whorl that represent branches. In the discussion below, pollutants are considered to be capable of influencing foliage longevity (and thus, the canopy interaction process) as well as the conversion of resource uptake into growth, which is represented as the production of a new height increment.

The calculation of multiple interactions between whorls is greatly simplified by dividing the plot into a grid of three-dimensional cells. The model looks at one cell at a time, determines which whorls overlap the cell, and then assigns radiation interception within that cell to those whorls. The cell-by-cell approach simplifies the tracking of irradiance levels as radiation passes through cells in the canopy. The cell's x, y, and z dimensions are chosen to balance the speed of the model program with the accuracy in assigning areas to whorls.

9.2.1 Assumptions

A model is defined by the list of all its assumptions, a feat exemplified by the competition models of Gates et al. (1979). The assumptions of the WHORL model areas follows.

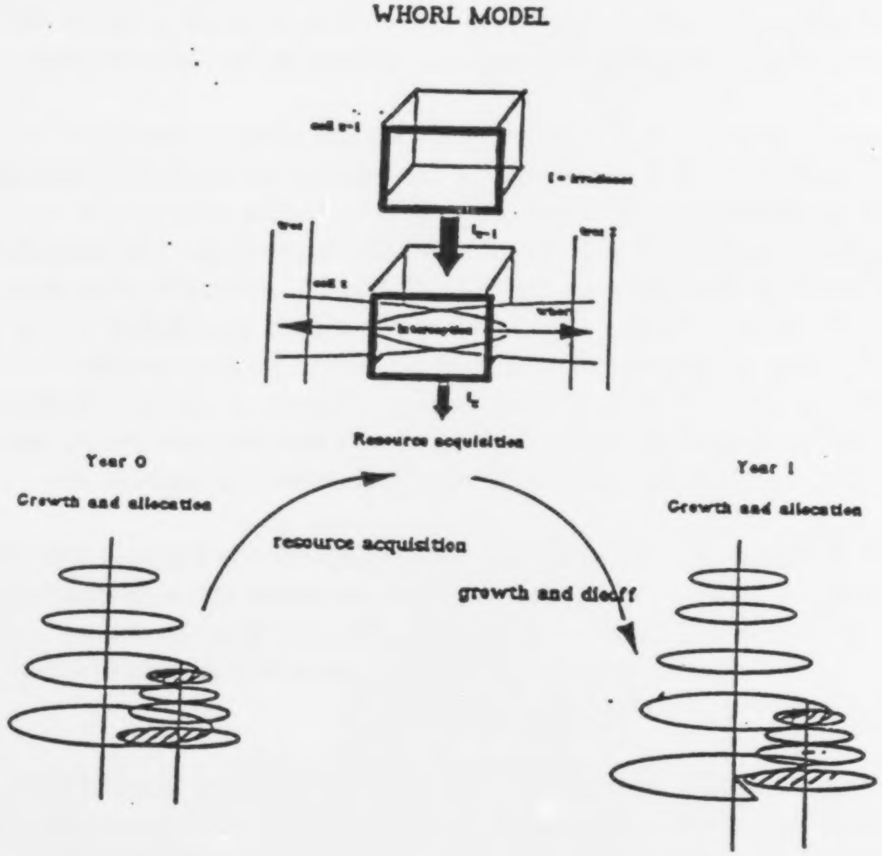
WHORL MODEL
Resource acquisition
Year 0
Growth and allocation
Year 1
Growth and allocation
resource acquisition
growth and dieoff

Figure 9-2. Representation of the process of canopy interaction in WHORL. The interaction between overlapping foliage from different trees is considered in successive cubes down through a vertical column and radiation intercepted in that cube is apportioned to the parent tree of that foliage. Growth of each tree is related to the total radiation intercepted and new growth produces a new structure for the next competition cycle. Foliage receiving radiation below a fixed level is assumed to die.

(1) *Competition for radiation: Competition for radiation dominates competition for other resources. Radiation, direct beam and diffuse, enters the canopy from directly overhead. Radiation entering at an angle is assumed negligible to simplify the computation.*

Directional radiation may influence competition but insufficient data are available to address this issue. This approach tackles other aspects of radiation first, such as foliage distribution, and then looks for evidence of a directional radiation effect in model residuals.

(2) *Competition between foliage elements: Competition for radiation occurs when foliage elements receive a reduced amount of direct radiation because of interception by other foliage elements.*

Competing foliage elements can occur on the same tree or on different trees. However, because of the first assumption, competing elements can only be directly vertically aligned or co-occurring in the same small volume.

(3) *Fractional interception: Each unit volume of a foliage element acquires and removes a fraction of the radiation present at its particular location. This fraction is the interception rate of the foliage.*

(4) *Crown structure.*

(a) *A tree crown is considered to be a series of two-dimensional whorls located at discrete points along a vertical axis.*

This representation differs from the more traditional solid cone representation in several ways. First, a solid cone gives greater importance to foliage on the outer surface of the cone than to foliage on the interior of the cone; the foliage on the outside of the cone creates a continuous surface that blocks radiation from the internal foliage. With discrete whorls, the unoccupied space between the whorls allows more radiation to the inner parts of the whorl than to the surface, which for some species is more realistic. Second, the whorls correspond to a history of height growth increments. This structure facilitates the incorporation of dynamic allocation to height growth versus branch extension. Third, different mean inter-whorl increments assign different individual crown densities in a natural manner. Kellomaki (1986) found branch densities (number of branches per unit bole length) of suppressed scotch pine (*Pinus sylvestris*) to be significantly higher than those of dominant trees. Finally, the location of the whorls can be used to more clearly represent the foliage overlap between trees; a whorl that partially extends directly above another whorl will have a vertical advantage. As discussed above, the vertical location of whorls are considered at some finite resolution, such as 10 cm, so that if two or more whorls overlap within this distance, no particular whorl is given a vertical advantage.

(b) *Whorls are initially formulated as a disk with four sectors that can function (grow or die) independently. A whorl is initially formulated with a constant foliage density representing an average of the foliage density generally clustered about a branch. This density changes as self-shading and competition are taken into account.*

To mimic branch distribution, the angle of orientation of each tree's sectors is random. This orientation is shifted by $\pi/4$ for alternating whorls of a given tree.

(5) *Foliage representation: Foliage is represented by the interception rate per area (r) and the efficiency of foliage in converting intercepted radiation to photosynthate.*

Transmittance of light through a whorl can be calculated based on the leaf area index using $P = \exp(-kLd)$, where P is the probability or rate of transmittance, L is leaf area density, d is the path distance through the foliage in the direction of the light beam, and k is the fraction of leaf area projected on a plane normal to the beam (Norman and Welles, 1983). If reflection is assumed negligible, there is a one-to-one correspondence between the interception rate, $r = 1 - P$ (see assumption 3 above) and foliage. Therefore, the interception rate is modeled as an analog of foliage density and the changes in interception rate are assumed to represent changes in foliage density.

The second attribute considered, foliage efficiency, is represented as a factor that converts intercepted radiation into photosynthetic uptake. That is, $uptake = rIE$, where I is the radiation flux and E is the efficiency factor. The efficiency of the foliage (e.g., shade foliage versus sun foliage) is a physiological attribute that may be affected by tree or branch status. Although the relative efficiency of all foliage is kept constant in this model, increased efficiency of shade foliage in very low radiation levels is considered in the calculation of foliage die-off with reduced radiation. That is, the density of shade foliage (and its interception rate) decreases more slowly under low radiation than does sun foliage.

(6) *Foliage die-off: Foliage density decreases with decreasing radiation at a rate dependent on the height class of the tree.*

This parameter was manipulated to simulate the effects of pollution. In the subsequent data analysis, it was observed that suppressed trees maintain and produce foliage at much lower levels in the canopy than medium and large trees. The physiological basis for longevity and photosynthetic efficiency of shade foliage is shown by Leverenz and Jarvis (1980).

(7) *Conversion of interception to uptake: Uptake is assumed to be a linear function of interception.*

Although the relative efficiency of photosynthate conversion may vary due to individual tree age and radiation environment, the relative efficiency of all foliage has been set at one to reduce the number of model parameters.

(8) *Sector growth and death: An entire sector grows as a function of its radiation environment and dies if this local environment is too poor to support the hypothetical branch wood.*

While the natural processes of branch extension and death are determined in part by the *net production* (i.e., production minus maintenance), a *relative production* measure of the form production/maintenance is used, where production and maintenance do not have to have the same units. Two measures are investigated. *Uptake per unit foliage* represents the requirements of maintaining foliage. *Uptake per unit area* of the sector represents the maintenance cost of large sectors. Large sectors, regardless of how full or scant the foliage is, have considerable maintenance costs. The radius of a sector grows as a function of the relative production term and dies if relative production falls below a specified level.

(9) *Height extension is a function of the relative production of the entire tree or of the top several whorls.*

Height extension is assumed to be a whole-tree response. It is affected only by the total amount, not the spatial distribution, of the resource acquisition. Therefore, biomass growth can be determined by measuring the *volume growth due to height increment*, defined as *Vgr.h*. Bole volume is calculated as the volume of a cone such that

$$Vgr.h(cm^3) = 1/3\pi (Diam_{initial}/2)^2 (H_{final} - H_{initial}) 100\ cm/m$$

(10) *Tree mortality: A tree dies when all its whorls have died.*

9.2.2 Calculation

9.2.2.1 Initialization of tree crowns. Predicting growth is often the objective, given the current size and spatial pattern of a particular data set. Thus, the current crowns must be estimated by assessing the effects of competition in the past. The relationships between tree height and crown shape are estimated from branch data collected from a section of the stand independent of that being modeled. The model then initializes crown structure for each tree based on its current height and the following crown shape relationships.

Mean inter-whorl distance:

$$\overline{dw} = \beta_0 + \beta_1(Height)$$

Crown apex angle coefficient (determines whorl radius at a given height):

$$cac = \exp\{\beta_2 + \beta_3(Height)\}$$

Crown length:

$$crlen = \beta_4 + \beta_5(Height)$$

These crown parameters specify the radius and position of each whorl assigned to a tree. However, the position of each whorl is constrained so that it occurs only at one of the horizontal layers created by the grid.

9.2.2.2 Interception. An initial radiation flux enters any cell at the top of the canopy (canopy depth $z = 0$) and, if unintercepted, passes through to the cell directly beneath it and continues through the vertical column of cells. When whorls from one or more trees are present, a fraction of the radiation is intercepted and assigned as *uptake* to the whorl sectors involved. Unintercepted radiation is passed down to the next cell (see Figure 9-2).

$$I_z = I_{z-1}(r - 1)$$

where: I_z = the current irradiance level μmoles/m^2/sec^1;
I_{z-1} = the level of irradiance incoming from above; and
r = the current interception rate for a single unit of foliage.

Let I_0 equal the full irradiance level above the canopy. The interception rate, r, *is a* function of radiation flux. At canopy depth z, the single interception rate is given by:

$$r_z = R(I_{z-1}/I_0)^K$$

where: R = maximum interception rate for foliage living in full radiation ($0 < R < 1$);

K = coefficient of decline of interception rate with radiation level ($0 < K_2 < 1$);
D = flux at which there is no living foliage, μmoles/m^2/sec. (If $K = 0$, the interception rate is constant at R).

Thus, radiation interception at progressively lower whorls is reduced by two factors: lower available radiation and lower interception rate. This form differs from current canopy radiation models (Norman and Jarvis, 1975; Oker-Blom and Kellomaki, 1983; Oker-Blom, 1986; Wang, 1988) in that foliage density is determined by the local radiation environment rather than being assumed in the form of a stochastic distribution or a function of canopy depth.

When the number of whorls occupying a volume, *nshare*, is greater than one, the whorls collectively intercept the same amount of radiation as *nshare* whorls occupying different vertical levels. The total interception (*TI*) is calculated and allocated equally between all of the *nshare* trees. Interception rate *r* is assumed constant within a cell, so total interception by k whorls is given by:

$$\begin{aligned} TI_k &= I\,(r + r(1-r) + r(1-r)^2 + \ldots + r(1-r)^{\wedge k}) \\ &= I\,(1-(1-r)^k) \end{aligned}$$

9.2.2.3 Annual Growth. After interception is calculated over all cells on the entire plot, the new height increment is predicted as a function of total uptake for a tree or uptake obtained only in the upper whorls. A new whorl disk is assigned at the old height. This new whorl is assigned a radius in accordance with the *cac* (crown angle coefficient) of its new height using the *cac* equation above. The radius of each sector of each whorl is extended as a function of its relative production. Similarly, the radius of a sector is permanently set to zero (sector death) if its relative production falls below a specified constant. The model repeats these processes using the new crown specifications.

9.3 ANALYSIS

WHORL was initially developed for use on a highly heterogeneous naturally regenerated stand of pacific silver fir (*Abies amabilis* (Douglas) Forbes). Before the removal of the adult trees 30 years prior to this study, the young trees occurring through natural regeneration were suppressed and were probably of similar size but of different ages. The spatial pattern is believed to have been aggregated and very dense.

9.3.1 Comparison to the APA Model

The parameters in WHORL are not assumed to be constant for different spatial conditions. Rather, how parameters change is investigated. However, data are available to estimate reasonable values, at least for the stand of white fir. In addition to indicating a range of parameter values, these data also provide a baseline by which to compare parameter differences. The following parameter estimates were used.

Rmax = 0.2: This is expected to be a constant for each species (and perhaps plot time stage); i.e., the portion of radiation intercepted by a whorl not under any competition is independent of plot history.

K, D: Note that K and D within {0.01 to 0.3} and {0 to 4}, respectively, are reasonable when radiation attenuation is considered.

Crown shape given height: This parameter depends on plot history, but here the crown shape estimates are based on single clumps of the trial woodland, and then compared with another crown shape relative to height that is designed. Plots with different spatial structures were available.

Tree class: Classes of trees with the same foliage survival at low radiation levels.

Sector die-off: This is dependent on Rmax, K, and D.

The model was extensively evaluated under the condition where whorls were represented as single discs (Sorrensen, 1989) rather than as four component sectors. A split-plot technique was used where parameters were estimated in one part of the plot and estimates were made on the other part. This was done for two plots with different densities and spatial arrangements of trees. The model was assessed on the basis of variation accounted for in predicting growth, including the spatial correlation of residuals and the prediction of crown length and light attenuation profiles. In assessing the predicted versus measured variables, particular attention was given to non-constant variance by plant size and non-normality of residuals, because of the wide range of plant densities involved and the potential for substantial change in the process of competition. An examination of WHORL was also made relative to the Area Potentially Available (APA) model of Nance et al. (1988). This comparison is interesting because of the following:

- WHORL produces a weighted three-dimensional crown area, but APA produces an unweighted "free from competition" two-dimensional area.

- WHORL uses heights of the trees, but APA bases its tessellation locations and constraining crown projections on tree diameter.

- WHORL assumes crown plasticity (die-off and altered height/branch extension relationship), but APA assumes a linear relationship between diameter and crown projection radius.

- WHORL uses multiple interactions to define neighbors, but APA uses a predominantly pair-wise definition.

WHORL: Several sets of interception parameters gave reasonable light attenuation and growth prediction, but among these no single set has emerged as clearly superior. Therefore, these sets, and others, continue to be observed in model runs. Crown parameters, *cac*, *crlen*, and *dw*, were kept as constant functions of height, as estimated from regressions of independent crown data.

APA: The model, and its assumptions, were used to specify the slope and intercept for what seemed to be a reasonable crown radius for open-grown trees: $radius(m) = 0.1 + 0.14 * D85(cm)$, which corresponds to a 1.5-m radius for a 6-m-tall tree. The default values for "density factor," a factor that diminishes the open-grown crown radius to reflect the density of the plot, were kept as specified in the model. The resulting radii may have been small because the map of APA on the plot left large gaps of no coverage, which is inconsistent with the data. However, use of larger crown radii gave much poorer predictions. Some of the smaller trees had to be removed for the model runs on one plot in order to fit within the limit of the APA program. Each model run was made using all trees in a given plot; only the non-border trees were used to predict growth.

Scatter plots of *predicted volume growth* on three predictor variables (uptake, APA, and initial volume) indicated linearity; data could be combined between plots. The only exception was four large trees that enhanced the range of any predictor, which suggested some nonlinearity. Consequently, the two transformations in addition to the untransformed data were examined:

(1) all trees - square-root transformation on both variables to include the influence of large *Vgr.h* values but to limit their potential bias; and

(2) untransformed data with trees having *H85* between 3 m and 5 m.

9.3.2 Variation Accounted for in Growth

Regression results are given in Table 9-1 for a two-year measurement and prediction interval. The square-root transformation gives the best overall comparison of the two models.

Table 9-1. Regression Results: Volume Growth over Two Years Simulated as Two Successive One-Year Periods

	WHORL	APA	Initial Volume
Transformation	R^2	R^2	R^2
Untransformed	0.85	0.75	0.84
Square Root	0.89	0.76	0.89

Two common problems are associated with competition models. These models are fitted to data from stands that have reached a certain size distribution, and they assume that the size of a tree is a good predictor of future growth. Competition models must provide the additional information that determines how size may *not* be a good predictor and how the status of a tree will change due to the effects of its neighbors. Table 9-1 indicates that initial volume is less effective in distinguishing potential variation in future size among large trees than among the whole population. This is because the conditions of canopy competition change more rapidly for large trees (i.e., from fully illuminated to partial shade) than for other trees, and this change depends upon neighbor proximity, not upon current size. For smaller trees, neighbor proximity has at least some impact on current size. WHORL captures the changing canopy process, APA does not.

9.3.3 Ten-Year Simulation to Compare Shade-Tolerant and Intolerant Canopies

Table 9-2 gives the corresponding partial R^2, i.e., the additional variation accounted for by the model when initial volume is already in the regression equation. The multiple R^2 is also given. For WHORL, these can be compared for improvement over the values in the Initial Volume column of Table 9-1. In the APA regression, there are slightly fewer trees (48 non-border trees shorter than 1 m were left out) and the R^2

values for initial volume for the untransformed and square root regressions are respectively (0.83, 0.88), a 0.01 reduction due to the removal of the small trees. For this situation, WHORL has substantial improvement over APA as a predictor of volume and, therefore, of height increment.

Table 9-2. Regression Results: Volume Growth Given Volume

	WHORL	APA
Transformation	$R^2(u,v)$ $R^2(v,u)$	$R^2(u,v)$ $R^2(v,u)$
Untransformed	0.32 0.89	0.04 0.84
Square Root	0.44 0.94	0.06 0.88

A simulation was created by constructing a 6 m x 6 m plot and placing various densities and arrangements of trees on it. Competition across plot edges was simulated by wrapping the plot as a torus. The growth of three stands was simulated for 10 successive years at the thickest stage of stand development and when any thinning effect would be expected to be at its maximum. All plants were given an initial height of 1 m. The simulations were duplicated for shade-tolerant and shade-intolerant conditions of foliage retention. Although simulations of red spruce and loblolly pine were not attempted, generally red spruce is considerably more shade tolerant than the pine. The stand conditions were as follows (Table 9-3):

(1) 100 trees in a square lattice;
(2) 100 trees in a random arrangement; and
(3) 300 trees in a random arrangement.

Table 9-3. **Stand Parameters After 10 Years of Growth for Shade-Tolerant and Shade-Intolerant Conditions of Foliar Retention at 3 Patterns of Stand Establishment(ΣF = Leaf Area Index; m = mean height; ΣB.A. = basal area in cm^2)**

Condition	100 regular trees	100 random trees	300 random trees
Shade tolerant foliage death = (4.0μ moles/m^2/sec)			
ΣF	11.7	11.75	12.0
Mean height	4.35	3.83	3.1
ΣB.A.	3052	2406	4223
Mean B.A.	30.52	24.06	14.1
Dead	0	0	0
Shade-intolerant foliage death = (10.0μ moles/m^2/sec)			
ΣF	8.85	8.79	8.89
Mean height	4.35	3.89	3.14
ΣB.A.	3051	2516	4368
Mean B.A.	30.51	25.16	14.5
Dead	0	0	0

The most obvious differences are between the amount of foliage in shade-tolerant and intolerant canopies; these differences were consistent between the establishment patterns. For both conditions, the 300 random trees had more foliage than the 100 random or regular spaced trees, suggesting slightly more efficient space packing. The effect of planting regularity in reducing competition and inducing more even growth is seen in the greater mean and total basal areas of the 100 regular compared with the 100 random trees. For both shade-tolerant and intolerant conditions, the 300-tree arrangement, while having smaller mean height and smaller mean basal area, had a greater total basal area. For the two conditions where competition is occurring, i.e. the random arrangements, the intolerant canopies produce slightly greater basal areas. In contrast, the additional foliage created in the tolerant canopy, while being a cost, actually absorbs very little additional radiation.

A comparison of stand structures between the three simulated shade-tolerant conditions simulated is shown in Figure 9-3. The differences in crown structures for large and small trees reflect differences in the intensity of competition. Crown structures of the same trees in a given spatial arrangement grown under the shade-intolerant conditions were almost identical when graphically represented.

9.4 APPLICATION

Two possible pollution conditions were considered: (1) an increase in the rate of foliage mortality, which was simulated by a 25% increase in the radiation level at which die-off occurs; and (2) a decrease in growth, which was simulated by a 25% decrease in the efficiency of translating intercepted radiation into tree height increments.

A reduction in foliage occurred in all six plots, creating a very mild thinning effect (Table 9-4). Very small increases occurred in basal area in both the shade-tolerant and intolerant plots. The other attempt to simulate pollution, a reduction in the "conversion" of radiation to growth by 25% on 50% of the trees, had a more dramatic effect.

Although foliage amounts were slightly increased, the most notable effect of this treatment was the reduction in basal area and, on the plots with 300 randomly distributed trees, the mortalities of 17 shade-tolerant and 50 shade-intolerant trees (Table 9-5). The range of final sizes was also greater under these treatments, and this reflected both lower minima (as would be expected) but also greater maxima, as some trees responded to the suppression "release" when the growth of neighbors was impaired (Figure 9-4). Although the canopy still develops effectively (and the reason(s) for the increases needs more study), the decline in growth rate of smaller trees cannot be compensated for by the growth of larger ones, at least under this range of treatments. A simulation combining both "pollution" treatments was dominated by the effects of the growth efficiency reduction. At these levels of the parameters no synergistic effect occurs.

9.5 CONCLUSIONS AND CRITIQUE

The model predicts the effects of reducing the growth of trees in some important respects. The model results are very similar to those found when making a thinning, and growth rate of some individuals increases because of the "release" from competition with neighbors. However, where individual growth conversions are reduced, the greater mean growth achieved by a few trees does not compensate for the loss of those "treated." Precise boundaries need to be established for these interactions.

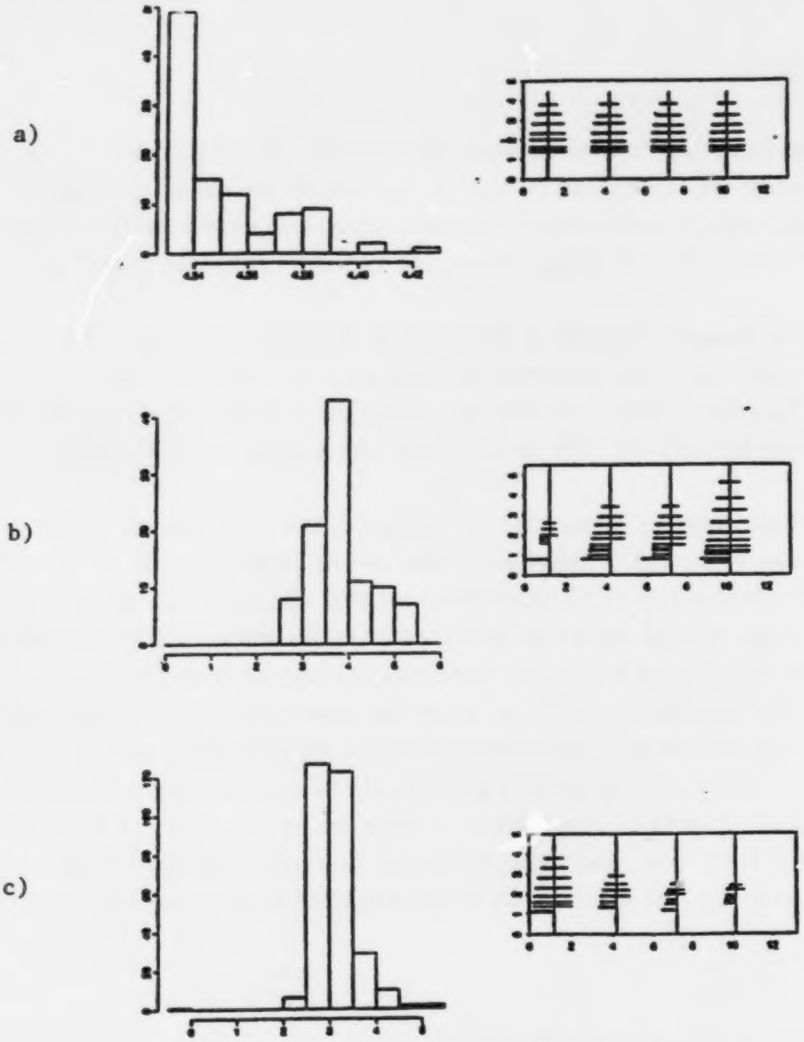

Figure 9-3. Height frequency distributions (note differences in scales of ordinates) and crown structures of four sample trees for each of initial spacing patterns, shade-tolerant foliage; a) 100 trees at equal spacing; b) 100 trees at random spacing; c) 300 trees at random spacing. Ten-year growth with all trees initially 1 m. The crown structures are spaced further apart than on the plot where extensive foliage overlap occurs.

Table 9-4. **Simulated Effects of Pollutants on Stand Growth over 10 Years under Three Different Spacings or Initial Distribution Patterns. The level of radiation at which foliage died was increased by 25% on half of the trees randomly selected (SF = Leaf Area Index; m = mean height; ΣB.A. = basal area in cm^2)**

Condition	100 regular trees	100 random trees	300 random trees
Shade tolerant			
ΣF	11.3	11.53	11.7
Mean height	4.35	3.84	3.1
ΣB.A.	3053	2418	4236
Mean B.A.	30.53	24.18	14.12
Dead	0	0	1

Table 9-5. **Simulated Effects of Pollutants on Stand Growth over 10 Years under Three Different Spacings or Initial Distribution Patterns (SF = Leaf Area Index; m = mean height; ΣB.A. = basal area in cm^2. Uptake -> Growth was decreased to 25% of baseline on 50% of trees.)**

Condition	100 regular trees	100 random trees	300 random trees
Shade tolerant			
ΣF	12.36	11.52	12.27
Mean height	2.99	2.65	2.27
ΣB.A.	1948	1425	2807
Mean B.A.	9.48	14.25	9.35
Dead	0	0	17

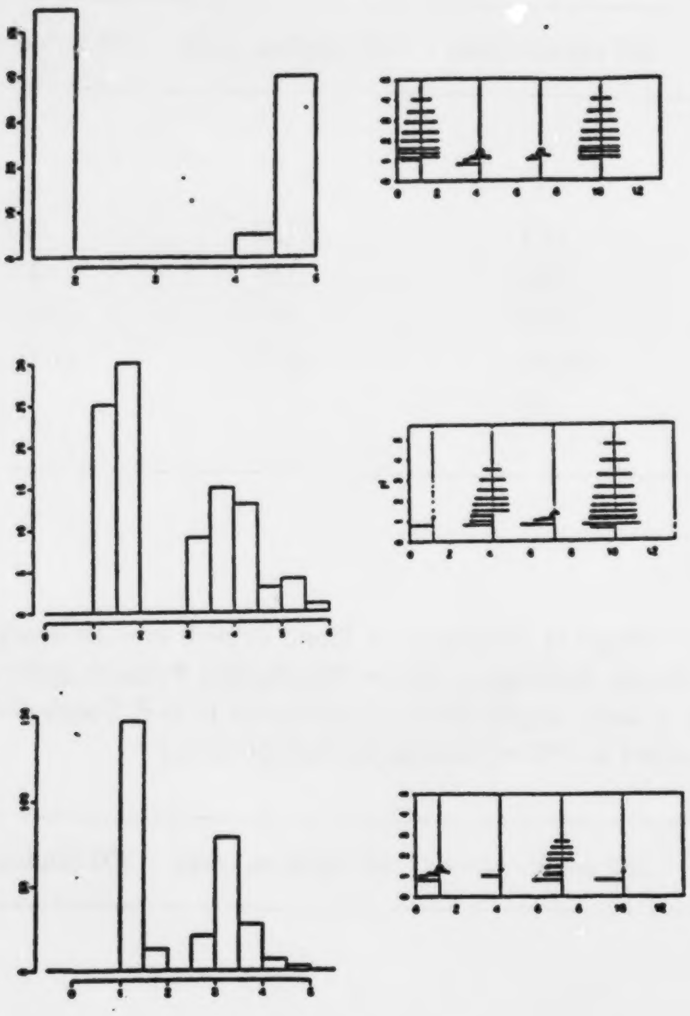

Figure 9-4. Height frequency distributions (note differences in scales of ordinates) and crown structures of four sample trees for each of initial spacing patterns, shade-tolerant foliage; a) 100 trees at equal spacing; b)100 trees at random spacing; c) 300 trees at random spacing. Ten-year growth with all trees initially 1 m. The crown structures are spaced further apart than on the plot where extensive foliage overlap occurs.

The potential for compensatory mechanisms at the stand level should be investigated using the levels of action and interaction explored in the BRANCH models. Different effects, such as increased foliage mortality, decreased photosynthetic rate, and possibly increased respiration rates, should be examined. Note that the first assumption of the model (i.e., that radiation is the limiting factor for growth) applies to the canopy of trees and not generally to the entire stand itself.

General principles can be illustrated with this model. However, this type of model can be organized and calibrated for individual species and conditions. Sufficient information exists in the literature for valuable commercial species such as loblolly pine.

SECTION 10. SUMMARY AND CONCLUSIONS

In this section, the models and the major conclusions derived from them are summarized. The limitations and uncertainties of the models are discussed. Conclusions for the two species of primary interest, red spruce and loblolly pine, are presented, and the impact that regulation of pollutant emissions may have on forest health is discussed.

10.1 SUMMARY OF THE FEEDBACK STRUCTURE OF THE MODELS

FOLIAR SENESCENCE

This model does not contain feedback mechanisms *per se*, but rather it calculates the effects of accelerated foliar senescence on photosynthate production (Figure 10-1).

FOLIAR SENESCENCE
Maturation of needles on single branch segment

Output: net photosynthesis
and area

+ relationship to:	- relationship to:
life span N content needle area	age N loss senescence ozone exposure

Figure 10-1. Structure of FOLIAR SENESCENCE.

BRANCH/FOLIAGE

The output of this model is usually export to trunk. For red spruce, however, where canopy vigor must be predicted, output can be regarded as foliage duration. Export to trunk is a balance between the production of photosynthate and the associated costs of producing that photosynthate by supporting foliage on the branch (Figure 10-2).

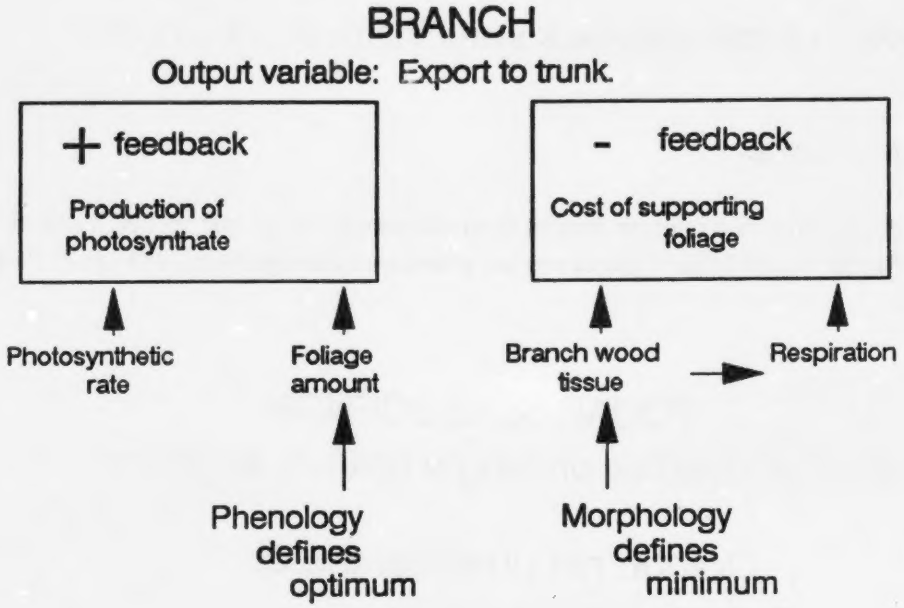
BRANCH
Output variable: Export to trunk.
+ feedback
Production of photosynthate
- feedback
Cost of supporting foliage
Photosynthetic rate
Foliage amount
Branch wood tissue
Respiration
Phenology defines optimum
Morphology defines minimum

Figure 10-2. Structure of BRANCH/FOLIAGE.

An increase in the overall level of photosynthetic rate will increase export to trunk without an associated increase in support costs, but an increase in photosynthetic rate at the higher end of the usual parameter range results in an increase in foliage amount. The activity of different meristems determines the balance between shoot extension, its associated foliage growth, and the time when export to trunk can occur. If the duration of shoot extension and foliage growth is short, then the amount of foliage is inadequate to benefit from the extended period during which export to trunk can occur. If the duration of shoot extension and foliage growth is long, the period during which export to trunk can take place is reduced. Furthermore, the branchwood material increases rapidly and the proportion of photosynthate required both for respiration and for wood production to support the increasing weight increases. The morphology of branchlet distribution defines the actual amount of supporting wood required; branches that extend far from their connection to the trunk require more supporting wood than branches that proliferate branchlets close to the main trunk.

SIMPLE WHOLE TREE

This model structure can be used in a range of spatial configurations to examine the effects of differences in spatial arrangement and timing of photosynthetic activity on growth rates (Figure 10-3). It is also used to examine the relationship between sink activity and the calculation of sink strength in the control of growth. Sink growth rate increases as both the amount of photosynthate produced and sink strength increase. The time required to reach an equilibrium sink growth rate increases as the distance between source and sink are increased. Also, a lower water potential at the source (foliage) than at the sink (cambium) causes the gradient in water potential along the translocation pathway to increase, and the time required to reach an equilibrium sink growth rate increases.

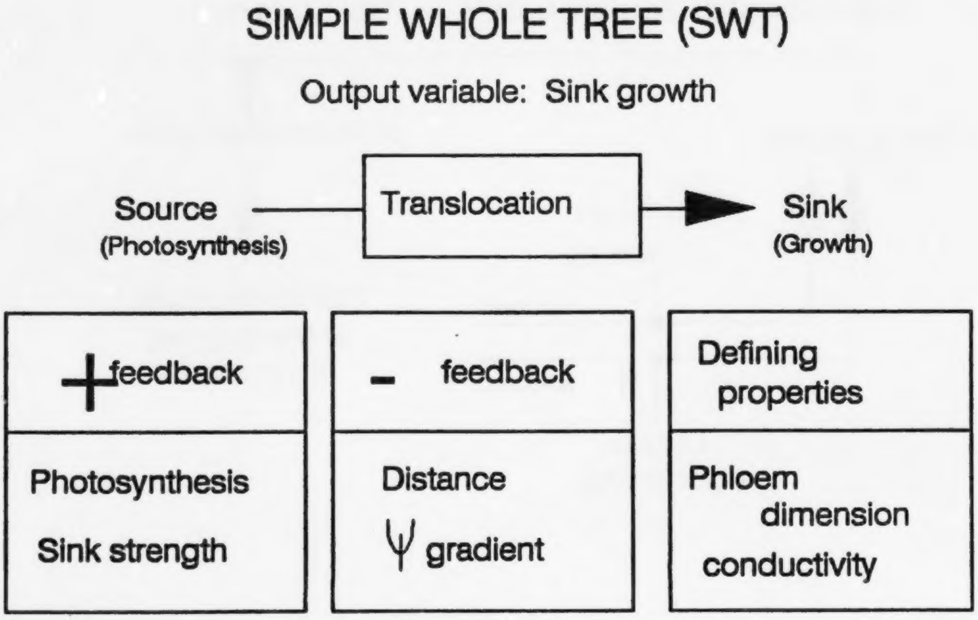
SIMPLE WHOLE TREE (SWT)
Output variable: Sink growth
Source
(Photosynthesis)
Translocation
Sink
(Growth)
+ feedback
Photosynthesis
Sink strength
- feedback
Distance
Ψ gradient
Defining properties
Phloem dimension
conductivity

Figure 10-3. Structure of SIMPLE WHOLE TREE.

ROOTS/SOIL

In this model, root growth occurs through a series of biologically based rules for branching, bending, and forking of roots (Figure 10-4). Nutrients are absorbed by roots in the soil. Nutrient uptake can occur only through diffusion or as a result of both diffusion and mass flow. Nutrient uptake results in distinctive spatial patterns of the nutrients that remain in the soil. In soil systems where diffusion is the primary uptake process, uptake continuously increases as the root system expands. However, as the root system grows and expands and the soil becomes fully occupied, root growth slows. New growth will depend on the rate of nutrient recharge in the system.

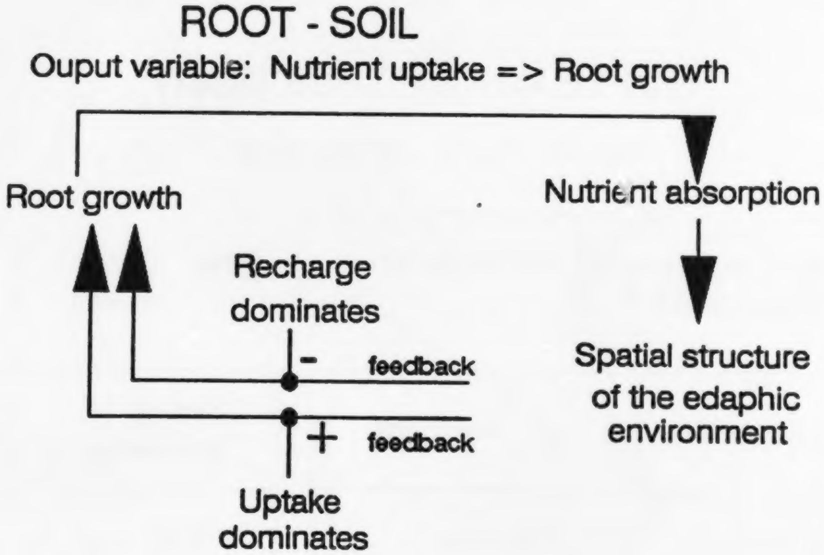
ROOT - SOIL
Ouput variable: Nutrient uptake => Root growth
Root growth
Nutrient absorption
Recharge dominates
-
feedback
+
feedback
Uptake dominates
Spatial structure of the edaphic environment

Figure 10-4. Structure of ROOTS/SOIL.

WHORL

In this model, the spatial structure of trees within a stand, both the distribution and relative sizes, defines the size and distribution of the foliage canopy (Figure 10-5). When the canopy is sparse, increased growth causes greater foliage growth, which in turn results in greater interception of light, a positive feedback. As this process continues, however, some individual trees will be shaded and receive a lower proportion of the light available, a negative feedback. The precise spatial location of the trees influences the rate at which changes in growth and distribution occur.

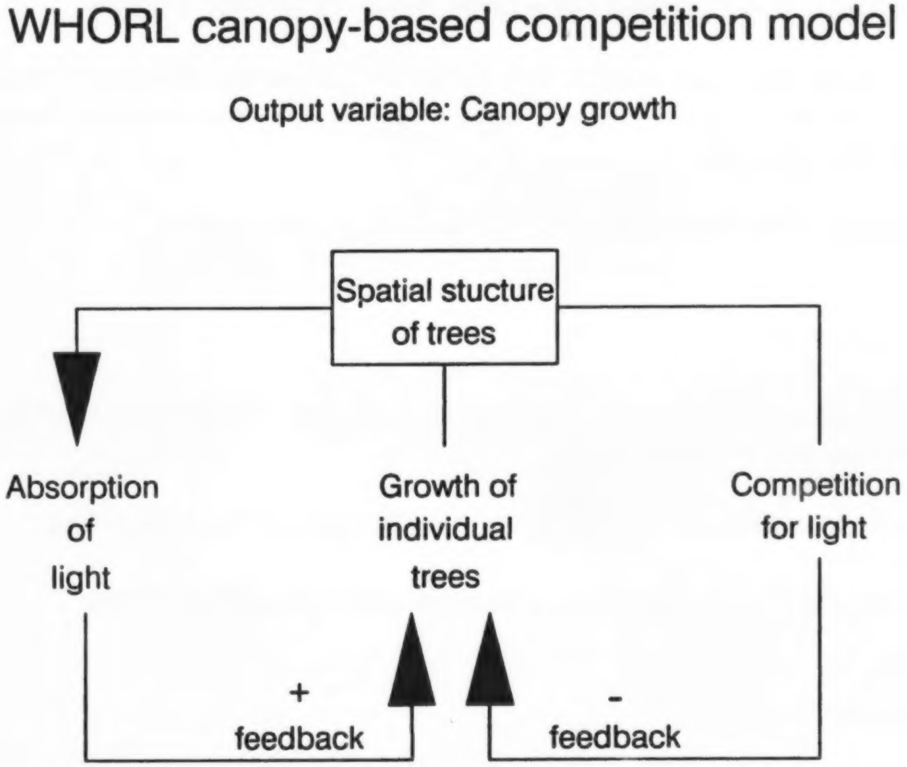
WHORL canopy-based competition model
Output variable: Canopy growth
Spatial stucture of trees
Absorption of light
Growth of individual trees
Competition for light
+
feedback
-
feedback

Figure 10-5. Structure of WHORL.

10.2 SUMMARY OF THE BASIC ASSUMPTIONS OF THE MODELS

FOLIAR SENESCENCE

- Response to ozone exposure is characterized by accelerated senescence.
- Foliage environment includes: 1) non-limiting water supply, 2) non-limiting ambient CO_2, and 3) location on an open-grown tree with negligible self-shading.
- Growth, maturation, and senescence are determined by an extension of the growth curve concept. Potential needle expansion is given by a sigmoid pattern, represented by the Gompertz equation (Gompertz, 1825).
- Photosynthesis is represented by a simple model by Landsberg (1986).
- The needle tissue that emerges first is the most ephemeral; tissue that emerges last is the most long-lived. The lifespan of any needle tissue is a linear function of its time of expansion.
- Abscission of senescent tissue occurs immediately upon death.

BRANCH/FOLIAGE

- Branch wood requirements can be predicted using the equations specified by McMahon and Kronauer (1976).
- Branch development is represented by a set of stochastic branching rules.
- Photosynthesis is represented by a simple model by Landsberg (1986).

SIMPLE WHOLE TREE

- Translocation occurs through the process specified in the Münch Hypothesis.
- Loading and unloading of sucrose (assimilate) can be specified by concentration differences and enzyme kinetics.
- The values of enzyme kinetics published for species other than those targeted for simulation of pollution effects will provide reasonable approximations.

ROOTS/SOIL

- Uptake is through a combination of diffusion and mass flow.
- Proliferation of roots can be expressed as a series of rules for branching, forking, and bending.
- Within the model, no representation currently exists of the feedback to root growth of carbon supply from the above-ground part of the plant.
- Transpiration through the root system is set as typical values and is not subject to environmental feedbacks.

WHORL

- Radiation penetration into the canopy is vertical (i.e., from above).
- There is a value of radiation intercepted below which foliage dies. This is a well-accepted assumption, i.e., the definition of a compensation point.
- The growth of individual trees can be related to the quantity of light they intercept.

10.3 SUMMARY OF THE ASSUMPTIONS OF POLLUTION EFFECTS

The following is a list of the assumed mechanisms of action for pollutants in the models. If no explicit mechanism is modeled, then the relevance for interpretation of pollution effects is given.

FOLIAR SENESCENCE

- Ozone causes premature aging and senescence.

BRANCH/FOLIAGE

- Increasing exposure of loblolly pine to ozone may decrease photosynthetic rate, decrease foliage longevity, and increase respiration rate. A synergistic effect occurs, decreasing both photosynthetic rate and foliage longevity.
- Pollution effects for red spruce were simulated as the effects of frost damage. The loss of foliage and changes in branch morphology were considered as frost damage.

SIMPLE WHOLE TREE

This model assesses the conditions under which a reduction in photosynthetic rate would actually cause a reduction in growth rate. It also defines the magnitude of the effect. Some reports indicate the translocation mechanism is influenced by pollution.

ROOTS/SOIL

At its current stage of development, the model indicates that experimental studies on seedlings must be interpreted cautiously with regard to mature trees because patterns of nutrient uptake from the soil vary for different aged trees.

WHORL

Pollution effects may operate at two points in this system: 1) through the death of foliage that influences competition for light; and 2) in the translation of the light received by an individual tree to growth. Simulations to date suggest the model output is more sensitive to the translation of light than to foliage mortality.

10.4 SUMMARY OF THE SENSITIVITY STUDIES

Each of the models has had sensitivity studies done on certain components. These components were selected because they were either a critical part of the dynamics or were based on poor empirical data.

FOLIAR SENESCENCE

Studies were performed on needle life span (the relationship of life span of the most durable to the most ephemeral tissue) and maximum carboxylation efficiency (Section 5).

BRANCH/FOLIAGE

The effect of variation in all major parameter values on the balance between positive and negative feedbacks has been examined (Ford et al., in press). A major effect of variations in morphology was discovered during this process. The existence of optima in photosynthetic rate and the duration of foliage production was determined (Ford et al., in press).

The loblolly pine and red spruce versions of the model were written as stochastic processes based on variation in measured morphological rules. The effects of this variation that have been explored through simulation were found to be of major importance and are reported in Section 6.

Sensitivity studies for the loblolly pine version were used to determine the percent of photosynthate exported to trunk during the first flush and the value of the maintenance respiration rate (Section 6).

SIMPLE WHOLE TREE

Studies were performed to assess the following (Section 7):

- Potential difference in sucrose concentration on specific mass transfer between source and sink.
- Variation in axial conductivity on specific mass transfer rates.
- Effects of water potential gradients on specific mass transfer rates for a range of sucrose concentration gradients.
- Effects of assumed phloem dimensions on translocation rates and of variation in the compensation point.

ROOTS/SOIL

The purpose of the principal sensitivity analysis currently underway is to examine the relative contributions of mass flow and diffusion to nutrient uptake as soil properties and root structure are varied (Section 8).

WHORL

Studies were performed to assess the variation in the density and initial spatial arrangement of the trees, variation in the translation of individual tree light intercepted to individual tree growth, and variation in the proportion of light intercepted per unit of foliage (Section 9).

10.5 CONCLUSIONS FROM MODELING

In Section 1, the purpose of this document was stated as the following:

> If there is a causal relationship, what is the dose-response relationship between acidic deposition, alone or in combination with other pollutants, and forest damage in North America?

The FRP has provided extensive experimental evidence that pollutants, particularly ozone, can directly influence growth and that acidic deposition may affect frost hardiness of red spruce (MPOs #3 and #4). Forest investigations, simulation studies, and transplant studies with seedlings also suggest that acid precipitation is likely to have an effect on both soil and growth processes, especially in montane habitats. Studies on geographical and altitudinal gradients show that changes in soil and plant chemistry occur with changes in pollution deposition load. Despite these studies, direct measurements of growth during periods of increased deposition have not found consistent or convincing statistical evidence that a widespread decline in forest growth exists (MPO #1&2), except in montane red spruce forests and ponderosa pine forests in southern California.

This study involves the construction of process-based models that incorporate the variability in biological and meteorological processes as an intrinsic characteristic of pollutant influence and response. Three issues led to this examination of the nature of dose-response relationships:

1) Growth, and the incidence of some pollutant effects, are stochastic processes. The stochastic nature of response is illustrated by the simulation of the processes of branch growth and the implications for tree growth as a whole (Section 6). The elements of the stochastic process include the development of different branching patterns and the weather. Variability is a fundamental aspect of these two processes. Variability in branching patterns is genetic and is due primarily to differences in the anatomy of bud development. Our expectation of variability in weather patterns was matched by our inability to predict them.

   The degree to which the stochastic element in these processes dominates our ability to detect pollution effects was an unexpected aspect of our results. This suggests that the analysis of forest measurements of growth or yield may not easily detect pollutant responses or the effects of potential regulation.

2) Trees and forest growth have component processes that compensate for environmental change. Direct compensation occurs in the competition process, and low levels of canopy reduction may actually enhance growth. However, there is a limit in the extent to which compensation can occur. Simulation of translocation suggests that the effects of reduced photosynthesis may be buffered by their effects on growth. In red spruce, the process of epicormic shoot production is a compensation mechanism for damage. Again, there is a limit to the extent of this compensation. The existence of compensatory or buffering mechanisms suggests that a threshold exposure dose must be reached before an effect will be seen in tree and forest growth.

3) A pollutant may have more than one effect on tree growth and the magnitude of these effects, when taken together, is greater than the sum of the individual effects. That is, the effects are synergistic. Simulations with the branch model of loblolly pine showed a synergism between photosynthetic rate and foliage mortality for ozone effect.

The combined compensatory mechanisms may sustain a certain level of damage, but the potential for synergistic effects indicates that the effects of pollution on trees will be nonlinear, increasing as the pollutant load increases.

In conclusion, the nature of the response has several characteristics. First, as pollution increases by small amounts, the effects are small due to buffering and compensating mechanisms. Most importantly, because of the stochastic nature of growth and environmental processes, these changes will not be easy to detect using standard statistical analyses on integrated measurements of growth or yield. Second, a point is reached where synergisms may occur and growth decreases markedly or ceases. Simulations of such critical threshold points indicate the relation of the ozone effect on loblolly pine and decreased frost resistance in red spruce in both reducing photosynthesis and decreasing foliage longevity. Consequently, species vulnerability to short intervals of successive damage increases. Extended simulations are underway to determine, within certain bounds, where the critical limits may be. However, it is important to note that the experimental conditions under which ozone exposures were made determine the type of limits that can be established, and a precise specification of particular environmental conditions that cause frost damage has not been made.

10.6 SPECIES DIFFERENCES

In addition to conforming to the general conclusions, the two most closely studied species have characteristic responses. The major pollutant of interest for loblolly pine is ozone, which affects both photosynthetic rate and needle life span in a possibly synergistic manner. Acidic deposition may ultimately affect soils, but the relation of this effect to root function is not yet known. The patterns of weather that actually cause winter damage and the relation to pollutant response in red spruce is not clear. Ozone damage to needle cuticle, consequent foliar leaching, and the possible compensation by root uptake, need further study.

10.7 MODEL LIMITATIONS AND UNCERTAINTIES

As with any modeling activity, major uncertainties are associated with the numerical results. Among these are untested assumptions; incomplete expression of interaction; incomplete understanding of functional relationships; and incomplete parameterization for the required species, sites, and situations of interest. Incomplete expression of interactions, such as the interaction of ozone and acidic precipitation in foliar leaching, probably results in models that underestimate the rate of change in growth that can take place in response to pollutants.

The lack of comprehensive data sets, in which all required parameters are measured at one site, is currently the most limiting aspect of the empirical studies that could validate these models. This results in the need to collate data from a range of different investigations, sometimes for different species. It also means that testing the model can only be partial. Future work must address this issue.

10.8 FORESTS AND LONG-TERM SOIL EFFECTS

Our models have been of trees and, to a limited extent, of forests. The next step is to relate these models to those produced in the studies of long-term acidification of forested watersheds and soils. The linkage between these areas of study must be made at the experimental level as well. The potential effects of long-term soil acidification on forests may be very nonlinear, but they remain a major area of uncertainty. The difference between a complete root and soil processes model, as specified by the workshop, and the status of ROOTS/SOIL at this time, is an indication of our overall uncertainty in this area. ROOTS/SOIL is only a beginning and it is clear this effort is insufficient.

10.9 DETECTING POLLUTION EFFECTS: CRITIQUE

Perhaps the most difficult problem addressed has been making rigorous deductions from the total body of work produced by the FRP. A classical statistical view is represented in Figure 10-6. The FRP initiated its work under six hypotheses of effect which were, as described in MPO #4, substantially developed and refined. Some of these hypotheses could be translated into models. Shortfalls include technical problems with regard to the soil-root system, and scientific with regard to the normal growth processes that operate in large, aging trees. The scientific shortfalls usually appear as assumptions that require further examination. The most notable assumptions concern the mobility of carbohydrate within branches as they grow, and carbon as a satisfactory primary currency for models. Advancement in scientific theory is evidenced by the attention currently being given to making a precise specification of the pollutant dose, λ.

A classical statistical view holds that complete testing of models requires the generation of matching outputs and the calculation of a series of values of B1, B2,..., Bn. If the specification of the dose-response system in forests is correct, then a series of B values capable of generating a positive effect would be possible only after a value of λ resulting in significant damage had been reached. Under a normal statistical framework, one can only be sure that pollution has an effect on the growth of trees when synergistic effects outweigh both compensatory mechanisms and the inherent variability of the systems. This is the condition when substantial damage will be observed. This dilemma has been pointed out by Bormann (1985).

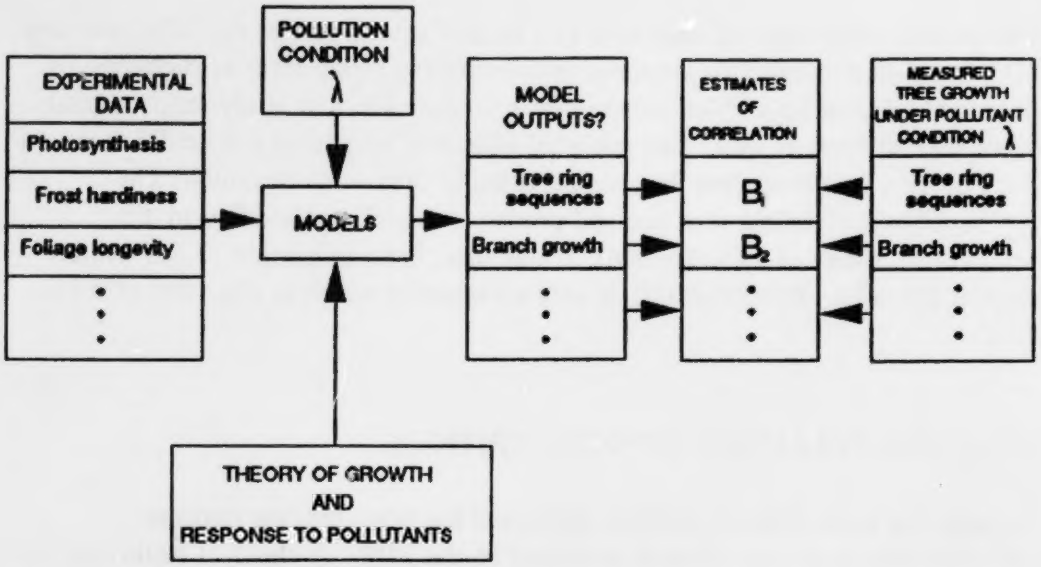
POLLUTION CONDITION λ
EXPERIMENTAL DATA
Photosynthesis
Frost hardiness
Foliage longevity
MODELS
MODEL OUTPUTS?
Tree ring sequences
Branch growth
ESTIMATES OF CORRELATION
B_1
B_2
MEASURED TREE GROWTH UNDER POLLUTANT CONDITION λ
Tree ring sequences
Branch growth
THEORY OF GROWTH AND RESPONSE TO POLLUTANTS

Figure 10-6. Modeling and hypothesis testing in the determination of pollutant effects on forests.

If we take the classical view and assume a null of hypothesis of no effect, we can conclude that the probability of accepting that hypothesis on a basis that includes field data is high. However, the crucial decision that a policy maker must make is whether to be more concerned with a Type I error (rejecting the null hypothesis when it should have been accepted) or a Type II error (accepting the null hypothesis when it should have been rejected). Given the possibility of threshold effects, which were indicated by the models, it would be prudent to be more concerned about falsely accepting the null hypothesis (Type II error). However, the decision as to which type of error to tolerate is not made on the basis of the scientific results alone, but rather on the scientific results in combination with other societal and economic factors included in all policy decisions.

The final conclusion of this study concerns the magnitude of potental changes in deposition: For changes in the levels of acidic deposition to have a detectable effect on the long-term health of forests, these changes will have to be of substantial magnitude. Small changes in emissions and consequent deposition will produce changes within the range of normal variability of tree and forest growth processes.

SECTION 11. LITERATURE CITED

Note:

Major Program Output (MPO) #1&2, see Reams et al.
Major Program Output (MPO) #3, see Peterson et al.
Major Program Output (MPO) #4, see Mattson et al.
State of Science Technology Report (SOS/T) #16, see Barnard et al.
State of Science Technology Report (SOS/T) #18, see Shriner et al.

Adams, M.B., J.M. Kelly, and J.T. Edwards. 1988. Growth of *Pinus taeda L.* seedlings varies with family and ozone exposure level. Water Air Soil Pollut. 38:137-150.

Adams, M.B., and C. Eagar, eds. 1989. Air pollution and winter injury of red spruce. Workshop Proceedings, April 17-18, 1989, Edinburgh, Scotland. USDA-Forest Service, Northeastern Forest Experiment Station.

Allen, H.L. Personal Communication. North Carolina State University, Raleigh, NC.

Assman, E. 1970. *The principles of forest yield study*. Pergamon Press, Oxford.

Avery, A., and A.R. Kiester. 1988. C Programming Standards for the Forest Response Program. U.S. Environmental Protection Agency, Internal Report, Environmental Research Laboratory, Corvallis, OR.

Baes, C.F., III, S.B. McLaughlin, and T.A. Hagan. 1984. Multi-elemental analysis of tree rings: Temporal accumulation patterns and relationships with air pollution, pp. 273. In: D.D. Davis, A.A. Millen, and L.S. Dochinger, eds. Air Pollution and the Productivity of the Forest. Proceedings of the Symposium, October 4-5, 1983. Washington, DC.

Baldwin, J.P., and P.H. Nye. 1974. A model to calculate the uptake by a developing root system or root hair system of solutes with concentration-variable diffusion coefficients. Plant and Soil. 40:703-706.

Baldwin, J.P., P.H. Nye, and P.B. Tinker. 1973. Uptake of solutes by multiple root systems from soil. III. A model for calculating the solute uptake by a randomly dispersed root system developing in a finite column of soil. Plant and Soil. 38:621-635.

Barnard, J., A. Lucier, A. Johnson, R. Brooks, D. Karnosky, and P. Dunn. 1990. Changes in Forest Health and Productivity in the United States and Canada. NAPAP Report 16, Acidic Deposition: State of Science and Technology, National Acid Precipitation Assessment Program, Washington, DC.

Barnes, A., and C.C. Hole. 1978. A theoretical basis of growth and maintenance respiration. Ann. Bot. 42:1217-1221.

Barrett, J.W. 1980. The northeastern region, pp. 25-65. In: J.W. Barrett, ed. *Regional Silviculture of the United States*. John Wiley & Sons, New York.

Bassow, S. 1989. Models of carbohydrate balance and translocation in trees. Master's thesis, University of Washington, Seattle, WA.

Bassow, S.L., E.D. Ford, and A.R. Kiester. 1990. A critique of carbon based tree growth models, pp. 50-57. In: R.K. Dixon, R.S. Meldahl, G.A. Ruark, and W.G. Warren, eds. *Process Modeling of Forest Growth Responses to Environmental Stress*. Timber Press, Portland, OR.

Batzer, H.O. 1973. Defoliation by the spruce budworm stimulated epicormic shoots on balsam fir. Environ. Entomol. 2:727-728.

Bella, I.E. 1971. A new competition model for individual trees. For. Sci. 17:364-372.

Binkley, D., and D. Richter. 1987. Nutrition cycles and H^+ budgets of forest ecosystems. Adv. Ecol. Res. 16:1-51.

Binkley, D., C.T. Driscoll, H.L. Allen, P. Schoeneberger, and D. McAvoy. 1989. *Acidic Deposition and Forest Soils: Context and Case Studies of Forest Soils in the Southeastern United States*. Springer-Verlag, New York. 149 pp.

Birk, E.M., and P.A. Matson. 1986. Site fertility affects seasonal carbon reserves in loblolly pine. Tree Physiol. 2:17-27.

Bonan, G.B. 1988. The size structure of theoretical plant populations: Spatial patterns and neighborhood effects. Ecology 69:1721-1730.

Bormann, F.H. 1985. Air pollution stress on forests: An ecosystem perspective. BioScience 35:434-441.

Bryan, J.A., and R.M. Lanner. 1981. Epicormic branching in Rocky Mountain Douglas-fir. Can. J. For. Res. 11(2):190-199.

Buol, C.W., F.D. Hole, and R.J. McCracken. 1973. *Soil Genesis and Classification*. Iowa State University Press, Ames, IA.

Cannell, M.G.R. 1985. Dry matter partitioning in tree crops. In: M.G.R. Cannell and J.E. Jackson, eds. *Attributes of Trees as Crop Plants*. Institute of Terrestrial Ecology, Abbots Ripton, England. pp. 160-193.

Cannell, M.G.R., P. Rothery, and E.D. Ford. 1984. Competition within stands of *Picea sitchensis* and *Pinus contorta*. Ann. Bot. 53:349-362.

Cannell, M.R., J. Sheppard, R.I. Smith, and M.B. Murray. 1985. Autumn frost damage on young *Picea sitchensis*. 2. Shoot frost hardening, and the probability of frost damage in Scotland. Forestry 58(2):145-166.

Canny, M.J. 1973. Phloem translocation. Cambridge University Press: Cambridge. 301 pp.

Chabot, B.F., and D.J. Hicks. 1982. The ecology of leaf life spans. Ann. Rev. Ecol. Syst. 13:229-259.

Cochrane, L.A., and E.D. Ford. 1978. Growth of a sitka spruce plantation: Analysis and stochastic description of the development of the branching structure. J. Appl. Ecol. 15:227-244.

Cole, D.W., and M. Rapp. 1981. Elemental cycling in forest ecosystems. In: D.E. Reichle, ed. *Dynamic Principles of Forest Ecosystems*. Cambridge Univ. Press, London & New York. pp. 341-409.

Cosby, B.J., G.M. Hornberger, J.N. Galloway, and R. F. Wright. 1985. Modeling the effects of acid deposition: Assessment of a lumped parameter model of soil water and stream chemistry. Wat. Resour. Res. 21:51-63.

Cosens, R.D. 1952. Epicormic branching on pruned white fir. J. For. 50:939-940.

Crafts, A.S., and C.E. Crisp. 1971. *Phloem Translocation in Plants*. W.H. Freeman and Company, San Francisco, CA. 481 pp.

Curry, J.R., and T.W. Church. 1952. Observations on winter drying of conifers in the Adirondacks. J. For. 50:114-116.

de Wit, C.T., and H. van Keulen. 1972. Simulation of transport processes in soils. Center for Agricultural Publishing and Documentation, Wageningen, The Netherlands. 100 pp.

Dean, T.J., and J.N. Long. 1986. Variation in sapwood area-leaf area relations within two stands of lodgepole pine. For. Sci. 32:749-758.

DeHayes, D.H., M.A. Ingle, and C.E. Waite. 1989. Developmental tolerance of red spruce and potential perturbations from natural and anthropogenic factors, pp. II-1 to II-10. In: M.B. Adams and C. Eagar, eds. Air pollution and winter injury of red spruce. Workshop Proceedings, April 17-18, 1989, Edinburgh, Scotland. USDA-Forest Service, Northeastern Forest Experiment Station.

Drew, M.C., and L.R. Saker. 1978. Nutrient supply and the growth of the seminal root system in barley. III. Compensatory increases in growth of lateral roots, and in rates of phosphate uptake, in response to a localized supply of phosphate. J. Exp. Bot. 29:435-451.

Eamus, D., I.D. Leith, and D. Fowler. 1989. Water relations of red spruce seedlings treated with acid mist. Tree Physiol. 5:387-397.

Eddleman, L.E. 1988. Precipitation throughfall, stemflow, and interception by western juniper canopies. Northwest Sci. 62(2) abstract #37.

Ek, A.R., and R.A. Monserud. 1974. Forest: a computer model for simulating the growth and reproduction of mixed species forest stands. Research Report R2635, University of Wisconsin, College of Agriculture and Life Sciences. 13 pp.

EPA. 1976. Quality Assurance Handbook for Air Pollution Measurement Systems: Vol. I. Principals. EPA 600/9-76-005, US Environmental Protection Agency, Office of Research and Development, Environmental Monitoring and Support Laboratory, Research Triangle Park, NC.

EPA. 1979. Handbook for Analytical Quality Control in Water and Wastewater Laboratories. EPA 600/4-79-019, US Environmental Protection Agency, Office of Research and Development, Environmental Monitoring and Support Laboratory, Cincinnati, OH.

EPA. 1982. Handbook for Sampling and Sample Preservation of Water and Wastewater. EPA 600/4-82-029, US Environmental Protection Agency, Office of Research and Development, Environmental Monitoring and Support Laboratory, Cincinnati, OH.

EPA. 1983. Methods for Chemical Analysis of Water and Waste. EPA 600/4-79-020, US Environmental Protection Agency, Office of Research and Development, Environmental Monitoring and Support Laboratory, Cincinnati, OH.

EPA. 1986. Quality Assurance Handbook for Air Pollution Measurement Systems: Vol. II. Ambient Air Specific Methods. EPA 600/4-77-027a, US Environmental Protection Agency, Office of Research and Development, Environmental Laboratory, Research Triangle Park, NC.

EPA. 1987. Quality Assurance Implementation Plan for the Forest Response Program. EPA/600/X-86/166, US Environmental Protection Agency Internal Report, Environmental Research Laboratory, Corvallis, OR. 75 pp.

Evans, L.S. 1986. Proposed mechanisms of initial injury-causing apical dieback in red spruce at high elevation in eastern North America. Can. J. For. Res. 16(5):1113-1116.

Evans, L.S., and P. Dougherty. 1986. Exposure systems and physiological measurements. Forest Response Quality Assurance Methods Manual. EPA/600/X-86/193a, US Environmental Protection Agency Internal Report, Environmental Research Laboratory, Corvallis, OR 99 pp.

Fahey, T.J., J.B. Yavitt, G. Joyce. 1988. Precipitation and throughfall chemistry in *Pinus contorta ss. latifolia* ecosystems, southeastern Wyoming. Can. J. For. Res. 18:337-345.

Fensom, D.S. 1981. Work with isolated phloem strands. In: M.H. Zimmermann and J.A. Milburn, eds. *Transport in Plants I: Phloem Transport*. Encyclopedia of Plant Physiology. New Series Volume 1. pp. 223-244.

Field, C. 1983. Allocating leaf nitrogen for the maximization of carbon gain: Leaf age as a control on the allocation program. Oceol. (Berlin). 56:341-347.

Fitter, A.H. 1985. Functional significance of root morphology and root system architecture. In: A.H. Fitter, D. Atkinson, D.J. Read, and M. Busher, eds. *Ecological Interactions in Soil.* Blackwell Scientific Publications, Oxford. pp. 87-106.

Fitter, A.H. 1987. An architectural approach to the comparative ecology of plant root systems. New Phytol. 106:61-77.

Ford, E.D. 1975. Competition and stand structure in some even-aged plant monocultures. J. Ecol. 63:311-333.

Ford, E.D. 1982a. Catastrophe and disruption in forest ecosystems and their implications for plantation forestry. Scot. For. 36:9-24.

Ford, E.D., A. Avery, and R. Ford. In press. Simulation of branch growth in the Pinaceae: Interactions of morphology, phenology, foliage productivity, and the requirement for structural support, on the export of carbon. J Theoret. Biol.

Ford, E.D., and S. Bassow. 1988. Modeling the influence of pollution on allocation. In: A.R. Ek, S.R. Shifley, and T.E. Burk, eds. *Proceedings of the International Union of Forestry Research Organizations Forest Growth Modelling and Prediction Conference*, Aug. 23-27, 1987, Minneapolis, MN. General Technical Report NC-120, USDA-Forest Service, North Central Forest Experiment Station, St. Paul, MN.

Ford, E.D., and J.D. Deans. 1977. Growth of a Sitka spruce plantation: Distribution and seasonal fluctuations of weights and carbohydrate concentrations of fine roots. Plant and Soil. 47:463-485.

Ford, E.D., and P.J. Diggle. 1981. Competition for light in a plant monoculture modelled as a spatial stochastic process. Ann. Bot. 48.

Ford, E.D., and A.R. Kiester. 1990. Modeling the effects of pollutants on the processes of tree growth, pp. 324-337. In: R.K. Dixon, R.S. Meldahl, G.A. Ruark, and W.G. Warren, eds. *Process Modeling of Forest Growth Responses to Environmental Stress*. Timber Press, Portland, OR.

Ford, R., and E.D. Ford. In press. Structure and basic equations of a simulator for branch growth in the Pinaceae. J. Theoret. Biol.

Franco, M. 1986. The influence of neighbours on the growth of modular organisms with an example from trees. Phil. Trans. Royal Soc. Lond. 313(B):209-225.

Gates, D.J., A.J. O'Connor, and M. Westcott. 1979. Partitioning the union of disks in plant competition models. Proc. Royal Soc. Lond. A. 367:59-79.

Gifford, R.M, and L.T. Evans. 1981. Photosynthesis, carbon partitioning, and yield. Ann. Rev. Plant Physiol. 32:485-509.

Gompertz, B. 1825. On the nature of the function expressive of the law of human mortality. Phil. Trans. Royal Soc. 36:513-585.

Gordon, J.C., and P.R. Larson. 1968. The seasonal course of photosynthesis, respiration, and distribution of 14C in young *Pinus resinosa* trees as related to wood formation. Plant Physiol. 43:1617-1624.

Grier, C.C., K.A. Vogt, M.R. Keyes, and R.L. Edmonds. 1980. Biomass distribution and above- and below-ground production in young and mature *Abies amabalis* zone ecosystems of the Washington Cascades. Can. J. For. Res. 11:155-167.

Guderian, R. (ed.) 1985. Air Pollution by photochemical oxidants. Ecological Studies 52. Berlin, Heidelberg, New York, Tokyo, Springer-Verlag.

Hari, P., E. Nikinmaa, and M. Holmberg. 1990. Photosynthesis, transpiration, and nutrient uptake in relation to tree structure, pp. 41-49. In: R.K. Dixon, R.S. Meldahl, G.A. Ruark, and W.G. Warren, eds. *Process Modeling of Forest Growth Responses to Environmental Stress*. Timber Press, Portland, OR.

Harper, J.L. 1967. A Darwinian approach to plant ecology. J. Ecol. 55:247-270.

Harper, J.L. 1977. *Population Biology of Plants*. Academic Press, London. pp. 892.

Haskins, J.L. In preparation. The movement of water through living conifer wood: Filling the gap between two spatial scales. Master's thesis, University of Washington, Seattle, WA.

Hatch, C.R, D.J. Gerrard, and J.C. Tappeiner, II. 1975. Exposed crown surface area: a mathematical index of individual tree growth potential. Can. J. For. Res. 5:224-228.

Henderson, R., E.D. Ford, and E. Renshaw. 1983b. Morphology of the structural root system of Sitka spruce, 2. Computer simulation of rooting patterns. Forestry 56:137-153.

Henderson, S., R.K. Olson, and R.F. Noss. 1989. Current and potential threats to biodiversity in forests of the lower Pacific Coast States, pp. 325-336. In: R.K. Olson and A.S. Lefohn, eds. *Effects of Air Pollution on Western Forests*. Transactions of the Air and Waste Management Association, Pittsburgh, PA.

Ho, L.C. 1988. Metabolism and compartmentation of imported sugars in sink organs in relation to sink strength. Ann. Rev. Plant Physiol. Plant Molec. Biol. 39:355-378.

Holley, D.L., and M.A. Veal. 1977. Economic impact of fusiform rust. In: R.J. Dinus and R.A. Schmidt, eds. *Management of Fusiform Rust in Southern Pines*. Symposium Proceedings, University of Florida, Gainesville, FL.

Hunt, W.F., and R.S. Loomis. 1979. Respiration modelling and hypothesis testing with a dynamic model of sugar beet growth. Ann. Bot. 44:5-17.

Johnson, A.H., A.J. Friedland, and J.G. Dushoff. 1986. Recent and historic red spruce mortality: Evidence of climatic influence. Water Air Soil Pollut. 30:319-330.

Johnson, I.R., and J.H.M. Thornley. 1987. A model of shoot:root partitioning with optimal growth. Ann. Bot. 60:133-142.

Johnson, J.D. 1984. A rapid technique for estimating total surface area of pine needles. For. Sci. 30(4):913-921.

Kellomaki, S. 1986. A model for the relationship between branch number and biomass in *Pinus sylvestris* crowns and the effect of crown shape and stand density on branch and stem biomass. Scand. J. For. Res. 1:455-472.

Kenkel, N.C. 1988. Pattern of self-thinning in jack pine: Testing the random mortality hypothesis. Ecology 69:1017-1024.

Khan, M.A., J. Antonovics, and A.D. Bradshaw. 1976. Adaption to heterogeneous Environments. II. Phenotypic plasticity in response to spacing in *Linum*. Aust. J. Agric. Res. 27:519-531.

Khan, M.A., J. Antonovics, and A.D. Bradshaw. 1976. Adaption to heterogeneous environments. III. The inheritance of response to spacing in flax and linseed (*Linum usitatissiumum*). Aust. J. Agric. Res. 27:649-659.

Kiester, A.R. 1988. Framework for the role of forest stand dynamics in estimating pollutant effects. Synthesis and Integration Report #16. US Environmental Protection Agency, Environmental Research Laboratory, Corvallis, OR. 20 pp.

Kiester, A.R. 1988. The roles of models in the forest response program. In: A.R. Ek, S.R. Shifley, and T.E. Burke, eds. *Proceedings of the International Union of Forestry Research Organizations Forest Growth Modelling and Prediction Conference*, Aug. 23-27, 1987, Minneapolis, MN. General Technical Report NC-120, USDA-Forest Service, Northeastern Forest Experiment Station, St. Paul, MN.

Kiester, A.R. 1990. Process modeling of tree and forest growth: Current perspectives and future needs, pp. 416-422. In: R.K. Dixon, R.S. Meldahl, G.A. Ruark, and W.G. Warren, eds. *Process Modeling of Forest Growth Responses to Environmental Stress*. Timber Press, Portland, OR.

Kinerson, R.S. 1975. Relationships between plant surface area and respiration in loblolly pine. J. Appl. Ecol. 12:965-71.

Kozlowski, T.T., and T. Keller. 1966. Food relations of woody plants. Bot. Rev. 32:294-382.

Kozlowski, T.T., and T.A. Peterson. 1962. Seasonal growth of dominant, intermediate and suppressed red pine trees. Bot. Gaz. 28:146-154.

Kress, L.W. Personal Communication. North Carolina State University, Raleigh, NC.

Landsberg, J.D., P.H. Cochran, M.M. Finck, and R.E. Martin. 1984. Foliar nitrogen content and tree growth after prescribed fire in ponderosa pine. USDA-Forest Service Research Note PNW-412.

Landsberg, J.J. 1986. *Physiological Ecology of Forest Production*. Academic Press, London. 198 pp.

Lanner, R.M., and J.A. Bryan 1981. Association of rhabdocline needle blight and epicormic branching in Douglas-fir (*Pseudotsuga menziestii, Rhabdocline pseudotsugae*, Utah.). Gr. Bas. Nat. 41(4):476-477.

Leveranz, J.W., and P.G. Jarvis. 1980. Photosynthesis in sitka spruce (*Picea sitchensis* (bong.) Carr.) X. Acclimation to quantum flux density within and between trees. J. Appl. Ecol. 17:697-708.

Little, C.H.A. 1970. Derivation of the springtime starch increase in balsam fir (*Abies balsamea*). Can. J. Bot. 48:1996-1999.

Lorenc-Plucinska, G. 1984. The uptake and translocation of ^{14}C in Scots pine seedlings of different susceptibility to sulfur dioxide. Eur. J. For. Path. 16:266-273.

Lorenc-Plucinska. G. 1986. Effect of sulfur dioxide on the partitioning of assimilates of Scots pine (*Pinus sylvestris L.*) seedlings of different susceptibility to this gas. Eur. J. For. Path. 16:266-273.

Lovett, G.M., R.K. Olson, W.A. Reiners, and D.A. Schaefer. 1984. Dynamics of potassium efflux during rain events in a balsam fir canopy: a mechanistic model. Bull. Ecol. Soc. Amer. 65(2): 238.

Lungley, D.R. 1973. The growth of root systems - The numerical computer simulation model. Plant and Soil. 38:145-159.

Luxmoore, R.J., J.L. Stolzy, and J.T. Holdeman. 1981. Sensitivity of a soil-plant-atmosphere model to changes in air temperature, dew point temperature and solar radiation. Agric. Meteor. 23:115-129.

Mäkelä, A. 1986. Implications of the pipe model theory on dry matter partitioning and height growth in trees. J. Theor. Biol. 123:103-120.

Mäkelä, A., and Sievänen, R.P. 1987. Comparison of two shoot-root partitioning models with respect to substrate utilization and functional balance. Ann. Bot. 59:129-140.

Maksymowich, R. 1973. Analysis of leaf development. In: M. Abercrombie, D.R. Newth, and J.G. Torrey, eds. *Development and Cell Biology Series*. University Press, Cambridge.

Mann, L.K., S.B. McLaughlin, and D.S. Shriner. 1980. Seasonal physiological response of white pine under chronic air pollution stress. Environ. Exp. Bot. 20:99-105.

Marshall, T.J., and J.W. Holmes. 1988. *Soil Physics*. Press Syndicate of the University of Cambridge, Second edition. 374 pp.

Mattson, K.G., L.Y. Arnaut, G.A. Reams, S.P. Cline, C.E. Peterson, and R.J. Vong. 1990. Response of forest trees to sulfur, nitrogen, and associated pollutants. Major Program Output #4, EPA/600/3-90/074, US Environmental Protection Agency, Environmental Research Laboratory, Corvallis, OR. 134 pp.

McLaughlin, S.B. 1985. Effects of air pollution in forests. J. Air Pollut. Control Assoc. 35:512-534.

McLaughlin, S.B. 1989. Carbon allocation processes as indicators of pollutant impacts on forest trees. In: *Biologic Markers of Air Pollution Stress and Damage in Forests*. National Academy Press, Washington, D.C. 363 pp.

McLaughlin, S.B., R.K. McConathy, D. Duvik, and L.K. Mann. 1982. Effects of chronic air pollution stress on photosynthesis, carbon allocation, and growth of white pine trees. For. Sci. 28:60-70.

McMahon, T.A., and R.E. Kronauer. 1976. Tree structures: Deducing the principle of mechanical design. J. Theor. Biol. 59:443-466.

McMurtrie, R., and L. Wolf. 1983. Above- and below-ground growth of forest stands: a carbon budget model. Ann. Bot. 52:437-448.

Meineke, E.P. 1917. Basic problems in forest pathology. J. For. 15:215-224.

Meinecke, E.P. 1928. The evaluation of loss from killing diseases in the young forest. J. For. 26:283-298.

Metz, J.A., and O. Diekmann. 1986. *The Dynamics of Physiologically Structured Populations*. Springer-Verlag, Berlin. 511 pp.

Miller, P.R., O.C. Taylor, and R.G. Wilhour. 1982. Oxidant air pollution effects on a western coniferous forest ecosystem. EPA-600/D-82-278, US Environmental Protection Agency, Environmental Research Brief.

Mitchell, K.J. 1975. Dynamics and simulated yield of Douglas-fir. For. Sci. Mon. 17. Supplement to For. Sci. (Suppl) 21. 39 pp.

Moore, J.A., C.A. Budelsky, and R.C. Schlesinger. 1973. A new index representing individual tree competitive status. Can. J. For. Res. 3:495-500.

Nance, W.L., J.E. Grissom, and W.R. Smith. 1988. A new competition index based on weighted and constrained area potentially available. In: A.R. Ek, S.R. Shifley, and T.E. Burk, eds. *Proceedings of the International Union of Forestry Research Organizations Forest Growth Modelling and Prediction Conference*, Aug. 23-27, 1987, Minneapolis, MN. General Technical Report NC-120, USDA-Forest Service, North Central Forest Experiment Station, St. Paul, MN.

Norman, J.M., and J.M. Welles. 1983. Radiative transfer in an array of canopies. Agron. J. 75:481-488.

Norman J.M., and P.G. Jarvis. 1975. Photosynthesis in sitka spruce (*Picea sitchensis* (bong.) Carr.) V. Radiation penetration theory and a test case. J. Appl. Ecol. 12:839-878.

Nye, P.H., and P.B. Tinker. 1977. *Solution Movement in the Soil-Root System*. Blackwell Scientific Publications, Oxford. 342 pp.

Oker-Blom, P. 1986. Photosynthetic radiation regime and canopy structure in modeled forest stands. ACTA For. Fenn. 197.

Oker-Blom, P., and S. Kellomaki. 1983. Effect of grouping of foliage on the within-stand and within-crown light regime: comparison of random and grouping canopy models. Agric. Met. 28:143-155.

Olson, R.K., W.A. Reiners, and G.M. Lovett. 1985. Trajectory analysis of forest canopy effects on chemical flux in throughfall. Biogeochem. 1:361-373

Öquist, G., and M. Strand. 1986. Effects of frost hardening on photosynthetic quantum yield, chlorophyll organization, and energy distribution between the two photosystems in Scots pine. Can. J. Bot. 64:748-754.

Oster. 1977. Lectures in population dynamics. In: R.C. DiPrima, ed. *Modern Modeling of Continuum Phenomona*. American Mathematical Society, Providence, RI. pp. 149-190.

Parthasarathy, M.V. 1975. Sieve-element structure. In: M.H. Zimmermann, and J.A. Milburn, eds. *Transport in Plants I: Phloem Transport*. Encyclopedia of Plant Physiology New Series Volume 1. pp. 3-38.

Peel, A.J. 1975. Investigations with aphid stylets into the physiology of the sieve tube. In: M.H. Zimmermann, and J.A. Milburn, eds. *Transport in Plants I: Phloem Transport*. Encyclopedia of Plant Physiology. New Series Volume 1. pp. 171-195.

Penning de Vries, F.W.T., J.M. Witlage, and D. Kremer. 1979. Rates of respiration and of increase in structural dry matter in young wheat, ryegrass and maize plants in relation to temperature, to water stress and to their sugar content. Ann. Bot. 44:595-609.

Peterson, C.E., K.G. Mattson, and R.A. Mickler. 1989. Seedling response to sulfur, nitrogen, and associated pollutants. Major Program Output #3, EPA/600/3-89/081, US Environmental Protection Agency, Environmental Research Laboratory, Corvallis, OR. 104 pp.

Porter, J.H., B. Klepper, and R.K. Belford. 1986. A model (WHTROOT) which synchronizes root growth and development with shoot development for winter wheat. Plant and Soil. 92:133-145.

Press, W.H., B.P. Flannery, S.A. Teukolsky, and W.T. Vetterling. 1988. *Numerical Recipes in C: The Art of Scientific Computing*. Cambridge University Press, Cambridge. 735 pp.

Prinz, B. 1987. Causes of forest damage in Europe: Major hypotheses and factors. Environment. 29(9):11-15, 32-37.

Pritchett, W.L., and R.E. Fisher. 1987. *Properties and Management of Forest Soils*. John Wiley & Sons, New York. 494 pp.

Reams, G.A., R.J. Vong, M. Böhm, K.G. Mattson, and L.Y. Arnaut. 1990. Extent and Magnitude of Recent Changes in Forest Condition and the Role of Air Pollution and Non-Air Pollution Factors. Major Program Output #1&2, EPA/600/3-90/042, US Environmental Protection Agency, Environmental Research Laboratory, Corvallis, OR. 152 pp.

Reich, P.B. 1987. Quantifying plant response to ozone: A unifying theory. Tree Physiol. 3:63-91.

Reynolds, J.F., B.R. Strain, G.L. Cunningham, and K.R. Knoerr. 1980. Predicting primary productivity for forest and desert ecosystem models. In: J.D. Hesketh and J.W. Jones, eds. *Predicting Photosynthesis for Ecosystem Models*. CRC Press, Boca Raton, FL. pp. 169-207.

Reynolds, J.F., and J.H.M. Thornley. 1982. A shoot:root partitioning model. Ann. Bot. 48:585-597.

Robarge, W.P., and I. Fernandez. 1987. Laboratory analytical techniques. Forest Response Program Quality Assurance Methods Manual. EPA/600/X-86/193c, US Environmental Protection Agency Internal Report, Revision 1. 218 pp.

Robinson, D., and I.H. Rorison. 1983. Relationships between root morphology and nitrogen availability in a recent theoretical model describing nitrogen uptake from soil. Plant Cell Environ. 6:641-647.

Running, S.W., R.R. Nemani, R.D. Hungerford. 1987. Extrapolation of synoptic meteorological data in mountainous terrain and its use for simulating forest evapotranspiration and photosynthesis. Can. J. For. Res. 17:472-483.

Russell, R.S. 1977. *Plant Root Systems: Their Function and Interaction with the Soil.* McGraw-Hill, London. 298 pp.

Sasek, T.W., and C.J. Richardson. 1989. Effects of chronic doses of ozone on loblolly pine: Photosynthetic characteristics in the third growing season. For. Sci. 35(3):745-755.

Sasser, C.I., and D. Binkley. 1989. Nitogen mineralization in high-elevation forests of the Appalachians. II. Patterns with stand development in fir waves. Biogeochem. 7:147-156.

Schroeder, P., and A.R. Kiester. 1989. The Forest Response Program: National research on forest decline and air pollution. J. For. 87:27-32.

Seemann, J.R., T.D. Sharkey, J. Wang, and C.B. Osmond. 1987. Environmental effects on photosynthesis, nitrogen-use efficiency, and metabolite pools in leaves of sun and shade plants. Plant Physiol. 84:796-802.

Sheppard, L.J., and E.D. Ford. 1987. Genetic and environmental control of crown development in *Picea sitchensis* and its relation to stem wood production. Tree Physiol. 1:341-352.

Shinozaki, K., K. Yoda, K. Hozumi, and T. Kira. 1964a. A quantitative analysis of plant form - The pipe model theory. I. Basic analyses. Jap. J. Ecol. 14:97-105.

Shinozaki, K., K. Yoda, K. Hozumi, and T. Kira. 1964b. A quantitative analysis of plant form - The pipe model theory. II. Further evidence of the theory and its application in forest ecology. Jap. J. Ecol. 14:133-139.

Shriner, D., W.W. Heck, S.B. McLaughlin, D.W. Johnson, J.D. Joslin, and C.E. Peterson. Changes in Forest Health and Productivity in the United States and Canada. NAPAP Report 18, Acidic Deposition: State of Science and Technology, National Acid Precipitation Assessment Program, Washington, DC.

Smith, K.C., C.E. Magnuson, J.D. Goeschl, and D.W. DeMichele. 1980. A time-dependent mathematical expression of the Münch hypothesis of phloem transport. J. Theor. Biol. 86:493-505.

Sorrensen, K.A. 1989. A three dimensional model of above ground competition incorporating crown plasticity and multiway interaction. Masters thesis. University of Washington, Seattle, WA.

Stanley, T.W., and S.S. Verner. 1985. The US EPA's quality assurance program. In: J.K. Taylor and T.W. Stanley, eds. *Quality Assurance for Environmental Measurements*. ASTM STP No. 867. pp. 12-19.

Stone, E.L., and M.H. Stone. 1943. "Dormant" versus "adventitious" buds. Science 98:62.

Stone, E.L. 1953. The origin of epicormic branches in fir. J. For. 51:366.

Strader, R.H., D. Binkley, and C.G. Wells. 1989. Nitogen mineralization in high-elevation forests of the Appalachians. I. Regional patterns in southern spruce-fir forests. Biogeochemistry 7:131-145.

Switzer, G.L., and L.E. Nelson. 1972. Nutrient accumulation and cycling in loblolly pine (*Pinus taeda L.*) plantation ecosystems: the first twenty years. Soil Sci. Soc. Amer. Proc. 36:143-147.

Taylor, G.E. Jr., R.J. Norby, et al. 1986. Carbon dioxide assimilation and growth of red spruce (*Picea rubrens Sarg.*) seedlings in response to ozone, precipitation chemistry, soil type. Oecologia. 70:163-171.

Thomas, H., and J. Stoddart. 1980. Leaf senescence. Ann. Rev. Plant Physiol. 31:83-111.

Thomasson, A.J. 1978. Towards an objective classification of soil structure. J. Soil Sci. 29:38-46.

Thornley, J.H.M. 1972. A balanced quantitative model for root:shoot ratios in vegetative plants. Ann. Bot. 36:431-441.

Ticha, I. 1981. Ontogeny of leaf morphology and anatomy. In: C.B. Johnson, ed. *Physiological Processes Limiting Plant Productivity*. Butterworths, London.

Tjoelker, M.G., R.J. Luxmoore, and O.J. Schwartz. 1989. Soil nitrogen and ozone effects on growth, physiology, and nutrition of loblolly pine and yellow-poplar seedlings. ORNL/TM-11065, Oak Ridge National Laboratory. Environmental Sciences Division Publication No. 3257, Oak Ridge, TN.

Tyree, M.T., A.L. Christy, and J.M. Ferrier. 1974. A simpler iterative steady state solution of Münch pressure flow systems applied to long and short translocation paths. Plant Physiol. 54:589-600.

van Praag, H.J., and F. Weissen. 1986. Foliar mineral composition, fertilization and dieback of Norway spruce in the Belgian Ardennes. Tree Physiol. 1:169-176.

VanSickle, J. 1977. Analysis of a distributed parameter population model based on physiological age. J. Theor. Biol. 64:571-586.

Vann, D.R. Personal Communication. University of Pennsylvania, Philadelphia, PA.

Walker, L.C. 1980. The southern pine region. In: J.W. Barrett, ed. *Regional Silviculture of the United States*. John Wiley & Sons, New York. pp. 231-276.

Waller, D.M., and D.A. Steingraeber. 1985. Branching and Modular Growth: Theoretical Models and Empirical Patterns, pp. 225-257. In: J.B.C. Jackson, L.W. Buss, and R.E. Cook, eds. Population Biology and Evolution of Clonal Organisms. Yale Univ. Press, New York.

Wang, Y. 1988. Description and validation of an array model - MAESTRO. Agric. For. Met.

Waring, R.H., and J.F. Franklin. 1979. Evergreen coniferous forests of the Pacific Northwest. Science 204:1380-1386.

Waring, R.H., and W.A. Schlesinger. 1985. *Forest Ecosystems: Concepts and Management*. Academic Press, New York. 340 pp.

Watson, M.A., and B.B. Casper. 1984. Morphogentic constraints on patterns of carbon distribution in plants. Ann. Rev. Ecol. Syst. 15:233-258.

Webb, C.D., and H.E. Burkhart. 1988. Modeling the effects of air pollution on forest productivity: sensitivity analysis using PTAEDA. In: A.R. Ek, S.R. Shifley, and T.E. Burk, eds. *Proceedings of the International Union of Forestry Research Organizations Forest Growth Modeling and Prediction Conference*, Aug. 23-27, 1987, Minneapolis, MN. General Technical Report NC-120, USDA-Forest Service, North Central Forest Experiment Station, St. Paul, MN. 610 pp.

Whitehead, D., W.R.N. Edwards, and P.G. Edwards. 1984. Conducting sapwood area, foliage area, and permeability in mature trees of *Picea sitchensis* and *Pinus contorta*. Can. J. For. Res. 14:940-947.

Yang, Y.S., J.M. Skelly, B.I. Chevone, and J.B. Birch. 1983. Effects of long term ozone exposure on photosynthesis and dark respiration of eastern white pine. Environ. Sci. Tech. 17:371-373.

Zedaker, S., and N. Nicholas. 1988. Site classification and field measurements. Forest Response Program Quality Assurance Methods Manual. EPA/600/X-86/193b, US Environmental Protection Agency Internal Report, Revision 2. 92 pp.

Zimmermann, M.H. 1971. Transport in the phloem, pp. 221-279. In: M.H. Zimmermann and C.L. Brown, eds. *Trees: Structure and Function*. Springer-Verlag, New York.